January 2010

Transient-State Kinetic Studies of The Mechanisms of Dna Unwinding And Translocation of The E. Coli Recbc And Recbcd Helicases

Colin Wu
Washington University in St. Louis

Washington University in St. Louis

Division of Biology and Biomedical Sciences

Program in Biochemistry

Dissertation Committee:

Timothy M. Lohman (Chairperson)
Peter Chivers
Tom Ellenberger
Carl Frieden
Roberto Galletto
John Majors

TRANSIENT-STATE KINETIC STUDIES OF THE MECHANISMS OF DNA UNWINDING AND TRANSLOCATION OF THE *E. coli* RecBC AND RecBCD HELICASES

by

Colin Galwun Wu

A dissertation presented to the
Graduate School of Arts and Sciences
of Washington University in
partial fulfillment of the
requirements for the degree
of Doctor of Philosophy

December 2010

Saint Louis, Missouri

ABSTRACT OF THE DISSERTATION

Transient-state kinetic studies of the mechanisms of DNA unwinding

and translocation of the *E. coli* RecBC and RecBCD helicases

by

Colin Galwun Wu

Doctor of Philosophy in Biochemistry

Washington University School of Medicine, 2010

Professor Timothy M. Lohman (thesis advisor)

This thesis presents mechanistic studies of the *E. coli* RecBC and RecBCD helicases using transient-state kinetic approaches to understand the relationship between DNA unwinding and ssDNA translocation. RecBC initiates unwinding from duplex DNA ends with pre-existing 5'-$(dT)_6$ and 3'-$(dT)_6$ ssDNA tails using a series of repeated rate-limiting steps with a rate of 345 ± 8 bp/sec and an average kinetic step-size of ~4 bp (20 mM Mops-KOH, pH 7.0 at 25°C, 30 mM NaCl, 10 mM $MgCl_2$, 5% glycerol, 1 mM 2-mercaptoethanol) while RecBCD unwinds these same DNA substrates with a rate of 745 ± 18 bp/sec using a more complicated mechanism which involves the loading of the 5' ssDNA end onto the RecD subunit. After DNA unwinding, RecBC can continue to translocate along a ssDNA extension in the 3' to 5' direction with a rate of 909 ± 51 nt/sec, consistent with the directionality of the RecB motor subunit. Surprisingly, RecBC also possesses a secondary translocase activity that enables it to move along a ssDNA extension of the opposite DNA strand with a similar rate (990 ± 49 nt/sec). Both

translocase activities are coupled to ATP hydrolysis from the RecB motor, and the primary translocase is sensitive to the polarity of the ssDNA backbone while the secondary translocase is not. RecBC can also translocate along two non-complementary ssDNA extensions simultaneously using both translocase activities. During DNA unwinding, RecBC consumes an average of 0.95 ± 0.08 ATP/bp unwound. The primary translocase activity utilizes 0.81 ± 0.05 ATP/nt translocated while its secondary translocase activity is less tightly coupled and requires 1.12 ± 0.06 ATP/nt. Translocation along two non-complementary ssDNA extensions has an ATP coupling stoichiometry of 1.07 ± 0.09 ATP/nt. These data indicate that the large majority, possibly all, of the ATP hydrolyzed by RecBC during DNA unwinding is used to fuel RecBC translocation along the nucleic acid rather than to facilitate base pair melting. These results suggest that RecBC uses a two step active mechanism to unwind DNA by first destabilizing the duplex using its binding free energy in an ATP-independent process, followed by ATP-dependent translocation along the resulting ssDNA.

Acknowledgements

I thank my family and friends for their continual support throughout my graduate school career. To my parents, I am eternally grateful for the hard work and sacrifices you have endured for the sake of my education. To my little brother Kelvin, do not hesitate to pursue your dreams. Thank you for keeping our folks out of trouble and for visiting me these past few years; it has been an amazing experience watching you grow up. To my girlfriend, the newly minted Dr. Erin O'Neal, you are my ATP. Your love and support have fueled me past every hurdle life has to offer. With all my heart, I thank you and your family for embracing me as an honorary member; I love you and I look forward to the next chapter of our journey together.

I extend my thanks to all former and current Lohman lab members for their help and wisdom, and especially: Dr. Jason "Guru" Wong for mentoring me when I was a rotation student; Drs. Aaron "Lucky" Lucius and Karl "The Monkey" Maluf for their constant motivation and scientific advice; Dr. Chris "Shark" Fischer for his expertise in everything related to data fitting and politics; Dr. Anita "Princess" Niedziela-Majka for her expertise in everything pertaining to protein biochemistry; Dr. Alex "The Tzar" Kozlov for sharing his knowledge of thermodynamics and for getting donuts for my group meetings. To my thesis committee members, you have been an invaluable resource. Thank you for your support and for your suggestions.

Finally, to my thesis advisor, Dr. Lohman, thank you for your guidance and for holding myself to a higher standard. Your training has improved my ability to think critically and has helped me evolve as a scientist. I am indebted to you for this research opportunity and I thank you for your mentorship…even if I am now a coffee addict.

Table of Contents

List of Figures

Chapter I

Chapter II

Chapter III

Chapter IV

List of Tables

Chapter II

Chapter III

Chapter IV

Chapter I

Introduction

DNA helicases are a ubiquitous class of motor proteins that couple the energy from 5'-nucleoside triphosphate (NTP) binding and hydrolysis in order to separate double-stranded (ds) DNA into transient single-strand (ss) intermediates that are required for DNA replication, recombination, and repair (Matson, Bean et al. 1994; Lohman and Bjornson 1996; Patel and Picha 2000; Delagoutte and von Hippel 2002; Lohman, Hsieh et al. 2003; Patel and Donmez 2006; Singleton, Dillingham et al. 2007). Since DNA helicase activity is essential for all aspects of DNA metabolism, defects and mutations in human enzymes are linked to a number of genetic disorders such as Bloom syndrome, Werner syndrome, xeroderma pigmentosum, and others as well (Ellis, Groden et al. 1995; Hickson, Davies et al. 2001; Hickson 2003; German, Sanz et al. 2007). In addition, a number of viral helicases which are essential for the replication of viral nucleic acids have been identified, such as the hepatitis C NS3 enzyme (Serebrov and Pyle 2004); therefore, understanding the molecular basis by which helicases function is paramount in aiding the design of potential therapeutics. To this end, this thesis describes mechanistic studies of DNA unwinding and translocation using the *E. coli* RecBCD and RecBC helicases as model systems.

RecBCD is a molecular motor possessing ATPase, DNA helicase, and nuclease activities (Smith 1990; Kowalczykowski, Dixon et al. 1994; Anderson and Kowalczykowski 1997). This heterotrimeric enzyme is composed of the RecB (134 kDa), RecC (129 kDa), and RecD (67 kDa) polypeptides, and is involved in the major pathway of recombination in *E. coli* by processing DNA ends at damaged induced dsDNA breaks (Finch, Storey et al. 1986; Finch, Storey et al. 1986; Finch, Wilson et al. 1986). To this date, there is a wealth of biochemical and genetic information available for this system, which has facilitated a number of equilibrium binding and DNA unwinding studies (Lucius, Vindigni et al. 2002; Dillingham 2003; Taylor and Smith 2003; Wong, Lucius et al. 2005). For the remainder of this introduction, I will highlight a subset of these studies that have laid the groundwork and have provided the motivation for this research. In addition, I will present any relevant background information regarding the structural features of RecBCD as well as its biochemical properties, and discuss its biological role *in vivo*.

Common Features

Helicases have been classified originally into superfamilies and families based on their amino acid patterns (Gorbalenya and Koonin 1993; Hall and Matson 1999). The largest two superfamilies, the SF1 and SF2 helicases, are each defined by seven conserved motifs in the primary sequence although not all seven regions are identical between the two superfamilies (Lohman, Tomko et al. 2008). Only motifs I and II, or the “Walker A” and “Walker B” boxes, are shared among all helicase superfamilies and familes; these motifs together form part of the NTP binding site required for nucleotide binding and hydrolysis. Since this classification method of helicases is based solely on amino acid sequence similarity, enzymes within a particular superfamily or family do not necessarily share the same unwinding properties and can act on a variety of nucleic-acid substrates. As a result, although still useful, this antiquated classification system provides no mechanistic information of how helicases function, and a refinement of classification has been suggested to differentiate between enzymes that translocate along ssDNA (type A) or dsDNA (type B) and is based also on the directionality of translocation (3' to 5' (type α) or 5' to 3' (type β)) (Singleton, Dillingham et al. 2007). To avoid further confusion, enzymes possessing helicase motifs but with unknown biochemical properties should be referred as nucleic-acid stimulated NTPases.

The *E. coli* RecBCD helicase is composed of two SF1 motor subunits: RecB (a 3' to 5' translocase or type Aα) and RecD (a 5' to 3' translocase or type Aβ) (Dillingham 2003). The RecC subunit lacks the amino acids that are required for ATP catalysis and functions instead as a processivity and regulatory factor (Singleton, Dillingham et al. 2004; Rigden 2005). Even though the RecB and RecD motor subunits have opposite strand translocation polarities, they function in unison within the RecBCD heterotrimer to unwind DNA in the same net direction by acting on opposite ends of the DNA duplex (Taylor and Smith 2003). Interestingly, the RecBC enzyme can still function as a rapid and processive helicase albeit with only one motor subunit (Korangy and Julin 1993) and therefore has a single ATP binding site, presumably; as a result, systematic studies of the RecBCD and RecBC enzymes can provide some insight to how the individual motor subunits function during DNA unwinding and ssDNA translocation.

Biological role and function of RecBCD

RecBCD is involved in the major pathway of homologous recombination in *E. coli* and functions to repair damaged induced dsDNA breaks (**Figure 1**). RecBCD first binds to a damaged induced blunt or nearly blunt-end with high affinity (Wong, Lucius et al. 2005), and then it will initiate unwinding of the DNA duplex upon ATP binding and hydrolysis with RecD serving as the lead motor (Spies, Amitani et al. 2007) and RecB as the trailing motor. Because the two motor subunits move with different rates, a ssDNA

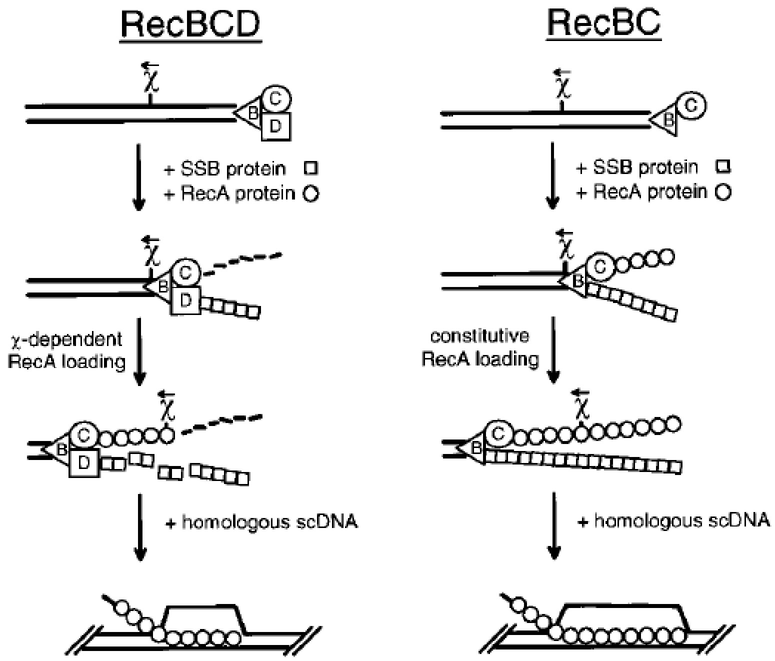

Figure 1. **Cartoon of RecBCD and RecBC mediated recombination *in vivo***. (**left panel**) RecBCD binds to a damaged DNA end and unwinds the duplex. RecBCD preferentially degrades the 3' terminating DNA strand until Chi is recognized, after which RecBCD degrades the 5' terminating strand and loads RecA onto the 3' terminating ssDNA. The RecA-ssDNA filament initiates recombinational repair of the DNA break. (**right panel**) RecBC also mediates recombinational repair but RecA loading is constitutive and independent of the Chi regulatory sequence. (Arnold and Kowalczykowski 2000).

loop is formed ahead of the slower RecB subunit as the duplex is unwound (Taylor and Smith 2003). During unwinding, RecBCD will degrade preferentially the 3' ended DNA strand (relative to the RecBCD loading site) while cleaving the 5' ended strand infrequently (Yu, Souaya et al. 1998; Yu, Souaya et al. 1998). This potent nuclease activity functions to degrade phage DNA which is devoid of a crossover hotspot instigator (Chi) regulatory sequence 5'-GCTGGTGG-3' that is over represented in the *E. coli* genome. RecBCD unwinding and nuclease activities will ensue until the complex encounters Chi, which is recognized by the RecC subunit, whereupon single-molecule studies have shown that RecBCD pauses for several seconds (Handa, Bianco et al. 2005; Spies, Amitani et al. 2007). After Chi recognition, DNA unwinding slows, and RecB then serves as the lead motor and the RecD subunit is inactivated (Spies, Amitani et al. 2007). Furthermore, the nuclease activity instead targets the 5' ended DNA strand, resulting in the formation of a 3' ssDNA overhang onto which RecBCD can load the

RecA protein (Arnold and Kowalczykowski 2000). The RecA coated ssDNA filament can then facilitate the invasion of a homologous piece of DNA and use it as a template to repair the original DNA break (Spies, Bianco et al. 2003; Spies, Dillingham et al. 2005)

The RecBC enzyme, although lacking the RecD motor subunit can still function as a processive and rapid helicase (Korangy and Julin 1993). Interestingly, the nuclease activity of RecBC is greatly diminished even though the nuclease domain is a part of the RecB subunit. Furthermore, DNA unwinding by the RecBC enzyme mimics a "post Chi" state since RecA loading is constitutive and independent of the Chi regulatory sequence. As a result, recD$^-$ *E. coli* cells are hyper-recombinogentic (Arnold and Kowalczykowski 2000).

Structural Features

A crystal structure of RecBCD bound to a 19 bp DNA hairpin was determined in 2004 (Singleton, Dillingham et al. 2004) (**Figure 2**). This complex was formed in presence of Ca^{2+} in order to inhibit the inherent Mg^{2+} dependent nuclease activity of RecBCD. The last 4 bp of the DNA duplex was observed to be "melted out," and the 3' end of the ssDNA was shown to interact with the RecB subunit, as expected for a 3' to 5' helicase, while the 5' ssDNA end was poised to interact with the RecD subunit although the DNA substrate was not sufficient in length to engage the motor. Equilibrium binding and DNA unwinding studies as well as computer modeling have suggested a 5' ssDNA tail length of ten nucleotides is required for the DNA end to reach the RecD subunit (Wong, Lucius et al. 2005; Wong, Rice et al. 2006). This is consistent with a more recent

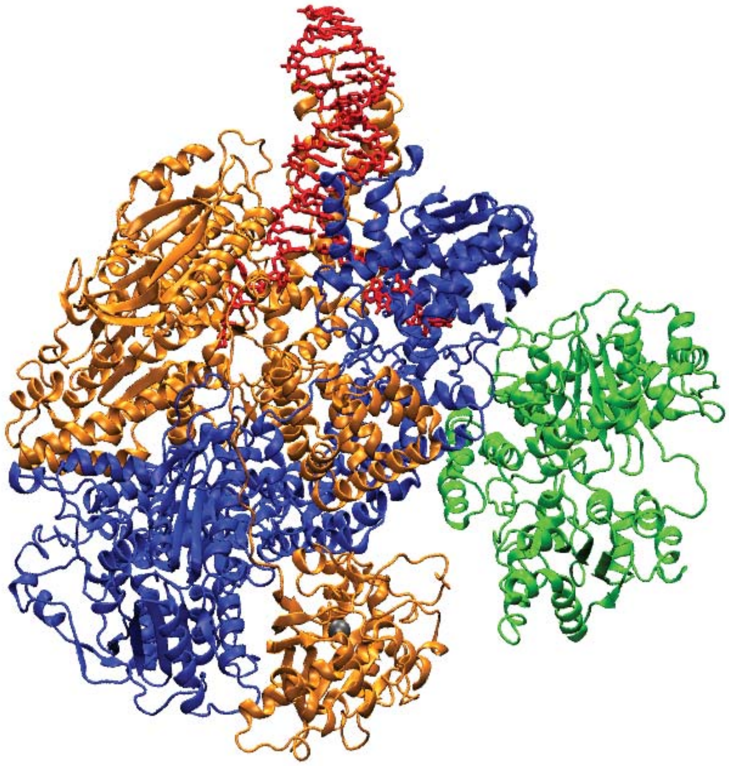

Figure 2. Crystal structure of a RecBCD-DNA complex. RecBCD is bound to a 19 bp blunt ended DNA hairpin. RecB is shown in orange, RecC is shown in blue, and RecD is shown in green; the DNA is shown in red. The RecBCD-DNA complex was formed in the presence of Ca^{2+} in order to attenuate its nuclease activity. A calcium ion (shown in gray) is observed to be bound to the RecB nuclease domain and the last 4 bp of the DNA substrate is observed to be melted. (Singleton, Dillingham et al. 2004)

crystal structure of RecBCD bound to a 19 bp DNA hairpin which has a 10 nt overhang on the 5'-end (Saikrishnan, Griffiths et al. 2008). An interesting structural feature to note is the "arm" region of RecB, which is shown to interact with the DNA duplex ahead of the unwinding fork; the implications of this arm domain on the mechanism of DNA unwinding and translocation will be discussed in Chapter 3 and Chapter 4. The ~ 30 kDa nuclease domain of RecB is tethered to the helicase domain through a long and flexible linker region (Singleton, Dillingham et al. 2004). Although this nuclease domain is observed to form many protein-protein interactions with RecC and RecD in the crystal structure, it likely adopts other conformations in solution using the flexible linker since RecBCD is able to degrade either DNA strand before Chi is recognized.

Interestingly, the RecC subunit, adopts a RecB-like fold even though the two polypetides share only 2-11% amino sequence identity and RecC does not possess any canonical catalytic helicase or nuclease residues; hence, it is considered motor and nuclease dead (Rigden 2005). RecC not only forms many protein-protein interactions with the RecB and RecD subunits, but also contacts both strands of the unwound ssDNA. The 5'-terminated DNA strand interacts with the dead nuclease region of RecC while the 3'-terminated strand, from which Chi is eventually recognized, interacts with the dead motor domain (Singleton, Dillingham et al. 2004; Rigden 2005; Saikrishnan, Griffiths et al. 2008).

Binding of RecBCD and RecBC to DNA ends

RecBCD and RecBC bind with high affinity to DNA ends (Wong, Lucius et al. 2005). Upon DNA binding, both RecBCD and RecBC can "melt out" the last 5-6 base pairs in a Mg^{2+} dependent but ATP independent manner. This was first demonstrated in footprinting studies by Farrah and Smith where they showed that the last 5-6 bases are susceptible to $KMnO_4$ attack when RecBCD binds to a DNA end (Farah and Smith 1997) which suggests base pair melting. In a crystal structure of a RecBCD-DNA complex, which is solved in presence of Ca^{2+} instead of Mg^{2+} in order to attenuate the nuclease activity of RecBCD, the last 4 base pairs are observed to be separated (Singleton, Dillingham et al. 2004; Saikrishnan, Griffiths et al. 2008). Consistent with these results, Wong et al have examined the energetics of RecBCD and RecBC binding to different

DNA ends using fluorescence titration and isothermal titration calorimetry (Wong, Lucius et al. 2005; Wong, Rice et al. 2006; Wong and Lohman 2008). These studies indicate that the affinity of RecBCD for a DNA end increases as the 5' ssDNA tail length is increased from 0 to 10 nucleotides, after which further extension of the 5' tail length does not influence the binding affinity. Interestingly, when the 3' ssDNA tail length is increased, the binding affinity increases from 0-6 nucleotides but decreases from 6-20 nucleotides. As a result, RecBCD binds with optimal affinity to a DNA end possessing pre-existing 5'-$(dT)_{10}$ and 3'-$(dT)_6$ ssDNA tails. A similar trend was observed with equilibrium studies of the RecBC heterodimer; however, this enzyme binds tightest to a DNA end possessing pre-formed 5'-$(dT)_6$ and 3'-$(dT)_6$ ssDNA tails. This result indicates that both RecBCD and RecBC can "melt out" ~ 6 bp upon DNA binding such that if either protein is presented with preformed ssDNA tails, it no longer has to melt out those base pairs resulting in an increase in binding affinity. Wong et al. later showed that the decrease in binding affinity when the 3' tail length is increased results from paying an unfavorable entropic cost for forming a ssDNA loop (Wong, Rice et al. 2006). I will discuss in Chapter 2 the effects of various DNA end structures (and also the influence of this ssDNA loop) on the mechanism of DNA unwinding initiation by RecBC and RecBCD. I note that the ssDNA loop Wong et al. observed is inherent to RecBC and RecBCD binding to DNA ends with a 3' ssDNA tail length > 6 nucleotides and differ from those previously observed during RecBCD catalyzed DNA unwinding (Taylor and Smith 2003); these loops result from the asymmetry in the unwinding rates of the RecB and RecD motor subunits.

Methods for studying DNA unwinding and translocation

There are a variety of experimental approaches used to study DNA unwinding and translocation; I will highlight several in this introduction. "All or none" experiments are especially powerful because they provide information not only on the rate/processivity of unwinding, but also yield an estimate of the kinetic step-size (Ali and Lohman 1997; Lucius, Vindigni et al. 2002). This technique requires labeling a reporter DNA strand either fluorescently or radioactively, and the substrate is designed such that unwinding is not detected until the entire strand is unwound and displaced by the protein. As a result, all or none unwinding time-courses display lag kinetics in which the initial lag phase is sensitive to the number of repeated steps similar rate constants the helicase must undergo (Lucius, Maluf et al. 2003). Unwinding experiments are typically performed as a function of reporter strand length and an average kinetic step-size can be estimated by analyzing such a set of time-courses. One disadvantage of this assay is that it is sensitive to re-annealing. Since DNA unwinding is not detected until the duplex is completely unwound, the unwound DNA can re-anneal behind the helicase which will influence the final amplitude of unwinding. Another type of unwinding assay commonly used involves intercalating agents (ie: YOYO-1 or Hoechst 33258) which have different fluorescence properties when bound to ssDNA versus dsDNA (Bianco, Brewer et al. 2001; Dillingham, Webb et al. 2005). DNA unwinding is observed by monitoring changes in fluorescence signal as a function of time. Alternatively, *E. coli* SSB binding to the newly unwound ssDNA can also be used as a signal to monitor DNA unwinding (Roman and Kowalczykowski 1989; Roman, Eggleston et al. 1992). In these experiments, one can either monitor changes in the intrinsic tryptophan fluorescence of SSB or SSB can be fluorescently labeled and yield a signal change when bound to ssDNA (Webb 2010).

RecBCD and RecBC catalyzed DNA unwinding

Previously, Lucius et al have determined the minimal kinetic mechanism by which RecBCD initiates DNA unwinding from blunt-ends using “all or none” pre-steady state rapid chemical quenched-flow and stopped-flow fluorescence approaches (Lucius, Vindigni et al. 2002; Lucius, Jason Wong et al. 2004; Lucius and Lohman 2004). RecBCD requires undergoing two to three initiation steps before DNA unwinding can proceed although the functional nature of these additional steps remains unclear. RecBCD unwinds DNA rapidly and processively (rates and conditions) with an average kinetic step-size of ~ 4 bp. This value is the same within error over a range of [ATP] and temperature examined which indicates that the same rate-limiting step remains rate-limiting over the range of conditions examined (Lucius and Lohman 2004). Single-molecule studies have revealed that upon recognizing the Chi sequence during DNA unwinding, RecBCD pauses for several seconds and then continues DNA unwinding albeit with a slower rate, and that RecBCD can undergo forward and reverse motions during DNA unwinding (Perkins, Li et al. 2004; Handa, Bianco et al. 2005). The estimated ATP coupling stoichiometry during RecBCD unwinding is reported to be ~ 2-3 ATP per base pair unwound, which equates to ~ 1-1.5 ATP per base pair per motor (Roman and Kowalczykowski 1989; Korangy and Julin 1994). However, these measurements were obtained by taking the ratio of the steady-state rate of DNA unwinding and the steady-state rate of ATP hydrolysis, which is influenced by slower processes such as protein dissociation and re-binding.

The RecBC enzyme, which possesses only the RecB ATPase motor, still functions as a helicase. Therefore, this simpler system provides a good model for studying how ATP binding and hydrolysis is coupled to DNA unwinding and translocation. However, to this date, the unwinding mechanism for RecBC remains unknown. In one interesting study, Bianco and Kowalczykowski inferred that RecBC translocates with strictly 3' to 5' directionality through DNA unwinding experiments in which the DNA substrate possessed a ssDNA gap in between two duplex regions (Bianco and Kowalczykowski 2000). When the intervening ssDNA is 3' to 5' relative to the RecBC loading site, the protein is able to bypass even a 30 nucleotide ssDNA gap and unwind a distal duplex with the same efficiency relative to when there is only a nick present. On the other hand, when the ssDNA region is 5' to 3' of the RecBC loading site, the protein has difficulty bypassing a 30 nucleotide ssDNA gap and a decrease in unwinding efficiency is observed in the unwinding of a distal duplex relative to when only a nick is present. The authors also observed that the gap size RecBC is able to traverse depends on the proximal duplex length and that on average RecBC takes a 23 nt step (Bianco and Kowalczykowski 2000). This led them to propose a quantum inchworm mechanism for RecBC unwinding in which a leading domain takes a 23 nt translocation step forward and then a trailing domain catches up to the leading domain and unwinds the DNA duplex with a smaller step size (Bianco and Kowalczykowski 2000; Lucius, Vindigni et al. 2002).

Research goals

The ultimate goal of this thesis research is to better understand the relationship between DNA unwinding and ssDNA translocation using the *E. coli* RecBC and RecBCD helicases. This dissertation presents pre-steady state kinetic studies of the RecBC and RecBCD helicases so that a direct comparison of these two activities can be made with these enzymes. Because RecBC is a processive helicase with only one motor subunit, it has a single ATP binding site (presumably) which will make the results from DNA unwinding and ssDNA translocation studies easier to interpret. Similar mechanistic studies can then be performed with the more complex RecBCD enzyme in order to determine and to dissect the relative contributions of each motor subunit to unwinding and translocation.

As stated in the beginning of this introduction, at the start of my research, the binding energetics of RecBC and RecBCD to different DNA ends was examined (Wong, Lucius et al. 2005; Wong, Rice et al. 2006; Wong and Lohman 2008) and the minimal kinetic mechanism required to describe RecBCD unwinding of DNA blunt ends was determined (Lucius, Vindigni et al. 2002; Lucius, Jason Wong et al. 2004; Lucius and Lohman 2004). However, the mechanism by which simpler RecBC helicase unwinds DNA remains unclear. My first goal will be to examine RecBC unwinding and compare these results with RecBCD in order to access whether RecBC unwinds DNA with the same rate and step-size as the RecBCD enzyme. I will also examine how different DNA end structures affect DNA unwinding initiation by RecBC and RecBCD and determine whether these effects are correlated with previous equilibrium binding measurements (ie: related to formation of a ssDNA loop on the 3' terminating DNA strand).

Since the directionality of RecBC translocation has thus far only been inferred using DNA unwinding studies (Bianco and Kowalczykowski 2000), I will monitor the ssDNA translocation activities of the RecB monomer as well as the RecBC heterodimer directly so that the ssDNA translocation rates can be compared with those of DNA unwinding under the same solution conditions. I will then determine the ATP coupling stoichiometry during unwinding as well as translocation, which will help us understand how ATP hydrolysis is coupled to fuel these two processes.

Chapter II

Influence of DNA End Structure on the Mechanism of Initiation of DNA Unwinding by the *E. coli* RecBCD and RecBC Helicases

Preface to Chapter II

This chapter presents DNA unwinding studies of the *E. coli* RecBCD and RecBC helicases using pre-steady state kinetic approaches. Previous unwinding experiments performed by Lucius et al (Lucius, Vindigni et al. 2002; Lucius, Jason Wong et al. 2004; Lucius and Lohman 2004) indicated that the RecBCD heterotrimer requires undergoing two to three initiation steps before it unwind DNA from a blunt-end, and that similar mechanistic studies were difficult to perform with the RecBC enzyme due to low unwinding amplitude. Wong et al (Wong, Lucius et al. 2005) showed subsequently using equilibrium approaches that RecBCD binds with optimal affinity to a duplex DNA end possessing 5'-$(dT)_{10}$, 3'-$(dT)_6$ pre-existing ssDNA tails, while the simpler RecBC binds with highest affinity to a DNA end with pre-existing 5'-$(dT)_6$, 3'-$(dT)_6$ ssDNA tails, and that both helicases can "melt out" ~ 6 bp upon DNA binding. Hence, the fundamental goals of the research described in this section are to determine the minimal kinetic mechanism which describes RecBC unwinding using its optimal binding substrate, and to investigate how various DNA end structures influence the mechanism by which RecBCD and RecBC initiate DNA unwinding. This chapter is based on the manuscript published in 2008 in the Journal of Molecular Biology (Wu and Lohman 2008), and additional data not presented in the original article is also included in this chapter.

doi:10.1016/j.jmb.2008.07.012 J. Mol. Biol. (2008) **382**, 312–326

JMB

Available online at www.sciencedirect.com
ScienceDirect

ELSEVIER

Influence of DNA End Structure on the Mechanism of Initiation of DNA Unwinding by the *Escherichia coli* RecBCD and RecBC Helicases

Colin G. Wu and Timothy M. Lohman*

Department of Biochemistry and Molecular Biophysics, Washington University School of Medicine, 660 South Euclid Avenue, Box 8231, St. Louis, MO 63110, USA

Received 17 April 2008; received in revised form 2 July 2008; accepted 3 July 2008
Available online 16 July 2008

Edited by D. E. Draper

Escherichia coli RecBCD is a bipolar DNA helicase possessing two motor subunits (RecB, a 3′-to-5′ translocase, and RecD, a 5′-to-3′ translocase) that is involved in the major pathway of recombinational repair. Previous studies indicated that the minimal kinetic mechanism needed to describe the ATP-dependent unwinding of blunt-ended DNA by RecBCD *in vitro* is a sequential *n*-step mechanism with two to three additional kinetic steps prior to initiating DNA unwinding. Since RecBCD can "melt out" ~6 bp upon binding to the end of a blunt-ended DNA duplex in a Mg^{2+}-dependent but ATP-independent reaction, we investigated the effects of noncomplementary single-stranded (ss) DNA tails [3′-$(dT)_6$ and 5′-$(dT)_6$ or 5′-$(dT)_{10}$] on the mechanism of RecBCD and RecBC unwinding of duplex DNA using rapid kinetic methods. As with blunt-ended DNA, RecBCD unwinding of DNA possessing 3′-$(dT)_6$ and 5′-$(dT)_6$ noncomplementary ssDNA tails is well described by a sequential *n*-step mechanism with the same unwinding rate ($mk_U = 774 \pm 16$ bp s^{-1}) and kinetic step size ($m = 3.3 \pm 1.3$ bp), yet two to three additional kinetic steps are still required prior to initiation of DNA unwinding ($k_C = 45 \pm 2$ s^{-1}). However, when the noncomplementary 5′ ssDNA tail is extended to 10 nt [5′-$(dT)_{10}$ and 3′-$(dT)_6$], the DNA end structure for which RecBCD displays optimal binding affinity, the additional kinetic steps are no longer needed, although a slightly slower unwinding rate ($mk_U = 538 \pm 24$ bp s^{-1}) is observed with a similar kinetic step size ($m = 3.9 \pm 0.5$ bp). The RecBC DNA helicase (without the RecD subunit) does not initiate unwinding efficiently from a blunt DNA end. However, RecBC does initiate well from a DNA end possessing noncomplementary twin 5′-$(dT)_6$ and 3′-$(dT)_6$ tails, and unwinding can be described by a simple uniform *n*-step sequential scheme, without the need for the additional k_C initiation steps, with a similar kinetic step size ($m = 4.4 \pm 1.7$ bp) and unwinding rate ($mk_{obs} = 396 \pm 15$ bp s^{-1}). These results suggest that the additional kinetic steps with rate constant k_C required for RecBCD to initiate unwinding of blunt-ended and twin $(dT)_6$-tailed DNA reflect processes needed to engage the RecD motor with the 5′ ssDNA.

Keywords: helicase; recombination; motor protein; fluorescence; kinetics

Introduction

DNA helicases are a diverse class of nucleic acid motor proteins that function by coupling the binding and hydrolysis of 5′-NTP to translocation along the DNA filament and unwinding of duplex DNA in order to form the single-stranded (ss) intermediates required for DNA replication, recombination, and repair.[1–7] Some helicases can also displace other proteins from the nucleic acid.[8–12] Because helicase function is involved in all aspects of DNA metabolism, defects in human helicases can give rise to genetic disorders, such as Bloom syndrome, Werner syndrome, Rothmund–Thomson syndrome, and xeroderma pigmentosum, among others.[13–16]

*Corresponding author. E-mail address: lohman@biochem.wustl.edu.

Abbreviations used: ss, single stranded; ds, double stranded; FRET, fluorescence resonance energy transfer; NLLS, nonlinear least squares; BSA, bovine serum albumin.

In *Escherichia coli*, the RecBCD pathway is the major pathway for homologous recombination and repair of double-stranded (ds) DNA breaks. RecBCD is an essential DNA helicase for this pathway and is composed of the RecB (134 kDa), RecC (129 kDa), and RecD (67 kDa) polypeptides.[17–19] This heterotrimeric enzyme processes dsDNA breaks with its dsDNA and ssDNA exonuclease, ssDNA endonuclease, DNA-dependent ATPase, and helicase activities, which are regulated by the crossover hotspot instigator (chi) regulatory sequence (5′-GCTGGTGG-3′).[20–23] RecBCD first binds to the damaged induced dsDNA break at a blunt or nearly blunt end and then unwinds the duplex in an ATP-dependent reaction. During DNA unwinding, its nuclease activity preferentially degrades the 3′ terminating DNA strand while cleaving the 5′ terminating strand infrequently.[24,25] These activities are modified when RecBCD recognizes a chi sequence, whereupon RecBCD first pauses and then continues to unwind DNA with a reduced rate.[26–28] Furthermore, the nuclease activity is altered such that it acts instead on the 5′ terminating strand preferentially. This generates a 3′ ssDNA overhang onto which RecBCD loads the RecA protein,[29] and the resulting RecA-coated DNA filament forms a joint molecule with a homologous piece of DNA and initiates recombinational repair of the nucleic acid.

RecB and RecD are both superfamily-1 helicases/translocases,[30] with opposite ssDNA translocation directionalities. Although the two motor subunits have opposite ssDNA translocation polarities (RecB is a 3′-to-5′ translocase, while RecD is a 5′-to-3′ translocase), they function in unison to unwind dsDNA in the same net direction within the RecBCD heterotrimer by interacting with opposite strands of the DNA end.[31,32] Interestingly, the RecBC enzyme, lacking the RecD subunit, is still a functional helicase. Both RecBCD and RecBC are processive helicases[26,33,34] that form stable heterotrimers and heterodimers, respectively, in solution.[35–37]

Equilibrium binding studies have indicated that RecBCD binds optimally to DNA ends possessing noncomplementary 5′-$(dT)_{10}$ and 3′-$(dT)_6$ ssDNA tails, while the RecBC binds optimally to DNA ends with 5′-$(dT)_6$ and 3′-$(dT)_6$ tails.[37] These results indicate that both the RecBCD and RecBC helicases are able to "melt out" 6 bp simply upon binding to a blunt-ended duplex in a Mg^{2+}-dependent but ATP-independent reaction.[38] In a crystal structure of a RecBCD–DNA complex, the last 4 bp are observed to be melted even though the complex was crystallized in the presence of Ca^{2+}.[39] Furthermore, the equilibrium binding studies suggest that additional 4 nt in the noncomplementary 5′ ssDNA tail are needed to facilitate interactions with the RecD subunit.[37]

Lucius *et al*.[40–42] previously determined a minimal kinetic mechanism by which RecBCD unwinds blunt-ended DNA duplexes *in vitro* using rapid kinetic methods under single-turnover conditions. A simple uniform *n*-step sequential scheme was not able to describe the time courses for RecBCD unwinding of blunt-ended DNA. In fact, the minimal kinetic mechanism required two to three additional kinetic steps, which made determination of the average DNA unwinding kinetic step size more difficult, although a well-constrained kinetic step size of 3.9 ± 0.5 bp that was independent of ATP concentration and temperature was determined.[40] The number (two to three) of these additional steps was found to be independent of DNA duplex length, suggesting that these steps are not associated with the repeated cycles of DNA unwinding and likely precede or occur at the early stages of DNA unwinding.[42] Here, we examine the effects of noncomplementary 3′ and 5′ ssDNA tails on the mechanism by which RecBCD and RecBC initiate and processively unwind DNA in order to probe the role of RecD in the initiation of DNA unwinding.

Results

The DNA substrates used in this study are shown schematically in Fig. 1, and the sequences of the individual DNA strands are given in Table 1. They consist of a DNA duplex containing two nicks with a hairpin structure on one end and noncomplementary ssDNA tails [$(dT)_n$] on the other that forms the site at which RecBCD or RecBC will initiate unwinding. With the exception of the DNA substrate used in the experiments shown in Fig. 3, which possesses a blunt end, the 3′ ssDNA tail length is 6 nt [$(dT)_6$], while the 5′ ssDNA length is either 6 nt [$(dT)_6$] or 10 nt [$(dT)_{10}$]. For the chemical quenched-flow unwinding experiments (see Fig. 2a), strand "A" is radiolabeled with ^{32}P on its 5′ end (denoted as an asterisk in Fig. 1a). Displacement of the radioactively labeled DNA is used to monitor DNA unwinding in a discontinuous assay (see Materials and Methods). For the stopped-flow fluorescence experiments (see Fig. 2b), Cy3 and Cy5 fluorophores are positioned on either side of a nick (see Fig. 1b) and changes in Cy3 and Cy5 fluorescence resulting from changes in fluorescence resonance energy transfer (FRET) are used to monitor DNA unwinding. Both assays are "all-or-none" assays since DNA unwinding is not detected until duplex "A" (see Figs. 1 and 2) is fully unwound; however, information on intermediate species present during unwinding can be obtained by analyzing a series of unwinding experiments performed as a function of DNA duplex length.[43,44]

RecBC initiates DNA unwinding poorly from a blunt DNA end

Single-turnover chemical quenched-flow kinetic studies were performed as described in Materials and Methods.[41] The kinetics of RecBC- and RecBCD-catalyzed unwinding of a 24-bp blunt-ended DNA [substrate I without the noncomplementary $(dT)_n$ tails] used in our previous studies[42] are shown in Fig. 3. Whereas RecBCD is able to initiate unwinding rapidly from a blunt DNA end, much less unwinding is catalyzed by RecBC. These single-turnover kinetic experiments were performed using

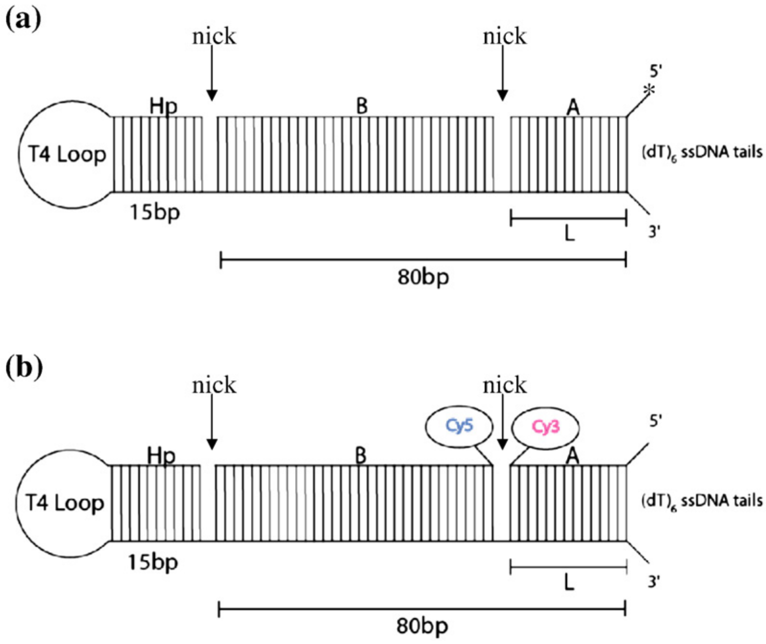

Fig. 1. Schematic representation of DNA substrates used in unwinding studies. Each DNA substrate is composed of three oligodeoxynucleotide strands, a constant bottom strand containing a hairpin (Hp) and two top strands—"A" and "B." These three DNA strands anneal to form a hairpin duplex containing two nicks. DNA substrates of different duplex lengths, *L*, are formed by varying the lengths of strands "A" and "B" while keeping their combined length constant. Because most substrates used in our unwinding studies possess noncomplementary ssDNA tails, *L* refers to the length of strand "A" that is base paired with the bottom strand and therefore must be unwound before DNA unwinding can be detected. (a) DNA substrates used in chemical quenched-flow unwinding experiments. Strand "A" is radiolabeled with ^{32}P at its 5′ end (denoted by an asterisk), and the release of this strand is used to monitor DNA unwinding. (b) DNA substrates used in stopped-flow fluorescence measurements. A Cy3 and Cy5 FRET pair is positioned across a nick as depicted, and changes in FRET signal are used to monitor DNA unwinding.

the same preincubation concentration for RecBCD and RecBC (40 nM). We note that in a multiple-turnover experiment, our preparation of RecBC enzyme shows DNA unwinding behavior similar to that of a blunt-ended DNA substrate as reported previously[45] (see Materials and Methods). One possibility is that the much lower amplitude of DNA unwinding by RecBC may result from a weaker affinity of RecBC for DNA blunt ends compared with RecBCD.[37] However, based on our

Table 1. Sequences of DNA unwinding substrates

DNA	Length (nt)[a]	DNA sequence
Strand "A"		
Ia	24	5′-(dT)$_n$ CCA TGG CTC CTG AGC TAG CTG CA(Cy3) G-3′
IIa	29	5′-(dT)$_n$ CCA TGG CTC CTG AGC TAG CTG CAG TAG C(Cy3)C-3′
IIIa	30	5′-(dT)$_n$ CCA TGG CTC CTG AGC TAG CTG CAG TAG CC(Cy3)T-3′
IVa	37	5′-(dT)$_n$ CCA TGG CTC CTGAGC TAG CTG CAG TAG CCT AAA GGA (Cy3)T-3′
Va	40	5′-(dT)$_n$ CCA TGG CTC CTG AGC TAG CTG CAG TAG CCT AAA GGA TGA C(Cy3)A-3′
VIa	43	5′-(dT)$_n$ CCA TGG CTC CTG AGC TAG CTG CAG TAG CCT AAA GGA TGA AAC (Cy3)T-3′
VIIa	48	5′-(dT)$_n$ CCA TGG CTC CTG AGC TAG CTG CAG TAG CCT AAA GGA TGA AAC TAG GA (Cy3)T-3′
VIIIa	53	5′-(dT)$_n$ CCA TGG CTC CTG AGC TAG CTG CAG TAG CCT AAA GGA TGA AAC TAG GAT CTT A(Cy3)T-3′
IXa	60	5′-(dT)$_n$ CCA TGG CTC CTG AGC TAG CTG CAG TAG CCT AAA GGA TGA AAC TAG GAT CTT ATG CTC CA(Cy3)T-3′
Strand "B"		
Ib	56	5′-(Cy5) TAG CCT AAA GGA TGA AAC TAG GAT CTT ATG CTC CAT GGA TAC GTC GAG TCG CAT CC-3′
IIb	51	5′-(Cy5) TAA AGG ATG AAA CTA GGA TCT TAT GCT CCA TGG ATA CGT CGA GTC GCA TCC-3′
IIIb	50	5′-(Cy5) AAA GGA TGA AAC TAG GAT CTT ATG CTC CAT GGA TAC GTC GAG TCG CAT CC-3′
IVb	43	5′-(Cy5) GAA ACT AGG ATC TTA TGC TCC ATG GAT ACG TCG AGT CGC ATC C-3′
Vb	40	5′-(Cy5) ACT AGG ATC TTA TGC TCC ATG GAT ACG TCG AGT CGC ATC C-3′
VIb	37	5′-(Cy5) AGG ATC TTA TGC TCC ATG GAT ACG TCG AGT CGC ATC C-3′
VIIb	32	5′-(Cy5) CTT ATG CTC CAT GCA TAC GTC GAG TCG CAT CC-3′
VIIIb	27	5′-(Cy5) GCT CCA TGG ATA CGT CGA GTC GCA TCC-3′
IXb	20	5′-(Cy5) GGA TAC GTC GAG TCG CAT CC-3′
Strand Hp		
Hp	120	5′-AGA TCC TAG TGC AGG TTT TCC TGC ACT AGG ATC TGG ATG CGA CTC GAC GTA TCC ATG GAG CAT AAG ATC CTA GTT TCA TCC TTT AGG CTA CTG CAG CTA GCT CAG GAG CCA TGG TTT TTT-3′

Substrate I is formed by annealing strand Ia, strand Ib, and the bottom strand Hp. Substrates II–IX are formed similarly. DNA strands "A" and "B" are fluorescently labeled with Cy3 and Cy5, respectively, for use in stopped-flow experiments.

[a] The length of DNA strand "A" refers to the number of base pairs that will form when annealed with the bottom strand (Hp) and therefore the DNA duplex length that is unwound in the kinetic experiment.

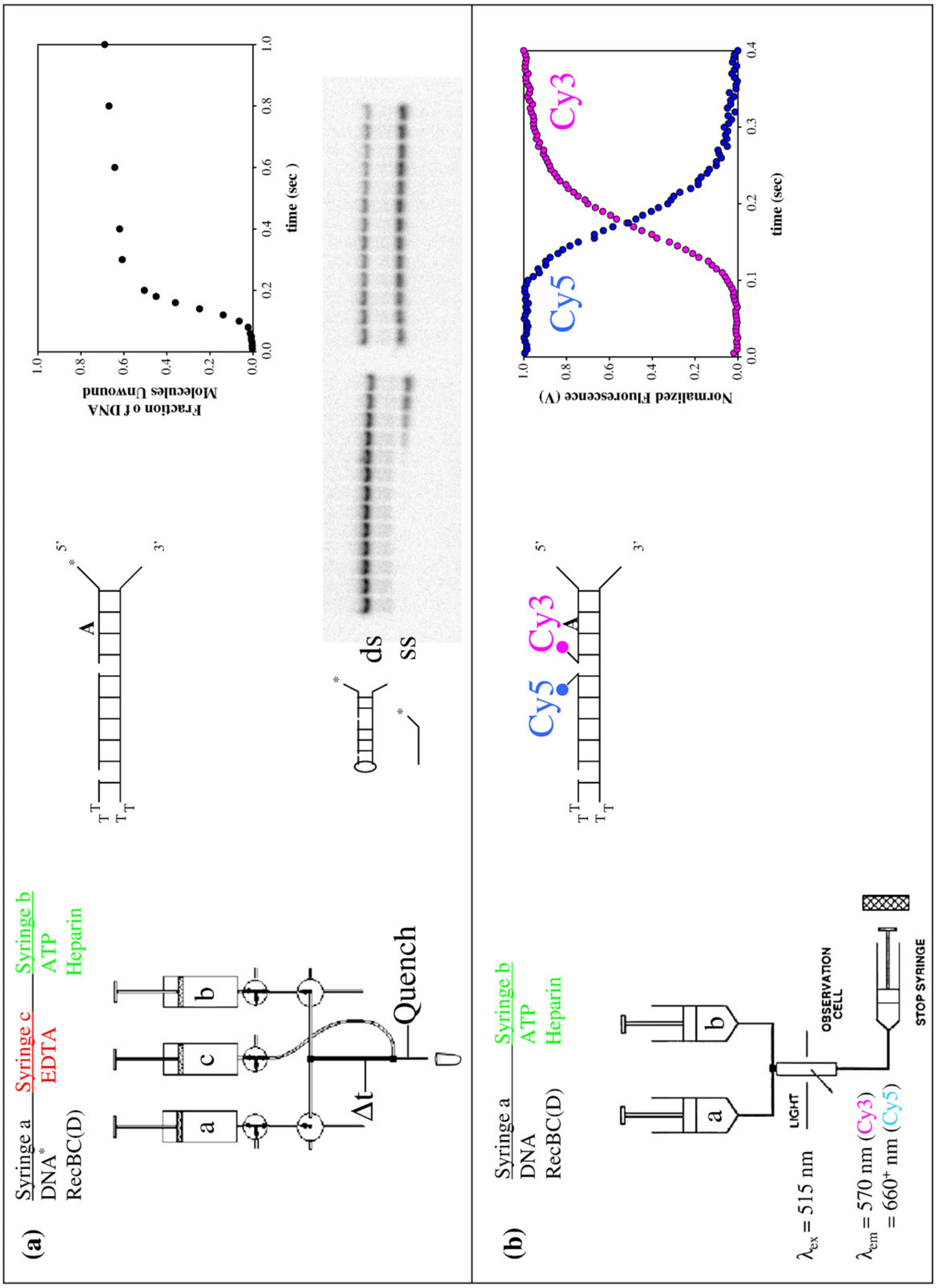

Fig. 2 *(legend on next page)*

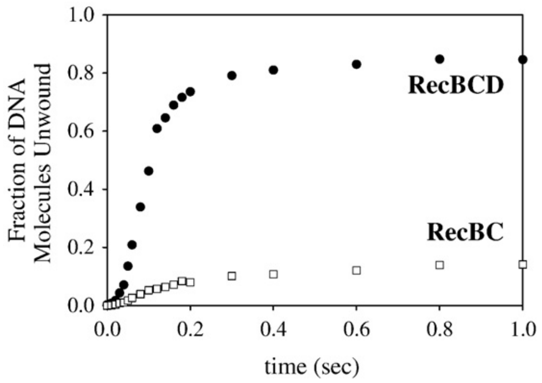

Fig. 3. Comparison of the kinetics of DNA unwinding of a 24-bp blunt-ended DNA substrate (substrate I without noncomplementary dT tails) by RecBCD and RecBC. Single-turnover time courses, obtained using the quenched-flow assay, show that RecBCD (filled circles) initiates unwinding from a blunt DNA end with much higher efficiency than does RecBC (open squares).

estimate of 2×10^7 M^{-1} for the equilibrium constant for RecBC binding to a blunt end under these conditions,[37] ~95% of the DNA ends should be bound with RecBC. Consistent with this conclusion, we observe no difference in the amplitude of unwinding when these experiments are performed using a 10-fold higher preincubation concentration (400 nM) of RecBC. This suggests that the majority of the RecBC enzyme must be bound in a nonproductive mode to a blunt duplex end. Previous studies have shown that RecBC binds with highest affinity to DNA ends possessing noncomplementary 5′-$(dT)_6$ and 3′-$(dT)_6$ ssDNA tails, while RecBCD binds optimally to DNA ends with noncomplementary 5′-$(dT)_{10}$ and 3′-$(dT)_6$ ssDNA tails.[37] Based on these, we examined the effect of such noncomplementary ssDNA tails on the kinetics and mechanism of DNA unwinding by both RecBC and RecBCD enzymes.

Minimal kinetic mechanism of RecBC-catalyzed DNA unwinding

We examined RecBC-catalyzed unwinding of a series of DNA duplexes possessing noncomplementary 5′-$(dT)_6$ and 3′-$(dT)_6$ ssDNA tails using rapid chemical quenched-flow and stopped-flow fluorescence techniques (see Materials and Methods). Quenched-flow experiments were performed with DNA substrates of the type shown in Fig. 1a, with duplex region "A" varying in length [24, 30, 40, 48, and 60 bp (substrates I, III, V, VII, and XI, respectively)]. Three independent sets of measurements were performed with each duplex length. The average time courses are plotted in Fig. 4a and were analyzed by global nonlinear least-squares (NLLS) analysis using Scheme 1 (Eq. (2)). The continuous curves in Fig. 4a are simulated time courses using Eq. (2) and the best-fit parameters (m=4.4±1.7 bp, k_{obs}=90±25 s^{-1}; mk_{obs}=396±15 bp/s, k_{NP}=1.7±0.5 s^{-1}). It is clear from the data in Fig. 4a that RecBC is able to initiate DNA unwinding from a DNA end possessing the noncomplementary 5′-$(dT)_6$ and 3′-$(dT)_6$ ssDNA tails with much higher efficiency than from a blunt DNA end (see Fig. 3).

As observed previously for RecBCD-catalyzed unwinding of blunt-ended DNA duplexes, the time courses all display a lag phase. This lag phase results from the fact that the assays used are of the all-or-none type and RecBC must proceed through a series of sequential kinetic steps (with similar rate constants, k_U) in order to fully unwind each duplex. The number of these unwinding steps, and thus the duration of the lag phase, increases with duplex length. In addition to this lag phase, we also observe a slower unwinding phase that is much smaller in amplitude. As discussed previously,[41] we attribute these two phases to DNA unwinding from two populations of initially bound RecBC–DNA complexes. One population of RecBC is bound in a productive mode that can initiate DNA unwinding rapidly upon the addition of ATP, while the other population of RecBC is bound in a nonproductive manner that must first undergo a slow isomerization, with rate constant k_{NP}, to form productive complexes before DNA unwinding can initiate.

Since RecBC-catalyzed unwinding of duplex DNA occurs via multiple (n) repeated steps, with the rate-limiting rate constant, k_U, the number of DNA unwinding steps, n, is expected to increase in direct proportion to the DNA duplex length, L. In fact, Fig. 4b shows that the values of n determined from NLLS fitting of the data to the simple Scheme 1 are directly proportional to L. A summary of the kinetic parameters obtained from the NLLS fitting is given in Table 2. In Scheme 1, productively bound RecBC can unwind the DNA in uniform steps with rate cons-

Fig. 2. Design of all-or-none chemical quenched-flow and stopped-flow fluorescence experiments to study single-turnover kinetics of DNA unwinding. (a) Quenched-flow assay. DNA substrates (radiolabeled with ^{32}P on the 5′ end of strand "A") are incubated with excess RecBCD or RecBC helicase in one syringe. DNA unwinding is initiated by rapid mixing with ATP and heparin. The unwinding reaction is quenched after a time interval (Δt) by rapid mixing with EDTA, and the ssDNA product produced after each time interval is separated from the native duplex DNA using nondenaturing PAGE and analyzed quantitatively after exposure to a phosphorimager (see Materials and Methods for details). (b) Stopped-flow assay. A DNA substrate labeled with donor (Cy3) and acceptor (Cy5) fluorophores as indicated is incubated with excess RecBCD or RecBC in one syringe, and DNA unwinding is initiated by rapid mixing with ATP and heparin. When Cy3 and Cy5 fluorophores are in close proximity, Cy3 fluorescence is decreased and Cy5 fluorescence is increased due to FRET. DNA unwinding is monitored in real time by the concomitant increase in Cy3 fluorescence and decrease in Cy5 fluorescence accompanying DNA unwinding and release of strand "A". Cy3 fluorescence is excited at 515 nm, and Cy3 fluorescence emission is monitored at 570 nm using an interference filter, while Cy5 fluorescence emission is monitored simultaneously at wavelengths above 665 nm using a long-pass filter.

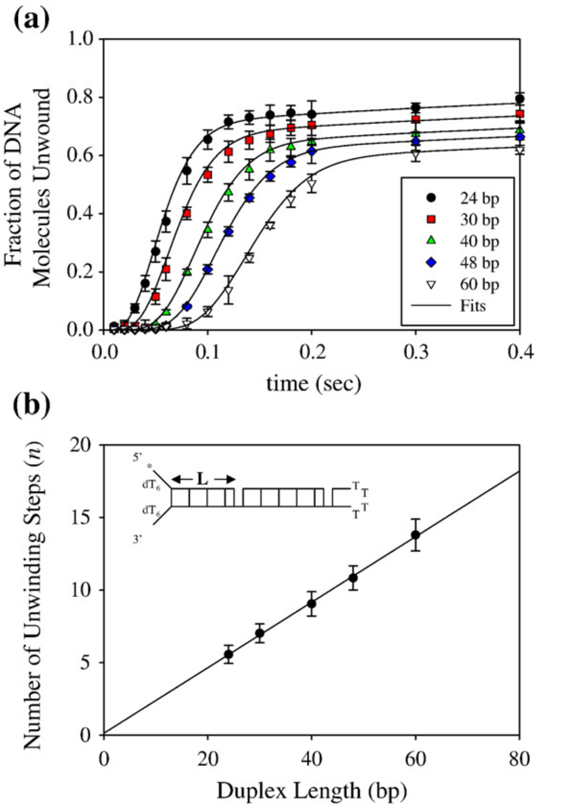

Fig. 4. Single-turnover kinetics of RecBC-catalyzed unwinding of DNA duplexes possessing noncomplementary 5′-$(dT)_6$ and 3′-$(dT)_6$ ssDNA tails. (a) Time courses as a function of duplex length [L=24 bp (black circles); L=30 bp (red squares); L=40 bp (green triangles); L=48 bp (blue diamonds); L=60 bp (open inverted triangles)] obtained using the quenched-flow assay. Data points correspond to the average of three independent measurements, and the error bars indicate the standard deviation of the data. Smooth curves are simulated time courses based on the global NLLS best fits to Scheme 1, with mk_{obs}=396±15 bp/s, m=4.4±1.7 bp, k_{obs}=90±25 s^{-1}, and k_{NP}=1.7±0.5 s^{-1}. (b) The number of steps n determined from global NLLS analysis using Scheme 1 plotted *versus* DNA duplex length L. The continuous line shows the linear least-squares fit through the data (n=0.23L+0.03).

tant k_U. The average kinetic step size, m, is defined as the average number of base pairs that are unwound between such two successive rate-limiting steps. Based on the NLLS fitting of the data in Fig. 4a, RecBC has an average kinetic step size of 4.4±1.7 bp for DNA unwinding, with a stepping rate of 90± 25 s^{-1}, resulting in a macroscopic unwinding rate mk_{obs} of 396±15 bp/s.

We also examined the kinetics of RecBC-catalyzed unwinding of DNA duplexes possessing noncomplementary twin 3′-$(dT)_6$ and 5′-$(dT)_6$ ssDNA tails using a stopped-flow fluorescence technique described previously.[42] These experiments were performed using a series of DNA substrates of the type shown in Fig. 1b, with duplex region "A" varying in length [24, 29, 37, 40, 43, 48, 53, and 60 bp (substrates I, II, IV, V, VI, VII, VIII, and IX, respectively)]. DNA unwinding was monitored by the loss of FRET between a Cy3 donor fluorophore and a Cy5 acceptor fluorophore. As indicated in Fig. 2b, the stopped-flow assay is also of the all-or-none type. When the DNA duplex is fully unwound and the labeled DNA strands are displaced, the two dyes become separated and thus Cy3 fluorescence increases, while there is a concomitant loss in Cy5 fluorescence due to the loss of energy transfer from Cy3 to Cy5.

The time courses monitoring the increase in Cy3 fluorescence (averages of three independent measurements) are plotted in Fig. 5a, and the continuous curves are global NLLS fits to the simple Scheme 1 (Eq. (2)) (m=4.4±0.1 bp, k_{obs}=79±11 s^{-1}; mk_{obs}= 348±5 bp/s, k_{NP}=1.1±0.1 s^{-1}). These time courses are also well described by Scheme 1, and the number of unwinding steps, n, determined from the data fitting is directly proportional to duplex length, L (Fig. 5b). The Cy5 fluorescence time courses (see Supplementary Fig. 1), which are exactly anticorrelated with the Cy3 fluorescence time courses, can be analyzed as well using Scheme 1 (Eq. (2)), yielding identical kinetic parameters. It is interesting to note that in previous RecBCD stopped-flow unwinding studies,[42] the resulting Cy5 fluorescence time courses showed a more complex time course that was not fully anticorrelated with the Cy3 fluorescence time course. This deviation[42] was attributed to the RecD subunit, which translocates along the 5′ ending DNA strand in the 5′-to-3′ direction, ultimately contacting the Cy3 fluorophore at the nick, resulting in an enhancement of the Cy3 fluorescence. This increase in Cy3 fluorescence was then transferred via FRET to the Cy5 fluorophore before the strands are separated, resulting in an additional increase in Cy5 fluorescence. This effect is not observed with the RecBC enzyme because of the absence of the RecD translocating motor and since RecB translocates along the 3′-ended strand in the 3′-to-5′ direction.

The advantage of the stopped-flow unwinding assay is that it is a continuous assay and thus many more time points can be obtained from a single experiment. As such, significantly more data

$$
\begin{array}{l}
(R \bullet D)_{NP} \\
\uparrow\downarrow k_{NP} \\
(R \bullet D)_{L} \xrightarrow{k_u} I_{(L-m)} \xrightarrow{k_u} \ldots I_{(L-im)} \cdots \xrightarrow{k_u} ssDNA
\end{array}
$$

Scheme 1.

Table 2. Summary of chemical quenched-flow and stopped-flow fluorescence unwinding kinetic results

	Quenched-flow results						
RecBCD	mk_U (bp/s)	k_U (s^{-1})	m (bp)	k_C (s^{-1})	h (steps)	k_{NP} (s^{-1})	x
Blunt ends[41]	790±23	196±77	3.9±1.3	29±3	2.0±0.2	1.1±0.2	0.84±0.02
5′/3′ T6	774±16	240±56	3.3±1.3	45±2	3.2±0.2	1.1±0.3	0.89±0.04
5′ T10, 3′ T6	538±24	138±37	3.9±0.5	–	0	6.7±1.8	0.81±0.03
	Quenched-flow results						
RecBC	mk_{obs} (bp/s)	k_{obs} (s^{-1})	m (bp)	k_C (s^{-1})	h (steps)	k_{NP} (s^{-1})	x
5′/3′ T6	396±15	90±25	4.4±1.7	–	0	1.7±0.5	0.81±0.02
5′ T10, 3′ T6	372±21	103±33	3.6±0.9		0	2.5±1.2	0.80±0.02
	Stopped-flow results						
RecBCD	mk_U (bp/s)	k_U (s^{-1})	m (bp)	k_C (s^{-1})	h (steps)	k_{NP} (s^{-1})	x
Blunt ends[46]	680±12	200±40	3.4±0.6	51±5	3.2±0.3	6.0±0.3	0.87±0.01
5′/3′ T6	745±18	220±28	3.4±0.5	58±2	3.2±0.1	6.7±0.3	0.83±0.01
5′ T10, 3′ T6	588±11	163±24	3.6±0.2	–	0	5.4±1.0	0.80±0.01
	Stopped-flow results						
RecBC	mk_{obs} (bp/s)	k_{obs} (s^{-1})	m (bp)	k_C (s^{-1})	h (steps)	k_{NP} (s^{-1})	x
5′/3′ T6	348±5	79±11	4.4±0.1	–	0	1.1±0.1	0.79±0.03
5′ T10, 3′ T6	320±7	92±12	3.5±0.1	–	–	1.9±0.6	0.81±0.02

from many more duplex lengths can be analyzed, yielding better estimates of the kinetic parameters. However, since the quenched-flow experiment yields a direct measure of the extent of DNA unwinding, we routinely perform and compare the results from both chemical quenched-flow and stopped-flow fluorescence studies. In this case, the kinetic parameters determined using both methods

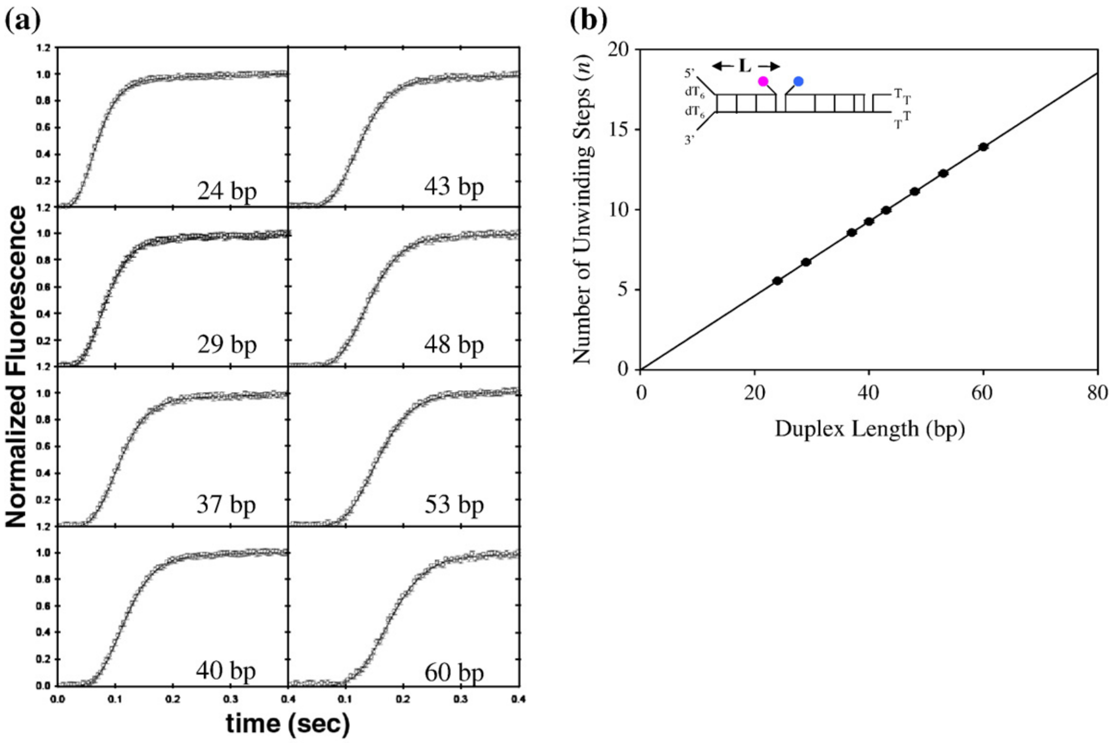

Fig. 5. Single-turnover kinetics of RecBC-catalyzed unwinding of DNA duplexes possessing noncomplementary 5′-$(dT)_6$ and 3′-$(dT)_6$ ssDNA tails using the stopped-flow fluorescence assay. (a) Cy3 fluorescence time courses as a function of duplex length (L=24, 29, 37, 40, 43, 48, 53, and 60 bp). Data points represent the average of three independent measurements, and the error bars indicate the standard deviation of the data. Smooth curves are simulated time courses based on the global NLLS best fits to Scheme 1, with mk_{obs}=348±5 bp/s, m=4.4±0.1 bp, k_{obs}=79±11 s^{-1}, and k_{NP}=1.1±0.1 s^{-1}. (b) The number of unwinding steps n determined from the global NLLS analysis using Scheme 1 plotted *versus* DNA duplex length L. The continuous line shows the linear least-squares fit through the data (n=0.23L−0.02).

are in good agreement, although some slight differences in the parameters are observed (see Table 2).

RecBCD-catalyzed unwinding of DNA duplexes with twin $(dT)_6$ ssDNA tails

We next compared RecBC and RecBCD unwinding directly. However, since the previous RecBCD experiments examined DNA unwinding from blunt DNA ends,[41,42] we needed to examine RecBCD unwinding of duplexes possessing the noncomplementary twin $(dT)_6$ tails used in the RecBC studies. Figure 6a shows the time courses determined using the chemical quenched-flow assay (the time courses determined using the stopped-flow assay are shown in Supplementary Fig. 2a). The data in Fig. 6a were analyzed by global NLLS analysis using the simple Scheme 1 (Eq. (2)), and the continuous curves are time courses simulated using Eq. (2) and the best-fit parameters. Based on the poor quality of these fits, Scheme 1 is not sufficient to describe these time courses. Consistent with this conclusion, Fig. 6b shows that a plot of the number of repeated rate-limiting kinetic steps, n, *versus* duplex length, L, exhibits a positive y-intercept. The fact that the fitted value of n is not directly proportional to L and that a positive y-intercept is observed suggest the presence of additional kinetic steps in the mechanism that are not directly associated with DNA unwinding.[41,44] As a result, we reanalyzed these time courses using the more complicated Scheme 2 (Eq. (4)), in which h additional kinetic steps with rate constant k_C are included in the mechanism, although these steps are not repeated within the series of DNA unwinding cycles. Scheme 2 is the same kinetic scheme that was used previously to analyze RecBCD-catalyzed unwinding of a series of blunt-ended DNA duplexes.[41,42] The time courses are well described by Scheme 2, as shown in Fig. 6c (m=3.3±1.3 bp, k_U=240±56 s^{-1}; mk_U=774±16 bp/s, h=3.2±0.2, k_C=45±2, k_{NP}=1.1±0.3 s^{-1}). Furthermore, after

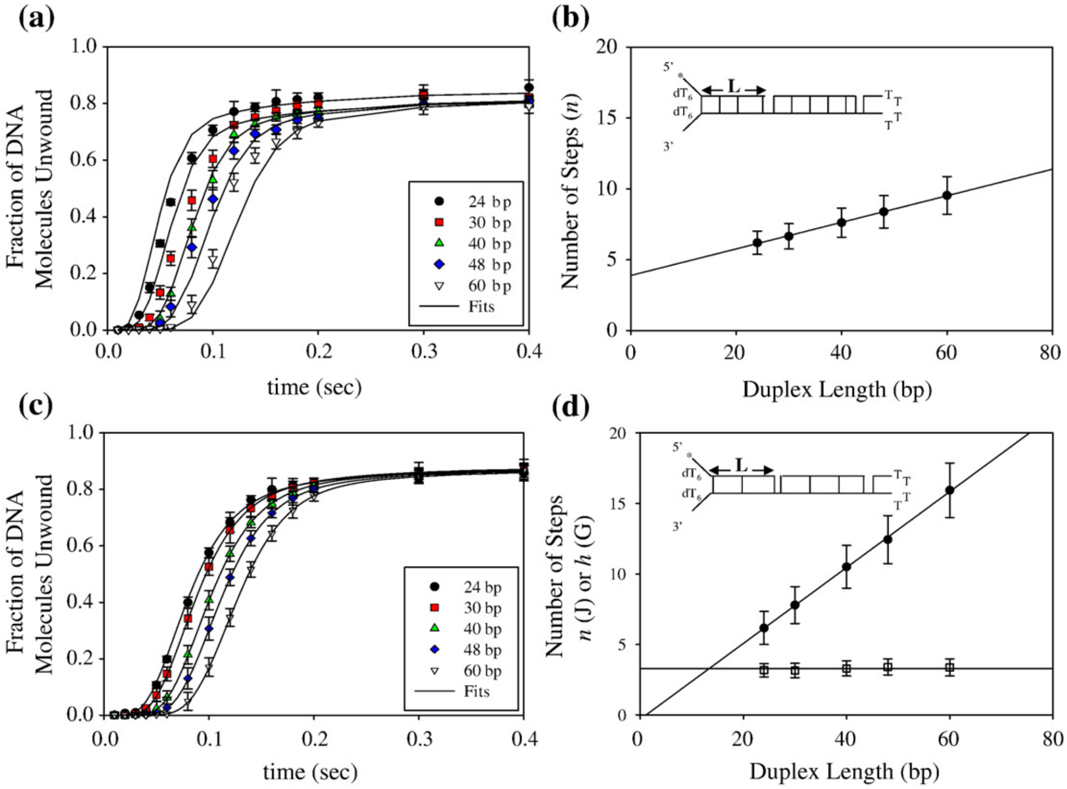

Fig. 6. Single-turnover kinetics of RecBCD-catalyzed unwinding of DNA duplexes possessing noncomplementary 5′-$(dT)_6$ and 3′-$(dT)_6$ ssDNA tails. (a) Time courses as a function of duplex length [L=24 bp (black circles); L=30 bp (red squares); L=40 bp (green triangles); L=48 bp (blue diamonds); L=60 bp (open inverted triangles)] obtained using the quenched-flow assay. Data points correspond to the average of three independent measurements, and the error bars indicate the standard deviation of the data. Smooth curves are simulated time courses based on the global NLLS best fits to Scheme 1, with mk_U=410±12 bp/s, m=10.1±0.9 bp, k_U=39±23 s^{-1}, and k_{NP}=5.9±1.8 s^{-1}. (b) The number of steps n determined from global NLLS analysis using Scheme 1 plotted *versus* DNA duplex length L. The continuous line shows the linear least-squares fit through the data (n=0.09L+3.88). (c) The same data from (a) were analyzed using Scheme 2, which includes the additional kinetic steps with rate constant k_C, which are not involved in DNA unwinding. Smooth curves are simulated time courses based on the global NLLS best fits to Scheme 2, with mk_U=774±16 bp/s, m=3.3±1.3 bp, k_U=240±56 s^{-1}, k_{NP}=1.1±0.3 s^{-1}, h=3.2±0.2 steps, and k_C=45±2 s^{-1}. (d) The number of unwinding steps n and additional kinetic steps h determined from global NLLS analysis using Scheme 2 plotted *versus* DNA duplex length L. The continuous line shows the linear least-squares fit through the data (n=0.27L−0.21; h=3.3).

$$\begin{array}{l}(R\bullet D)_{NP}\\ \downarrow k_{NP}\\ (R\bullet D)_L \xrightarrow{k_c} (R\bullet D)_L^1 \xrightarrow{k_c} \ldots(R\bullet D)_L^h \xrightarrow{k_u} I_{(L-m)} \xrightarrow{k_u} \ldots.I_{(L-im)}\ldots \xrightarrow{k_u} ssDNA\end{array}$$

Scheme 2.

incorporating the additional k_C steps into the mechanism, the number of steps involved in unwinding, n, is found to be directly proportional to duplex length, L, while the number of additional steps, h, is independent of L, as shown in Fig. 6d. A summary of the kinetic parameters obtained from the fits of the quenched-flow and fluorescence time courses to Scheme 2 is given in Table 2.

RecBCD-catalyzed unwinding of DNA possessing noncomplementary 5′-(dT)$_{10}$ and 3′-(dT)$_6$ ssDNA tails

Previous equilibrium binding experiments have shown that RecBCD binds optimally to DNA duplex ends possessing noncomplementary 5′-(dT)$_{10}$ and 3′-(dT)$_6$ ssDNA tails;[37] hence, we next examined RecBCD unwinding of DNA substrates possessing this DNA end structure under the same solution conditions used above. We first obtained time courses for five duplex lengths using the chemical quenched-flow unwinding assay. These time courses, shown in Fig. 7a, also display lag kinetics and are biphasic. Interestingly, in contrast to the time courses obtained with the DNA substrates possessing twin (dT)$_6$ ssDNA tails, these time courses are well described by the simple n-step sequential kinetic mechanism of Scheme 1 as shown by the continuous curves in Fig. 7a (m=3.9±0.5 bp, k_U= 138±37 s^{-1}; mk_U=538±24 bp/s, k_{NP}=6.7±1.8 s^{-1}). Furthermore, Fig. 7b indicates that the number of steps involved in unwinding, n, is directly proportional to duplex length, L. The two to three additional steps, with rate constant k_C, that are part of Scheme 2 and required for RecBCD to initiate DNA unwinding from blunt ends and duplexes with twin (dT)$_6$ tails are not necessary to describe these time courses. This conclusion is also supported by time courses obtained for eight duplex lengths using the stopped-flow fluorescence assay (Supplementary Fig. 3a and b). Table 2 provides a summary of the kinetic parameters obtained from these experiments. RecBCD has the same average kinetic step size for unwinding (~4 bp) all three of the DNA molecules, independent of the end structure [blunt end, twin (dT)$_6$, and 5′-(dT)$_{10}$ as well as 3′-(dT)$_6$].

Discussion

In previous studies of the mechanism of RecBCD-catalyzed unwinding of DNA using single-turnover methods, Lucius *et al.*[40–42] found that the time course for RecBCD unwinding of blunt-ended DNA cannot be described by a simple sequential n-step kinetic model, such as that shown in Scheme 1. In fact, Scheme 2, which includes additional kinetic steps, was needed to describe the time courses for a range of duplex DNA lengths. The need to include these additional kinetic steps made it more difficult to

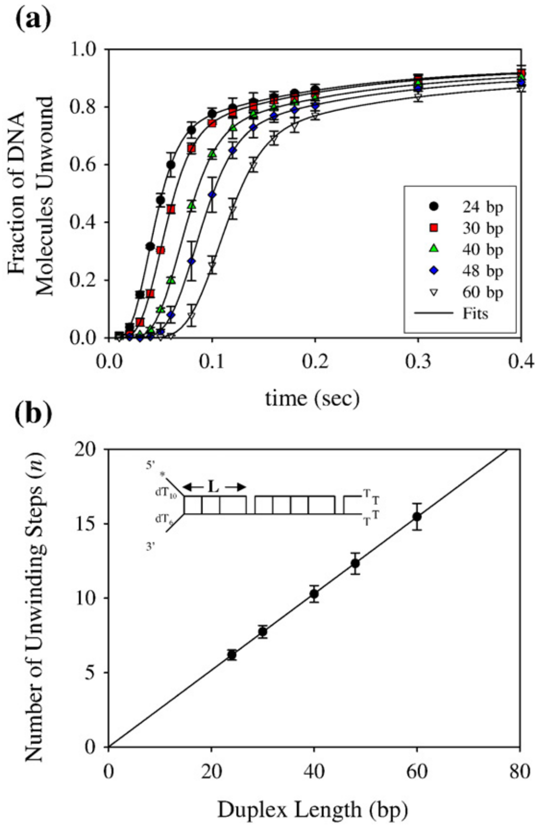

Fig. 7. Single-turnover kinetics of RecBCD-catalyzed unwinding of DNA duplexes possessing noncomplementary 5′-(dT)$_{10}$ and 3′-(dT)$_6$ ssDNA tails obtained. (a) Time courses obtained as a function of duplex length [L=24 bp (black circles); L=30 bp (red squares); L=40 bp (green triangles); L=48 bp (blue diamonds); L=60 bp (open inverted triangles)] using the chemical quenched-flow assay. Data points represent the average of three independent measurements, and the error bars indicate the standard deviation of the data. Smooth curves are simulated time courses based on the global NLLS best fits to Scheme 1, with mk_U=538±24 bp/s, m=3.9±0.5 bp, k_U=138±37 s^{-1}, and k_{NP}=6.7±1.8 s^{-1}. (b) Plot of the number of unwinding steps n *versus* duplex length L. The continuous line shows the linear least-squares fit through the data (n=0.26L).

estimate the DNA unwinding kinetic step size for RecBCD, although a well-constrained kinetic step size independent of ATP concentration and temperature of 3.9±0.5 bp was determined.[40] The number (two to three) of these additional steps with rate constant k_C was found to be independent of DNA duplex length; hence, these steps do not appear to be part of the repeated cycles of DNA unwinding and likely precede DNA unwinding.[42]

The experiments described in our current study show that these additional steps are still required for RecBCD to initiate unwinding from a duplex end possessing noncomplementary 5′-$(dT)_6$ and 3′-$(dT)_6$ ssDNA tails, yet they are not needed to describe the unwinding of DNA possessing a noncomplementary 5′-$(dT)_{10}$ tail in the presence of a 3′-$(dT)_6$ ssDNA tail. Interestingly, these additional steps are also not needed to describe the time course of RecBC-catalyzed unwinding of DNA duplexes possessing noncomplementary twin $(dT)_6$ ssDNA tails (Table 2). These results further support the conclusion that the additional k_C steps represent a real aspect of the mechanism for RecBCD initiation of DNA unwinding at a blunt-ended DNA. Furthermore, the less complex kinetic traces for RecBCD unwinding of duplex DNA possessing the noncomplementary 5′-$(dT)_{10}$ and 3′-$(dT)_6$ ssDNA tails are well described by the simple sequential n-step kinetic model (Scheme 1) and yield the same average kinetic step size (~4 bp) as previously reported for RecBCD unwinding of blunt-ended DNA, thus supporting the previous analyses.[40–42]

Functional significance of the additional k_C steps

The results from the current study, along with recent DNA binding[37] and structural[39] studies, suggest a role for these additional kinetic steps with rate constant k_C. A crystal structure of RecBCD bound to a blunt-ended duplex shows 4 bp melted from the blunt end within the complex;[39] however, the 4 nt that are not base paired on the 5′ ssDNA end do not contact any part of the RecD subunit. Equilibrium DNA binding studies[37] suggest that a 5′ ssDNA tail of at least 10 nt [$(dT)_{10}$] is needed to make full contact with the RecD subunit within the RecBCD–DNA complex. Computer modeling studies also suggest that extension of the 5′ ssDNA tail to 10 nt is needed to contact the RecD subunit.[47] These findings suggest that the additional k_C steps that are required to describe RecBCD-catalyzed unwinding from a blunt-ended DNA duplex or a DNA duplex possessing twin $(dT)_6$ ssDNA tails reflect the process of initiating binding of the RecD subunit with the 5′ ssDNA tail. This might involve pausing or molecular rearrangement steps that take place after the 5′ ssDNA end becomes sufficient in length to reach RecD, thereby enabling this subunit to initiate DNA unwinding. In this scenario, upon ATP binding and hydrolysis, the RecB motor in the RecBCD–DNA complex acting on the 3′ ssDNA strand would begin to unwind the duplex and translocate along the DNA until it creates a 5′ ssDNA tail long enough, at least 10 nt, so that RecD can interact with the 5′ ssDNA strand and initiate translocation. Studies of the $RecB^{K29Q}CD$ protein, where the RecB motor is inactivated via a mutation in the ATP binding site,[48] showed that a 4-nt 5′ ssDNA tail on the DNA end is required for DNA unwinding. This observation is consistent with our results since upon melting of the 6 bp at the duplex DNA end, this would yield a 10-nt-long 5′ ssDNA tail, which would allow interaction of RecD.

Interestingly, although the additional k_C steps are not needed to describe RecBCD unwinding of duplex DNA possessing noncomplementary 5′-$(dT)_{10}$ and 3′-$(dT)_6$ ssDNA tails, the macroscopic rate of DNA unwinding that we estimate is slightly slower (538±24 bp s^{-1}) than that for RecBCD unwinding of a blunt-ended DNA (790±23 bp s^{-1}) or a duplex DNA possessing noncomplementary twin $(dT)_6$ tails (774±16 bp s^{-1}). Currently, we cannot explain this slower observed rate of DNA unwinding. However, it has recently been shown that the rate of RecBCD unwinding becomes slower after RecBCD interacts with a "chi" sequence in the unwound ssDNA due to a switching of the lead motor from RecD to RecB.[23] In light of this, it is possible that when RecBCD initiates unwinding from a blunt-ended DNA or a duplex end possessing noncomplementary 3′-$(dT)_6$ and 5′-$(dT)_6$ tails, it starts in a "pre-chi" state with a faster rate. However, when RecBCD initiates unwinding from a duplex end possessing an extended 5′ ssDNA tail of 10 nt, it may initiate unwinding as if it were in a "post-chi" state. Further experiments will be needed to test this hypothesis.

We note that there is a potential ambiguity in the analyses of the experiments reported here, specifically with regard to the actual length of duplex DNA that should be considered unwound by RecBCD or RecBC during its ATP-dependent unwinding (helicase) reaction. We find that the kinetic parameters determined for RecBCD unwinding of a series of blunt-ended DNA duplexes varying in length, L (bp), are identical within experimental error with the kinetic parameters determined for RecBCD unwinding of a series of DNA duplexes possessing noncomplementary 5′- and 3′-$(dT)_6$ tails. However, when RecBCD forms an initiation complex with a blunt duplex DNA end, the enzyme can melt out 5–6 bp in a Mg^{2+}- or Ca^{2+}-dependent reaction;[37–39] hence, the effective duplex length with prebound RecBCD is potentially ~5–6 bp shorter than the actual length of the duplex region. Yet, when RecBCD binds to a DNA end possessing noncomplementary twin $(dT)_6$ ssDNA tails or 5′-$(dT)_{10}$ and 3′-$(dT)_6$ ssDNA tails, no additional base pair melting presumably occurs.[37] This becomes an issue when we relate the number of kinetic steps, n, determined from the NLLS analysis to the length of the duplex DNA that is unwound, which in turn would potentially affect the estimation of the kinetic step size, m. In an attempt to assess the effects of this ambiguity, we reanalyzed the time courses for RecBCD-catalyzed unwinding of blunt-ended DNA in two ways. We assumed that each DNA duplex length is actually $(L-6)$ bp rather than L bp when RecBCD is initially bound to the blunt-ended DNA but before unwinding is initiated. We then compared the plots of n *versus* $(L-6)$ and n *versus* L for the blunt-ended duplexes with the plot of n *versus* L for RecBCD unwinding of the twin $(dT)_6$-tailed DNA substrate. We find that the kinetic parameters determined from these three analyses are identical within our experimental uncertainty; hence, this potential ambiguity has no influence on the kinetic parameters that we report here. On the other hand, even though RecBCD melts out 5–6 bp upon binding to a blunt DNA end, the enzyme may still need to proceed through the same number, n, of repeated rate-limiting steps to fully unwind a blunt-ended DNA of duplex length, L, or a DNA with duplex length $(L-6)$ bp that possesses noncomplementary twin $(dT)_6$ tails. This could result if the n repeated rate-limiting kinetic steps are not associated with the actual DNA unwinding process, which may be much faster, but with a slower process (e.g., a protein conformational change) that is repeated every ~4 bp (on average) during the unwinding cycle. Hence, even if 5–6 bp of a duplex end are premelted, the "kinetic step" may not be complete until it proceeds through the rate-limiting step and thus the total number of rate-limiting steps needed to fully unwind the DNA could be unchanged.

RecBC and RecBCD display the same average kinetic step size for DNA unwinding

We have shown that RecBC initiates DNA unwinding poorly from a blunt DNA end and that its ability to initiate unwinding is greatly enhanced when RecBC is prebound to a duplex possessing noncomplementary twin $(dT)_6$ ssDNA tails. We have recently shown that RecBC appears to be able to melt out at least 4 bp upon binding to a blunt DNA duplex end in a Mg^{2+}-dependent but ATP-independent reaction,[46] similar to the reaction demonstrated for RecBCD.[38] However, the kinetic results reported here suggest that the complex formed by RecBC upon binding to a blunt DNA end must differ in some important functional manner from the RecBCD complex. Yet, once initiated, RecBC unwinds DNA with an average kinetic step size of ~4 bp, which is the same as the average kinetic step size for RecBCD unwinding. RecBC unwinding studies performed as a function ATP concentration (C. Wu and T. M. Lohman, unpublished data) indicate that this average kinetic step size is also independent of ATP concentration, as observed previously for RecBCD.[40] These data suggest that the same rate-limiting kinetic process is repeated every ~4 bp on average during DNA unwinding by both RecBCD and RecBC, although the rate of this process is slower for RecBC.

It is not clear how the kinetic step size measured in our single-turnover ensemble studies may relate to a mechanical step size, as measured in a single-molecule experiment. However, it is worth noting that these should only be the same if the process that limits the rate of DNA unwinding is the same as the process that limits the rate of the mechanical step. For example, Bianco and Kowalczykowski[45] proposed a "quantum-inch worm model" for RecBC unwinding and translocation based on the observation that RecBC is able to bypass flexible ssDNA gaps in duplex DNA as large as ~23 nt. In this model, the enzyme is viewed as having two DNA binding sites such that DNA unwinding occurs in a series of small steps of a few base pairs, whereas larger translocation steps of ~23 bp can also occur. In this model, the unwinding step size could be smaller than the translocation step size. Based on the experiments reported here, we observe a smaller (~4 bp) kinetic step size for RecBC unwinding. However, if translocation and unwinding occur with different step sizes, the relative rates of the steps limiting unwinding *versus* translocation would determine which step is observed in a measurement of a kinetic step size. Previous single-molecule studies of RecBCD unwinding[49] were unable to resolve individual steps, although those experiments placed an upper limit for the step size of a few base pairs.

Materials and Methods

Buffers and reagents

Buffers were prepared with reagent-grade chemicals and doubly distilled water that was deionized further using a Milli-Q purification system (Millipore Corp., Bedford, MA). All buffers and reagents were filtered using 0.2-μm filters after preparation. RecBCD storage buffer is buffer C: 20 mM KP_i, pH 6.8 at 25 °C, 0.1 mM 2-mercaptoethanol, 0.1 mM ethylenediaminetetraacetic acid (EDTA), and 10% (v/v) glycerol. DNA unwinding reaction buffer is buffer M: 20 mM Mops–KOH, pH 7.0 at 25 °C, 30 mM NaCl, 10 mM $MgCl_2$, 1 mM 2-mercaptoethanol, and 5% (v/v) glycerol.

Heparin stock solutions were prepared by dissolving heparin sodium salt (lot no. 114K1328; Sigma, St. Louis, MO) in buffer M and dialyzing it further against buffer M using a 3500-molecular-weight-cutoff dialysis tubing. Heparin stock concentrations were determined by titration with Azure A as described previously[50] and stored at 4 °C until use.

ATP stock solutions were prepared by dissolving adenosine 5′-triphosphate sodium salt (lot no. 016K7008; Sigma) in water and adjusting the pH to 7.0 with NaOH. Stock aliquots were stored at −20 °C until use, and stock concentrations were determined spectrophotometrcally using an extinction coefficient of $\varepsilon_{260}=1.5\times10^4$ M^{-1} cm^{-1}.[51]

Proteins

E. coli RecB and RecC were purified and stored in buffer C at −80 °C as described previously.[41,42] The RecBC enzyme was reconstituted by mixing equimolar RecB and RecC on ice. RecBC was dialyzed against buffer M at 4 °C before use, and its concentration was determined spectrophotometrically using an extinction coefficient of $\varepsilon_{280}=3.9\times10^5$ M^{-1} cm^{-1}.[37] We have examined and compared our RecBC preparation with RecBC that was purified from *E. coli* directly as the heterodimer [kindly provided by A. Taylor and G. Smith (Fred Hutchinson Cancer Center, Seattle, WA)] and observed no difference between the two preparations with respect to DNA binding[37] and single-turnover DNA unwinding. On the other hand, in multiple-turnover experiments, Bianco and Kowalczykowski[45] observed that ~65% of a blunt-ended DNA substrate is unwound after 2 min. For comparison, we also performed multiple-turnover unwinding experiments with a 24-bp blunt-ended DNA substrate [substrate I without the noncomplementary $(dT)_n$ tails] under the same solution conditions used in that study[45] and observed similar results (~56% unwinding after 2 min).

E. coli RecBCD was purified as a heterotrimer and stored in buffer C at −80 °C as described previously.[36,41,52,53] RecBCD was dialyzed against buffer M at 4 °C before use, and its concentration was determined spectrophotometrically using an extinction coefficient of $\varepsilon_{280}=4.5\times 10^5$ M^{-1} cm^{-1}.[36,41,52,53] Dialyzed RecBCD and RecBC were used immediately (within 1 day) since a loss of activity (5%–15%) occurred after 5 days at 4 °C in buffer M.[36,37,41,52,53]

Bovine serum albumin (BSA) was purchased from Roche (Indianapolis, IN) and dialyzed against buffer M at 4 °C. Dialyzed BSA stock was stored at 4 °C until use, and stock concentration was determined spectrophotometrically using an extinction coefficient of $\varepsilon_{280}=4.3\times 10^4$ M^{-1} cm^{-1}.[37,54]

Oligodeoxynucleotides

Oligodeoxynucleotides were synthesized using an ABI model 391 synthesizer (Applied Biosystems, Foster City, CA) as described previously.[55] Unlabeled DNA was purified using PAGE under denaturing conditions followed by gel electroelution, while Cy3- and Cy5-labeled DNA was further purified by reversed-phase HPLC using an XTerra MS C18 column (Waters, Milford, MA).[55] The concentrations of each stock of DNA strands were determined by digesting each strand with phosphodiesterase I (Worthington, Lakewood, NJ) in 100 mM Tris–HCl, pH 9.2 at 25 °C, and 3 mM $MgCl_2$ and analyzing the resulting mixture of mononucleotides spectrophotometrically using the following extinction coefficients:[51] $\varepsilon_{260,AMP}=15{,}340$ M^{-1} cm^{-1}, $\varepsilon_{260,CMP}=7600$ M^{-1} cm^{-1}, $\varepsilon_{260,GMP}=12{,}160$ M^{-1} cm^{-1}, $\varepsilon_{260,TMP}=8700$ M^{-1} cm^{-1}, $\varepsilon_{260,Cy3}=5000$ M^{-1} cm^{-1}, and $\varepsilon_{260,Cy5}=10{,}000$ M^{-1} cm^{-1}.

DNA substrate design

The DNA substrates used for DNA unwinding studies were composed of three DNA strands that form a hairpin structure when annealed together with the exception of two nicks as shown in Fig. 1.[36,41,42] For chemical quenched-flow experiments, strand "A" was radiolabeled on its 5′ end as depicted in Fig. 1a with ^{32}P using T4 polynucleotide kinase (USB, Cleveland, OH) and $\gamma^{32}P$-ATP (Perkin Elmer, Waltham, MA) as described previously.[55] The radiolabeled strand "A" was mixed with an equal molar ratio of strand "B" and 25% excess of the bottom strand. The resulting DNA stock solution was heated to 94 °C for 5 min, followed by slow cooling to 25 °C to allow annealing. For stopped-flow unwinding experiments, strand "A" was fluorescently labeled with a Cy3 donor, while strand "B" was labeled with a Cy5 acceptor as depicted in Fig. 1b. These two fluorescently labeled DNA strands were mixed and annealed to the bottom strand as described above.

Rapid chemical quenched-flow DNA unwinding kinetics

DNA unwinding experiments were performed at 25 °C using a quenched-flow apparatus (KinTek RQF-3, University Park, PA) as described previously.[41] RecBCD or RecBC (20 nM) was preincubated with ^{32}P-labeled DNA substrate (2 nM) and BSA (6 μM) on ice for 20 min in buffer M, and this mixture was then loaded into one loop of the quenched-flow apparatus. Equilibrium binding experiments indicate that all unwinding substrates were saturated under these solution conditions and at these protein and DNA concentrations.[37] A solution containing ATP (10 mM) and heparin trap (15 mg/ml) in buffer M was loaded into the other loop. After equilibration at 25 °C for 5 min, DNA unwinding was initiated by rapidly mixing these solutions together (1:1) and quenching the reaction after a predefined time interval (Δt) by mixing with 0.4 M EDTA and 10% (v/v) glycerol; the zero time point was determined by performing a "mock reaction" (without ATP). Quenched reactions collected at each time point were kept on ice until all samples were collected, and the unwound ssDNA was separated from the native duplex DNA using nondenaturing [10% (w/v)] PAGE. The gel was exposed to a phosphor screen (Molecular Dynamics, Sunnyvale, CA) for 1 h, after which the screen was scanned using a Storm 840 phosphorimager (Molecular Dynamics). The radioactivity of each band was quantified using the ImageQuant software (Molecular Dynamics), and the fraction of DNA molecules unwound at each time point, $f_{ss}(t)$, was calculated using Eq. (1):[41]

$$f_{ss}(t) = \frac{\frac{C_S(t)}{C_S(t)+C_D(t)} - \frac{C_{S,0}}{C_{S,0}+C_{D,0}}}{1-\frac{C_{S,0}}{C_{S,0}+C_{D,0}}} \tag{1}$$

where $C_S(t)$ and $C_D(t)$ reflect the radioactive counts for the unwound ssDNA and the native duplex DNA, respectively, at time t, while $C_{S,0}$ and $C_{D,0}$ represent the corresponding quantities at time zero. Unwinding time courses were collected as a function of duplex length ($L=24$, 30, 40, 48, and 60 bp), and the averages of three independent unwinding time courses for each duplex length were subjected to global NLLS analysis.

Stopped-flow fluorescence unwinding kinetics

Fluorescence DNA unwinding experiments were performed at 25 °C using a stopped-flow apparatus (SX.18MV, Applied Photophysics Ltd., Leatherhead, UK) as described previously.[40,42] RecBC or RecBCD (200 nM) was preincubated with each Cy3- and Cy5-labeled DNA substrate (40 nM) and BSA (6 μM) on ice for 20 min in buffer M. Equilibrium binding experiments indicate that all unwinding substrates were saturated under these solution conditions and at these protein and DNA concentrations.[37] This mixture was then loaded into one syringe of the stopped-flow apparatus, and a solution containing ATP (10 mM) and heparin (15 mg/ml) in buffer M was loaded into the other syringe of the device. Both solutions were equilibrated to 25 °C for 5 min, after which DNA unwinding was initiated by rapid mixing of the two solutions (1:1). The Cy3 fluorophore was excited at 515 nm, and its emission was monitored at 570 nm with an interference filter (Oriel Corp., Stradford, CT); Cy5 emission was monitored simultaneously at all wavelengths >665 nm using a long-pass filter (Oriel Corp.). Ten individual Cy3 FRET time courses were collected and averaged, and unwinding experiments were performed as a function of duplex length (L=24, 29, 37, 40, 43, 48, 53, and 60 bp). The results from three independent measurements were averaged and subjected to global NLLS analysis. Since all Cy3 FRET time courses exhibit a lag phase before fluorescence enhancement, this initial signal was assumed to represent 100% duplex DNA and thus reflect zero DNA unwinding. Hence, the first 10 data points from each time course were averaged and subtracted from all data points, thereby constraining each time course to start at zero.[42]

Analysis of DNA unwinding kinetics

Global NLLS analysis of DNA unwinding kinetics was performed as described previously[41,42,44] using Conlin[56] (kindly provided by Dr. Jeremy Williams and modified by Dr. Chris Fischer) and IMSL C Numerical Libraries (Visual Numeric Incorporated, Houston, TX). The uncertainties reported reflect 68% confidence interval limits determined from a 50-cycle Monte Carlo analysis as described previously.[41] Entire time courses with data collected out to 10 s were used in the analysis, although only data out to 0.4 s were plotted here for clarity. Fitting of the time courses to a particular kinetic scheme was performed by obtaining the time-dependent formation of ssDNA, $f_{ss}(t)$, as the inverse Laplace transform of $F_{ss}(s)$ using numerical methods as described previously.[41,44] For Scheme 1, $f_{ss}(t)$ is given by Eq. (2):

$$f_{ss}(t) = A_T\mathcal{L}^{-1}F_{ss}(s) = A_T\mathcal{L}^{-1}\left(\frac{k_U^n(k_{NP}+sx)}{s(k_{NP}+s)(k_U+s)^n}\right) \quad (2)$$

where $F_{ss}(s)$ is the Laplace transform of $f_{ss}(t)$, $\mathcal{L}^{-1}$ is the inverse Laplace transform operator with s as the Laplace variable, A_T is the total amplitude for a given duplex length L, n is the number of unwinding steps with k_U being the rate constant in between two successive unwinding steps, k_{NP} is the rate constant for the isomerization reaction from nonproductive, $(RD)_{NP}$, to productive, $(RD)_L$, RecBC(D)–DNA complexes, and x is the fraction of productively bound RecBC(D)–DNA complexes defined by Eq. (3):

$$x = \frac{(RD)_L}{(RD)_L + (RD)_{NP}} \quad (3)$$

$f_{ss}(t)$ for Scheme 2 is given by Eq. (4) in which h additional kinetic steps with rate constant k_C that are not directly associated with DNA unwinding have been included in the mechanism:

$$f_{ss}(t) = A_T\mathcal{L}^{-1}F_{ss}(s) = A_T\mathcal{L}^{-1}\left(\frac{k_C^h k_U^n(k_{NP}+sx)}{s(k_C+s)^h(k_{NP}+s)(k_U+s)^n}\right) \quad (4)$$

In Figs. 4b–7b, A_T, n, h (where appropriate), and x were allowed to float for each duplex length, while k_C (where appropriate), k_U, and k_{NP} were constrained to be global parameters. In Figs. 4a–7a, n in Eqs. (2) and (4) was replaced with L/m, where L is duplex length in base pairs and m is the average unwinding kinetic step size. In this analysis, A_T and x (as well as h, where appropriate) were floated for each time course at every duplex length, while k_U, k_{NP}, and m (as well as k_C, where appropriate) were constrained to be global parameters.

Acknowledgements

This work was supported in part by the National Institutes of Health through grant GM045948. We thank Thang Ho for synthesis and purification of all DNA substrates; Drs. Gerald Smith and Doug Julin for providing plasmids and cell lines; and Drs. Aaron Lucius, Anita Niedziela-Majka, Jason Wong, and Tom Perkins for valuable discussions.

Supplementary Data

Supplementary data associated with this article can be found, in the online version, at doi:10.1016/j.jmb.2008.07.012

References

1. Lohman, T. M. & Bjornson, K. P. (1996). Mechanisms of helicase-catalyzed DNA unwinding. *Annu. Rev. Biochem.* **65**, 169–214.
2. Lohman, T. M., Hsieh, J., Maluf, N. K., Cheng, W., Lucius, A. L., Fischer, C. J. *et al.* (2003). DNA helicases, motors that move along nucleic acids: lessons from the SF1 helicase superfamily. In *The Enzymes* (Tamanoi, F. & Hackney, D. D., eds), vol. XXIII, pp. 303–369, Academic Press, New York, NY.
3. Matson, S. W., Bean, D. W. & George, J. W. (1994). DNA helicases: enzymes with essential roles in all aspects of DNA metabolism. *BioEssays*, **16**, 13–22.
4. Patel, S. S. & Donmez, I. (2006). Mechanisms of helicases. *J. Biol. Chem.* **281**, 18265–18268.
5. Patel, S. S. & Picha, K. M. (2000). Structure and function of hexameric helicases. *Annu. Rev. Biochem.* **69**, 651–697.
6. Delagoutte, E. & von Hippel, P. H. (2002). Helicase mechanisms and the coupling of helicases within macromolecular machines: Part I. Structures and properties of isolated helicases. *Q. Rev. Biophys.* **35**, 431–478.
7. Singleton, M. R., Dillingham, M. S. & Wigley, D. B. (2007). Structure and mechanism of helicases and nucleic acid translocases. *Annu. Rev. Biochem.* **76**, 23–50.
8. Flores, M. J., Sanchez, N. & Michel, B. (2005). A fork-clearing role for UvrD. *Mol. Microbiol.* **57**, 1664–1675.
9. Jankowsky, E., Gross, C. H., Shuman, S. & Pyle, A. M. (2001). Active disruption of an RNA–protein interaction by a DExH/D RNA helicase. *Science*, **291**, 121–125.
10. Veaute, X., Delmas, S., Selva, M., Jeusset, J., Le Cam, E., Matic, I. *et al.* (2005). UvrD helicase, unlike Rep helicase, dismantles RecA nucleoprotein filaments in *Escherichia coli*. *EMBO J.* **24**, 180–189.
11. Eggleston, A. K., O'Neill, T. O., Bradbury, E. M. & Kowalczykowski, S. C. (1995). Unwinding of nucleosomal DNA by a DNA helicase. *J. Biol. Chem.* **270**, 2024–2031.
12. Byrd, A. K. & Raney, K. D. (2006). Displacement of a

DNA binding protein by Dda helicase. *Nucleic Acids Res.* **34**, 3020–3029.
13. German, J., Sanz, M. M., Ciocci, S., Ye, T. Z. & Ellis, N. A. (2007). Syndrome-causing mutations of the BLM gene in persons in the Bloom's Syndrome Registry. *Hum. Mutat.* **28**, 743–753.
14. Ellis, N. A., Groden, J., Ye, T.-Z., Straughen, J., Lennon, D., Ciocci, J. *et al.* (1995). The Bloom's syndrome gene product is homologous to RecQ helicases. *Cell*, **83**, 655–666.
15. Hickson, I. D., Davies, S. L., Li, J. L., Levitt, N. C., Mohaghegh, P., North, P. S. & Wu, L. (2001). Role of the Bloom's syndrome helicase in maintenance of genome stability. *Biochem. Soc. Trans.* **29**, 201–204.
16. Hickson, I. D. (2003). RecQ helicases: caretakers of the genome. *Nat. Rev. Cancer*, **3**, 169–178.
17. Finch, P. W., Storey, A., Brown, K., Hickson, I. D. & Emmerson, P. T. (1986). Complete nucleotide sequence of *recD*, the structural gene for the α subunit of exonuclease V of *Escherichia coli*. *Nucleic Acids Res.* **14**, 8583–8594.
18. Finch, P. W., Storey, A., Chapman, K. E., Brown, K., Hickson, I. D. & Emmerson, P. T. (1986). Complete nucleotide sequence of the *Escherichia coli recB* gene. *Nucleic Acids Res.* **14**, 8573–8582.
19. Finch, P. W., Wilson, R. E., Brown, K., Hickson, I. D., Tomkinson, A. E. & Emmerson, P. T. (1986). Complete nucleotide sequence of the *Escherichia coli recC* gene and of the *thyA–recC* intergenic region. *Nucleic Acids Res.* **14**, 4437–4451.
20. Anderson, D. G. & Kowalczykowski, S. C. (1997). The translocating RecBCD enzyme stimulates recombination by directing RecA protein onto ssDNA in a χ-regulated manner. *Cell*, **90**, 77–86.
21. Kowalczykowski, S. C., Dixon, D. A., Eggleston, A. K., Lauder, S. D. & Rehrauer, W. M. (1994). Biochemistry of homologous recombination in *Escherichia coli*. *Microbiol. Rev.* **58**, 401–465.
22. Smith, G. R. (1990). RecBCD enzyme. In *Nucleic Acids and Molecular Biology* (Eckstein, F. & Lilley, D. M. J., eds), pp. 78–98, Springer–Verlag, Berlin, Germany.
23. Spies, M., Amitani, I., Baskin, R. J. & Kowalczykowski, S. C. (2007). RecBCD enzyme switches lead motor subunits in response to chi recognition. *Cell*, **131**, 694–705.
24. Yu, M., Souaya, J. & Julin, D. A. (1998). The 30-kDa C-terminal domain of the RecB protein is critical for the nuclease activity, but not the helicase activity, of the RecBCD enzyme from *Escherichia coli*. *Proc. Natl Acad. Sci. USA*, **95**, 981–986.
25. Yu, M., Souaya, J. & Julin, D. A. (1998). Identification of the nuclease active site in the multifunctional RecBCD enzyme by creation of a chimeric enzyme. *J. Mol. Biol.* **283**, 797–808.
26. Bianco, P. R., Brewer, L. R., Corzett, M., Balhorn, R., Yeh, Y., Kowalczykowski, S. C. & Baskin, R. J. (2001). Processive translocation and DNA unwinding by individual RecBCD enzyme molecules. *Nature*, **409**, 374–378.
27. Handa, N., Bianco, P. R., Baskin, R. J. & Kowalczykowski, S. C. (2005). Direct visualization of RecBCD movement reveals cotranslocation of the RecD motor after chi recognition. *Mol. Cell*, **17**, 745–750.
28. Spies, M., Bianco, P. R., Dillingham, M. S., Handa, N., Baskin, R. J. & Kowalczykowski, S. C. (2003). A molecular throttle: the recombination hotspot chi controls DNA translocation by the RecBCD helicase. *Cell*, **114**, 647–654.
29. Arnold, D. A. & Kowalczykowski, S. C. (2000). Facilitated loading of RecA protein is essential to recombination by RecBCD enzyme. *J. Biol. Chem.* **275**, 12261–12265.
30. Gorbalenya, A. E. & Koonin, E. V. (1993). Helicases: amino acid sequence comparisons and structure–function relationships. *Curr. Opin. Struct. Biol.* **3**, 419–429.
31. Dillingham, M. S., Spies, M. & Kowalczykowski, S. C. (2003). RecBCD enzyme is a bipolar helicase. *Nature*, **423**, 893–897.
32. Taylor, A. F. & Smith, G. R. (2003). RecBCD enzyme is a DNA helicase with fast and slow motors of opposite polarity. *Nature*, **423**, 889–893.
33. Roman, L. J., Eggleston, A. K. & Kowalczykowski, S. C. (1992). Processivity of the DNA helicase activity of *Escherichia coli* recBCD enzyme. *J. Biol. Chem.* **267**, 4207–4214.
34. Roman, L. J. & Kowalczykowski, S. C. (1989). Characterization of the helicase activity of the *Escherichia coli* RecBCD enzyme using a novel helicase assay. *Biochemistry*, **28**, 2863–2873.
35. Masterson, C., Boehmer, P. E., McDonald, F., Chaudhuri, S., Hickson, I. D. & Emmerson, P. T. (1992). Reconstitution of the activities of the RecBCD holoenzyme of *Escherichia coli* from the purified subunits. *J. Biol. Chem.* **267**, 13564–13572.
36. Taylor, A. F. & Smith, G. R. (1995). Monomeric RecBCD enzyme binds and unwinds DNA. *J. Biol. Chem.* **270**, 24451–24458.
37. Wong, C. J., Lucius, A. L. & Lohman, T. M. (2005). Energetics of DNA end binding by *E. coli* RecBC and RecBCD helicases indicate loop formation in the 3′-single-stranded DNA tail. *J. Mol. Biol.* **352**, 765–782.
38. Farah, J. A. & Smith, G. R. (1997). The RecBCD enzyme initiation complex for DNA unwinding: enzyme positioning and DNA opening. *J. Mol. Biol.* **272**, 699–715.
39. Singleton, M. R., Dillingham, M. S., Gaudier, M., Kowalczykowski, S. C. & Wigley, D. B. (2004). Crystal structure of RecBCD enzyme reveals a machine for processing DNA breaks. *Nature*, **432**, 187–193.
40. Lucius, A. L. & Lohman, T. M. (2004). Effects of temperature and ATP on the kinetic mechanism and kinetic step-size for *E. coli* RecBCD helicase-catalyzed DNA unwinding. *J. Mol. Biol.* **339**, 751–771.
41. Lucius, A. L., Vindigni, A., Gregorian, R., Ali, J. A., Taylor, A. F., Smith, G. R. & Lohman, T. M. (2002). DNA unwinding step-size of *E. coli* RecBCD helicase determined from single turnover chemical quenched-flow kinetic studies. *J. Mol. Biol.* **324**, 409–428.
42. Lucius, A. L., Wong, C. J. & Lohman, T. M. (2004). Fluorescence stopped-flow studies of single turnover kinetics of *E. coli* RecBCD helicase-catalyzed DNA unwinding. *J. Mol. Biol.* **339**, 731–750.
43. Ali, J. A. & Lohman, T. M. (1997). Kinetic measurement of the step-size of DNA unwinding by *Escherichia coli* UvrD helicase. *Science*, **275**, 377–380.
44. Lucius, A. L., Maluf, N. K., Fischer, C. J. & Lohman, T. M. (2003). General methods for analysis of sequential "*n*-step" kinetic mechanisms: application to single turnover kinetics of helicase-catalyzed DNA unwinding. *Biophys. J.* **85**, 2224–2239.
45. Bianco, P. R. & Kowalczykowski, S. C. (2000). Translocation step size and mechanism of the RecBC DNA helicase. *Nature*, **405**, 368–372.
46. Wong, C. J. & Lohman, T. M. (2008). Kinetic control of Mg^{2+}-dependent melting of duplex DNA ends by *E. coli* RecBC. *J. Mol. Biol.* **378**, 759–775.
47. Wong, C. J., Rice, R. L., Baker, N. A., Ju, T. & Lohman, T. M. (2006). Probing 3′-ssDNA loop formation in

E. coli RecBCD/RecBC–DNA complexes using non-natural DNA: a model for "chi" recognition complexes. *J. Mol. Biol.* **362**, 26–43.
48. Dillingham, M. S., Webb, M. R. & Kowalczykowski, S. C. (2005). Bipolar DNA translocation contributes to highly processive DNA unwinding by RecBCD enzyme. *J. Biol. Chem.* **280**, 37069–37077.
49. Perkins, T. T., Li, H. W., Dalal, R. V., Gelles, J. & Block, S. M. (2004). Forward and reverse motion of single RecBCD molecules on DNA. *Biophys. J.* **86**, 1640–1648.
50. Mascotti, D. P. & Lohman, T. M. (1995). Thermodynamics of charged oligopeptide–heparin interactions. *Biochemistry*, **34**, 2908–2915.
51. Gray, D. M., Hung, S. H. & Johnson, K. H. (1995). Absorption and circular dichroism spectroscopy of nucleic acid duplexes and triplexes. *Methods Enzymol.* **246**, 19–34.
52. Amundsen, S. K., Taylor, A. F., Chaudhury, A. M. & Smith, G. R. (1986). *recD*: the gene for an essential third subunit of exonuclease V. *Proc. Natl Acad. Sci. USA*, **83**, 5558–5562.
53. Taylor, A. F. & Smith, G. R. (1985). Substrate specificity of the DNA unwinding activity of the recBC enzyme of *Escherichia coli*. *J. Mol. Biol.* **185**, 431–443.
54. Lohman, T. M., Chao, K., Green, J. M., Sage, S. & Runyon, G. (1989). Large-scale purification and characterization of the *Escherichia coli rep* gene product. *J. Biol. Chem.* **264**, 10139–10147.
55. Wong, I., Chao, K. L., Bujalowski, W. & Lohman, T. M. (1992). DNA-induced dimerization of the *Escherichia coli rep* helicase. Allosteric effects of single-stranded and duplex DNA. *J. Biol. Chem.* **267**, 7596–7610.
56. Williams, D. J. & Hall, K. B. (2000). Monte Carlo applications to thermal and chemical denaturation experiments of nucleic acids and proteins. *Methods Enzymol.* **321**, 330–352.

Single-turnover kinetics of RecBC-catalyzed unwinding of DNA duplexes possessing noncomplementary 5′-$(dT)_6$ and 3′-$(dT)_6$ ssDNA tails. (a) Cy5 fluorescence time courses (inverted about the *x*-axis) as a function of duplex length (L = 24, 29, 37, 40, 43, 48, 53, and 60 bp) obtained using the stopped-flow fluorescence assay. Data points represent the average of three independent measurements, and the error bars indicate the standard deviation of the data. Smooth curves are simulated time courses based on the global NLLS best fits to Scheme 1, with $mk_{obs} = 339 \pm 9$ bp/s, $m = 4.3 \pm 0.1$ bp, $k_{obs} = 77 \pm 13\ s^{-1}$, and $k_{NP} = 1.0 \pm 0.1\ s^{-1}$. (b) The number of unwinding steps n determined from global NLLS analysis using Scheme 1 plotted *versus* DNA duplex length L. The continuous line shows the linear least-squares fit through the data ($n = 0.24L - 0.01$).

Single-turnover kinetics of RecBCD-catalyzed unwinding of DNA duplexes possessing noncomplementary 5′-$(dT)_6$ and 3′-$(dT)_6$ ssDNA tails. (a) Cy3 fluorescence time courses as a function of duplex length (L = 24, 29, 37, 40, 43, 48, 53, and 60 bp) obtained using the stopped-flow assay. Data points represent the average of three independent measurements, and the error bars indicate the standard deviation of the data. Smooth curves are simulated time courses based on the global NLLS best fits to Scheme 2, with $mk_U = 745 \pm 18$ bp/s, $m = 3.4 \pm 0.5$ bp, $k_U = 220 \pm 28\ s^{-1}$, $k_{NP} = 6.7 \pm 0.3\ s^{-1}$, $h = 3.2 \pm 0.1$ steps, and $k_C = 58 \pm 2\ s^{-1}$. (b) The number of unwinding steps n and additional kinetic steps h determined from global NLLS analysis using Scheme 2 plotted *versus* DNA duplex length L. The continuous line shows the linear least-squares fit through the data ($n = 0.29L - 0.06$; $h = 3.2$).

Single-turnover time courses of RecBCD-catalyzed unwinding of DNA duplexes possessing noncomplementary 5′-$(dT)_{10}$ and 3′-$(dT)_6$ ssDNA tails. (a) Cy3 fluorescence time courses as a function of duplex length (L = 24, 29, 37, 40, 43, 48, 53, and 60 bp) obtained using the stopped-flow assay. Data points represent the average of three independent measurements, and the error bars indicate the standard deviation of the data. Smooth curves are simulated time courses based on the global NLLS best fits to Scheme 1, with $mk_U = 588 \pm 11$ bp/s, $m = 3.6 \pm 0.2$ bp, $k_U = 163 \pm 24\ s^{-1}$, and $k_{NP} = 5.4 \pm 1.0\ s^{-1}$. (b) The number of unwinding steps n as a function of duplex length L. The continuous line shows the linear least-squares fit through the data ($n = 0.28L - 0.01$).

Single-turnover kinetics of RecBC-catalyzed unwinding of DNA duplexes possessing noncomplementary 5′-$(dT)_{10}$ and 3′-$(dT)_6$ ssDNA tails. (a) Cy3 fluorescence time courses as a function of duplex length (L = 24, 29, 37, 40, 43, 48, 53, and 60 bp) obtained using the stopped-flow assay. Data points represent the average of three independent measurements, and the error bars indicate the standard deviation of the data. Smooth curves are simulated time courses based on the global NLLS best fits to Scheme 1, with $mk_{obs} = 320 \pm 7$ bp/s, $m = 3.5 \pm 0.1$ bp, $k_{obs} = 92 \pm 12\ s^{-1}$, and $k_{NP} = 1.9 \pm 0.6\ s^{-1}$. (b) The number of unwinding steps n determined from global NLLS analysis using Scheme 1 as a function of duplex length L. The continuous line shows the linear least-squares fit through the data ($n = 0.29L - 0.41$).

A.

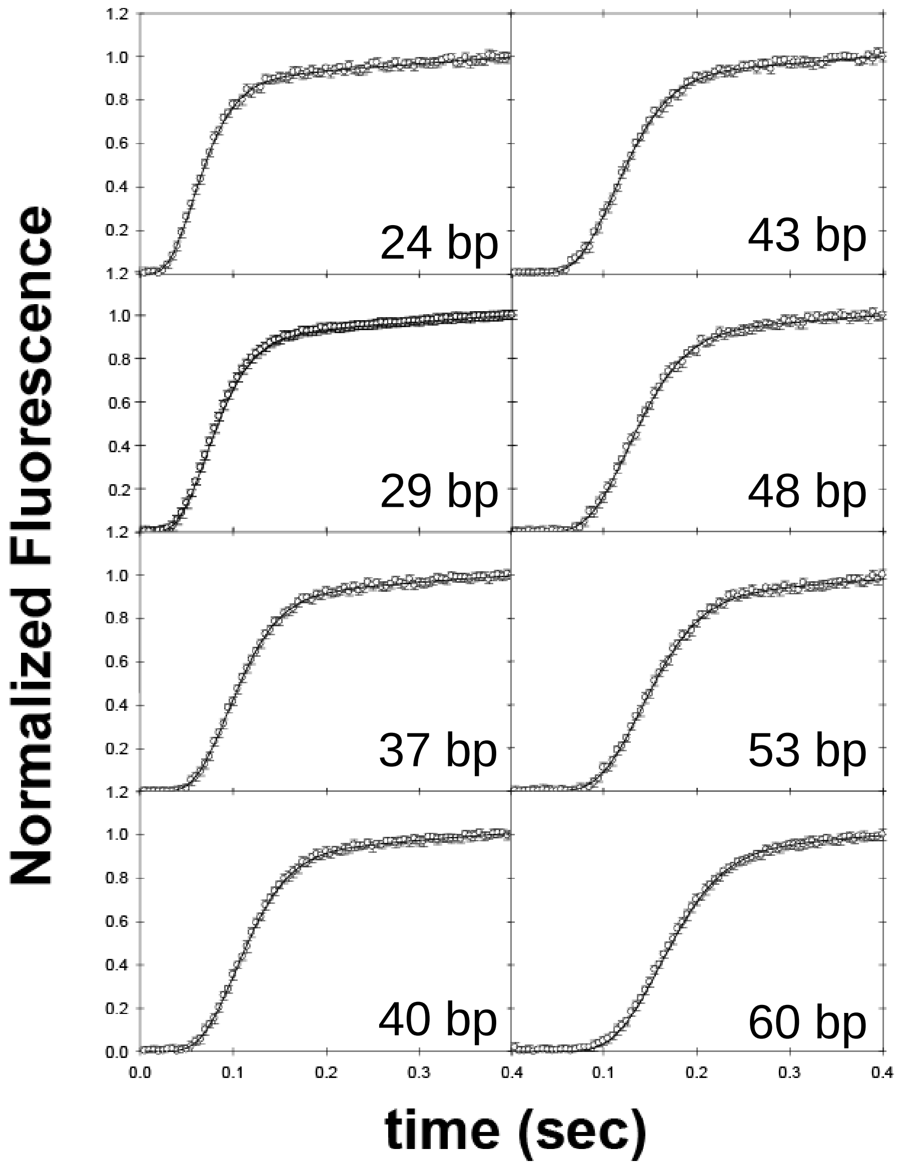

B.

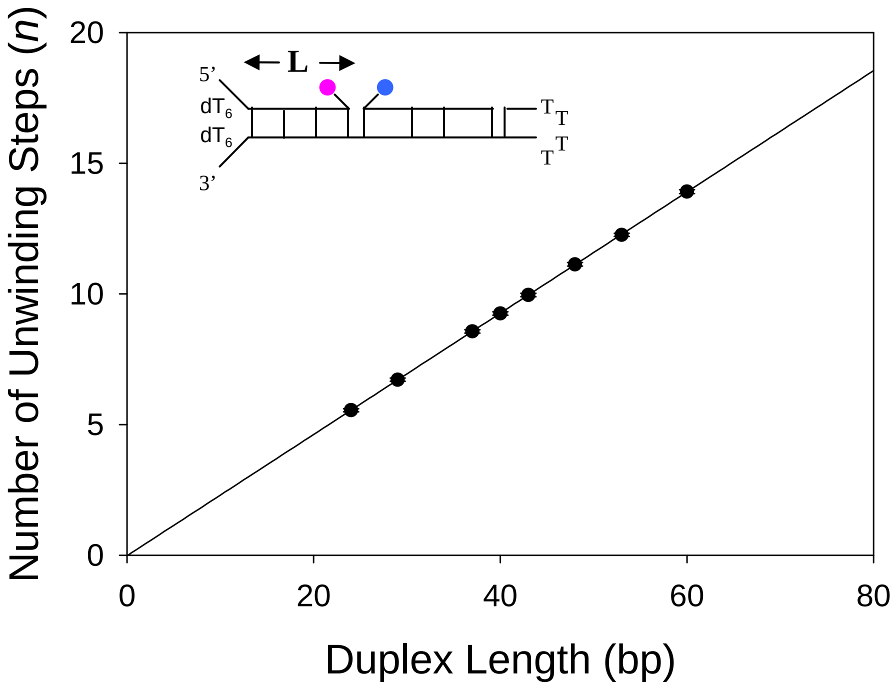

Supplementary Figure 1

A. B.

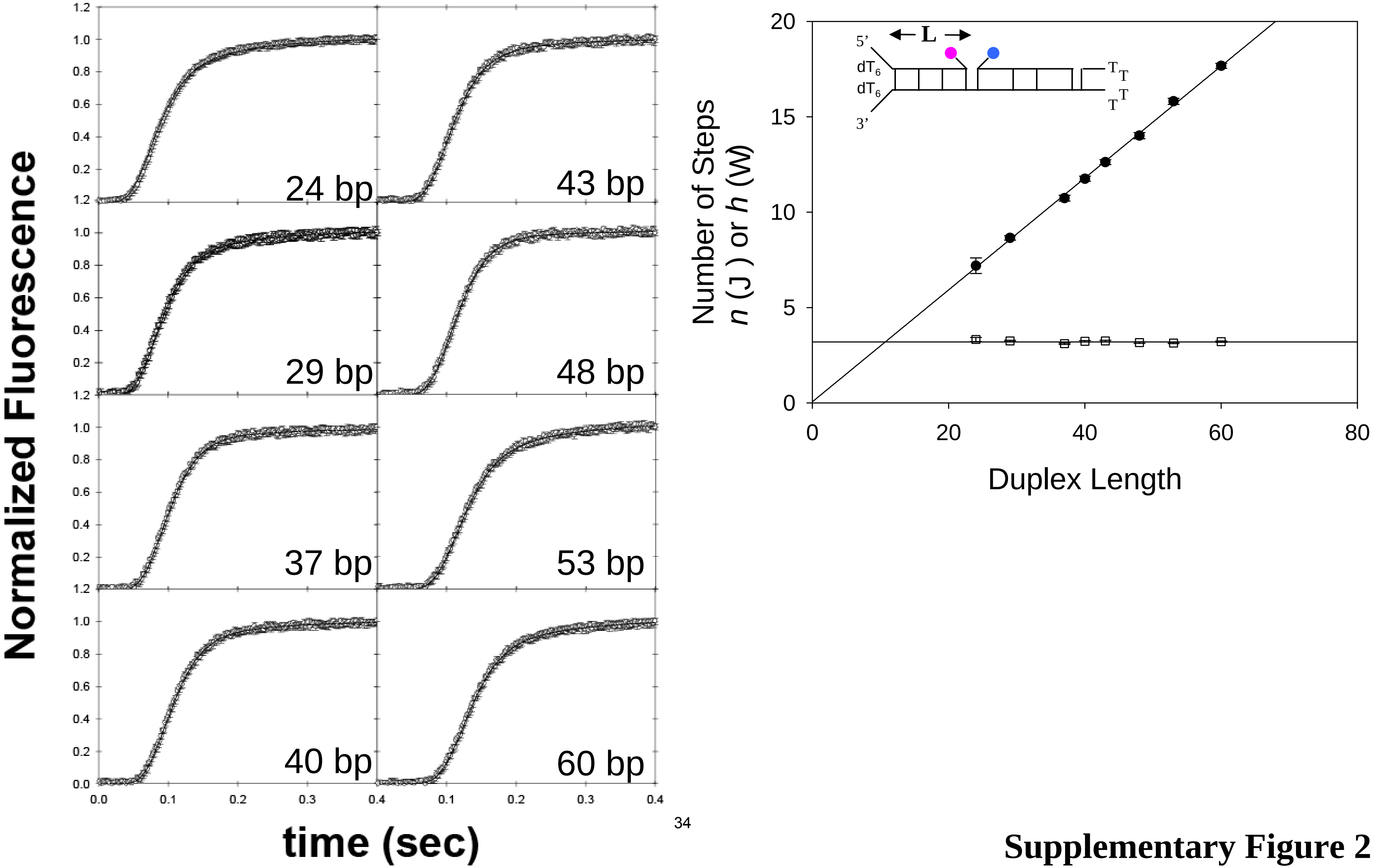

Supplementary Figure 2

A.

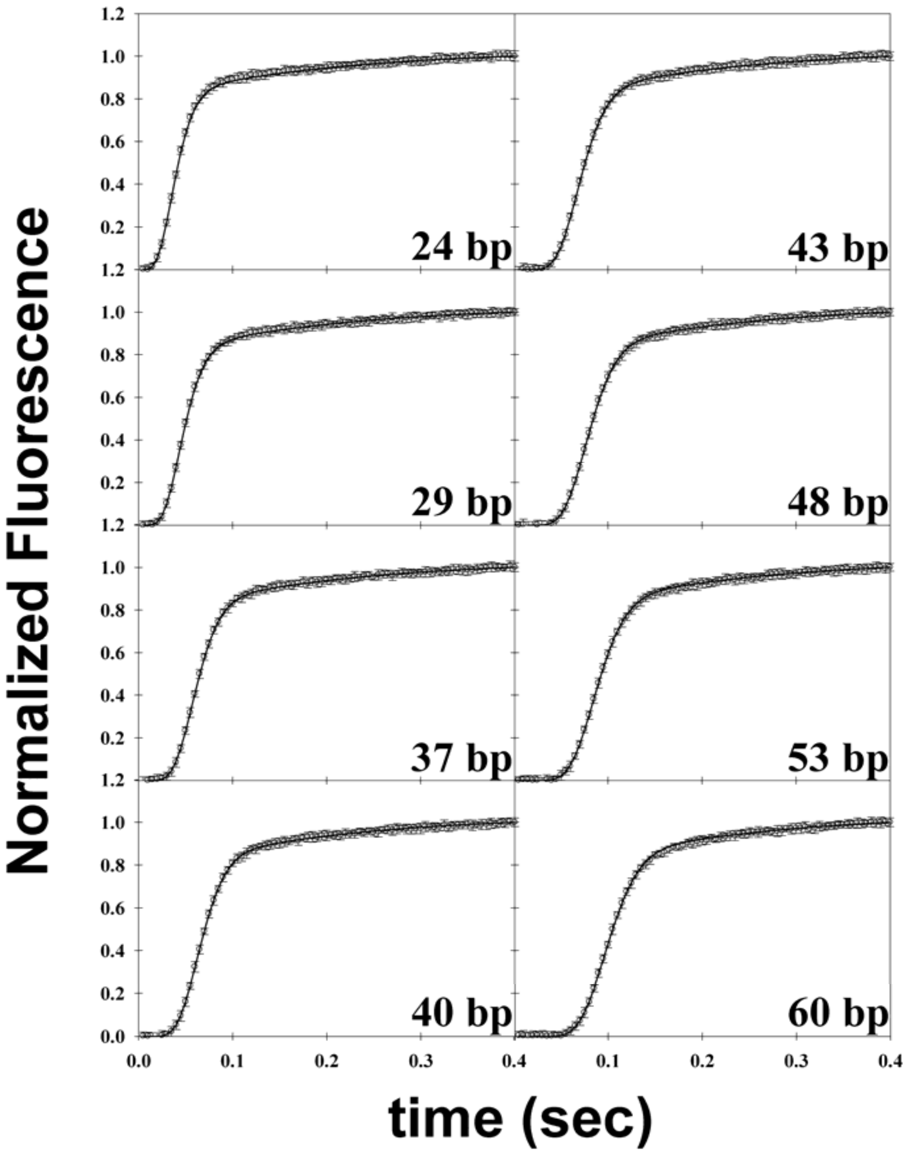

B.

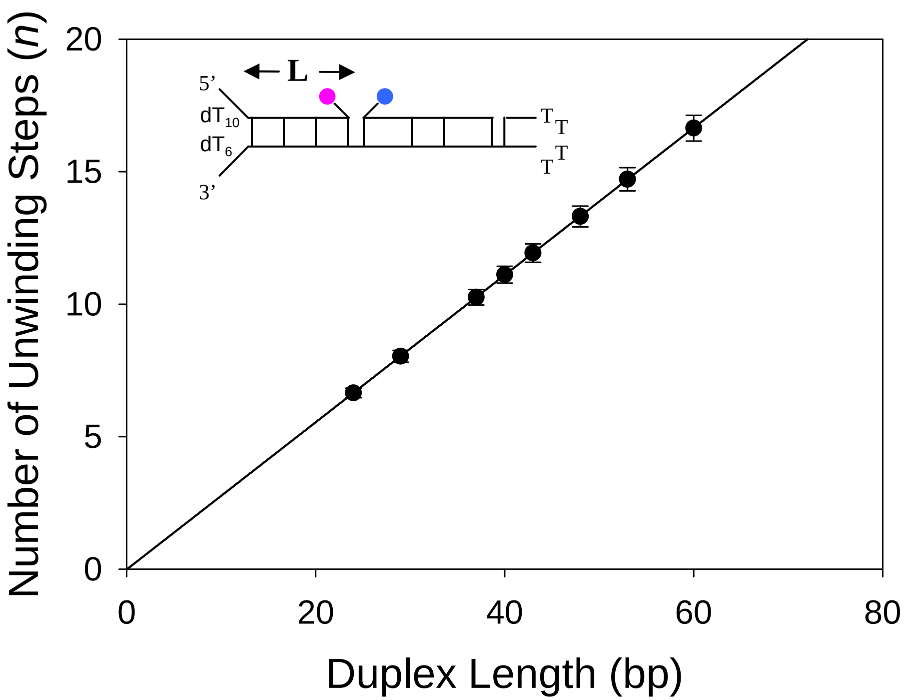

Supplementary Figure 3

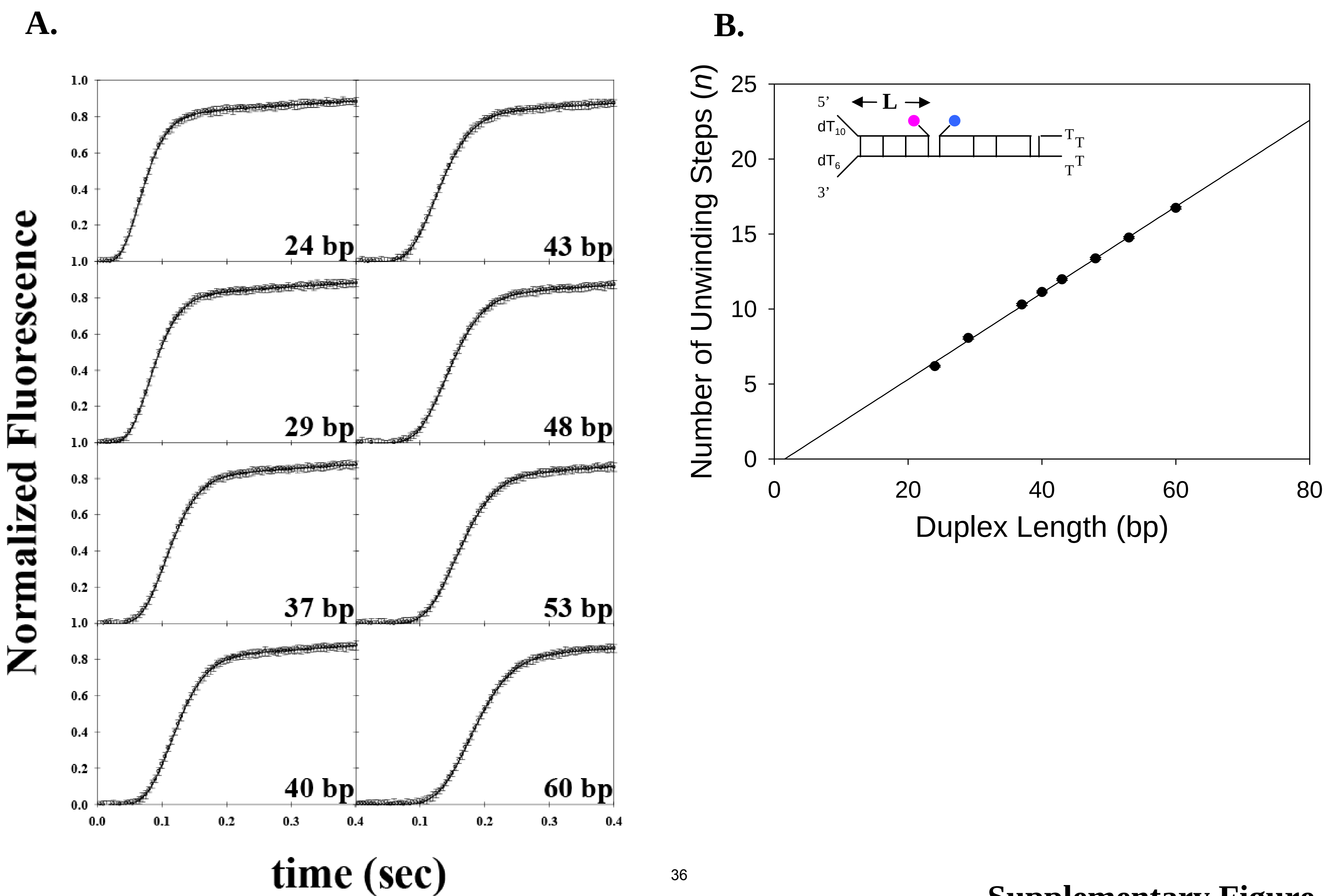

Supplementary Figure 4

Appendix to Chapter II

[NaCl] dependence on RecBC catalyzed DNA unwinding

RecBC unwinding of a 24 bp duplex was examined as a function of NaCl concentration in order to test whether [NaCl] influences the rate of DNA unwinding or processivity. Unwinding time courses collected at 30 mM NaCl, 60 mM, 120 mM, and 250 mM NaCl (**Figure 2-S5**) are analyzed using **Equation 1** (Chapter 2) based on the *n*-step sequential mechanism shown in **Scheme 1** (Chapter 2) with m = 5.0 bp (constrained). These time courses not only show identical lag phases, but also k_{obs} is the same within error across the range of NaCl concentration examined. However, the final unwinding amplitude decreases with increasing NaCl concentration. This indicates that although RecBC unwinds DNA with the same unwinding rate, it is less processive at higher NaCl concentrations. One important note is that although the unwinding rate is invariant across the range of [NaCl] examined, the average unwinding kinetic step-size, m, was fixed in the analysis. These experiments will ultimately have to be performed as a function of DNA duplex length in addition to [NaCl] in order to determine whether RecBC takes larger or smaller (or the same) steps at higher NaCl concentrations.

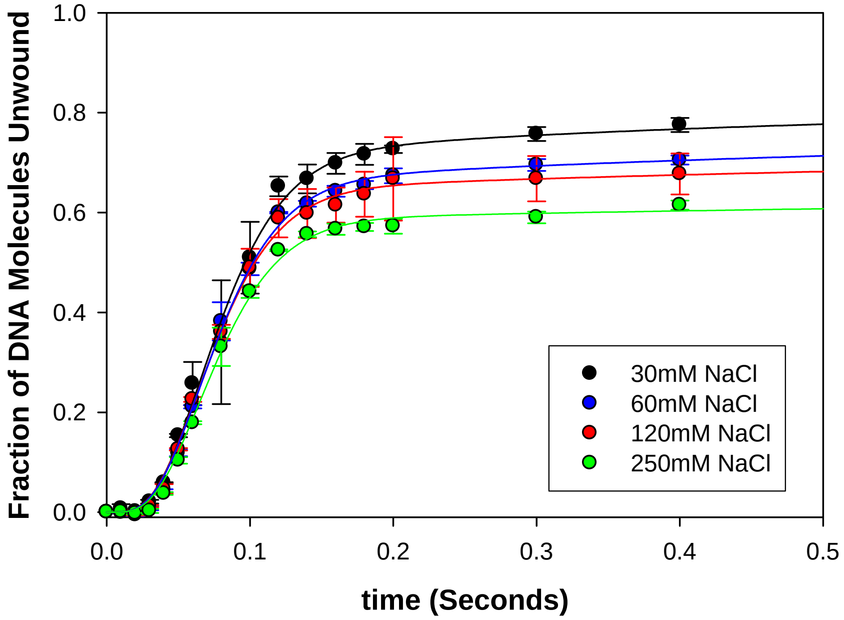

Figure 2-S5. RecBC unwinding of a 24 bp duplex with pre-formed twin dT_6 ssDNA tails as a function of [NaCl]. 200 nM RecBC pre-bound to 2 nM radiolabeled DNA substrate was rapidly mixed with 10 mM ATP and 15 mg/mL heparin. Time courses were analyzed using **Equation 1** based on **Scheme 1** (Chapter 2) with m = 5.0 bp (fixed) (●) Reaction in buffer M: 20 mM Mops-KOH pH 7.0 at 25°C, 30 mM NaCl, 10 mM $MgCl_2$, 1 mM 2-mercaptoethanol, 5% (v/v) glycerol. x = 0.88 ± 0.05, k_{np} = 2.6 ± 0.7 s^{-1}, k_{obs} = 58 ± 6 s^{-1}, A = 0.81 ± 0.03. (●) Reaction in buffer M with 60 mM NaCl. x = 0.87 ± 0.05, k_{np} = 1.8 ± 0.5 s^{-1}, k_{obs} = 59 ± 3 s^{-1}, A = 0.76 ± 0.02. (●) Reaction in buffer M with 120 mM NaCl. x = 0.90 ± 0.06, k_{np} = 1.6 ± 0.5 s^{-1}, k_{obs} = 60 ± 3 s^{-1}, A = 0.72 ± 0.02. (●) Reaction in buffer M with 250 mM NaCl. x = 0.90 ± 0.04, k_{np} = 1.1 ± 0.3 s^{-1}, k_{obs} = 59 ± 4 s^{-1}, A = 0.65 ± 0.02. Based on this data (only one duplex length) the unwinding rate is unaffected by [NaCl] but the overall extent of unwinding decreases with increasing [NaCl].

Does the DNA re-anneal behind RecBC during unwinding?

RecBC unwinding time courses shown in **Figure 2-S6** exhibit a decrease in the final unwinding amplitude as duplex length increases. There two potential explanations for this observation. Either RecBC has limited processivity or the DNA substrates can re-anneal behind the protein as it unwinds the duplex. Similar unwinding experiments with the RecBCD enzyme do not show this decrease in the extent of DNA unwinding as a function of duplex length because RecBCD is not only highly processive, but also DNA unwinding is coupled to nuclease activity, which prevents any re-annealing that may occur. To test whether the DNA can re-anneal behind RecBC as it unwinds DNA, I performed an unwinding experiment at lower ATP concentration (10 µM ATP after mixing) and in the presence of *E. coli* SSB. If transient ssDNA intermediates are formed, SSB will bind to it and prevent the two strands from re-annealing. **Figure 2-S6** shows that with a 60 bp DNA substrate, the final unwinding amplitude of RecBC is independent of *E. coli* SSB concentration. This indicates that either re-annealing does not occur or that the transiently formed ssDNA intermediates are not long enough for SSB to bind and the two DNA strands are still able to re-anneal behind RecBC. These experiments will need to be repeated using bacteriophage T4 g32 protein which has a smaller binding site size for ssDNA in order to test these two possibilities. If SSB is assumed to bind to any available ssDNA formed transiently in these experiments, then these results indicate that RecBC has limited unwinding processivity under these assay conditions (Buffer M).

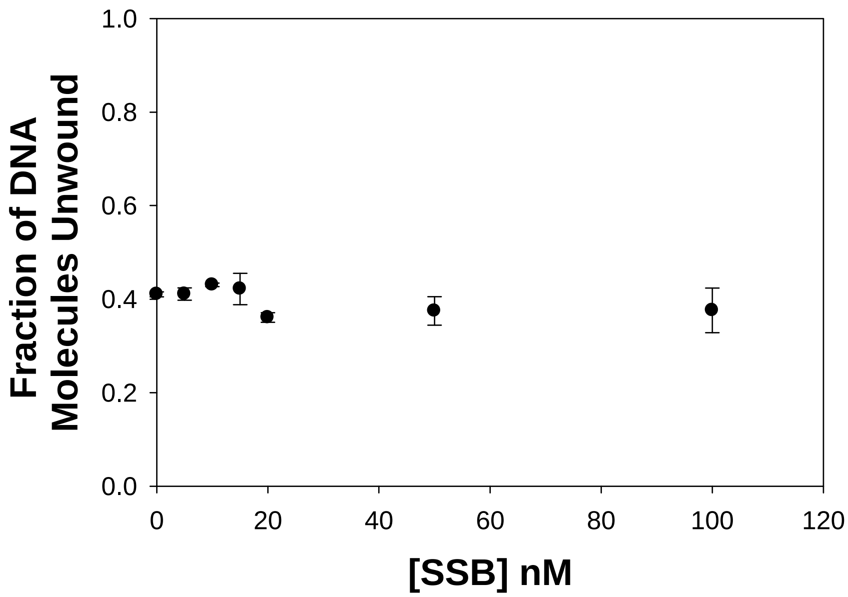

Figure 2-S6. Influence of E. coli SSB on RecBC unwinding. 20 nM RecBC was pre-bound to 2 nM radiolabeled DNA (60 bp duplex with twin dT_6 ssDNA tails) and unwinding was initiated by manual mixing with 20 µM ATP and 10 mg/mL heparin. Single time point measurements were collected after 30 seconds (reaction quenched with 0.4 M EDTA). The final unwinding amplitude is independent of [SSB] suggesting that no significant re-annealing occurs behind RecBC during DNA unwinding.

Heparin as a protein trap for RecBC during DNA unwinding

In a typical single-turnover unwinding experiment, RecBC is pre-bound to the DNA substrate and DNA unwinding is initiated by mixing with ATP and heparin. Heparin "traps" any RecBC molecules that are initially free in solution and also prevents any RecBC that dissociate during DNA unwinding from rebinding to the substrate and reinitiating the unwinding of the duplex. A heparin "trap test" is performed routinely to access how much heparin is required in our unwinding experiments. Instead of pre-forming the RecBC-DNA complex, RecBC is mixed with a solution containing ATP, DNA substrate, and X mg/mL heparin. If the amount of heparin in solution is insufficient to function as an effective trap, then RecBC will be able to bind to the DNA substrate and initiate DNA unwinding. **Figure 2-S7** shows that in the absence of heparin, RecBC can unwind ~30% of a 60 bp DNA substrate (at 10 µM ATP after mixing) but at 3 mg/mL heparin (1.5 mg/mL after 1:1 mixing), the amount of DNA unwound is decreased significantly (~ 4%). At 6 mg/mL heparin (3 mg/mL after 1:1 mixing), RecBC is unable to bind to DNA substrate and no DNA unwinding is observed.

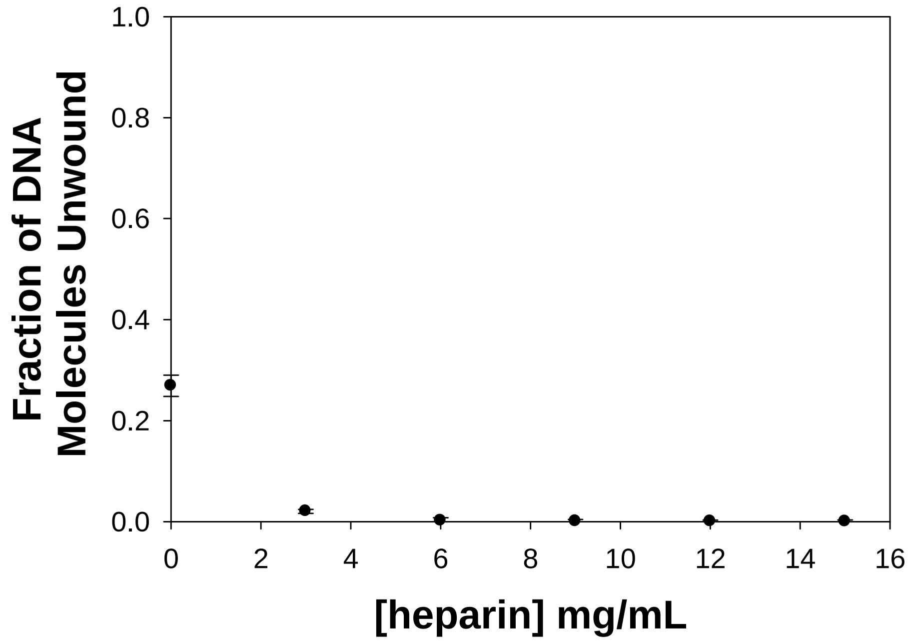

Figure 2-S7. Trap test for RecBC unwinding. 20 nM RecBC was mixed with a solution containing 2 nM radiolabeled DNA substrate (60 bp DNA duplex with twin dT_6 ssDNA tails), 20 µM ATP, and X mg/mL heparin. Single time point measurement was collected after 30 seconds. RecBC is unable to bind to the DNA substrate and initiate unwinding at [heparin] > 6 mg/mL.

Influence of 3' ssDNA tail length on RecBC unwinding imitation

Wong et al. (Wong, Lucius et al. 2005) have observed that the binding affinity of RecBC and RecBCD for a DNA end increases when the 3' ssDNA tail length increases from 0-6 nts but then the affinity decreases dramatically if the 3' ssDNA tail length is extended beyond 6 nt (up to 20 nt). This decrease in binding affinity results from paying an unfavorable entropic cost for forming a ssDNA loop on the 3' terminating DNA strand (Wong, Rice et al. 2006). I was therefore interested in whether the formation of this ssDNA loop influences RecBC unwinding. Using a 24 bp DNA substrate with a pre-formed 5'-$(dT)_6$ ssDNA tail, I have examined the effects of the 3' ssDNA tail length (3'-$(dT)_L$) on the initiation of DNA unwinding by RecBC. The unwinding time courses collected for L = 0-30 nts are shown in **Figure 2-S8A** and the unwinding kinetics were analyzed using **Equation 1** (Chapter 2) based on the *n*-step sequential mechanism shown in **Scheme 1** (Chapter 2) with m = 5.0 bp (constrained). The resulting best fit kinetic parameters are plotted versus 3' ssDNA tail length in **Figure 2-S8B**: the total unwinding amplitude A_t (as well as the fast and slow phase components) along with k_{obs} (microscopic unwinding rate), k_{np} (isomerization rate for converting between productive and non-productive RecBC-DNA complexes), and x (fraction of productive RecBC-DNA complexes).

Interestingly, the total unwinding amplitude increases as the 3' ssDNA tail length is increased from 0-6 nts and decreases when the tail is extended beyond 6 nts. This correlates well with the binding affinity measurements by Wong et al (Wong, Lucius et al. 2005). A control unwinding experiment performed with the 5' ssDNA tail extended to 15 nts (while keeping the 3' tail at 6 nts) indicate that the 5' tail length has no effect on unwinding initiation. The unwinding contribution from the fast phase of unwinding (resulting from productive RecBC-DNA complexes) also correlates well with previous equilibrium studies and decreases when the 3' ssDNA tail length is extended beyond 6 nts. This indicates that formation of the ssDNA loop on the 3' terminating DNA strand promotes the formation of non-productive RecBC-DNA complexes. Additional unwinding experiments employing a similar strategy as Wong et al (Wong, Rice et al. 2006) by incorporating regions of PEG in the 3' ssDNA tail can be used to test whether preventing loop formation rescues DNA unwinding by forming productive RecBC-DNA complexes.

A.

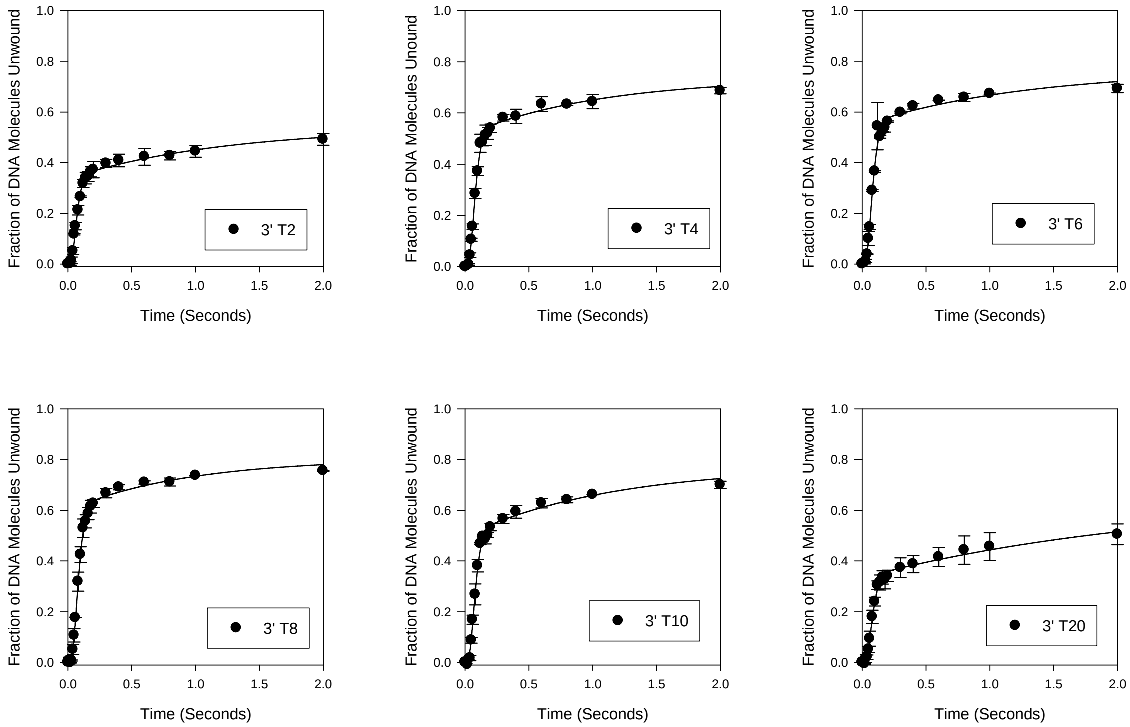

Fraction of DNA Molecules Unwound
Time (Seconds)
3' T2
Fraction of DNA Molecules Unound
3' T4
3' T6
3' T8
3' T10
3' T20

B.

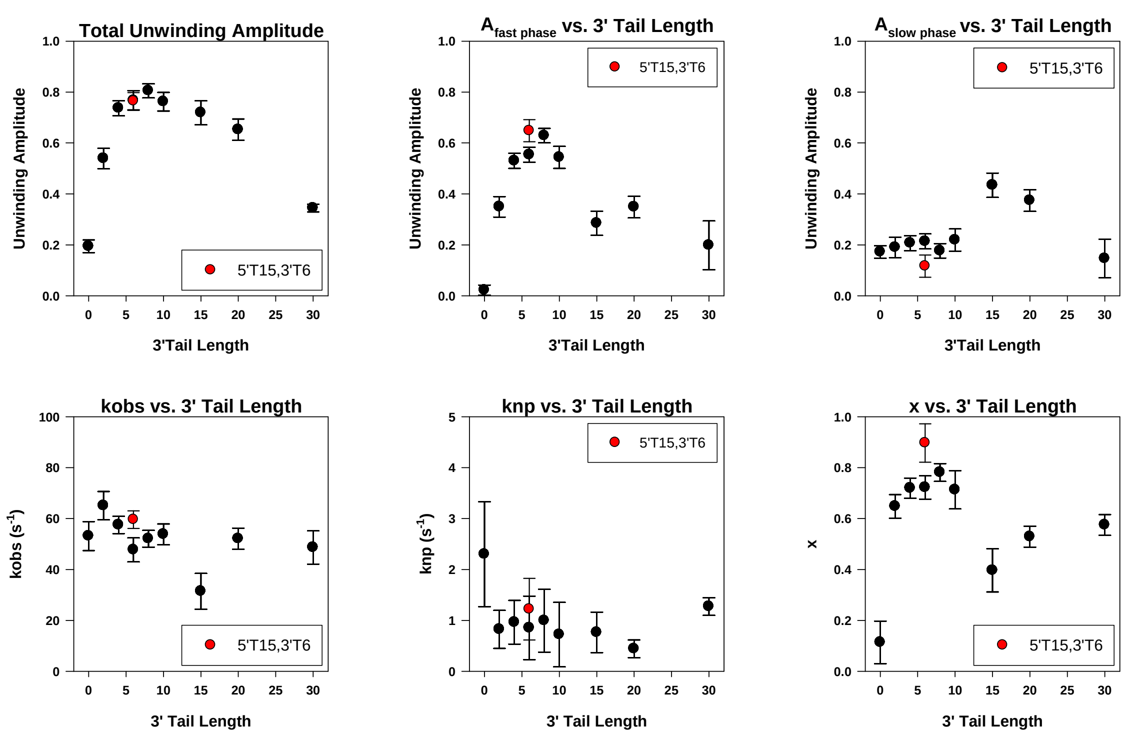

Total Unwinding Amplitude
Unwinding Amplitude
3'Tail Length
5'T15,3'T6
A fast phase vs. 3' Tail Length
A slow phase vs. 3' Tail Length
kobs vs. 3' Tail Length
kobs (s-1)
3' Tail Length
knp vs. 3' Tail Length
knp (s-1)
x vs. 3' Tail Length
x

Figure 2-S8. RecBC unwinding of a 24 bp substrate possessing pre-existing 5'-(dT_6), and 3'-$(dT)_L$ ssDNA tails. Experiments were performed by pre-mixing 20 nM RecBC with 2 nM DNA substrate (radiolabeled with ^{32}P) and unwinding was initiated by rapid mixing with 10 mM ATP and 15 mg/mL heparin. **A.)** Unwinding time courses for L = 2, 4, 6, 8, 10, and 20 are shown. Unwinding kinetics were analyzed using **Equation 1** (based on the *n*-step sequential mechanism shown in **Scheme 1** in Chapter 2) with m = 5.0 bp (fixed) and the smooth black curves are simulations based on the best fit parameters. **B).** The best fit parameters are plotted versus 3' ssDNA tail length. These include the total unwinding amplitude A_t (as well as the fast/slow phase components), k_{obs}, k_{np}, and x. (●) A control experiment in which the DNA substrate possesses pre-formed 5'dT_{15}, 3'dT_6 tails.

Chapter III

E. coli RecBC Helicase Has Two Translocase Activities Controlled by a Single ATPase Motor

Preface to Chapter III

This chapter presents pre-steady state translocation kinetic studies of the RecBC enzyme to better understand the relationship between DNA unwinding and translocation. Thus far, RecBC translocation activity and directionality have been inferred indirectly by Bianco and Kowalczykowski through a series of unwinding experiments in which the DNA substrate contains a ssDNA gap in between two duplex regions (Bianco and Kowalczykowski 2000). When the 3' to 5' DNA strand (relative to the RecBC loading site) is continuous, then RecBC can bypass even a 30 nt gap and unwind the distal duplex with the same efficiency versus when there is a nick present. If however the 5' to 3' ssDNA strand is continuous instead, then a decrease in efficiency is observed for the unwinding of the distal duplex when a 30 nt gap is present rather than a nick. Based on these results, Bianco and Kowalczykowki concluded that RecBC unwinds and translocates strictly with 3' to 5' directionality using a quantum inchworm mechanism. To characterize this activity further, I first examined the translocation activity of the RecB monomer, and then I monitored RecBC translocation not only directly using a stopped-flow fluorescence assay, but also indirectly using a similar approach as Bianco and Kowalczykowski (Bianco and Kowalczykowski 2000). This chapter is based on a manuscript that has been submitted in 2010 to Nature Structural and Molecular Biology (currently in press); translocation data not included in the original paper are also presented in this chapter.

E. coli RecBC Helicase has Two Translocase Activities Controlled by a Single ATPase Motor

Colin G. Wu, Christina Bradford and Timothy M. Lohman*

Department of Biochemistry and Molecular Biophysics

Washington University School of Medicine

660 S. Euclid Avenue, Box 8231

Saint Louis, MO 63110

Running title: Two concerted translocase activities within RecBC

Keywords: allostery, translocation, DNA, fluorescence, recombination

*Address correspondence to: T. M. Lohman

Department of Biochemistry and Molecular Biophysics

Washington University School of Medicine

660 S. Euclid Avenue, Box 8231

Saint Louis, MO 63110

(314)-362-4393

(314)-362-7183 (Fax)

lohman@biochem.wustl.edu

Abstract

Escherichia coli RecBCD is a DNA helicase with two ATPase motors (RecB, a 3´ to 5´ translocase, and RecD, a 5´ to 3´ translocase) that functions in repair of double-stranded DNA breaks. The RecBC heterodimer, with only the RecB motor, remains a processive helicase. Here we examined RecBC translocation along single stranded (ss) DNA. Surprisingly, we find that RecBC displays two translocase activities: the primary translocase moves 3´ to 5´, while the secondary translocase moves RecBC along the opposite strand of a forked DNA at a similar rate. The secondary translocase is insensitive to the ssDNA backbone polarity, and we propose that its function may be to fuel RecBCD translocation along double stranded DNA ahead of the unwinding fork, and to ensure that the unwound single strands move through RecBCD at the same rate after interaction with a Chi sequence.

Escherichia coli RecBCD is a molecular motor possessing ATPase, DNA helicase, and nuclease activities. This hetero-trimeric enzyme initiates repair of double strand (ds) DNA breaks via homologous recombination and degrades foreign DNA [1]. RecBCD possesses two motor subunits, RecB (134 kDa), a 3′ to 5′ DNA helicase and nuclease, and RecD (67 kDa), a 5′ to 3′ DNA helicase [2-4]. RecC (129 kDa) is a processivity and regulatory factor that interacts with both RecB and RecD and is structurally homologous to RecB but with non-functional helicase and nuclease domains [5-6]. Although RecB and RecD translocate with opposite directionalities along single stranded (ss) DNA, they function within RecBCD to unwind DNA in the same net direction by translocating along complementary DNA strands of the duplex [6], as depicted in **Figure 1**. To initiate recombinational DNA repair, RecBCD first binds to a dsDNA break and unwinds the DNA using its bipolar helicase activity. At first, RecD is the faster motor [4,7] and the RecB nuclease activity preferentially degrades the 3′ ssDNA end until the complex recognizes a Chi (crossover hotspot instigator) sequence (5′–GCTGGTGG) within the unwound 3′-ssDNA. At this point, the enzyme pauses then continues to unwind at a reduced rate with RecB as the faster motor. In addition, the nuclease selectivity switches to act exclusively on the 5′-ssDNA end, producing a 3′-ssDNA end onto which RecA enzyme is loaded. The resulting RecA filament then initiates homologous recombination to repair of the dsDNA break [1]. RecB and RecD are both superfamily 1 (SF1) DNA helicases, each with a functional ATPase motor[2]. In the absence of RecD, a stable heterodimeric RecBC complex retains highly processive and rapid helicase activity[4,8-10].

The DNA binding [11-14] and helicase properties of RecBCD and RecBC [3-4,8,10,15-20] have been studied, and structures of RecBCD bound to a duplex DNA end have been determined [6,21] (**Fig. 1**). Upon binding to a blunt ended DNA duplex, both RecBCD and RecBC [6,11,13,22] melt out 5–6 base pairs (bp) in a Mg^{2+}-dependent, but ATP-independent reaction. However, RecBCD unwinds DNA more rapidly than RecBC [4]; (774 ± 16 bp s^{-1} vs. 348 ± 5 bp s^{-1}) under the same conditions [10,18-19].

To unwind DNA processively, a helicase must also translocate along DNA. From DNA unwinding experiments, Bianco and Kowalczykowski [8] inferred that RecBC translocates along ssDNA with 3′ to 5′ directionality, consistent with the directionality of the RecB motor [23-24]. However, the ssDNA translocation properties of RecB, RecBC and RecBCD have not been examined directly, and thus, the relationship between ssDNA translocation and DNA unwinding is not established. Here, we examined ssDNA translocation of RecB and RecBC and show that RecBC not only possesses its expected primary 3′ to 5′ ssDNA translocase activity, but also a second previously undetected translocation activity, both of which are controlled by the RecB motor. This discovery has important implications for the mechanism and regulation of DNA unwinding activities by RecBC and RecBCD.

Results

<u>RecB monomer translocation along ssDNA</u>

A stopped-flow fluorescence approach [25] (see **Methods**) was used to monitor RecB translocation along a series of ss oligodeoxythymidylates, $(dT)_L$, L nucleotides long with a fluorophore (Cy3 or Oregon Green (OG)) attached on the 5′- or the 3′-end. When

RecB reaches the ssDNA end labeled with Cy3 or OG, Cy3 fluorescence is enhanced, whereas OG fluorescence is quenched; hence, one can monitor the kinetics of RecB arrival at the ssDNA ends. Use of a two-fold molar excess of ssDNA over RecB ensures that no more than one RecB monomer is bound to each ssDNA. Translocation was initiated by mixing pre-formed RecB–$(dT)_L$ complexes with ATP and heparin, the latter serving as a trap to prevent rebinding to the DNA of any RecB that dissociates during translocation or that was initially free. Hence, a single round of translocation is monitored, although multiple rounds of ATP hydrolysis occur.

The translocation time courses for different DNA lengths (**Fig. 2a** and **2b**) indicate that RecB monomers bind randomly to $(dT)_L$ and translocate with 3′ to 5′ directionality [25]. Identical experiments performed with a $(dT)_{54}$ substrate with Cy3 on the 3′ end of the ssDNA, show an exponential decrease in Cy3 fluorescence (**Fig. 2c**), the rate of which is independent of ssDNA length (data not shown) indicating RecB translocates away from the 3′-end. These data indicate that RecB translocates along ssDNA with biased 3′ to 5′ directionality.

The time courses in **Figure 2a** and **2b** were analyzed using the *n*-step sequential translocation model in **Scheme 1 (Eq. S1**), to obtain fluorophore-independent estimates of the translocation kinetic parameters (**Table 1**). A dissociation rate constant, $k_d = 7.5 \pm 0.3\ s^{-1}$, determined from independent RecB–poly(dT) dissociation experiments (see **Supplementary Fig. 1**), was constrained in the analysis of the translocation time courses as described [26]. This analysis indicates that RecB translocates along ssDNA in the 3′ to 5′ direction with a macroscopic rate of $m_t k_t = 803 \pm 13$ nucleotides per second (nt s^{-1}). The smooth curves in **Figure 2** show that the *n*-step sequential model provides a good description of the translocation kinetics.

ssDNA translocation by RecBC

We next examined ssDNA translocation of RecBC using the same 5′–Cy3–$(dT)_L$ substrates; however, no translocation activity was detected. In fact, **Figure 2d** shows exponential decreases in Cy3 fluorescence when pre-bound RecBC–DNA complexes (5′–Cy3–$(dT)_{54}$ or $(dT)_{54}$–Cy3–3′) were mixed with ATP and heparin, suggesting that RecBC is unable to initiate translocation on ssDNA alone and instead dissociates from the ssDNA. Based on the structures of RecBCD–DNA complexes [6,21] (**Fig. 1**), we hypothesize that it is difficult for ssDNA to be threaded into the RecBC complex to properly engage the RecB motor and designed a different DNA substrate to monitor RecBC translocation.

RecBC binds weakly to ssDNA and blunt duplex DNA ends, but binds with high affinity to a DNA end possessing twin 5′-dT_6 and 3′-dT_6 tails [13] and RecBC can rapidly initiate DNA unwinding from such a site [10]. Therefore, we hypothesized that once RecBC initiates DNA unwinding from this loading site, it might continue to translocate in the 3′ to 5′ direction along a $(dT)_L$ ssDNA extension. The modified DNA substrates used to test for RecBC translocation along ssDNA are shown schematically in **Figure 3a** and **3b**. These substrates contain a 24 bp duplex with a high affinity RecBC loading site at one end. On the other end of the duplex is a ssDNA ($(dT)_L$) extension of length, *L*, labeled on its 5′-end with either Cy3 or Fluorescein (F); these substrates should detect 3′ to 5′ translocation of RecBC along the ss-$(dT)_L$ extensions. To differentiate between the two

DNA strands in these molecules, we refer to them as the 3′-terminated strand and the 5′-terminated strand, where the 3′ or 5′ denotes the duplex end containing the RecBC loading site. Hence, in **Figure 3a,** the strand with the ssDNA extension is the 3′-terminated strand. To ensure that RecBC initiates at the high affinity loading site, a two-fold molar excess of DNA (200 nM) over RecBC (100 nM) was used. If all RecBC enzymes initiate DNA unwinding from this unique site, we expect a measurable lag time before RecBC arrives at the fluorophore-labeled 5′-ssDNA end [27].

The results of experiments with RecBC and these DNA substrates show a lag phase (**Fig. 3a–3b**), the duration of which increases with ssDNA extension length, *L*, consistent with RecBC translocating along the extension in the 3′ to 5′ direction after unwinding the 24 bp duplex. For the 5′–Cy3–$(dT)_L$ extensions (**Fig. 3a**), Cy3 fluorescence increases after the lag, reflecting arrival of RecBC at the 5′-end, after which Cy3 fluorescence decreases to its starting value after ~ 2 seconds, reflecting RecBC dissociation. The same trend, but with a transient quenching of fluorescein fluorescence is observed for DNA with 5′–F–$(dT)_L$ extensions (**Fig. 3b**).

We analyzed these time courses using two approaches**:** an analysis of the "lag time" (defined in **Supplementary Fig. 2**) and an analysis of the complete time course (described in **Supplementary Data**). The "lag time" for each time course reflects the average time for RecBC to reach the 5′ end of the ssDNA and is linearly dependent on the $(dT)_L$ extension length, *L* (see **Fig. 3e**), consistent with directional translocation. The reciprocal slope of these plots yields an estimate of the 3′ to 5′ translocation rate, which is the same for both substrates (909 ± 51 nt s^{-1} (Cy3); 1,030 ± 53 nt s^{-1} (F)). Since all

DNA molecules contain the same 24 bp duplex, these rates only reflect ssDNA translocation.

We also analyzed the full time courses in **Figure 3a** and **3b** using **Scheme 2** (**Eq. S2**), which combines two tandem *n*-step sequential schemes, reflecting the unwinding of the 24 bp duplex by RecBC, followed by translocation of RecBC along the $(dT)_L$ extensions. In this analysis, the DNA unwinding kinetic parameters (k_U and m_U) were constrained to the values determined from a previous study of DNA unwinding by RecBC performed under the same solution conditions [10], allowing us to float only the kinetic parameters for RecBC translocation. The resulting ssDNA translocation rate of 920 ± 33 nt s^{-1} is the same within error as the rates determined from the “lag time” analyses. Both Cy3 and fluorescein time courses are well described by this mechanism and the parameters in **Table 1**, as shown by the simulated curves in **Figure 3a** and **3b**.

RecBC has a distinct secondary translocase activity

We next performed control experiments with RecBC using a similar set of partial duplex substrates but with the fluorophore-labeled $(dT)_L$ ssDNA extending from the 5´-terminated strand. If RecBC translocates along ssDNA with strict 3´ to 5´ directionality, then no length dependent translocation signal should be observed on these substrates since the strand along which RecB translocates stops at the end of the duplex; therefore, RecBC would be expected to either dissociate or become stuck after unwinding the 24 bp duplex. To our great surprise, we observed the characteristic signature of ssDNA translocation (length-dependent lag, followed by a peak (trough) in fluorescence) (**Fig. 3c–3d**) indicating movement of RecBC in the unexpected 5´ to 3´ direction.

“Lag time” analyses (**Fig. 3e**) show linear dependences on ssDNA length, consistent with RecBC translocation in the 5′ to 3′ direction with rates of 990 ± 49 nt s^{-1} (Cy3) and 1187 ± 61 nt s^{-1} (F), which are the same within error as the rates determined for RecBC translocation in the 3′ to 5′ direction. Although the time courses observed for the two types of DNA substrates ($(dT)_L$ extensions on the 3′-terminated strand (**Fig. 3a–b**) versus on the 5′-terminated strand (**Fig. 3c–3d**)) show the same qualitative characteristics, they differ in detail and are not superimposable (see **Supplementary Fig. 3**). The amplitudes of the fluorescence changes (both Cy3 and F) are larger and the dissociation rates of RecBC are slower for the DNA substrates that monitor 3′ to 5′ translocation. Furthermore, the complete time courses for the DNA substrates that monitor 5′ to 3′ translocation are not described as well by the simple tandem *n*-step sequential model of **Scheme 2**, suggesting that additional steps (e.g., pausing or conformational rearrangement or multistep dissociation from the ssDNA end) may occur. From here on, we will refer to the 3′ to 5′ translocation activity as the “primary” RecBC translocase, and the apparent 5′ to 3′ translocation activity as the “secondary” RecBC translocase.

We note that when RecB alone is examined using the DNA substrates in **Figure 3a** and **3c**, we observe translocation profiles similar to those shown in **Figure 2a** and **2c** (data not shown), indicating that RecB preferentially loads onto the ssDNA extensions at random sites and moves with 3′ to 5′ directionality. When RecC alone is examined with any of the DNA substrates described above, no translocation activity is observed. We also note that the RecBC used here was purified from *E. coli* strains that do not express RecD and thus the secondary translocase activity is not due to RecD contamination.

ATP-dependence of the primary and secondary translocase activities

We next examined the effect of [ATP] on the primary and secondary translocase activities of RecBC. Cy3 time courses were obtained for all five $(dT)_L$ extension lengths at each [ATP]. Both primary and secondary translocation rates, determined from "lag time" analyses (see **Supplementary Fig. 4**), display hyperbolic dependences on [ATP] (**Fig. 3f**) and were fit to the Michaelis-Menton model (**Eq. S4**). The primary translocase has V_{max} = 946 ± 64 nt s^{-1} and K_M = 203 ± 32 μM while the secondary translocase has V_{max} = 1,055 ± 75 nt s^{-1} and K_M = 123 ± 28 μM; hence, both K_M values are similar. Translocation by the RecB monomer alone has V_{max} = 860 ± 53 nt s^{-1} and K_M = 125 ± 38 μM (**Fig. 3f**).

The primary 3′ to 5′ translocation activity of RecBC was anticipated, but our discovery of a secondary 5′ to 3′ translocase activity was surprising. Both translocase rates are similar over a range of [ATP] and [NaCl] (**Supplementary Fig. 6)**, suggesting that they are both driven by the same motor (RecB). Since RecB ATPase activity is strongly stimulated by binding ssDNA [23,28], it would seem necessary for the primary ssDNA binding site of RecB to remain bound to ssDNA during the course of both translocase activities. This suggests that in order for RecBC to translocate in the 5′ to 3′ direction after unwinding the 24 bp duplex (**Fig. 3c**), the primary ssDNA binding site within RecB must remain bound to the short unwound 3′-terminated ssDNA strand. If instead, RecBC translocated off the end of the unwound ssDNA, then RecB ATPase activity would decrease dramatically and would not support the secondary translocation activity.

We designed two DNA substrates (see **Fig. 4a** and **4b**) to test whether the primary RecBC translocase stops and remains bound to the end of the short ssDNA after unwinding the 24 bp duplex. The ends of the $(dT)_{60}$ extensions are labeled with Cy3, while the ends of the shorter strand that forms the 24 bp duplex are labeled with Cy5. The Cy3 (donor) and Cy5 (acceptor) fluorophores can undergo fluorescence resonance energy transfer (FRET) that can be monitored as a change in the Cy5 acceptor fluorescence when the Cy3 donor is excited. Thus, if one of either translocase gets stuck at the end of the 24 bp duplex, the Cy3 will be brought closer to the Cy5 resulting in a transient increase in Cy5 fluorescence. However, if RecBC translocates past the Cy5 donor and releases the short Cy5 labeled strand after unwinding, then a decrease in Cy5 fluorescence should be observed.

The results of the two FRET experiments are shown in **Figure 4a** and **4b**. The substrate in **Figure 4a** shows a lag followed by a transient increase in Cy5 fluorescence and then a decrease, consistent with the primary translocase remaining bound to the end of the unwound duplex while the secondary translocase continues to move along the other strand. Superimposed on the Cy5 time course is the time course of arrival of RecBC at the 3′–Cy3 labeled end (determined using a DNA containing only the Cy3 fluorophore). The peak in Cy5 fluorescence occurs slightly before the peak in the Cy3 fluorescence, as expected. In contrast, the substrate in **Figure 4b** shows only a decay in Cy5 fluorescence, suggesting dissociation of the Cy5 labeled strand after the 24 bp duplex is unwound since the primary RecBC translocase can translocate uninterrupted on this DNA. These results indicate that when RecBC reaches an end or gap in the 3′-terminated DNA strand, the primary translocase stops and remains bound to the ssDNA while continuing to hydrolyze ATP which drives the secondary translocase. Hence, we conclude that the RecB ATPase motor drives both the primary and secondary translocase activities.

Simultaneous translocation of RecBC along both strands of ssDNA

Although both translocase activities are fueled by the RecB motor, we anticipate that RecBC uses two distinct DNA binding sites for the two translocation activities. Hence, we designed DNA substrates, shown schematically in **Figure 5a**, to examine whether RecBC can translocate along the two single strands simultaneously. These substrates possess the same 24 bp duplex with a RecBC loading site on one end, but two non-complementary ssDNA ($(dT)_L$) extensions of equal length on the other. The $(dT)_L$ extensions are labeled either on the 5′-end or the 3′-end with Cy3 to independently monitor the primary or secondary translocase, respectively. RecBC shows identical time courses (when normalized to the peak fluorescence) for translocation along either strand, as shown in **Figure 5a**. In fact, only a slightly (~15%) larger Cy3 enhancement is observed when Cy3 is on the 5′-end of the DNA extension (**Supplementary Fig. 5**). The fact that the normalized translocation time courses are identical (for a given L), regardless of which strand is monitored, indicates that RecBC translocates along both DNA strands simultaneously and with identical rates.

Consistent with directional translocation, we observe lag kinetics for all time courses and the lag times increase with increasing L (**Fig. 5b**). Interestingly, when RecBC translocates along both strands simultaneously, the rate of translocation is substantially slower (671 ± 47 nt s^{-1} (5′–Cy3), 621 ± 43 nt s^{-1} (3′–Cy3)) than when only one strand is present (~900–1,100 nt s^{-1}). This indicates that both strands participate in RecBC translocation. Furthermore, the rates for both the primary and secondary ssDNA translocases are identical, and slightly faster than the DNA unwinding rate of RecBC measured under the same solution conditions (348 ± 5 bp s^{-1}) [10].

RecBC translocation on DNA with reversed polarity backbone linkages

We next examined whether either translocase is affected by reversing the polarity of the phosphodiester backbone in the ssDNA extension. Since the primary ssDNA binding site of the RecB motor (1A and 2A sub-domains) binds ssDNA with a distinct polarity [6,11,21] (see **Fig. 1**), the primary (3′ to 5′) translocase should stop if the motor encounters a 5′–5′ phosphodiester linkage within the ssDNA extension. We introduced a 5′–5′ linkage in the lower (3′-terminated) strand just after the 24 bp duplex region (**Fig. 5c**), which reverses the backbone polarity of the $(dT)_{75}$ extension in that strand. The polarity of the 5′-terminated strand was not changed. We generated two DNA substrates (indicated I and II in **Fig. 5c**), differing only by which ssDNA extension was labeled with Cy3, so that translocation along each strand could be monitored independently. The time courses in **Figure 5c** indicate that reversing the backbone polarity of the bottom (3′-terminated) strand (DNA II) blocks the primary RecBC translocase, as expected. However, the secondary translocase still moves along the top (5′-terminated) strand (DNA I).

We then introduced a 3′–3′ linkage in the top (5′-terminated) strand (**Fig. 5d**, DNA III and IV). Since the backbone polarity of the bottom ssDNA extension is not interrupted there was no effect on the primary translocation activity. However, the secondary translocase was also functional, even though the backbone polarity of the top (5′-terminated) strand was reversed. This indicates that the secondary translocase of RecBC is insensitive to the ssDNA backbone polarity. This surprising conclusion is further supported by comparisons of other variants of reversed polarity substrates (see **Supplementary Fig. 5)**. In all cases, the primary translocase is blocked by a polarity reversal in the 3′-terminated strand, whereas the secondary translocase is unaffected by a polarity reversal in the 5′-terminated strand.

As a further test of whether RecBC translocates along both ssDNA extensions, we examined a DNA substrate with two ssDNA extensions that are both end labeled, one with Cy3 and one with Cy5 (**Fig. 5e**). With this DNA, changes in FRET between Cy3 and Cy5 should occur if the ends of the ssDNA extensions are brought closer together as RecBC translocates. **Figure 5e** shows the anti-correlated Cy3 and Cy5 time courses consistent with FRET resulting from the simultaneous translocation of the DNA strands through the RecBC enzyme. Reversing the backbone polarity within the top (5′-terminated) ssDNA extension does not affect the secondary translocase activity (**Figure 5f**).

Re-initiation of DNA unwinding after RecBC crosses a ssDNA gap

Previous studies inferred a 3′ to 5′ directionality for RecBC ssDNA translocation by examining its ability to unwind two DNA duplexes separated by ssDNA gaps [8]. We therefore performed experiments using similar gapped DNA substrates (**Fig. 6**), which contain a RecBC loading site on one end of a 24 bp (proximal) duplex, followed by a ssDNA ($(dT)_L$) extension and then a 40 bp (distal) duplex. Two types of DNA substrates were made such that a gap occurs in either strand of the duplex DNA, with gap lengths of L = 2, 21 or 41 nucleotides. The 5′-ends of one strand of both DNA duplexes were radiolabeled with ^{32}P so that unwinding of both duplexes could be monitored in the same experiment[10,18]. RecBC initiates only from the high affinity loading site since it binds weakly and initiates unwinding poorly from blunt ends[13,10]. Because DNA was in excess over RecBC and single-round conditions were used, the maximum amount of DNA unwinding is limited by the RecBC concentration (2 nM).

In the substrates used in **Figure 6a**, the ssDNA connecting the proximal and distal duplexes is the strand along which the primary RecBC translocates (3′ to 5′). For the substrates in **Figure 6b**, the ssDNA in the gap is the strand along which the secondary RecBC translocates. For both substrates, RecBC unwinds ~85% of the 24 bp proximal duplex with time courses consistent with previous RecBC studies [10]. Furthermore, RecBC can re-initiate unwinding of the distal 40 bp DNA duplex equally well for ssDNA gaps of different lengths, regardless of which strand spans the gap. The extent of the lag phase increases with increasing gap length, L. Since the proximal (24 bp) and the distal (40 bp) duplexes are identical in all substrates, the shifts in lag times reflect only the additional time required for RecBC to traverse the progressively longer ssDNA gaps.

We analyzed these time courses using **Scheme 3** (**Eq. S3**), which assumes three stages, with RecBC starting from the high affinity loading site: (1)-unwinding of the proximal duplex, (2)- translocation along the ssDNA region, and (3)- unwinding of the distal duplex. The RecBC DNA unwinding rates were constrained to those determined previously (396 ± 15 bp s^{-1}) [10], while the ssDNA translocation kinetic parameters were allowed to float. This analysis indicates that RecBC translocates along ssDNA in the 3′ to

5′ direction using its primary translocase with a rate of 928 ± 38 nt s^{-1}, and along the other strand in the 5′ to 3′ direction using its secondary translocase with the same rate (919 ± 42 nt s^{-1}). The observation that the primary and secondary translocases move with the same rates supports our earlier conclusions obtained using the fluorescently labeled DNA (**Fig. 3a–d**).

Discussion

RecBC has two translocase activities, both controlled by the RecB motor

To date, SF1 translocases containing only one ATPase motor have been observed to translocate uni-directionally along ssDNA[29-33]. It was therefore unexpected to find that RecBC, possessing only a single canonical motor (RecB), displays two distinct translocase activities. The primary translocase activity is sensitive to the phosphodiester backbone polarity and moves only in a 3′ to 5′ direction, consistent with the translocation properties of the isolated RecB motor. However, the secondary translocase, which moves at the same rate as the primary, is insensitive to the ssDNA backbone polarity. Our studies with the RecB subunit alone show no evidence of the secondary translocase activity. Hence it appears that the interaction of RecB with RecC is needed to form the secondary ssDNA translocase site or to support its interactions with DNA.

The regions of RecBC that form the channel for the unwound 5′-terminated ssDNA, and thus likely involved in the secondary translocase activity, are well removed from the ATP binding site of RecB and the channel for the unwound 3′-terminated ssDNA, along which the primary translocase moves (see **Fig. 1**)[6]. Thus, the DNA binding site associated with the secondary translocase must be distinct from the ssDNA binding site responsible for the primary translocase, hence the concerted control of both translocase activities by the RecB motor must occur allosterically. Both RecBC translocases display the same rates of translocation and are ATP-dependent with K_M values similar to that measured for RecB translocation, consistent with both activities being driven by the single RecB motor.

Interestingly, when RecBC translocates along only one strand of DNA the rate is ~1,000 nt s^{-1}, whereas the rate is reduced to ~ 650 nt (or "bp") s^{-1} when it translocates along both single strands simultaneously. However, this translocation rate is still faster than the DNA unwinding rate of RecBC under the same conditions (~350 bp s^{-1}), although slower than the RecBCD unwinding rate (~750 bp s^{-1}) [10]. Importantly, the primary and secondary translocation rates of RecBC are identical when both ssDNA extensions are present. Thus both DNA strands move through the enzyme at the same rates preventing any loop formation during unwinding.

<u>Implications for RecBC translocation and DNA unwinding mechanisms.</u>

Bianco & Kowalczykowski[8] previously examined the ability of RecBC to initiate unwinding of a short DNA duplex (proximal), followed by unwinding of a second (distal) DNA duplex separated by a ssDNA gap. Using DNA substrates similar to those shown in **Figure 6**, they observed that the efficiency with which RecBC could traverse the ssDNA gap was lower when the gap was in the strand along which the primary RecBC translocase operates and concluded that RecBC translocation along ssDNA occurred strictly in the 3′ to 5′ direction. This differs from our conclusion that RecBC has two translocase activities. They[8] also observed that RecBC could traverse ssDNA gaps in the

3′-terminated strand as large as 23 ± 2 nucleotides and proposed a “quantum inch-worm” unwinding model. However, RecBC was still observed to unwind ~16% of the distal DNA duplexes, even with a gap of 30 nucleotides in that strand. Our finding that RecBC can bypass ssDNA gaps in either strand and then re-initiate DNA unwinding is qualitatively consistent with this observation[8]. However, we do not observe a difference in unwinding efficiency regardless of which strand contains the gap. These differences may be due to the absence of *E. coli* single stranded binding (SSB) protein in our experiments.

Interestingly, Bianco & Kowalczykowski[8] also observed that the ability to traverse a gap was dependent upon the length of the proximal duplex DNA that preceded the gap, and concluded that RecBC stepping was not only quantized with a periodicity of 23 ± 2 nucleotides, but also that the placement of the next step was determined by where the enzyme initiated. Although our experiments do not address this result, it seems likely that the secondary translocase activity of RecBC that we report is related to this “quantum inch-worm” behavior[8].

Where in RecBC is the secondary translocase activity and what is its function?

The general view of the mechanism of ssDNA translocation by an SF1 helicase is that ATP-hydrolysis drives coupled motions between the two RecA-like sub-domains (1A and 2A) whose interface forms the ATP binding site (**Fig. 1b**). One proposal is that these two sub-domains each contain a sub-site for binding ssDNA and these sub-sites cycle between high and low ssDNA affinity based on the nucleotide binding state (i. e., ATP, ADP–Pi, ADP, etc.), resulting in an inch-worm mechanism that moves the motor uni-directionally along the ssDNA backbone[2]. This type of motor activity is likely responsible for the primary translocase of RecBC. However, the secondary RecBC translocase must involve a distinctly different region of the enzyme, but one that is controlled allosterically by the same ATPase motor within RecB.

We suggest that the secondary translocase activity resides either in the arm region of RecB and (or) the dead nuclease domain of RecC (see **Fig. 1b**) [6]. These regions contact either the duplex DNA ahead of the fork or the 5′-terminated ssDNA. Although we detect the secondary translocase activity of RecBC as an ability to translocate along the 5′-terminated ssDNA, its actual function may be to interact with and translocate along the duplex DNA ahead of the fork. This would explain the lack of sensitivity of the secondary translocase activity to the backbone polarity of ssDNA. Hence, the RecB "arm" is a likely candidate since it contacts the dsDNA ahead of the fork.

The function of this secondary translocase may be to load the other (5′-terminated) single strand of DNA into the RecD motor. When RecBCD binds to a blunt ended DNA duplex, 5–6 bp are melted in a Mg^{2+}-dependent but ATP-independent process to form an initiation complex[6,12-13,22]. In this initiation complex, the 3′-terminated ssDNA is bound in a channel containing the RecB motor and thus is ready to be translocated upon ATP binding and hydrolysis. However, the initial length of the 5′-terminated ssDNA (5–6 nt) is not long enough to reach the motor region of RecD, although RecD can be crosslinked to this strand [12]. In fact, a 5′-terminated ssDNA of at least 10 nucleotides is needed to functionally engage the RecD motor [10,13,20]. As such, the secondary RecBC translocase activity may function to load the 5′-terminated ssDNA into the RecD motor.

The secondary translocase activity may also function after RecBCD recognizes the recombination hotspot, Chi. Following RecBCD initiation of unwinding at a blunt DNA end, the RecD motor moves faster than the RecB motor generating a ssDNA loop ahead of the fork, in the 3′-terminated ssDNA along which the primary RecB translocase operates [4]. During this time, the RecB nuclease preferentially digests the 3′-terminated strand. However, once a Chi site is recognized by RecC, the relative speeds of the RecB and RecD motors switch [7] and the nuclease selectively degrades the 5′-terminated strand. After Chi, the now faster RecB motor will eventually catch up to the RecD motor. At this point, if RecB remains faster than RecD, a different loop would form in the 5′-terminated strand ahead of the enzyme; however, this has not been observed [4]. The existence of the secondary RecBC translocase may ensure that the two unwound single strands move through RecBCD at the same rates and thus prevent loop formation after Chi recognition. The existence of concerted translocase activities would also prevent dissociation of RecBCD if a ssDNA gap is encountered on either strand during DNA unwinding after Chi.

In addition to RecBCD, two other classes of double strand DNA break resecting enzymes have been described that are hetero-dimeric and thus more similar to RecBC in that they do not possess a second RecD-like motor. AddAB from *Bacillus subtilis* has one motor subunit, AddA, but two RecB-like nuclease domains, one each on AddA and AddB [34]. AdnAB from *Mycobacterium smegmatis* has two active motors and two active nuclease domains [35]. It will be interesting to determine whether these hetero-dimeric enzymes also possess a secondary translocase activity similar to *E. coli* RecBC.

Acknowledgements

We thank Drs. R. Galletto, C. Fischer, A. Lucius, K. Maluf, E. Galburt, N. Baker, P. Burgers, G. Smith, T. Ellenberger, S. Kowalczykowski, and E. Antony for valuable discussions and comments on the manuscript, Drs. G. Smith (Fred Hutchinson Cancer Research Center, Seattle, WA), A. Taylor (Fred Hutchinson Cancer Research Center, Seattle, WA) and D. Julin (University of Maryland, College Park, MD) for plasmids and cell lines and T. Ho (Washington University School of Medicine, St. Louis, MO) for synthesis and purification of DNA. This work was supported in part by NIH GM045948 (to TML).

Author contributions

C.W. and T.M.L. designed the experiments. C.W. purified the protein, performed the stopped-flow and DNA unwinding experiments, and analyzed the data; C.B. and C.W. performed the FRET and RecBC translocation experiments as a function of [NaCl]. T.M.L. supervised the study and C.W. and T.M.L. wrote the manuscript.

Figure Legends

Figure 1. RecBCD and RecBC structures. RecB (orange), RecC (blue), and RecD (green) subunits are indicated. **(a)**. Ribbon diagram of a RecBCD–DNA complex [6,21]. **(b).** Cartoon depiction of a RecBC–DNA complex. RecB motor, nuclease, and arm domains are indicated along with the catalytically dead RecC motor and nuclease domains. The paths of the 3´- and 5´-terminated unwound ssDNA are shown.

Figure 2. RecB translocates with 3′ to 5′ directionality along ssDNA.

(a). RecB monomer translocation kinetics for a series of 5′–Cy3–$(dT)_L$ DNA (**Supplementary Table 1**, DNA I–VIII). Cy3 fluorescence from DNA alone (DNA I) is shown in filled black circles. **(b).** RecB monomer translocation kinetics for a series of 5′–OG–$(dT)_L$ substrates. OG (Oregon Green) fluorescence from DNA alone (DNA I) is shown in filled black circles. Smooth black curves in panels A and B are simulated time courses using **Equation S1** and the best fit kinetic parameters (**Table 1**). **(c).** Time course obtained with RecB and $(dT)_{54}$ –Cy3–3′ (**Supplementary Table 1**, DNA IX). **(d).** Time course obtained with RecBC and 5′–Cy3–$(dT)_{54}$ (filled circles) or $(dT)_{54}$–Cy3–3′ (opened circles).

Figure 3. RecBC displays both a primary (3′ to 5′) and secondary (5′ to 3′) translocase activity. RecBC translocation time courses obtained using the DNA substrates depicted which possesses a 24 bp duplex with a high affinity (twin-dT_6) RecBC loading site on one end and either 5′– or 3′–$(dT)_L$ ssDNA extensions on the other end. **(a).** DNA substrates labeled with Cy3 on the 5′ end of the $(dT)_L$ extension. **(b).** DNA substrates labeled with fluorescein (F) on the 5′ end of the $(dT)_L$ extension. **(c).** DNA substrates labeled with Cy3 on the 3′ end of the $(dT)_L$ extension. **(d).** DNA substrates labeled with fluorescein (F) on the 3′ end of the $(dT)_L$ extension. Smooth black curves in panels a–d are simulated time courses using **Equation S2** and the kinetic parameters in **Table 1**. **(e).** Dependence of the lag time on ssDNA extension length, L. Cy3 data from panel **a** (opened circles) (Lag time = 0.00110 L + 0.0095) (909 ± 51 nt s^{-1}). Fluorescein data from panel **b** (filled circles) (Lag time = 0.000971 L + 0.0110) (1,030 ±

53 nt s^{-1}). Cy3 data from panel **c** (opened squares) (Lag time = 0.00101 L + 0.0093) (990 ± 49 nt s^{-1}). Fluorescein data from panel **d** (filled squares) (Lag time = 0.000843 L + 0.0134) (1,187 ± 61 nt s^{-1}). **(f).** [ATP] dependence of RecBC translocation rates (from lag time analyses) for the (circles)-primary (3′ to 5′) (V_{max} = 946 ± 64 nt s^{-1}, K_M = 203 ± 32 μM); and (squares)-secondary (5′ to 3′) (V_{max} = 1,055 ± 75 nt s^{-1}, K_M = 123 ± 28 μM) translocases. (triangles)-Effects of [ATP] on RecB monomer translocation (V_{max} = 860 ± 53 nt s^{-1}, K_M = 125 ± 38 μM). Smooth curves represent fits to the Michaelis-Menton equation (**Eq. S4**) and the best fit parameters summarized in **Table 1**.

Figure 4. The primary RecBC translocase site remains bound to ssDNA upon reaching a 5′-end, while its secondary translocase continues. (a). RecBC translocation along a partial duplex substrate with a 5′ to 3′ dT_{60} ssDNA extension, doubly labeled with Cy3 and Cy5 as shown. Time course monitoring FRET as Cy5 fluorescence (filled circles) (due to exciting Cy3 donor) shows that the 3′-terminated ssDNA remains bound to RecBC while the secondary translocase continues; x Translocation time course for the same DNA, but without the Cy5 label (opened squares). **(b).** RecBC translocation along a partial duplex substrate with a 3′ to 5′ dT_{60} ssDNA extension doubly labeled with Cy3 and Cy5 as shown. Time course monitoring FRET as Cy5 fluorescence (filled circles) (due to exciting Cy3 donor) shows dissociation of the 5′-terminated ssDNA; Translocation time course for the same DNA, but without the Cy5 label (opened squares).

Figure 5. primary and secondary RecBC translocases operate simultaneously along two ssDNA extensions. Translocation of RecBC along DNA substrates containing a 24

bp duplex region with high affinity RecBC loading site on one end and two $(dT)_L$ extensions of equal length (L = 15, 30, 45, 50, 75 nucleotides) and labeled with Cy3 on one of the two ends as depicted. **(a).** Normalized time courses for DNA substrates 5′–Cy3 labeled DNA (filled circles) and 3′–Cy3 labeled DNA (opened circles) for L = 30, 45, and 75 nucleotides. **(b).** Lag time analyses of time courses; 5′–Cy3 labeled DNA (filled circles) (Lag time = 0.00149 L + 0.0098) (671 ± 47 nt s^{-1}). 3′–Cy3 labeled DNA (opened circles) (Lag time = 0.00161 L + 0.0016) (621 ± 43 nt s^{-1}). **(c).** Backbone polarity of the ssDNA extension along which the primary (3′ to 5′) translocase operates is reversed using a 5′–5′ linkage at the position indicated (red **X**). DNA I - top strand end-labeled with Cy3; DNA II - bottom strand end-labeled with Cy3. **(d).** Backbone polarity of the ssDNA extension along which the secondary translocase operates is reversed using a 5′–5′ linkage at the position indicated (red **X**); DNA III - top strand end-labeled with Cy3; DNA IV - bottom strand end-labeled with Cy3. **(e).** FRET experiment monitoring Cy3 (purple circles) and Cy5 fluorescence (blue circles) performed using the DNA substrate double labeled with Cy3 and Cy5 as depicted. Red and black squares show the time courses for a DNA possessing both ssDNA extensions, but containing only a Cy3 fluorophore (as in panel (**b**) , with L = 60)). **(f).** FRET experiment monitoring Cy3 (purple squares) and Cy5 fluorescence (blue squares) performed as in panel **(e)**, but with a DNA substrate in which the backbone polarity of the top ssDNA extension was reversed using a 3′–3′ linkage at the position indicated (red **X**).

Figure 6. RecBC re-initiation of DNA unwinding after a ssDNA gap. DNA substrates contain a proximal 24 bp duplex with a RecBC loading site (twin dT_6 fork), a ssDNA gap

of length, $L = 2$, 21 or 41 nucleotides, followed by a distal 40 bp duplex DNA. The ssDNA connecting the proximal and distal duplexes runs either 3′ to 5 (panel **a**) or 5′ to 3′ (panel **b**) relative to the RecBC loading site. **(a).** Single round time course for RecBC unwinding the proximal 24 bp duplex (diamonds) and the distal 40 bp duplex connected by a 3′ to 5′ ssDNA with $L = 2$ nt (circles), 21 nt (squares), or 41 nt (triangles). Smooth curves indicate fits to **Scheme 3** (**Eq. S3**) using the parameters ($m_t k_t = 928 \pm 38$ nt s^{-1}; $m_U k_U = 396 \pm 15$ bp s^{-1} (constrained)). **(b).** Single round time course for RecBC unwinding the proximal 24 bp duplex (diamonds) and the distal 40 bp duplex connected by a 5′ to 3′ ssDNA with $L = 2$ nt (circles), 21 nt (squares), or 41 nt (triangles). Smooth curves indicate fits to **Scheme 3** (**Eq. S3**) using the parameters ($m_t k_t = 919 \pm 42$ nt s^{-1}; $m_U k_U = 396 \pm 15$ bp s^{-1} (constrained)). Models for re-initiation of DNA unwinding by RecBC after traversing a ssDNA gap in either strand are shown below each panel.

Methods

Buffers and Reagents. Buffers were prepared with distilled, de-ionized water and filtered through 0.2 micron filters. Buffer M is 20 mM Mops-KOH (pH 7.0 at 25ºC), 30 mM NaCl, 10 mM $MgCl_2$, 1 mM 2-mercaptoethanol (2-ME), and 5% (v/v) glycerol. RecB and RecC storage buffer is Buffer C: 20 mM K phosphate (pH 6.8 at 25), 0.1 mM 2-mercaptoethanol, 0.1 mM ethylenediaminetetraacetic acid (EDTA), and 10% (v/v) glycerol. Heparin stock solutions were prepared in Buffer M as described [32]. ATP stock solutions were prepared and concentrations determined as described [10].

Proteins. *E. coli* RecB was overexpressed in *E. coli* strain V186 (which contains a deletion of the chromosomal *recB, recC and recD* genes [23] carrying pPB700 (*recB*$^{+}$) and pNM52 (*lacI*^{q}). *E. coli* RecC was overexpressed *E. coli* strain V186 carrying pBP500 (*recC*+) and pNM52. In this way we avoided any possible contamination of the RecBC prep with RecD. RecB and RecC proteins were expressed and purified separately, and stored in Buffer C as described [36]. RecB was dialyzed versus Buffer M at 4ºC before use and its concentration determined using an extinction coefficient of ε_{280} = 1.9 x 10^{5} M^{-1} cm^{-1} [36]. RecBC enzyme was reconstituted and dialyzed against Buffer M at 4ºC before use, and its concentration determined using ε_{280} = 3.9 x 10^{5} M^{-1} cm^{-1} [36].

DNA. Oligodeoxynucleotides, either unlabeled or labeled covalently with fluorescein, Cy3 or Cy5, or containing reversed polarity phosphodiester backbones were synthesized and purified and their concentrations determined as described [10]; stock solutions were dialyzed versus Buffer M and stored at –20ºC. DNA labeled with Oregon Green was purchased (Integrated DNA Technologies, Coralville, IA). The sequences of the DNA substrates used are given in **Supplementary Tables 1–3**.

Stopped-flow fluorescence experiments. Translocation kinetics experiments were performed in Buffer M at 25ºC using an SX.18MV stopped-flow fluorescence instrument (Applied Photophysics Ltd., Leatherhead, UK). RecB (50 nM) or RecBC (100 nM) were pre-mixed with DNA present in excess (100 nM or 200 nM) in one syringe of the stopped-flow apparatus, and translocation was initiated by mixing with 10 mM ATP and 8 mg mL^{-1} heparin in the other syringe. Heparin "trap tests" were performed by including the DNA substrate with the ATP and heparin solution. When mixed with RecBC no translocation signal was observed indicating that heparin trapped all of the free RecBC. Cy3 fluorescence was excited at 515 nm, and its emission was monitored at wavelengths > 570 nm using a long pass filter. Oregon Green fluorescence was excited at 508 nm, and its emission was monitored at wavelengths > 520 nm using a long pass filter. For FRET experiments, Cy3 fluorescence was excited at 515 nm and its emission was monitored at 570 nm using an interference filter while Cy5 fluorescence was monitored at wavelengths > 665 nm using a long pass filer. Analysis of translocation time courses is described in **Supplementary Data**.

DNA Unwinding. DNA unwinding kinetics was performed in Buffer M at 25ºC using a KinTek RQF-3 rapid quenched-flow instrument (University Park, PA). DNA substrates were composed of three DNA strands as depicted in **Figure 6** (**sequences in Supplementary Table 3**, **Supplementary Data**) which when annealed together, form a proximal (24 bp) and distal (40 bp) duplex DNA regions that are separated by a ssDNA $(dT)_L$ region of length L nucleotides with either 3´ to 5´ or 5´ to 3´ polarity [8]. Reporter strands from the proximal and distal duplex were radiolabeled on the 5´ end with ^{32}P as described [10]. An excess of annealed DNA unwinding substrate (20 nM) was pre-incubated with RecBC (2 nM) in one syringe and reactions were initiated by rapid mixing with an equal volume of 10 mM ATP and 8 mg mL^{-1} heparin, followed by mixing with an equal volume of 0.4 M EDTA and 10% (v/v) glycerol to quench the reaction after a predefined time interval (Δt). Unwound DNA products were resolved from the native substrates using non-denaturing polyacrylamide gel electrophoresis (PAGE) and quantified as described [10,18] Analysis of unwinding time courses is described in **Supplementary Data**.

References

1 Dillingham, M. S. & Kowalczykowski, S. C. RecBCD enzyme and the repair of double-stranded DNA breaks. *Microbiol Mol Biol Rev* **72**, 642-671 (2008).

2 Singleton, M. R., Dillingham, M. S. & Wigley, D. B. Structure and Mechanism of Helicases and Nucleic Acid Translocases. *Annu Rev Biochem* **76**, 23-50 (2007).

3 Dillingham, M. S., Spies, M. & Kowalczykowski, S. C. RecBCD enzyme is a bipolar DNA helicase. *Nature* **423**, 893-897 (2003).

4 Taylor, A. F. & Smith, G. R. RecBCD enzyme is a DNA helicase with fast and slow motors of opposite polarity. *Nature* **423**, 889-893 (2003).

5 Rigden, D. J. An inactivated nuclease-like domain in RecC with novel function: implications for evolution. *BMC Struct Biol* **5**, 9 (2005).

6 Singleton, M. R., Dillingham, M. S., Gaudier, M., Kowalczykowski, S. C. & Wigley, D. B. Crystal structure of RecBCD enzyme reveals a machine for processing DNA breaks. *Nature* **432**, 187-193 (2004).

7 Spies, M., Amitani, I., Baskin, R. J. & Kowalczykowski, S. C. RecBCD Enzyme Switches Lead Motor Subunits in Response to chi Recognition. *Cell* **131**, 694-705 (2007).

8 Bianco, P. R. & Kowalczykowski, S. C. Translocation step size and mechanism of the RecBC DNA helicase. *Nature* **405**, 368-372. (2000).

9 Korangy, F. & Julin, D. A. Efficiency of ATP Hydrolysis and DNA Unwinding by the RecBC Enzyme from *Escherichia coli*. *Biochemistry* **33**, 9552-9560 (1994).

10 Wu, C. G. & Lohman, T. M. Influence of DNA end structure on the mechanism of initiation of DNA unwinding by the Escherichia coli RecBCD and RecBC helicases. *J Mol Biol* **382**, 312-326 (2008).

11 Ganesan, S. & Smith, G. R. Strand-specific binding to duplex DNA ends by the subunits of the *Escherichia coli* RecBCD enzyme. *J.Mol.Biol.* **229**, 67-78 (1993).

12 Farah, J. A. & Smith, G. R. The RecBCD Enzyme Initiation Complex for DNA Unwinding: Enzyme Positioning and DNA Opening. *J.Mol.Biol.* **272**, 699-715 (1997).

13 Wong, C. J., Lucius, A. L. & Lohman, T. M. Energetics of DNA end binding by *E.coli* RecBC and RecBCD helicases indicate loop formation in the 3´-single-stranded DNA tail. *J. Mol. Biol.* **352**, 765-782 (2005).

14 Wong, C. J., Rice, R. L., Baker, N. A., Ju, T. & Lohman, T. M. Probing 3´-ssDNA Loop Formation in *E. coli* RecBCD/RecBC-DNA Complexes Using Non-natural DNA: A Model for "Chi" Recognition Complexes. *J. Mol. Biol.* **362**, 26-43 (2006).

15 Taylor, A. & Smith, G. R. Unwinding and Rewinding of DNA by the RecBC Enzyme. *Cell* **22**, 447-457 (1980).

16 Bianco, P. R. *et al.* Processive translocation and DNA unwinding by individual RecBCD enzyme molecules. *Nature* **409**, 374-378 (2001).

17 Spies, M. *et al.* A molecular throttle: the recombination hotspot chi controls DNA translocation by the RecBCD helicase. *Cell* **114**, 647-654 (2003).

18 Lucius, A. L. *et al.* DNA unwinding step-size of E. coli RecBCD helicase determined from single turnover chemical quenched-flow kinetic studies. *J Mol Biol* **324**, 409-428 (2002).

19 Lucius, A. L. & Lohman, T. M. Effects of temperature and ATP on the kinetic mechanism and kinetic step-size for *E.coli* RecBCD helicase-catalyzed DNA unwinding. *J. Mol. Biol.* **339**, 751-771 (2004).

20 Dillingham, M. S., Webb, M. R. & Kowalczykowski, S. C. Bipolar DNA translocation contributes to highly processive DNA unwinding by RecBCD enzyme. *J Biol Chem* **280**, 37069-37077 (2005).

21 Saikrishnan, K., Griffiths, S. P., Cook, N., Court, R. & Wigley, D. B. DNA binding to RecD: role of the 1B domain in SF1B helicase activity. *EMBO J* **27**, 2222-2229 (2008).

22 Wong, C. J. & Lohman, T. M. Kinetic control of Mg2+-dependent melting of duplex DNA ends by Escherichia coli RecBC. *J Mol Biol* **378**, 759-775 (2008).

23 Boehmer, P. E. & Emmerson, P. T. The RecB subunit of the *Escherichia coli* RecBCD Enzyme Couples ATP Hydrolysis to DNA Unwinding. *J.Biol.Chem.* **267**, 4981-4987 (1992).

24 Phillips, R. J., Hickleton, D. C., Boehmer, P. E. & Emmerson, P. T. The RecB protein of *Escherichia coli* translocates along single-stranded DNA in the 3′ to 5′ direction: a proposed ratchet mechanism. *Mol. Gen. Genet.* **254**, 319-329 (1997).

25 Fischer, C. J., Maluf, N. K. & Lohman, T. M. Mechanism of ATP-dependent translocation of E.coli UvrD monomers along single-stranded DNA. *J Mol Biol* **344**, 1287-1309 (2004).

26 Fischer, C. J. & Lohman, T. M. ATP-dependent translocation of proteins along single-stranded DNA: models and methods of analysis of pre-steady state kinetics. *J Mol Biol* **344**, 1265-1286 (2004).

27 Lucius, A. L., Maluf, N. K., Fischer, C. J. & Lohman, T. M. General methods for analysis of sequential "n-step" kinetic mechanisms: application to single turnover kinetics of helicase-catalyzed DNA unwinding. *Biophys J* **85**, 2224-2239 (2003).

28 Hickson, I. D., Robson, C. N., Atkinson, K. E., Hutton, L. & Emmerson, P. T. Reconstitution of RecBC DNase activity from purified Escherichia coli RecB and RecC proteins. *J Biol Chem* **260**, 1224-1229 (1985).

29 Brendza, K. M. *et al.* Autoinhibition of *Escherichia coli* Rep monomer helicase activity by its 2B subdomain. *Proc Natl Acad Sci U S A* **102**, 10076-10081 (2005).

30 Dillingham, M. S., Wigley, D. B. & Webb, M. R. Direct measurement of single-stranded DNA translocation by PcrA helicase using the fluorescent base analogue 2-aminopurine. *Biochemistry* **41**, 643-651 (2002).

31 Niedziela-Majka, A., Chesnik, M. A., Tomko, E. J. & Lohman, T. M. Bacillus stearothermophilus PcrA Monomer Is a Single-stranded DNA Translocase but Not a Processive Helicase in Vitro. *J. Biol. Chem.* **282**, 27076-27085 (2007).

32 Tomko, E. J., Fischer, C. J., Niedziela-Majka, A. & Lohman, T. M. A Nonuniform Stepping Mechanism for E. coli UvrD Monomer Translocation along Single-Stranded DNA. *Molecular Cell* **26**, 335-347 (2007).

33 Antony, E. *et al.* Srs2 disassembles Rad51 filaments by a protein-protein interaction triggering ATP turnover and dissociation of Rad51 from DNA. *Mol Cell* **35**, 105-115 (2009).

34 Yeeles, J. T. & Dillingham, M. S. A Dual-nuclease Mechanism for DNA Break Processing by AddAB-type Helicase-nucleases. *J Mol Biol* **371**, 66-78 (2007).

35 Unciuleac, M. C. & Shuman, S. Characterization of the mycobacterial AdnAB DNA motor provides insights into the evolution of bacterial motor-nuclease machines. *J Biol Chem* **285**, 2632-2641 (2010).

36 Lucius, A. L., Jason Wong, C. & Lohman, T. M. Fluorescence stopped-flow studies of single turnover kinetics of *E.coli* RecBCD helicase-catalyzed DNA unwinding. *J. Mol. Biol.* **339**, 731-750 (2004).

Table 1. RecB and RecBC translocation kinetics summary

NLLS fit to Eq S1 (Scheme 1)	$m_t k_t$ (nt s^{-1})	k_t (s^{-1})	m_t (nt)	k_d (s^{-1})	k_{end} (s^{-1})	d (nt)	r
RecB	803 ± 13	168 ± 25	4.8 ± 0.3	7.5 ± 0.3 (constrained)	11 ± 3	18 ± 2	0.8 ± 0.1
NLLS fit to Eq S2 (Scheme 2)	**$m_t k_t$ (nt s^{-1})**	**k_t (s^{-1})**	**m_t (nt)**	**$m_U k_U$ (bp s^{-1})**	**k_U (s^{-1})**	**m_U (bp)**	**k_{end} (s^{-1})**
RecBC (3′ to 5′) primary along ssDNA	920 ± 33	260 ± 41	3.5 ± 0.2	348 ± 5 (constrained)	79 ± 11 (constrained)	4.4 ± 0.1 (constrained)	2.7 ± 0.1
“lag time” analysis	**$m_t k_t$(Cy3) (nt s^{-1})**	**$m_t k_t$(F) (nt s^{-1})**					
RecBC (3′ to 5′) primary along ssDNA	909 ± 51	1,030 ± 53					
RecBC (5′ to 3′) secondary along ssDNA	990 ± 49	1,187 ± 61					
RecBC along both ssDNA strands (5′ Cy3)	671 ± 47						
RecBC along both ssDNA strands (3′ Cy3)	621 ± 43						

Fit to Eq S4	V_{max} (nt s^{-1})	K_M (μM)				
RecB	860 ± 53	125 ± 38				
RecBC (3′ to 5′) Primary	946 ± 64	203 ± 32				
RecBC (5′ to 3′) Secondary	1,055 ± 75	123 ± 28				
NLLS fit to Eq S3 (Scheme 3)	**$m_t k_t$ (nt s^{-1})**	**k_t (s^{-1})**	**m_t (nt)**	**$m_U k_U$ (bp s^{-1})**	**k_U (s^{-1})**	**m_U (bp)**
RecBC gap unwinding 3′ to 5′ ssDNA gap	928 ± 38	242 ± 60	3.8 ± 0.4	396 ± 15 (constrained)	90 ± 25 (constrained)	4.4 ± 1.7 (constrained)
RecBC gap unwinding 5′ to 3′ ssDNA gap	919 ± 42	262 ± 57	3.5 ± 0.2	396 ± 15 (constrained)	90 ± 25 (constrained)	4.4 ± 1.7 (constrained)

The best fit parameters for RecB and RecBC translocation are summarized. The equations and kinetic schemes used to analyze the data are given in **Supplementary Data**. Errors denote s.d.

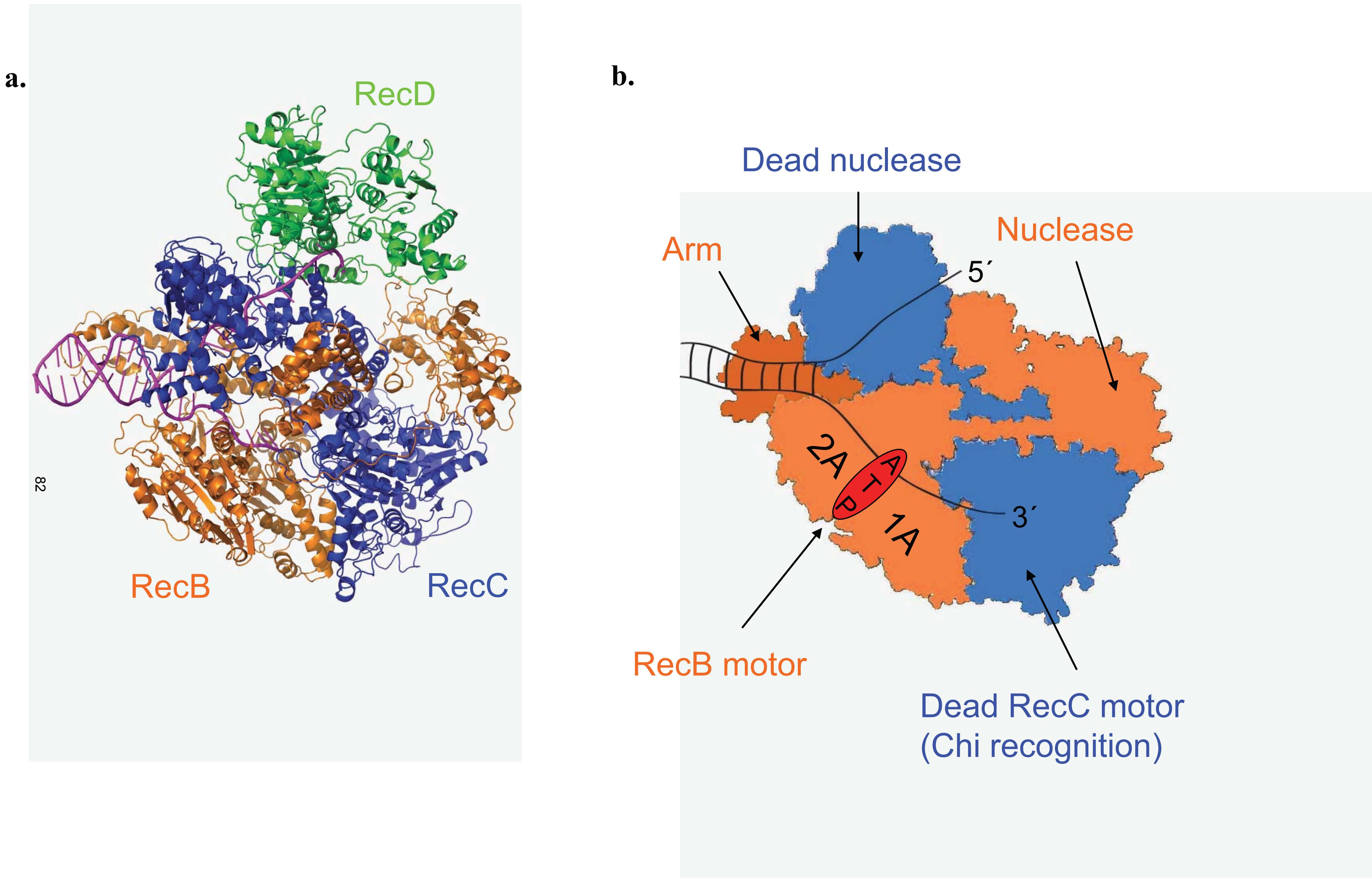
a.
RecD
RecB
RecC
b.
Dead nuclease
Nuclease
Arm
5´
3´
2A
ATP
1A
RecB motor
Dead RecC motor
(Chi recognition)

Figure 1

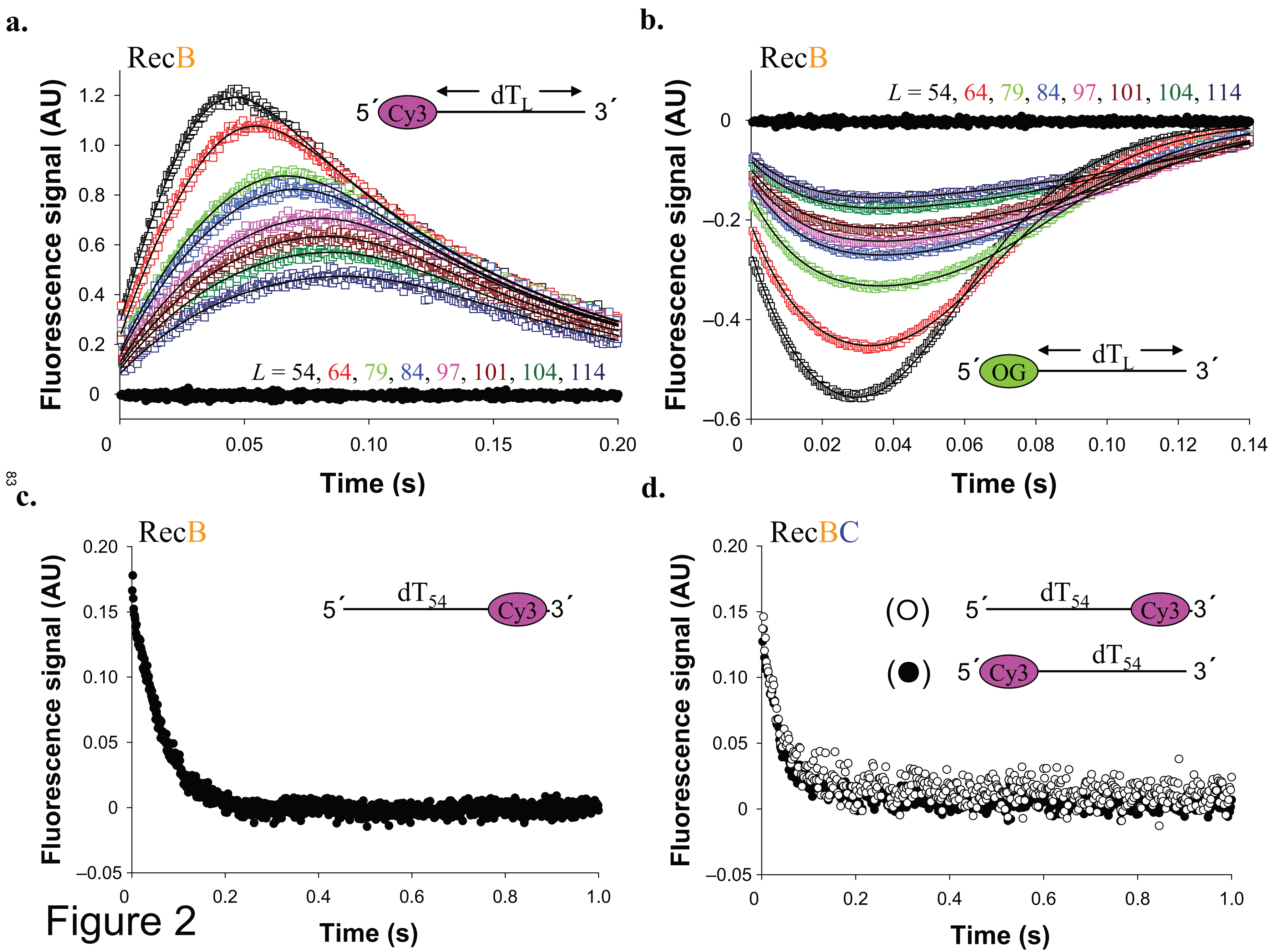
a.
RecB
5´ Cy3 dTL 3´
L = 54, 64, 79, 84, 97, 101, 104, 114
Fluorescence signal (AU)
Time (s)
b.
RecB
L = 54, 64, 79, 84, 97, 101, 104, 114
5´ OG dTL 3´
Fluorescence signal (AU)
Time (s)
c.
RecB
5´ dT54 Cy3 3´
Fluorescence signal (AU)
Time (s)
d.
RecBC
(O) 5´ dT54 Cy3 3´
(●) 5´ Cy3 dT54 3´
Fluorescence signal (AU)
Time (s)

Figure 2

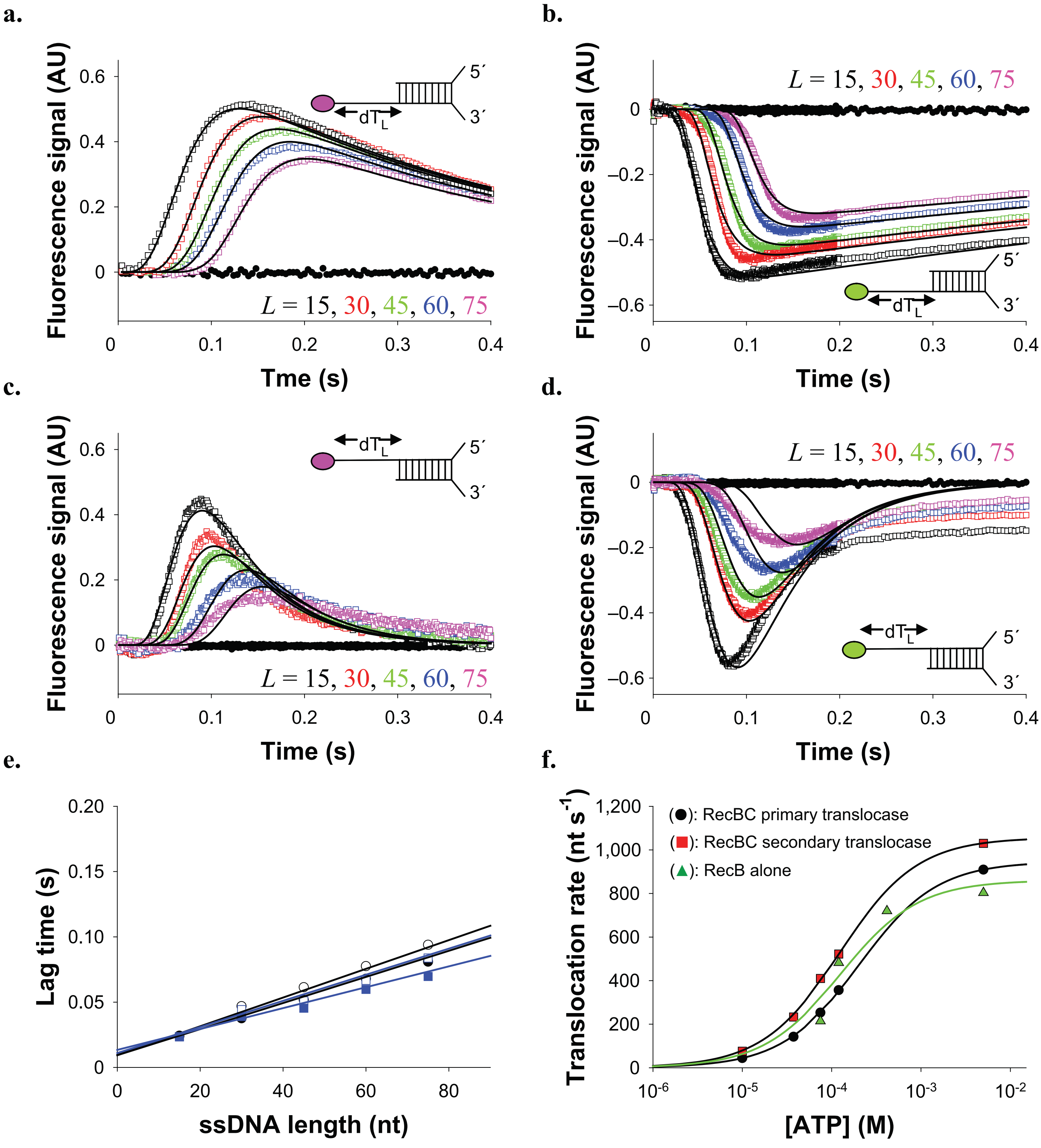
a.
Fluorescence signal (AU)
0.6
0.4
0.2
0
5´
3´
dT_L
L = 15, 30, 45, 60, 75
0
0.1
0.2
0.3
0.4
Tme (s)
b.
Fluorescence signal (AU)
0
−0.2
−0.4
−0.6
L = 15, 30, 45, 60, 75
5´
3´
dT_L
Time (s)
c.
Fluorescence signal (AU)
dT_L
5´
3´
L = 15, 30, 45, 60, 75
Time (s)
d.
Fluorescence signal (AU)
L = 15, 30, 45, 60, 75
dT_L
5´
3´
Time (s)
e.
Lag time (s)
0.20
0.15
0.10
0.05
0
0
20
40
60
80
ssDNA length (nt)
f.
Translocation rate (nt s-1)
1,200
1,000
800
600
400
200
0
(●): RecBC primary translocase
(■): RecBC secondary translocase
(▲): RecB alone
10-6
10-5
10-4
10-3
10-2
[ATP] (M)

Figure 3

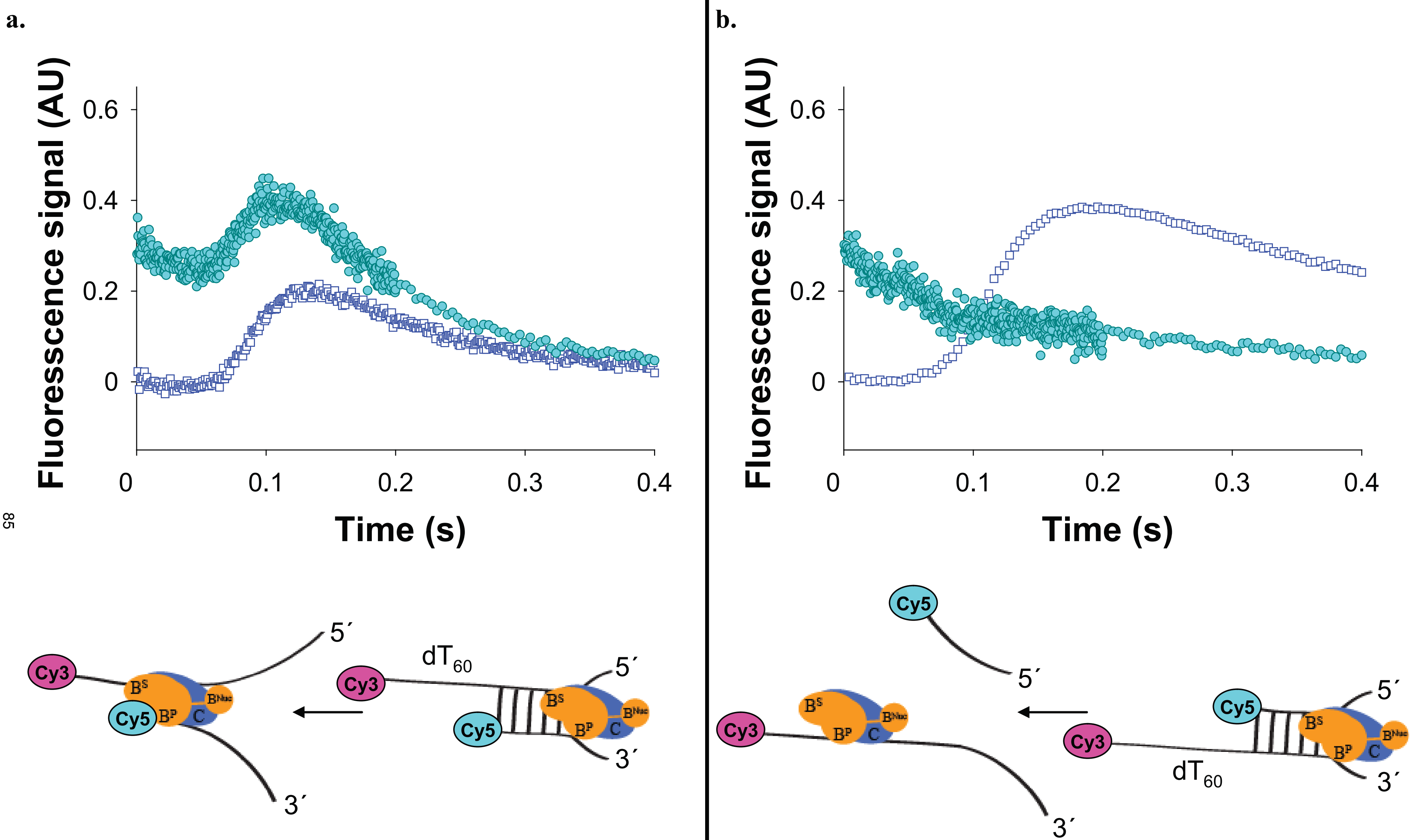
a.
b.
Fluoresscence signal (AU)
0.6
0.4
0.2
0
Time (s)
0
0.1
0.2
0.3
0.4
Cy3
Cy5
dT60
5´
3´
B^S
B^P
B^Nuc
C

Figure 4

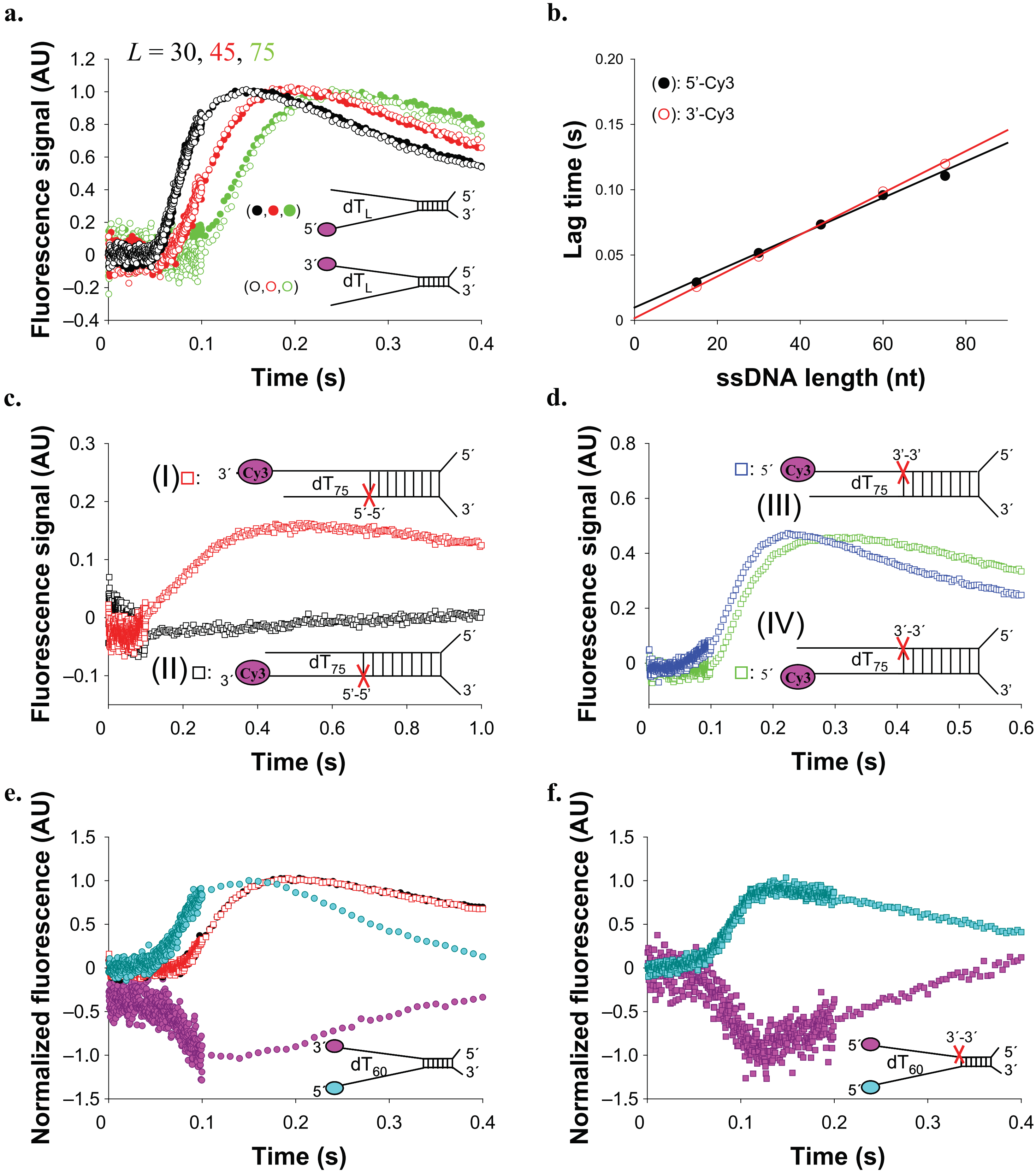
a.
L = 30, 45, 75
Fluorescence signal (AU)
Time (s)
dT$_L$
b.
(●): 5'-Cy3
(○): 3'-Cy3
Lag time (s)
ssDNA length (nt)
c.
(I)□:
(II)□:
Cy3
dT$_{75}$
5′-5′
Fluorescence signal (AU)
Time (s)
d.
(III)
(IV)
3′-3′
Cy3
dT$_{75}$
Fluorescence signal (AU)
Time (s)
e.
dT$_{60}$
Normalized fluorescence (AU)
Time (s)
f.
3′-3′
dT$_{60}$
Normalized fluorescence (AU)
Time (s)

Figure 5

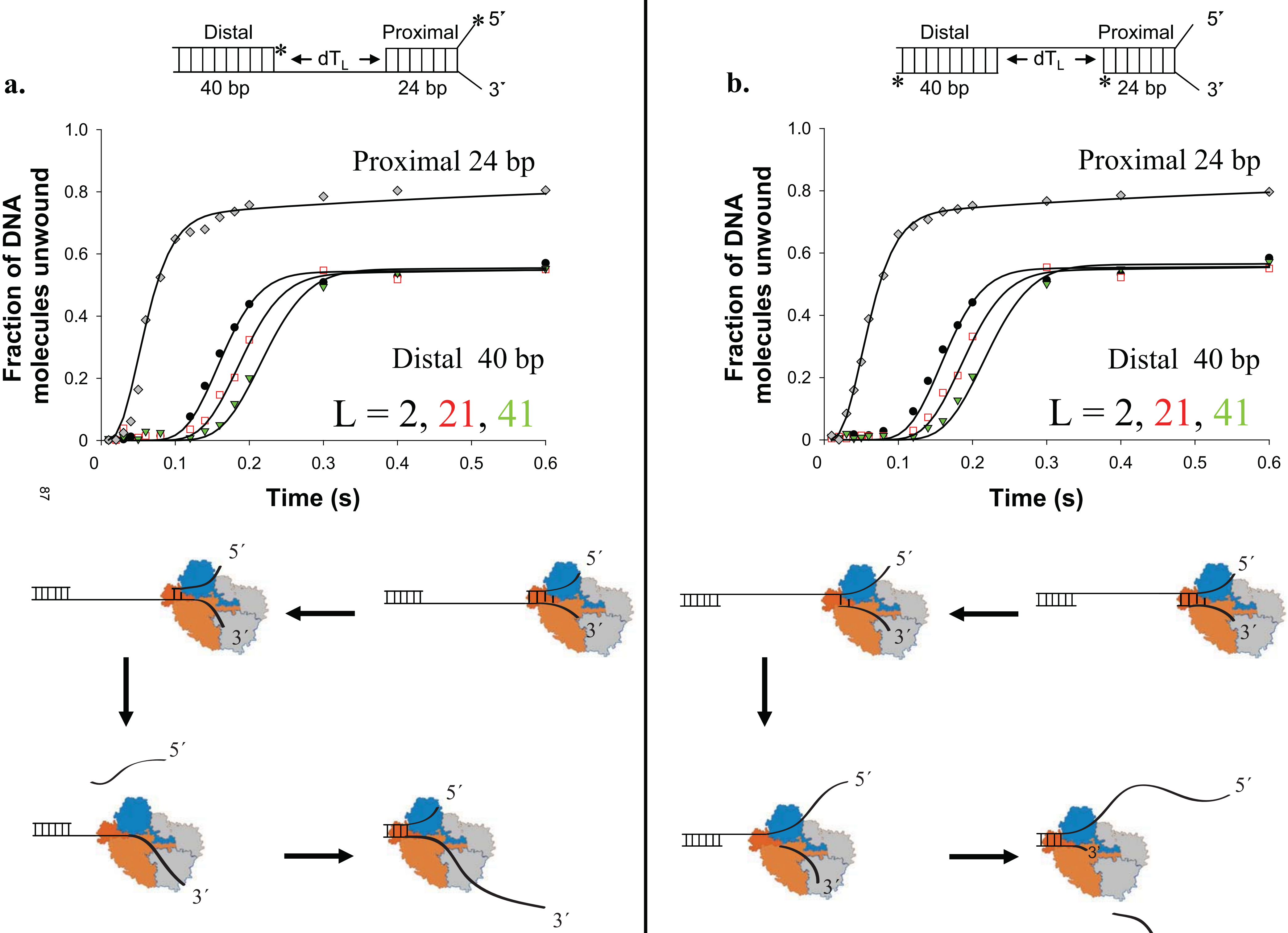

a.
Distal
Proximal
dT$_L$
40 bp
24 bp
5′
3′
Fraction of DNA molecules unwound
Time (s)
Proximal 24 bp
Distal 40 bp
L = 2, 21, 41
b.
Distal
Proximal
dT$_L$
40 bp
24 bp
5′
3′
Fraction of DNA molecules unwound
Time (s)
Proximal 24 bp
Distal 40 bp
L = 2, 21, 41

Figure 6

Supplementary Information

E. coli RecBC Helicase has Two Translocase Activities Controlled by a Single ATPase Motor

Colin G. Wu, Christina Bradford and Timothy M. Lohman

Supplementary Methods

Buffers and Reagents. RecB and RecC storage buffer is Buffer C: 20 mM K phosphate (pH 6.8 at 25ºC), 0.1 mM 2-mercaptoethanol, 0.1 mM ethylenediaminetetraacetic acid (EDTA), and 10% (v/v) glycerol. Poly-(dT) was purchased from Midland Certified Reagents Inc. (Midland, TX) and fractionated as described [1-2] to obtain a weight average length of 3.2 kb.

RecB dissociation kinetics during ssDNA translocation. RecB dissociation kinetics during ssDNA translocation was examined by monitoring the increase in RecB intrinsic tryptophan fluorescence, which is quenched when RecB is bound to ssDNA[1]. 50 nM RecB was pre-mixed with 20 μM poly-(dT) (nucleotides concentration) in Buffer M on ice for five minutes and the mixture was loaded into one syringe of the stopped-flow apparatus. Translocation was initiated by mixing with 10 mM ATP and 8 mg mL^{-1} heparin. RecB tryptophan fluorescence was excited at 280 nm and fluorescence emission was monitored at 350 nm using an interference filter (Oriel Corp., Stratford, CT). RecB dissociation time courses were fit to a single exponential function ($f(t) = Ae^{(-k_{d,obs}t)}$; A = –0.21 ± 0.02 (AU), $k_{d,obs}$ = 7.5 ± 0.3 s^{-1}) since photobleaching was not observed within the time scale of the experiment. We note that the value of $k_{d,obs}$ remains constant over a range constant [heparin] (up to 15 mg mL^{-1} after mixing, data not shown); therefore, heparin does not displace RecB monomers from the ssDNA during translocation.

Analysis of ssDNA translocation and DNA unwinding kinetic time courses. RecB monomer translocation kinetics along ssDNA was analyzed using non-linear least squares (NLLS) methods as described previously [1,3]. Cy3 and Oregon Green time courses were analyzed globally using **Scheme 1** and **Equation S1**, where *f*(*t*) describes the time dependent fluorescence signal resulting from RecB monomer translocating to the 5′ end of the ssDNA. $\mathcal{L}^{-1}$ is the inverse Laplace transform operator and *s* is the Laplace variable. The fluorescence amplitude (*A*) and the

$$f(t) = \frac{A}{1+nr}\mathcal{L}^{-1} \times \left(\frac{1}{s+k_{end}} \left(1 + \frac{k_t r}{s+k_d} \left(1 - \left(\frac{k_t}{s+k_t+k_d} \right)^n \right) \right) \right) \qquad \textbf{(Equation S1)}$$

number of translocation steps (*n*) were floated for each ssDNA length (*L*) while the microscopic translocation rate (k_t), the end dissociation rate constant (k_{end}), and *r* (which is the fraction of RecB bound to any position other than the 5′ end of the ssDNA to that of the 5′ end) were constrained to be global parameters. The average kinetic step-size for translocation, m_t, was determined by replacing *n* in **Equation S1** with $(L–d)/m_t$, where *d* is the contact size of RecB in nucleotides. The value for k_d was fixed at 7.5 s^{-1} in the analysis, which was determined independently as described above.

The rates reported for RecBC translocation along ssDNA were estimated using two methods: examining the dependence of the lag phase of the translocation time courses on ssDNA extension length, or fitting the entire time courses to a kinetic scheme which describes the initial unwinding of the 24 bp duplex and subsequent ssDNA translocation. The duration of the lag phase was estimated as the intersection point of two linear fits (see **Supplementary Fig. 2**) which describe the lag phase and the initial increase (or decrease for fluorescein labeled substrates) in fluorescence signal. Simulated time courses have shown[4] that a plot of the "time to reach the lag" as well as "peak position" versus ssDNA length always provides an accurate estimate of the macroscopic translocation rate if the translocase initiates from a unique site on the DNA as in this case. Such an analysis does not generally provide accurate estimates of the translocation rate if the translocase initiates from random sites on the DNA as is the case for RecB, UvrD, PcrA, and Rep monomer translocation on ssDNA[1,4-6]. In that case, the full time course must be analyzed to obtain accurate translocation rates [1,3]. We also analyzed the full time courses for RecBC translocation along ssDNA using **Equation S2** based on the kinetic mechanism shown in **Scheme 2**, in which RecBC first unwinds a duplex region of length L_{ds} followed by translocation along ssDNA of length L_{ss}. The DNA unwinding parameter L_{ds} was fixed at 24 bp, and average kinetic step-size and microscopic rate constant for DNA unwinding were constrained to the values determined in previous stopped-flow fluorescence experiments under the same solution conditions (m_U = 4.4 ± 0.1 bp, $k_U = 79 \pm 11$ s^{-1}; $mk_U = 348 \pm 5$ bp s^{-1}) [7]. The fluorescence amplitude (A) was floated at each ssDNA length (L_{ss}) while the translocation step-size (m_t), microscopic translocation rate (k_t), and end dissociation rate constant (k_{end}) were constrained to be global parameters.

$$f(t) = A \times \mathcal{L}^{-1}\left(\frac{k_t^{L_{ss}/m_t} k_u^{L_{ds}/m_U}}{(s+k_t)^{L_{ss}/m_t}(s+k_u)^{L_{ds}/m_U}(s+k_{end})} \right) \qquad \textbf{(Equation S2)}$$

Analysis of DNA unwinding kinetics. DNA unwinding time courses from **Figure 6** were analyzed using **Equation S3** based on the kinetic mechanism shown in **Scheme 3**, which describes the initial unwinding of a proximal duplex followed by translocation along a ssDNA gap and subsequent re-initiation of the unwinding of a 40 bp distal duplex. As written in **Scheme 3**, the unwinding parameters for the proximal and distal duplexes are assumed to be the same, therefore, L_{ds} was fixed at 64 bp (24 bp proximal, 40 bp distal), and m_{U} and k_{U}

$$f_{ss}(t) = A \times \mathcal{L}^{-1}\left(\frac{k_U^{L_{ds}/m_U} k_t^{L_{ss}/m_t}}{s(k_U+s)^{L_{ds}/m_U}(k_t+s)^{L_{ss}/m_t}} \right) \qquad \textbf{(Equation S3)}$$

were constrained to values determined previously using chemical quenched-flow under the same solution conditions ($m_U = 4.4 \pm 1.7$ bp, $k_U = 90 \pm 25\ \mathrm{s}^{-1}$; $m_U k_U = 396 \pm 15$ bp s^{-1}). The extent of DNA unwinding (A) was floated for each ssDNA gap length (L_{ss}), while m_t and k_t were constrained to be global parameters.

The RecBC translocation rates determined from "lag time" analysis as a function of [ATP] were fit to the Michaelis-Menton equation (**Equation S4**).

$$m_t k_t = \frac{V_{\max}[ATP]}{K_M + [ATP]} \qquad \textbf{(Equation S4)}$$

Supplemental References

1 Fischer, C. J., Maluf, N. K. & Lohman, T. M. Mechanism of ATP-dependent translocation of E.coli UvrD monomers along single-stranded DNA. *J Mol Biol* 344, 1287-1309 (2004).

2 Tomko, E. J., Fischer, C. J., Niedziela-Majka, A. & Lohman, T. M. A Nonuniform Stepping Mechanism for E. coli UvrD Monomer Translocation along Single-Stranded DNA. *Molecular Cell* 26, 335-347 (2007).

3 Fischer, C. J. & Lohman, T. M. ATP-dependent translocation of proteins along single-stranded DNA: models and methods of analysis of pre-steady state kinetics. *J Mol Biol* 344, 1265-1286 (2004).

4 Tomko, E. J. *Transient-State Kinetic Studies of the E. coli UvrD Monomer Translocation Along Single-Stranded DNA* Ph.D thesis, Washington University School of Medicine, (2010).

5 Brendza, K. M. *et al.* Autoinhibition of *Escherichia coli* Rep monomer helicase activity by its 2B subdomain. *Proc Natl Acad Sci U S A* 102, 10076-10081 (2005).

6 Niedziela-Majka, A., Chesnik, M. A., Tomko, E. J. & Lohman, T. M. Bacillus stearothermophilus PcrA Monomer Is a Single-stranded DNA Translocase but Not a Processive Helicase in Vitro. *J. Biol. Chem.* 282, 27076-27085, (2007).

7 Wu, C. G. & Lohman, T. M. Influence of DNA end structure on the mechanism of initiation of DNA unwinding by the Escherichia coli RecBCD and RecBC helicases. *J Mol Biol* 382, 312-326 (2008).

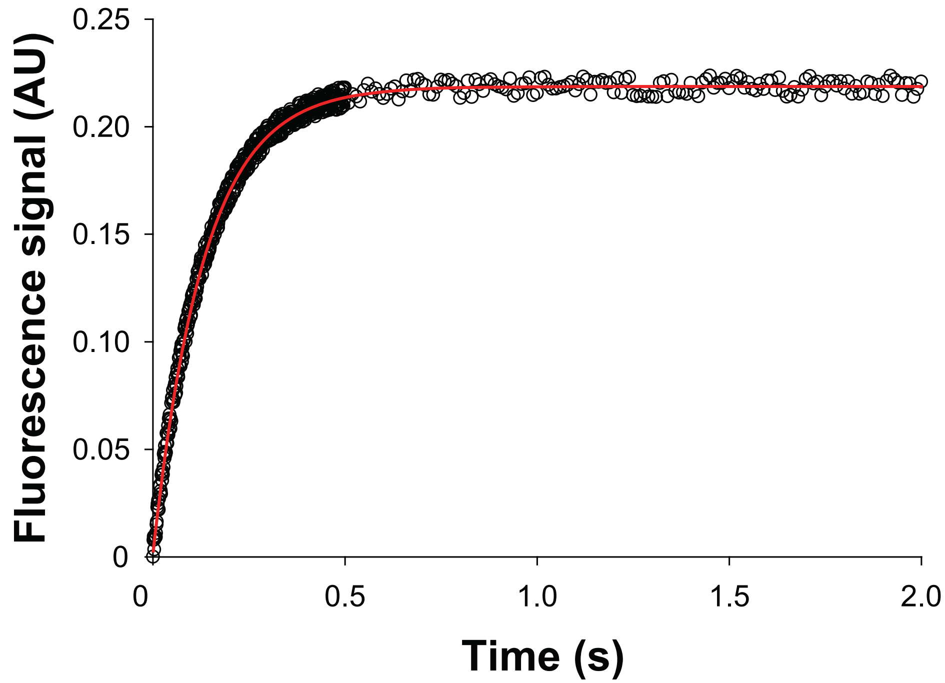

Supplementary Figure 1. RecB monomer dissociation kinetics. RecB monomer dissociation kinetics during 3′ to 5′ ssDNA translocation was examined by monitoring the increase in intrinsic trypophan fluorescence of RecB, which is quenched when bound to ssDNA. The dissociation time course was fit to a single exponential function ($f(t) = Ae^{(-k_{d,obs}t)}$; A = -0.21 ± 0.02 (AU), $k_{d,obs}$ = 7.5 ± 0.3 s^{-1}) as indicated by the smooth red curve. This value of $k_{d,obs}$ was independent of [heparin] (up to 15 mg mL^{-1} after mixing) and was constrained in the analysis of RecB monomer translocation kinetics (see **Fig. 2a–2b**).

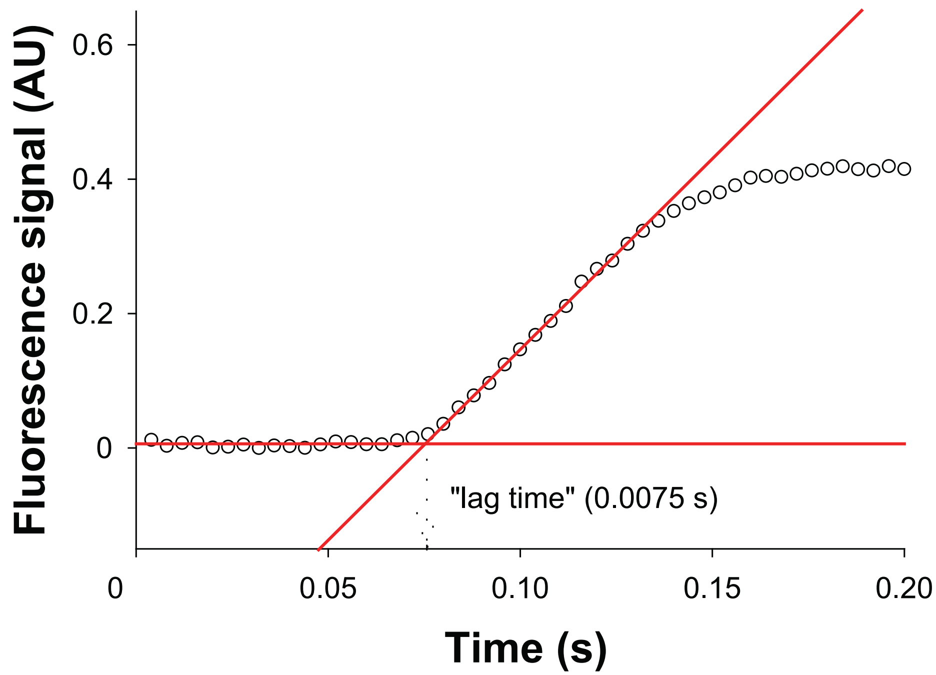

Supplementary Figure 2. “Lag time” analysis of a RecBC translocation time course. Data from **Figure 3a** is plotted (L = 60 nucleotides). The duration of the lag was estimated as the intersection point of two linear fits which describe the lag phase and the initial increase (or decrease with fluorescein labeled substrates) in fluorescence intensity. This value was determined for each L (see **Fig. 3e**) and the dependence of the lag time on L was used to estimate the translocation rate.

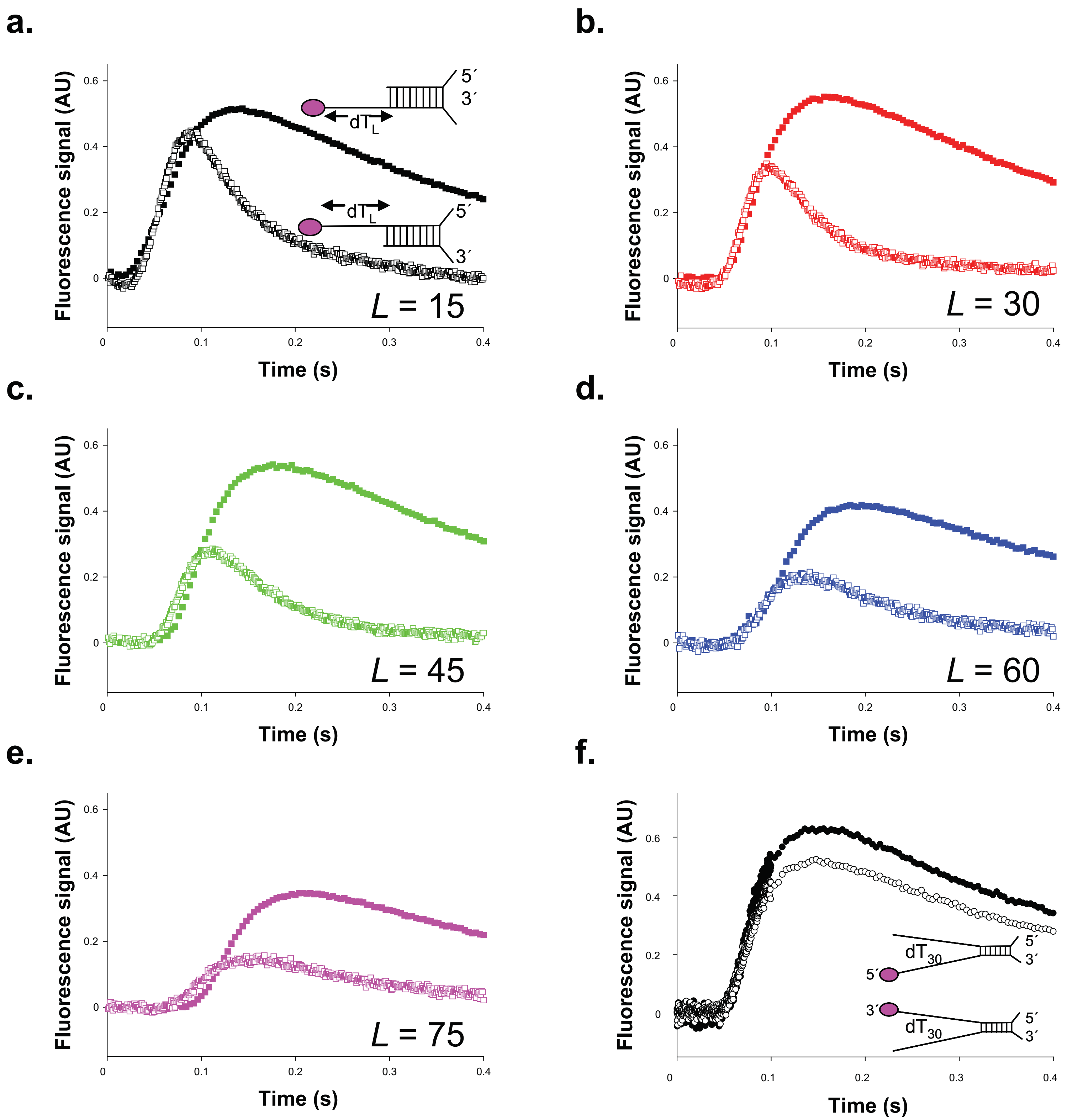

Supplementary Figure 3. Comparison of RecBC primary and secondary translocase time courses. (a–e). Data from **Figure 3a** and **3c** are overlaid for L = 15, 30, 45, 60, and 75 nucleotides. Closed squares (■) indicate primary translocase time courses shown in **Figure 3a** and opened squares (□) denote secondary translocase kinetics shown in **Figure 3c**. Although the duration of the lag phase and initial increase of fluorescence intensity are similar for each L, the translocation kinetics differ in the peak positions of fluorescence as well as the dissociation rates from the ssDNA ends. **(f).** Overlay of the raw fluorescence intensity for the data shown in **Figure 5a** (L = 30). The two time courses are obtained from DNA substrates possessing two $(dT)_{30}$ ssDNA extensions and are labeled either on the 3´-end (○) or 5´-end with Cy3 (●). Although the normalized translocation kinetics are identical for the two substrates (see **Fig. 5a**), the total extent of fluorescence increase is ~ 15% larger for the 5´-end labeled DNA substrate.

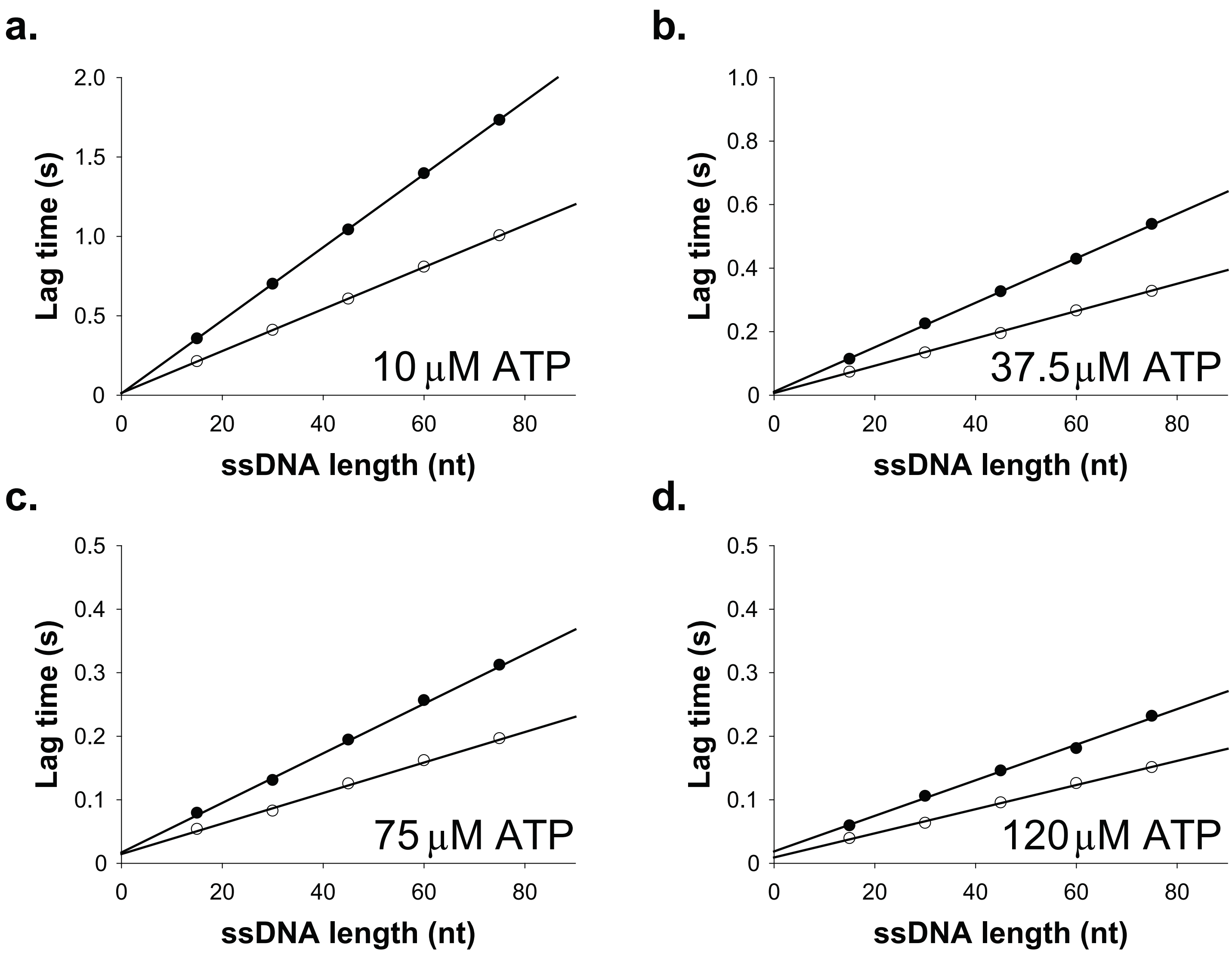

Supplementary Figure 4. Translocation rates of RecBC primary and secondary activities as a function of [ATP] determined from "lag time" analyses. The translocation rates determined from this analysis are plotted versus [ATP] in **Figure 3f** and fit to the Michaelis-Menton Equation (**Eq. S4**) (see **Fig. 3f**). (●) 3′ to 5′ primary translocase data; (○) 5′ to 3′ secondary translocase data. **(a).** 10 μM ATP (after mixing). Smooth curves indicate linear fits: "time" = 0.0232*L* + 0.0111 (primary), "time" = 0.0132*L* + 0.014 (secondary). **(b).** 37.5 μM ATP (after mixing). Smooth curves indicate linear fits: "time" = 0.0074*L* + 0.0109 (primary), "time" = 0.0043*L* + 0.0068 (secondary). **(c).** 75 μM ATP (after mixing). Smooth curves indicate linear fits: "time" = 0.0039*L* + 0.0171 (primary), "time" = 0.0024*L* + 0.0146 (secondary). **(d).** 120 μM ATP (after mixing). Smooth curves indicate linear fits: "time" = 0.0028*L* + 0.0187 (primary), "time" = 0.0019*L* + 0.0092 (secondary).

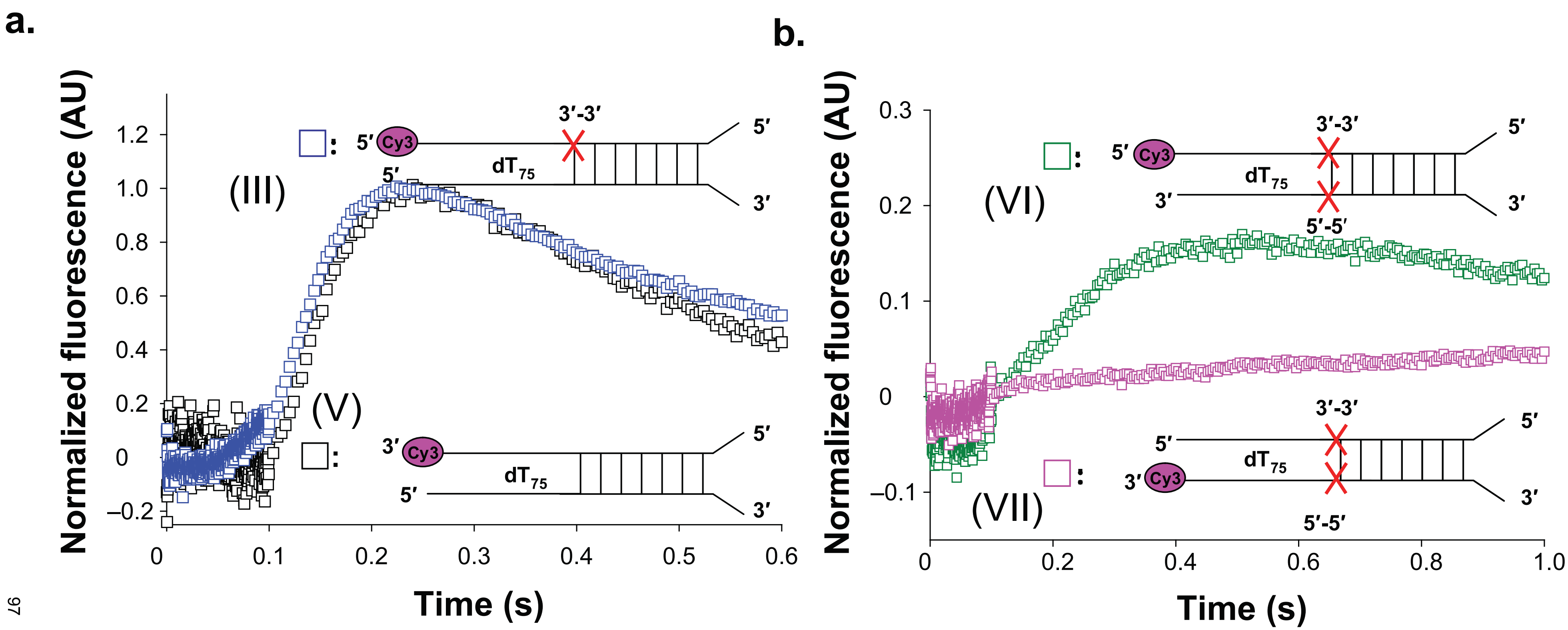

Supplementary Figure 5. RecBC primary translocase is sensitive to ssDNA backbone polarity but the secondary translocase is not. (a). Overlay of the time courses shown in **Figure 5a** and **5d**, which were normalized to the maximum fluorescence intensity. DNA III, as shown in **Figure 5d**, contains a 3′–3′ phosphodiester linkage ("X") that reverses the backbone polarity on the 5′-terminating strand. The ssDNA backbone polarity is unchanged in DNA V (*L* = 75 in **Figure 5a**). The translocation time courses obtained for both DNA substrates are identical indicating that the secondary translocase in not sensitive to the ssDNA backbone polarity. **(b).** The backbone polarity of both 5′-terminating and 3′-terminating strands are reversed ("X") after the initial 24 bp duplex. DNA VI is labeled with Cy3 at the end of the 5′-terminating strand while DNA VII is labeled with Cy3 at the end of the 3′-terminating strand. The primary translocase is blocked by the reverse polarity backbone (see **Fig. 5c**) while the secondary translocase is unaffected.

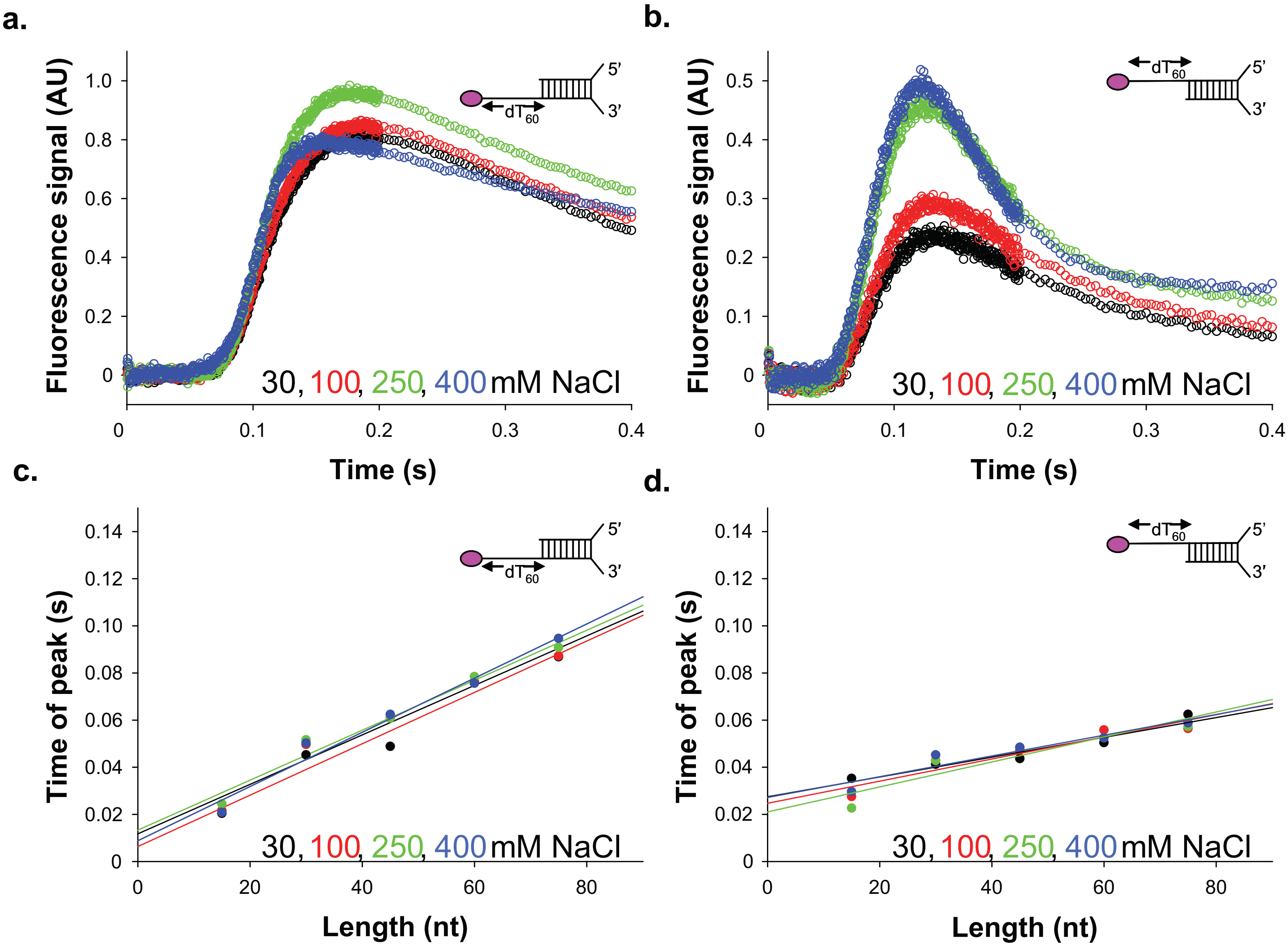

Supplementary Figure 6. [NaCl] dependence on RecBC primary and secondary translocase activities. (a). Primary translocase activity was examined using the DNA substrates shown in **Figure 3a** at 30, 100, 250, and 400 mM NaCl. **(b).** Secondary translocase activity was examined using the DNA substrates shown in **Figure 3c** at 30, 100, 250, and 400 mM NaCl. **(c).** lag time analysis of the primary translocase at different [NaCl]. (●) 30 mM NaCl: "time" = 0.0011*L* + 0.0064; (●) 100 mM NaCl: "time"= 0.0011*L* + 0.0117; (●) 250 mM NaCl: "time"= 0.0011*L* + 0.0133; (●) 400 mM NaCl: "time"= 0.0012*L* + 0.0088. **(d).** lag time analysis of the secondary translocase at different [NaCl]. (●) 30 mM NaCl: "time" = 0.0007*L* + 0.0275; (●) 100 mM NaCl: "time"= 0.0008*L* + 0.0247; (●) 250 mM NaCl: "time"= 0.0009*L* + 0.021; (●) 400 mM NaCl: "time"= 0.0007*L* + 0.0272.

Supplementary Table 1. DNA substrate sequences used for examining RecB monomer translocation

DNA	Length (nt)	DNA sequence
I	54	5′-X $(dT)_{54}$-3′
II	64	5′-X $(dT)_{64}$-3′
III	79	5′-X $(dT)_{79}$-3′
IV	84	5′-X $(dT)_{84}$-3′
V	97	5′-X $(dT)_{97}$-3′
VI	101	5′-X $(dT)_{101}$-3′
VII	104	5′-X $(dT)_{104}$-3′
VIII	114	5′-X $(dT)_{114}$-3′
IX	54	5′-$(dT)_{54}$ (Cy3)T-3′

DNA substrates I-VIII are fluorescently labeled on the 5′ end (designated as “X”) with either Cy3 or Oregon Green, and are used to monitor RecB monomer translocation along ssDNA in the 3′ to 5′ direction (**Fig. 2a-2b**). DNA IX is fluorescently labeled on the 3′ end with Cy3 and is used to test whether RecB can translocate along ssDNA with 5′ to 3′ directionality (**Fig. 2c**).

Supplementary Table 2. DNA substrate sequences used for examining RecBC translocation along ssDNA

DNA	Length (nt)	DNA sequence
A	30	5´-$(dT)_6$ CCA TGG CTC CTG AGC TAG CTG CAG (ZT)-3´
Ia	45	5´-(Y)$(dT)_{15}$ CTG CAG CTA GCT CAG GAG CCA TGG $(dT)_6$-3´
IIa	60	5´-(Y)$(dT)_{30}$ CTG CAG CTA GCT CAG GAG CCA TGG $(dT)_6$-3´
IIIa	75	5´-(Y)$(dT)_{45}$ CTG CAG CTA GCT CAG GAG CCA TGG $(dT)_6$-3´
IVa	90	5´-(Y)$(dT)_{60}$ CTG CAG CTA GCT CAG GAG CCA TGG $(dT)_6$-3´
Va	105	5´-(Y)$(dT)_{75}$ CTG CAG CTA GCT CAG GAG CCA TGG $(dT)_6$-3´
B	30	5´-(Z) CTG CAG CTA GCT CAG GAG CCA TGG $(dT)_6$-3´
Ib	45	5´-$(dT)_6$ CCA TGG CTC CTG AGC TAG CTG CAG $(dT)_{15}$ (YT)-3´
IIb	60	5´-$(dT)_6$ CCA TGG CTC CTG AGC TAG CTG CAG $(dT)_{30}$ (YT)-3´
IIIb	75	5´-$(dT)_6$ CCA TGG CTC CTG AGC TAG CTG CAG $(dT)_{45}$ (YT)-3´
IVb	90	5´-$(dT)_6$ CCA TGG CTC CTG AGC TAG CTG CAG $(dT)_{60}$ (YT)-3´
Vb	105	5´-$(dT)_6$ CCA TGG CTC CTG AGC TAG CTG CAG $(dT)_{75}$ (YT)-3´

DNA substrates from **Figure 3a-3b** are formed by annealing DNA strand A with DNA strands Ia-Va, which are fluorescently labeled on the 5´ end with Cy3 or fluorescein (denoted as "Y" where appropriate). This forms a 24 bp duplex with a twin $(dT)_6$ high affinity loading site for RecBC on one end of the duplex, and a series of $(dT)_L$ ssDNA extensions (L = 15, 30, 45, 60, 75 nucleotides) on the other end of the 3´-terminating DNA strand, which allows us to examine the primary 3´ to 5´ translocase activity of RecBC. DNA substrates from **Figure 3c-3d** are formed by annealing DNA strand B with DNA strands Ib-Vb, which are fluorescently labeled on the 3´ end with Cy3 or fluorescein (denoted as "Y" where appropriate). These substrates also form a 24 bp duplex with a high affinity RecBC loading site, but the $(dT)_L$ extensions now reside on the 5´-terminating DNA strand and are used to examine the secondary 5´ to 3´ translocase activity of RecBC.

DNA substrates from **Figure 4a-4b** are formed by annealing DNA strand B with IVb and DNA strand A with IVa as described above but now the A and B strands are labeled with Cy5 (denoted as "Z").

DNA substrates from **Figure 5a-5b**, which are used to examine RecBC translocation along the two ssDNA extensions simultaneously, are formed by annealing DNA strands Ia-Va with Ib-Vb such that either the a or b strands are labeled with Cy3 (designated as "Y"). Substrates with reverse polarity linkages on the DNA backbone have the same sequences but 5´-5´ or 3´-3´ linkages are introduced to the DNA backbone as depicted in **Figure 5c-5d** ("**X**"). For **Figure 5e-5f**, DNA strand IVb (Y=Cy3) was annealed with IVa (Y=Cy5).

Supplementary Table 3. DNA substrate sequences used for examining unwinding reinitiation by RecBC

DNA	Length (nt)	DNA sequence
Strand ´A´		
Ia	30	5´-CTG CAG CTA GCT CAG GAG CCA TGG $(dT)_6$-3
IIa	30	5´-$(dT)_6$ CCA TGG CTC CTG AGC TAG CTG CAG-3´
Strand ´B´		
Ib	40	5´-GGA TGC GAC TCG ACG TAT CCA TGG AGC ATA AGA TCC TAG T-3´
IIb	40	5´-ACT AGG ATC TTA TGC TCC ATG GAT ACG TCG AGT CGC ATC C-3´
Strand ´C´		
Ic	66	5´-$(dT)_6$ CCA TGG CTC CTG AGC TAG CTG CAG $(dT)_2$ ACT AGG ATC TTA TGC TCC ATG GAT ACG TCG AGT CGC ATC C-3´
IIc	84	5´-$(dT)_6$ CCA TGG CTC CTG AGC TAG CTG CAG $(dT)_{20}$ ACT AGG ATC TTA TGC TCC ATG GAT ACG TCG AGT CGC ATC C-3´
IIIc	105	5´-$(dT)_6$ CCA TGG CTC CTG AGC TAG CTG CAG $(dT)_{41}$ ACT AGG ATC TTA TGC TCC ATG GAT ACG TCG AGT CGC ATC C-3´
IVc	66	5´-GGA TGC GAC TCG ACG TAT CCA TGG AGC ATA AGA TCC TAG T$(dT)_2$ CTG CAG CTA GCT CAG GAG CCA TGG $(dT)_6$-3´
Vc	84	5´-GGA TGC GAC TCG ACG TAT CCA TGG AGC ATA AGA TCC TAG T $(dT)_{20}$ CTG CAG CTA GCT CAG GAG CCA TGG $(dT)_6$-3´
VIc	105	5´-GGA TGC GAC TCG ACG TAT CCA TGG AGC ATA AGA TCC TAG T$(dT)_{41}$CTG CAG CTA GCT CAG GAG CCA TGG $(dT)_6$-3´

DNA substrates from **Figure 6a**, which possess 3´ to 5´ ssDNA gaps of dT_2, dT_{20}, and dT_{41} are formed by annealing DNA strands IIa, IIb, and IV-VIc. This forms a 24 bp proximal duplex with a high affinity loading site for RecBC on one end and a gap region on the other end, followed by a distal duplex of 40 bp. Similarly, DNA substrates from **Figure 6b** are formed by annealing DNA strands Ia, Ib, and I-IIIc. These DNA possess 5´ to 3´ ssDNA gaps of dT_2, dT_{20}, and dT_{41} in between the proximal and distal duplexes.

Scheme 1

$$
\begin{array}{ccccccccccccc}
I_n & \xrightarrow{k_t} & I_{n-1} & \xrightarrow{k_t} & \cdots & \xrightarrow{k_t} & I_i & \xrightarrow{k_t} & \cdots & \xrightarrow{k_t} & I_1 & \xrightarrow{k_t} & I_{\mathrm{end}} \\
\downarrow k_d & & \downarrow k_d & & & & \downarrow k_d & & & & \downarrow k_d & & \downarrow k_{\mathrm{end}} \\
P_f & & P_f & & & & P_f & & & & P_f & & P_f
\end{array}
$$

Scheme 2

$$
\begin{array}{ccccccccccc}
(R \bullet D)_{L_{ds}} & \xrightarrow{k_U} & (R \bullet D)^{1}_{(L_{ds}-m_U)} & \xrightarrow{k_U} & \ldots(R \bullet D)^{n_U}_{(L_{ds}-n_U m_U)} & \xrightarrow{k_t} & I_{(L_{ss}-m_t)} & \xrightarrow{k_t} & \ldots I_{(L_{ss}-n_t m_t)}\cdots & \xrightarrow{k_t} & I_{end} \\
\downarrow \mathrm{k_d} & & \downarrow \mathrm{k_d} & & \downarrow \mathrm{k_d} & & \downarrow \mathrm{k_d} & & \downarrow \mathrm{k_d} & & \mathrm{k_{end}} \downarrow
\end{array}
$$

Scheme 3

$$
\begin{array}{ccccccccccc}
(R \bullet D)_{L_{ds}} & \xrightarrow{k_U} & (R \bullet D)^{1}_{(L_{ds}-m_U)} & \xrightarrow{k_U} & \ldots(R \bullet D)^{n_U}_{(L_{ds}-n_U m_U)} & \xrightarrow{k_t} & I_{(L_{ss}-m_t)} & \xrightarrow{k_t} & \ldots I_{(L_{ss}-n_t m_t)}\cdots & \xrightarrow{k_U} & \ldots ssDNA \\
\downarrow \mathrm{k_d} & & \downarrow \mathrm{k_d} & & \downarrow \mathrm{k_d} & & \downarrow \mathrm{k_d} & & \downarrow \mathrm{k_d} & &
\end{array}
$$

Appendix to Chapter III

Apparent 5' to 3' translocation is RecBC specific

In Chapter 3, I have shown that the RecBC enzyme possesses two distinct translocase activities which are controlled by a single ATPase motor (RecB). RecBC uses its secondary translocase activity to move along a 5' to 3' ssDNA extension after unwinding a 24 bp duplex. Since this is a novel and provocative observation, we have tested whether this is reproducible with another helicase. **Figure 3-S7** shows similar translocation experiments presented in Chapter 3 using the *E. coli* UvrD enzyme. The DNA substrate possesses a 24 bp duplex with 5'-$(dT)_6$,3'$(dT)_6$ on one end of the duplex, and a dT_{60} nucleotide ssDNA extension (fluorescently labeled with Cy3 at the 3' or 5' end) from either the 5' or 3'-erminating DNA strand as depicted in **Figure 3-S7**. No 5' to 3' translocation is not observed with a UvrD monomer since Cy3 fluorescence intensity decreases when the ssDNA extension on the 5'-terminating DNA strand. This decrease indicates that UvrD can bind to the ssDNA tail and translocate away from the fluorescently labeled 3' end with 3' to 5' directionality, as expected of the UvrD monomer (Tomko, Fischer et al. 2007; Tomko 2010). A control experiment where the ssDNA extension is on the 3'-terminating strand was performed and 3' to 5' translocation is observed as predicted. These experiments served as an initial control to show that the apparent 5' to 3' translocation activity observed for RecBC is specific for that system and that the DNA substrates are not mislabeled.

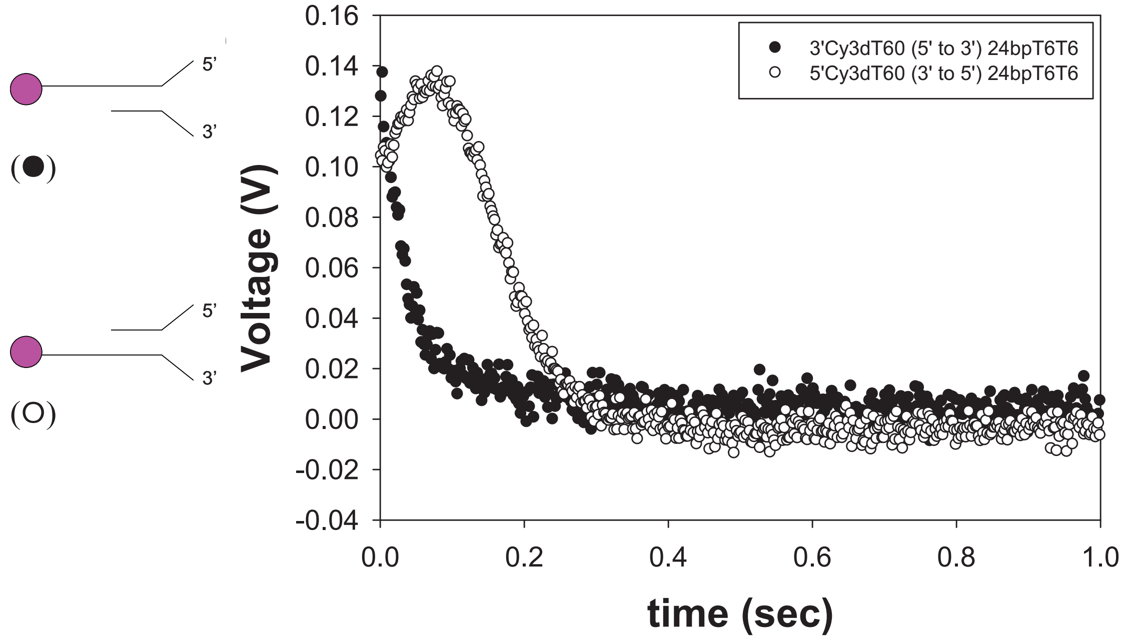

Figure 3-S7. *E. coli* UvrD translocation on a partial duplex substrate. 200 nM DNA substrate (24 bp duplex with twin dT_6 ssDNA tails on one end and either a 3' to 5' (O) or 5' to 3' (●) dT_{60} Cy3 end-labeled ssDNA extension on the other) was pre-bound to 40 nM UvrD. Translocation was initiated by mixing with 10 mM ATP and 8 mg/mL heparin. No apparent 5' to 3' translocation activity was detected. UvrD binds to the ds/ss junction and translocates towards the 5' end.

Influence of DNA length on RecBC primary translocase activity when the polarity of the ssDNA backbone is reversed

Since RecBC uses its primary translocase activity to move along a ssDNA extension in the 3' to 5' direction, I have tested whether reversing the polarity of the ssDNA backbone influences translocation along this strand. As presented in Chapter 3, the DNA substrate contains a 24 bp duplex with a high affinity RecBC loading site and a ssDNA extension along which the primary translocase normally operates (3'-terminating). The DNA substrate is designed such that after DNA unwinding, RecBC can continue to translocate along the ssDNA extension for 30 nts using its primary translocase activity, after which the polarity of the ssDNA backbone is reversed with a 5'-5' linker. The length of this "reversed" region is varied from 30-75 nucleotides. The translocation time courses shown in **Figure 3-S8A** indicate that the kinetics of translocation is identical for the different DNA substrates although the final amplitude decreases as the length of the reversed region increases. This is further illustrated in **Figure 3-S8B** in which the time courses are normalized and all the traces are superimposable and have identical kinetics. These results indicate that after RecBC unwinds the 24 bp duplex, it can translocate along the 30 nt ssDNA extension but then it becomes stuck when it encounters the 5'-5' linkage in the ssDNA backbone; however, it is still able to influence the fluorescence intensity of Cy3 from a distance. As the length of the reversed region is lengthened, RecBC unwinds, translocates, and then becomes stuck at the same location (after translocating 30 nts with its primary translocase activity) but since the Cy3 labeled DNA end is further away, the overall fluorescence amplitude is decreased.

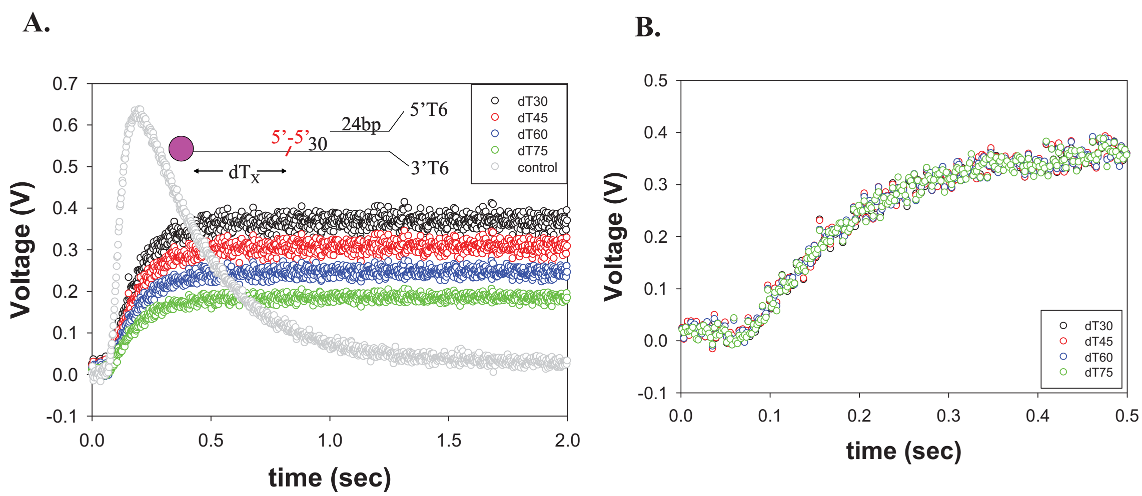

Figure 2-S8. Influence of the length of reverse polarity backbone on RecBC primary translocase activity. A). RecBC translocation time courses from DNA substrates with a dT_{30} ssDNA extension on the 3'-terminating strand (along which the primary translocase operates) after a 24 bp duplex. The backbone polarity of this DNA strand is reversed after the dT_{30} extension and is further extended for *L* nucleotides (*L* = 30, 45, 60, 75). (○) RecBC translocation along a dT_{30} control substrate (no 5'-5' linker). **B).** Fluorescence intensities from the time courses in panel A are normalized. The kinetics are identical between the time courses and are superimposable.

RecB monomer dissociation kinetics from internal sites

Results from RecB monomer translocation along ssDNA were presented in Chapter 3. The translocation time courses were analyzed using an *n*-step sequential mechanism as discussed in that chapter. Since this model requires a large number of kinetic parameters, I have determined the value of the dissociation rate of RecB from internal sites of the DNA (k_d) independently and constrained it during data analysis. RecB monomer dissociation experiments were performed by pre-forming the RecB-DNA complex and then initiating translocation by mixing with ATP and heparin. When RecB is bound to ssDNA, its tryptophan fluorescence is quenched; hence, when RecB dissociates from the DNA during translocation, an increase in tryptophan fluorescence intensity is observed. For these experiments, a long DNA substrate is typically required so that the signal change is not dominated by RecB dissociation from the end of the DNA. To that end (no pun intended), I have used m13ssDNA which is closed-circular DNA of mixed sequences (7249 nts), poly(dT) with a weight average length of 3200 nts, and dT_{114}. RecB dissociation time courses collected from all three DNA substrates well described by a single exponential function since little to no photobleaching is observed within the timescale of the experiment, as shown in **Figure 3-S9**. The value of $k_{d,obs}$ obtained from m13ssDNA is 6.8 ± 0.4 sec^{-1} (**Figure 3-S9A**) while the value of $k_{d,obs}$ obtained from poly(dT) is 7.5 ± 0.3 sec^{-1} (**Figure 3-S9B**) The value of $k_{d,obs}$ determined from dT_{114} is 10.2 ± 0.4 sec^{-1} (**Figure 3-S9C**) indicating that there is a significant end effect when a shorter oligo is used to determine the dissociation rate relative to poly(dT) or m13ssDNA.

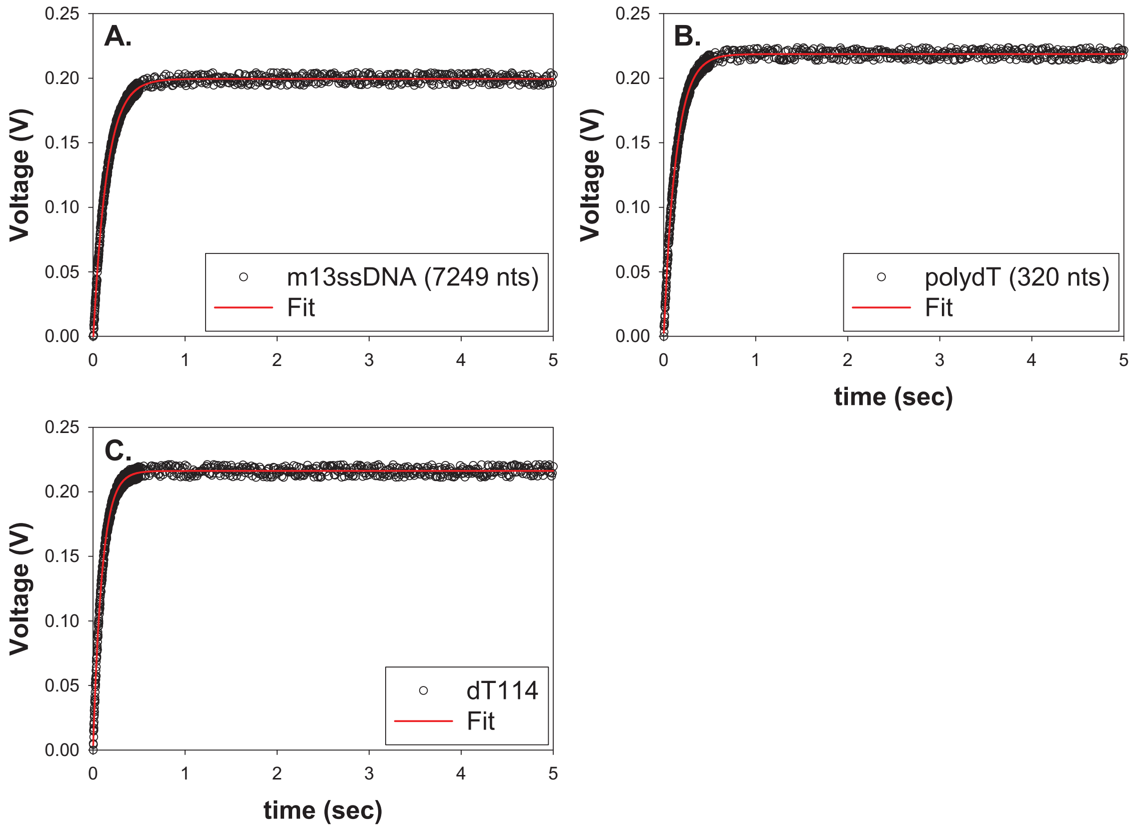

Figure 3-S9. RecB monomer dissociation kinetics during ssDNA translocation. RecB (50 nM) monomer is pre-bound to DNA substrate (20 μM nucleotides) and translocation is initiated by mixing with ATP (10 mM) and heparin (10 mg/mL). Intrinsic tryptophan fluorescence is monitored to examine RecB dissociation during translocation. Time courses are fit to a single exponential function $A\,e^{(-k_d \times t)}$. **A).** Dissociation experiment from m13ssDNA (A = -0.20 ± 0.03, k_d = 6.8 ± 0.4 sec^{-1}). **B).** Dissociation experiment from poly(dT) with a weight average length of 320 nts (A = -0.21 ± 0.02, k_d = 7.5 ± 0.3 sec^{-1}). **C).** Dissociation experiment from dT_{114} (A = -0.21 ± 0.02, k_d = 10.2 ± 0.4 sec^{-1}).

RecBΔ2BΔNuc monomer translocation kinetics along ssDNA

Studies of *E. coli* Rep have shown that the Rep monomer is able to translocate along ssDNA but is unable to unwind dsDNA processively (Brendza, Cheng et al. 2005). However, when the 2B subdomain is removed, thus forming the RepΔ2B monomer, this enzyme can not only move along ssDNA with a faster translocation rate, but also RepΔ2B is able to unwind longer DNA duplexes as a monomer; hence, this 2B subdomain is autoinhibitory in Rep and removing alleviates the inhibition and stimulates both translocation and unwinding activities (Brendza, Cheng et al. 2005). I have tested whether the 2B subdomain plays a similar role in *E. coli* RecB since both Rep and RecB are SF1 helicases. Constructs of RecBΔ2B were poorly expressed but I was able to express and purify the RecBΔ2BΔNuc protein in which the nuclease domain is also removed. RecBΔ2BΔNuc translocation along ssDNA was monitored as described in Chapter 3 using a series of DNA oligos of varying length (dT_L) and the 5' ssDNA end is fluorescently labeled with Cy3. Similar to RecB monomer translocation experiments, RecBΔ2BΔNuc monomer translocation along ssDNA is also well described by **Equation 1** (Chapter 3) and **Scheme 1** (Chapter 3). The macroscopic translocation rate is 1310 ± 11 nt/sec which is faster than RecB monomer translocation (mk_t = 803 ± 13 nt/sec). However, these experiments will need to be repeated with DNA oligos labeled another fluorophore (Oregon Green or fluorescein) so that the time courses can be analyzed globally in order to obtain fluorophore independent measurements of the kinetic parameters.

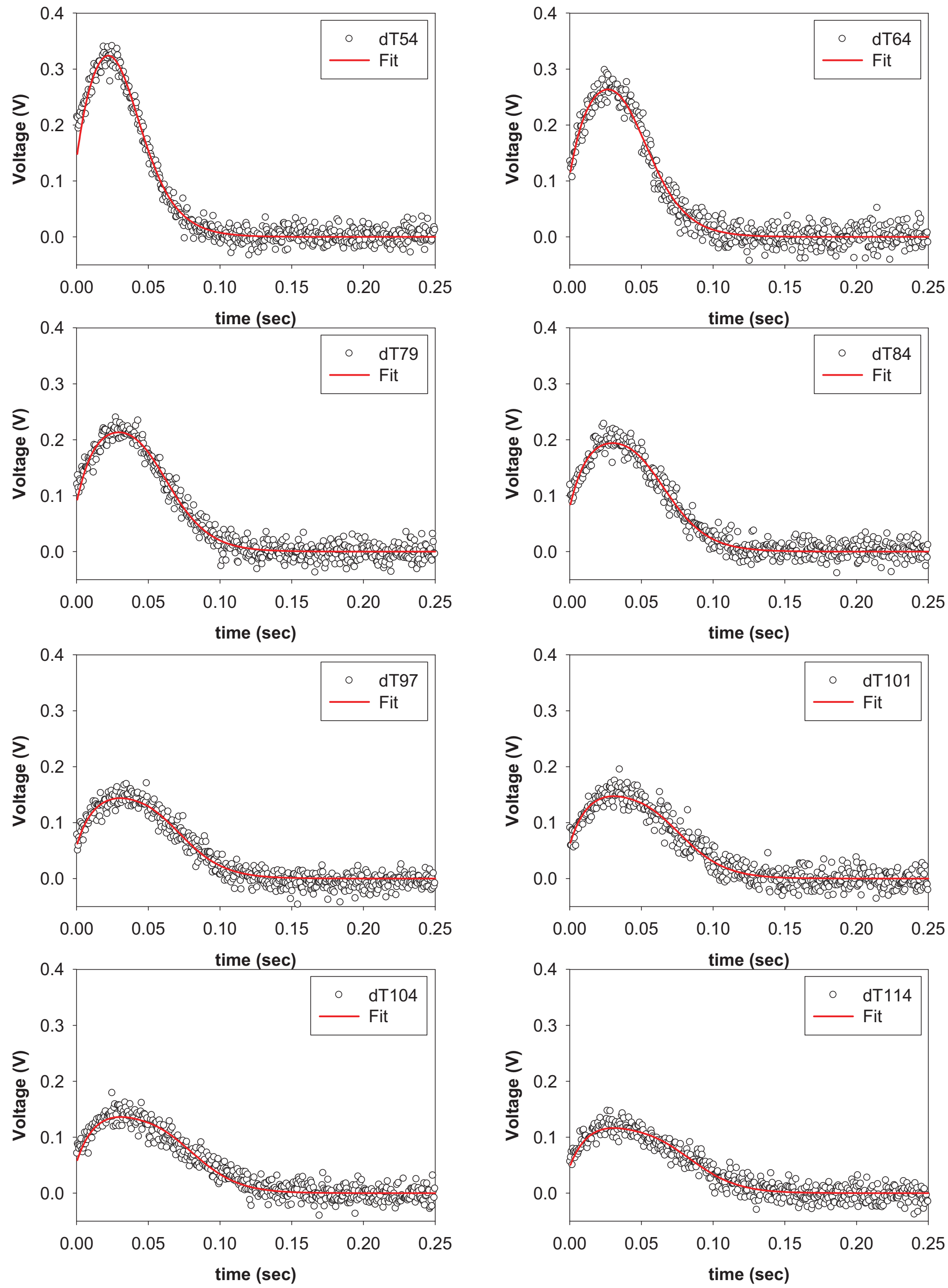

Figure 3-S10. RecBΔ2BΔnuc translocation along ssDNA. 5'-Cy3-dT$_L$ (100 nM) was mixed with 50 nM protein and translocation was initiated by mixing with ATP (10 mM) and heparin (10 mg/mL). Time courses are fit to **Scheme 1** using **Equation 1** described in Chapter 3. $m = 5.8 \pm 0.6$ nt, $k_t = 228 \pm 19$ sec^{-1}, $mk_t = 1310 \pm 11$ nt/sec, $k_d = 8.2 \pm 1.3$ sec^{-1}, $k_{end} = 65 \pm 10$ sec^{-1}, r = 0.9 ± 0.3, d = 3 ± 1 nt.

Can the RecBC primary or secondary translocase activity displace SSB during ssDNA translocation?

Since RecBC unwinding and translocation can be synchronized to initiate from a unique loading site using the partial duplex substrates described in Chapter 3, I have investigated whether the RecBC primary or secondary translocase activities can displace *E. coli* SSB during ssDNA translocation. Preliminary studies shown in **Figure 3-S11A** suggests that RecBC may be able to displace SSB as it translocates along the ssDNA extension using its primary translocase activity, since a peak in fluorescence intensity is observed when SSB is present (**Figure 3-S11A**, blue time course) and this peak occurs at a later time when compared with a time course without SSB (**Figure 3-S11A**, black time course). However, these results are difficult to interpret for several reasons. First, SSB binding to the Cy3 containing ssDNA also has an effect on Cy3 fluorescence intensity. Also, under these solution conditions (Buffer M), SSB binds to ssDNA in the 65 binding mode which wraps the around the DNA molecule, binging the ds/ss junction close to the Cy3 labeled DNA end. It is unclear whether the ds/ss junction influences Cy3 fluorescence when SSB is bound. Similar translocation experiments monitoring RecBC secondary translocase activity is interesting in that a peak in fluorescence intensity is not observed when SSB is present (**Figure 3-S11B**, blue time course). However, interpreting this data is also difficult because it is unclear to which process the initial decrease in fluorescence intensity corresponds. Additional work characterizing how SSB binding to the ssDNA and how the junction influences Cy3 fluorescence will be necessary to better understand these results.

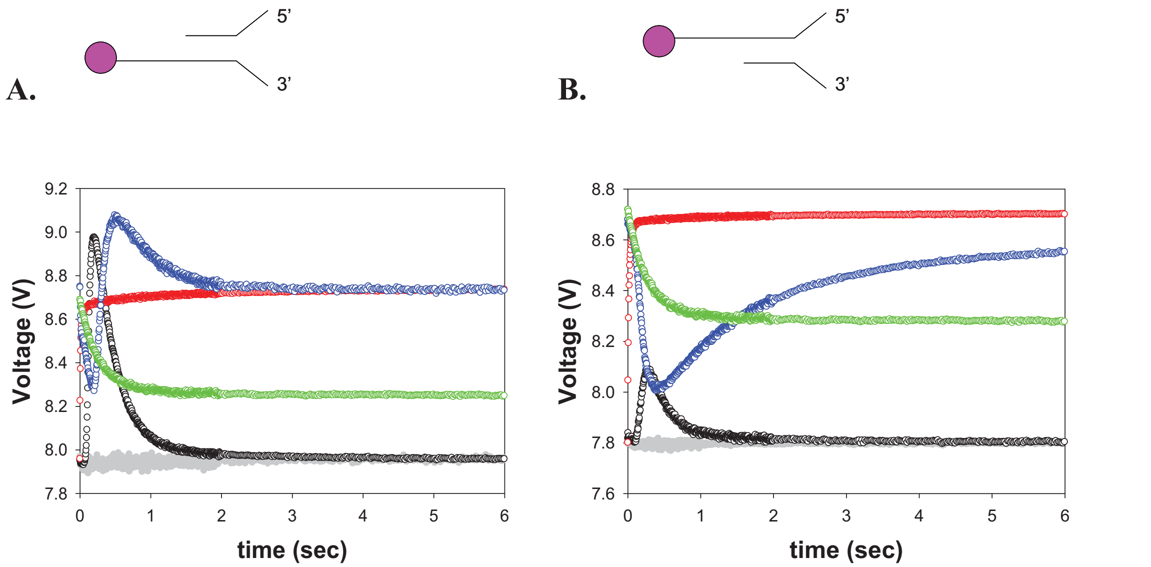

Figure 3-S11. Effect of SSB on the RecBC primary and secondary translocases. A). Primary translocase data. (●) translocation time course of a dT$_{75}$ ssDNA extension (24 bp duplex with a twin dT$_6$ RecBC loading site) collected with 100 nM RecBC and 200 nM DNA (as described in Chapter 3). (●) Fluorescence intensity of the DNA substrate alone. (●) 500 nM SSB (tetramer) binding to 200 nM DNA substrate. (●) translocation experiment in presence of 500 nM SSB. (●) SSB-DNA complex mixed with ATP and heparin. **B). Secondary translocase data.** (●) translocation time course of a dT$_{75}$ ssDNA extension (24 bp duplex with a twin dT$_6$ RecBC loading site) collected with 100 nM RecBC and 200 nM DNA (as described in Chapter 3). (●) Fluorescence intensity of the DNA substrate alone. (●) 500 nM SSB (tetramer) binding to 200 nM DNA substrate. (●) translocation experiment in presence of 500 nM SSB. (●) SSB-DNA complex mixed with ATP and heparin.

Chapter IV

Comparison of ATP Hydrolysis During DNA Unwinding and ssDNA Translocation by the *E. coli* RecBC Helicase

Preface to Chapter IV

In Chapter 3, I have shown that the RecBC helicase not only possesses a primary translocase activity with an expected 3' to 5' directionality, but also has a distinct secondary translocase activity which enables it to move along the opposite DNA strand. Although RecBC has two different translocase activities, they are both controlled by the RecB ATPase motor, and it remains unclear how ATP binding and hydrolysis is utilized to fuel DNA unwinding and translocation. Thus far, an ATP coupling stoichiometry for RecBCD catalyzed DNA unwinding has been estimated to be ~ 2-3 ATP/bp (1-1.5 ATP/bp for each motor) and the efficiency of ATP hydrolysis during RecBC unwinding is estimated to be ~ 1.2-1.4 ATP/bp (Roman and Kowalczykowski 1989; Korangy and Julin 1994). These measurements were obtained using steady state approaches and under multiple turnover conditions by taking the ratio of the steady state unwinding rate and the steady state rate of ATP hydrolysis, and as a result, these values can be influenced by slower processes such as protein dissociation and protein rebinding rather than DNA unwinding. In an effort to overcome such limitations and to potentially obtain a more accurate estimate of the efficiency of ATP hydrolysis during DNA unwinding and translocation by RecBC, this chapter describes pre-steady state phosphate release kinetic studies, which measure the amount of inorganic phosphate that is released during ATP hydrolysis. These experiments were performed with DNA unwinding substrates and also with substrates that monitor only the primary translocase, the secondary translocase, or translocation along both strands of ssDNA. This chapter is based on a manuscript which will soon be submitted for publication in the Journal of Molecular Biology (2010).

Comparison of ATP Hydrolysis During DNA Unwinding and Single-Stranded DNA Translocation by the *E. coli* RecBC Helicase

Colin G. Wu and Timothy M. Lohman*

Department of Biochemistry and Molecular Biophysics

Washington University School of Medicine

660 S. Euclid Avenue, Box 8231

Saint Louis, MO 63110

Running title: ATP Coupling Stoichiometry of RecBC During DNA Unwinding vs. ssDNA Translocation

*Address correspondence to: Timothy M. Lohman

Department of Biochemistry and Molecular Biophysics

Washington University School of Medicine

660 S. Euclid Avenue, Box 8231

Saint Louis, MO 63110

(314)-362-4393

(314)-362-7183 (Fax)

lohman@biochem.wustl.edu

Abstract

We have shown that the *E. coli* RecBC helicase possesses two distinct, but coupled ssDNA translocase activities controlled by the RecB ATPase motor. In order to better understand the relationship between RecBC translocation along ssDNA and its DNA unwinding activity, we have examined the efficiency of ATP hydrolysis during RecBC unwinding of DNA as well as during ssDNA translocation using stopped-flow fluorescence and a phosphate release assay. DNA unwinding by RecBC consumes an average of 0.95 ± 0.08 ATP/bp unwound while its primary translocase activity, which enables RecBC to translocate along ssDNA in the 3' to 5' direction, utilizes an average of 0.81 ± 0.05 ATP/nt translocated. The secondary translocase activity, which enables RecBC translocation along the opposite DNA strand, is less tightly coupled to ATP hydrolysis and uses an average of 1.12 ± 0.06 ATP/nt. When RecBC uses its two translocase activities to move along two non-complementary strands of ssDNA simultaneously, it consumes an average of 1.07 ± 0.09 ATP/nt, which is the same within error as the amount of ATP consumed during RecBC unwinding. The relative rate of DNA unwinding by RecBC is only about two fold slower than the rate of ssDNA translocation. Taken together, these results indicate that the large majority, possibly all, of the ATP hydrolyzed by RecBC during DNA unwinding is used to fuel translocation along the nucleic acid rather than to facilitate base pair melting. These results suggest that RecBC uses a two step active mechanism to unwind DNA by first using its binding free energy to destabilize multiple base pairs within the duplex in an ATP-independent process, followed by ATP-dependent translocation along the resulting ssDNA.

Introduction

DNA helicases are a ubiquitous class of motor proteins that function by coupling nucleoside triphosphate (NTP) binding and hydrolysis to unwind duplex DNA in order to produce the transient single stranded (ss) DNA intermediates required for all aspects of DNA metabolism (Abdel-Monem, Durwald et al. 1976; Abdel-Monem and Hoffmann-Berling 1976; Abdel-Monem, Durwald et al. 1977; Scott, Eisenberg et al. 1977; Kornberg, Scott et al. 1978; Yarranton, Das et al. 1979; Matson, Bean et al. 1994; Patel and Picha 2000; Delagoutte and von Hippel 2002; Lohman, Tomko et al. 2008). The *E. coli* RecBCD enzyme is a molecular motor possessing DNA helicase, ATPase, and nuclease activities, and is involved in the major pathway of homologous recombination in *E. coli* (Smith 1990; Kowalczykowski, Dixon et al. 1994; Anderson and Kowalczykowski 1997). In particular, RecBCD functions to repair damaged induced double stranded (ds) DNA breaks in *E. coli*. This heterotrimer possesses two superfamily-1 (SF1) motor subunits: RecB (134 kDa), a 3' to 5' helicase, and RecD (67 kDa), a 5' to 3' helicase (Finch, Storey et al. 1986; Finch, Wilson et al. 1986; Dillingham 2003; Taylor and Smith 2003). RecC (129 kDa) while structurally homologous to the RecB subunit, is devoid of the amino acids required for ATP hydrolysis and functions instead as a processivity and regulatory factor (Rigden 2005). Although the two motor subunits have opposite single strand translocation directionalities, they function in unison within the RecBCD heterotrimer and unwind dsDNA in the same net direction by translocating along the complementary strands of the duplex (Dillingham 2003; Taylor and Smith 2003). RecBCD first binds to the damaged DNA at a blunt or nearly blunt end and then unwinds the duplex in an ATP-dependent manner with RecD serving as the leading motor (Spies, Amitani et al. 2007). During unwinding, RecBCD preferentially degrades the 3' terminating DNA strand while cleaving the 5' terminating strand infrequently (Yu, Souaya et al. 1998; Yu, Souaya et al. 1998). These activities ensue until RecBCD recognizes the crossover hotspot instigator (chi) regulatory sequence (5'-GCTGGTGG-3') within the unwound DNA, whereupon RecBCD first pauses and then continues to unwind the DNA with a slower rate with RecB now as the leading motor (Handa, Bianco et al. 2005). The nuclease activity after chi recognition is modified such that it degrades instead the 5' terminating strand, thereby creating a 3' ssDNA overhang onto which RecBCD can load the RecA protein (Arnold and Kowalczykowski 2000; Spies, Bianco et al. 2003). The resulting RecA coated ssDNA filament forms a joint molecule with a homologous piece of DNA and initiates recombinational repair of the break.

Interestingly, the RecBC enzyme, without the RecD subunit, still functions as a rapid and processive helicase but its nuclease activity is greatly attenuated (Korangy and Julin 1993). Since RecBC possesses a single ATPase motor, this simpler enzyme is a good model system with which to study how ATP binding and hydrolysis is coupled to DNA unwinding and translocation. RecBC binds with optimal affinity to DNA ends with pre-existing 5'-$(dT)_6$ and 3'-$(dT)_6$ ssDNA tails since RecBC can "melt-out" six base pairs upon DNA binding in a Mg^{2+} dependent but ATP independent manner (Farah and Smith 1997; Singleton, Dillingham et al. 2004; Wong, Lucius et al. 2005). RecBC can initiate DNA unwinding from this "pre-melted" DNA end structure using a simple *n*-step sequential mechanism with an average kinetic step-size of 4.4 ± 0.1 bp and a macroscopic unwinding rate of 348 ± 5 bp/sec (20 mM Mops-KOH, pH 7.0 at 25ºC, 10 mM NaCl, 10 mM $MgCl_2$, 5% (v/v) glycerol, 1 mM 2-mercaptoethanol) (Wu and Lohman 2008)

We have shown that RecBC possesses two distinct translocase activities that are controlled by the single ATPase motor within RecB. The primary translocase activity enables RecBC to translocate along ssDNA in the expected 3' to 5' direction while the secondary translocase activity facilitates translocation along the other DNA strand, but surprisingly is not sensitive to the polarity of the ssDNA backbone. RecBC can use its two translocase activities to move along two non-complementary strands of ssDNA simultaneously. To better understand the relationship between DNA unwinding and translocation, we have compared the ATP coupling stoichiometry of RecBC catalyzed DNA unwinding with that of its translocase activities using a stopped-flow fluorescence phosphate release assay. This method utilizes the *E. coli* phosphate binding protein (PBP) A197C mutant, which can be labeled fluorescently with coumarin (MDCC) (Brune, Hunter et al. 1998). The resulting protein, PBP-MDCC, exhibits a large increase in fluorescence intensity when it binds to inorganic phosphate and therefore functions as a phosphate sensor by detecting the amount of phosphate released in solution; this probe has been used to examine the ATPase activity of a number of helicases (Dillingham, Wigley et al. 2000; Dillingham, Wigley et al. 2002; Kim, Narayan et al. 2002; Tomko, Fischer et al. 2007). Previous studies of the efficiency of ATP hydrolysis during DNA unwinding by RecBCD has estimated ~ 2-3 ATP/bp unwound or ~ 1-1.5 ATP/bp per motor, and the ATP coupling stoichiometry during RecBC unwinding is estimated to be ~1.2-1.4 ATP/bp unwound (Roman and Kowalczykowski 1989; Korangy and Julin 1994). Using a stopped-flow fluorescence phosphate release assay, we have examined the pre-steady kinetics of ATP hydrolysis during both RecBC unwinding and ssDNA translocation under single-turnover conditions, which allows us to examine the relative contributions of ATP hydrolysis to each activity.

Results

RecBC-catalyzed DNA unwinding kinetics as a function of [ATP]

We have determined previously the minimal kinetic mechanism to describe RecBC unwinding at saturating ATP concentration (5 mM after 1:1 mixing) (Wu and Lohman 2008). Here we examine the kinetics of DNA unwinding as a function of [ATP]. These studies are needed to allow us to compare DNA unwinding rates with phosphate release studies, which had to be performed at 75 μM ATP in order to minimize the amount of PBP-MDCC used in those experiments.

Stopped-flow fluorescence unwinding experiments were performed as described in Materials and Methods and also previously (Lucius, Jason Wong et al. 2004; Wu and Lohman 2008) using the DNA substrates depicted in **Figure 1** and also presented in Chapter 2 (DNA sequences are given in **Table S1**). These DNA substrates are composed of three strands and possess a Cy3-Cy5 FRET pair when annealed together (**Figure 1**). Initially, in the duplex DNA, Cy3 fluorescence is quenched by the Cy5 fluorophore due to its close proximity. After RecBC unwinds and displaces the Cy3 containing DNA strand, Cy3 fluorescence intensity increases. The opposite trend is observed for Cy5 fluorescence intensity since initially FRET efficiency is high with the Cy3 labeled strand in close proximity, and FRET efficiency decreases when the Cy3 containing strand is displaced. RecBC unwinding experiments were performed at 10 μM, 37.5 μM, 75 μM, 120 μM, 416 μM, 1.4 mM, and 5 mM ATP, and the resulting time courses are shown in **Figure 1A-G**. The DNA unwinding kinetics at all [ATP] are described well by **Equation 1** based on the simple *n*-step sequential model shown in **Scheme 1**. The solid curves are simulations based on the best fit kinetic parameters in **Table 1**. Consistent with previous unwinding studies (Wu and Lohman 2008), the number of unwinding steps, *n*, is directly proportional to duplex length, *L*, at all [ATP] examined as shown in **Figure 2A-G**. The average kinetic step-size as well as the macroscopic unwinding rate determined at each [ATP] (**Table 1**) is plotted versus [ATP] and shown in **Figure 3A** and **3B**. As observed for RecBCD (Lucius, Jason Wong et al. 2004; Lucius and Lohman 2004), the average kinetic step-size for DNA unwinding is independent of [ATP] (4.0 ± 0.3 bp) and the macroscopic unwinding rate exhibits a hyperbolic dependence with [ATP] as shown in **Figure 3B**. Fitting this data to the Michaelis-Menton equation (**Equation 2**) yields K_M = 131 ± 23 μM and V_{max} = 317 ± 14 bp/s, which is consistent with the unwinding rate determined for RecBC under saturating ATP concentration (5 mM ATP, 347 ± 5 bp/sec) (Wu and Lohman 2008). In comparison, RecBC translocates along two non-complementary ssDNA extensions with a rate 671 ± 47 nt/sec under the same solution conditions (Chapter 3) (20 mM Mops-KOH, pH 7.0 at 25°C, 30 mM NaCl, 10 mM MgCl2, 5% (v/v) glycerol, 1 mM 2-mercaptoethanol, 5 mM ATP); hence, RecBC has a $V_{un}/V_{trans} \approx 0.52$ where V_{un} and V_{trans} are the DNA unwinding and ssDNA translocation rates, respectively.

ATP coupling stoichiometry during DNA unwinding by RecBC

Phosphate release experiments were performed as described in Materials and Methods. The DNA hairpin substrates used to study DNA unwinding were not used for these experiments since RecBC can unwind beyond the reporter strand and continue to unwind the rest of the substrate and hydrolyze ATP. We have therefore used DNA substrates which possess a high affinity RecBC loading site followed by a duplex region of length *L* and a 40 nt 3' ssDNA overhang as depicted in **Figure 4A**. RecBC binds and initiates unwinding preferentially at the 5'-$(dT)_6$, 3'-$(dT)_6$ loading site when DNA is present in excess (200 nM) over RecBC (20 nM). Furthermore, the binding affinity of RecBC for a DNA end decreases dramatically for ends with a 3' ssDNA tail length greater than six nucleotides (Wong, Rice et al. 2006), thus favoring initiation at the DNA end possessing the high affinity loading site. DNA unwinding is initiated by 1:1 mixing with 150 μM ATP, 10 mg/mL heparin trap, and 40 μM PBP-MDCC. Final conditions therefore are 100 nM DNA, 10 nM RecBC, 75 μM ATP, 5 mg/mL heparin, and 20 μM PBP-MDCC. A mock phosphate release experiment was performed the same way but in the absence of the DNA substrate to determine the amount of phosphate contamination within the buffers and reagents, and also to measure any background ATP hydrolysis that may occur when RecBC is not bound to DNA. PBP-MDCC was calibrated as described in Materials and Methods by mixing the same ATP, heparin, and PBP-MDCC solution with known concentrations of phosphate standard in order to relate the observed fluorescence intensity to the amount of phosphate present (**Supplementary Figure 1**). Calibrated phosphate release time-courses corrected for phosphate contamination are shown in **Figure 4A**. Control experiments indicate that under these conditions, PBP-

MDCC binding to phosphate is not rate limiting, and heparin does not stimulate the ATPase activity of RecBC (**data not shown**).

When RecBC unwinds the DNA substrate, there is a burst of phosphate released followed by a slower steady-state release of phosphate. We have shown that after RecBC unwinds a duplex, it can remain bound to the ds/ss junction and use its secondary translocase activity to reel in a 5' to 3' ssDNA extension. As a result, the burst phase reflects the amount of ATP consumed during the unwinding of L (L = 24, 29, 37, 40, 43, 48, 53, and 60 bp) and also the translocation along the 40 nt ssDNA extension; an overlay of an unwinding time course collected also at 75 μM ATP (**Figure 1,** L = 40) and the phosphate release time course for a L = 40 substrate is shown in **Supplementary Figure 2**. The long lived steady-state phase of phosphate release corresponds to futile ATP hydrolysis which occurs due to RecBC molecules remaining bound to the DNA substrate after DNA unwinding and ssDNA translocation. The time-courses in **Figure 4A** are analyzed using **Equation 3** which describes the initial burst phase followed by the slower linear phase, and the resulting parameters are summarized in **Table 2**. The burst amplitudes determined from this analysis for each DNA substrate (L = 24, 29, 37, 40, 43, 48, 53, and 60 bp) are plotted versus the corresponding duplex length (**Figure 4B**). Since each DNA substrate has the same 40 nt ssDNA extension, the slope of this plot reflects the amount of ATP hydrolyzed during RecBC catalyzed DNA unwinding only, which indicating an average of 0.95 ± 0.08 ATP/bp unwound.

ATP coupling stoichiometry during ssDNA translocation by RecBC

We have shown that after unwinding a DNA duplex, RecBC can use its primary translocase activity to translocate along a 3' to 5' ssDNA extension and/or also use its secondary translocase activity to move along a 5' to 3' ssDNA extension. In fact, these two activities enable RecBC to translocate simultaneously along substrates with two strands of non-complementary ssDNA. We have performed phosphate release experiments to determine the ATP coupling stoichiometry during these RecBC translocation activities. The DNA substrates used in these studies (shown schematically in **Figure 5A**, **6A**, and **7A**) possess a 24 bp duplex region with a 5'-$(dT)_6$, 3'-$(dT)_6$ RecBC loading site on one end of the duplex. Flanking the other end of the duplex are either a series of 3' to 5' ssDNA extensions, 5' to 3' ssDNA extensions, or twin extensions of length L (L = 15, 30, 45, or 60 nts).

Phosphate release time courses examining the primary translocase activity of RecBC (3' to 5' ssDNA translocation) are shown in **Figure 5A**. A burst phase of release of phosphate is observed followed by a slower linear phase as was observed for RecBC unwinding. This burst phase also represents the amount of ATP hydrolyzed during RecBC unwinding of the initial duplex followed by translocation along the ssDNA extension; an overlay of a time course monitoring 3' to 5' ssDNA translocation (L = 45) and the phosphate release time course (L = 45) is shown in **Supplementary Figure 3**. The time courses in **Figure 5A** were fit to **Equation 3** and a summary of the resulting kinetic parameters are given in **Table 2**. Since all the DNA substrates possess the 24 bp initial duplex, the burst amplitudes are plotted versus ssDNA extension length in **Figure 5B** and the slope of this plot reflect the amount of ATP hydrolyzed during RecBC translocation only. The primary RecBC translocase uses an average of 0.81 ± 0.05

ATP/nt. Similar experiments were performed to monitor the release of phosphate associated with the secondary translocase activity of RecBC, and the results are plotted in **Figure 6A**. An overlay of the translocation kinetics of the RecBC secondary translocase and the phosphate release kinetics are shown in **Supplementary Figure 4** (L = 45). The time courses in **Figure 6A** are also well described by **Equation 3** (parameters summarized in **Table 2**). A plot of the burst amplitude versus ssDNA extension length is shown in **Figure 6B** and the slope of this plot indicates that on average, the secondary translocase of RecBC consumes 1.12 ± 0.06 ATP/nt translocated, which is slightly larger than the value determined for the primary translocase.

Since RecBC can utilize both translocase activities to move along two non-complementary ssDNA extensions simultaneously, we have also examined the phosphate release kinetics using the substrates depicted in **Figure 7A**. These phosphate release time courses analyzed using **Equation 3** (parameters given in **Table 2**) and analysis of the burst amplitude as a function of the length of the two non-complementary strands of ssDNA extensions (**Figure 7B**) indicates that on average RecBC utilizes 1.07 ± 0.09 ATP/nt translocated on these substrates.

Discussion

RecBC-catalyzed DNA unwinding as a function of [ATP]

My previous RecBC-catalyzed DNA unwinding studies performed under the same solution conditions but at 5 mM ATP (final concentration after 1:1 mixing) indicated that RecBC initiates DNA unwinding from duplexes with pre-existing 5'-$(dT)_6$, 3'-$(dT)_6$ ssDNA tails using a simple n-step sequential mechanism with a macroscopic unwinding rate of 348 ± 5 bp/sec and an average kinetic step-size of 4.4 ± 0.1 bp (Wu and Lohman 2008). Here we show that DNA unwinding time courses collected over a wide range of [ATP] are also well described by this simple *n*-step sequential model and the average unwinding kinetic step-size is not sensitive to [ATP] (4.0 ± 0.3 bp). Similar unwinding experiments conducted by Lucius et al. (Lucius and Lohman 2004) have shown that the average kinetic step-size for RecBCD unwinding is independent of both [ATP] and temperature (~ 4 bp). Taken together, these results suggest that in between two successive rate-limiting steps during the repeated DNA unwinding cycles, RecBC and RecBCD unwind an average of 4 base pairs. However, it remains unclear what process is reflected in this repeated slow step such as protein conformational change, product release, and so forth. Because RecBC and RecBCD have a similar average kinetic step-size for DNA unwinding, the same process(es) likely contribute to the repeated slow step, which remains rate-limiting over the range of [ATP] examined for both helicases. We can conclude at a minimum, based on simulations of unwinding data (Lucius and Lohman 2004), that this repeated slow step is coupled to ATP binding and that there cannot be any additional fast steps in between the ATP binding step and the repeated step; otherwise, a transition would occur in the apparent kinetic step-size (Lucius and Lohman 2004), which was not observed experimentally.

We note the caveat that the step-size analysis of our DNA unwinding experiments will be affected by the presence of static heterogeneity (or "static disorder") if present in the protein population since our analysis assume a homogenous protein population. Based on single-molecule unwinding and translocation studies of the RecBCD (Bianco, Brewer et al. 2001; Handa, Bianco et al. 2005) and UvrD (Lionnet, Dawid et al. 2006) helicases, significant variations in the rate of DNA unwinding and ssDNA translocation have been observed in the protein population although any given helicase molecule has a characteristic rate which persists throughout the reaction. As a result, although the average rate of unwinding for many single molecules is comparable to the ensemble measured average, these large variations in the kinetic rates in the population can lead to an overestimate of the apparent step-size for DNA unwinding using our methods. It is unclear whether static disorder is present in our protein molecules or what may be the source of this heterogeneity; as a result, we conclude that the average kinetic step-size for RecBC and RecBCD unwinding can be no greater than ~ 4 bp.

RecBC unwinds DNA using an active mechanism

Two limiting cases have been considered for mechanisms of helicase-catalyzed DNA unwinding, namely a passive and an active mechanism (Lohman 1992). In an active mechanism, the helicase lowers the activation energy for duplex DNA separation by direct participation in destabilizing the duplex DNA (Betterton and Julicher 2005; Manosas, Xi et al. 2010). As a result, the unwinding rate of a fully active helicase is limited by how quickly it can translocate along the newly generated ssDNA and is not limited by base pair melting ($V_{un}/V_{trans} \approx 1$ where V_{un} and V_{trans} are the unwinding and ssDNA translocation rates, respectively) (Manosas, Xi et al. 2010). On the other hand, a passive helicase must instead wait for the duplex DNA to open transiently through thermal fluctuations and then advance into the fork using its unidirectional translocation activity thereby preventing the two DNA strands from reannealing (Lohman 1992). Since a passive helicase does not influence the height of the energy barrier required to separate the DNA duplex, the unwinding rate of a passive helicase is expected to be much slower than its translocation rate. Based on a model from Betterton and Julicher (Betterton and Julicher 2005), Manosas et al (Manosas, Xi et al. 2010) define a passive helicase to have $V_{un}/V_{trans} < 0.25$, and an active helicase to have $V_{un}/V_{trans} \geq 0.25$; this is based upon the assumption that the helicase has a step size of 1 bp and can lower the free energy of the fork by 1 K_BT. The macroscopic unwinding rate of RecBC at 5 mM ATP is 348 ± 5 bp/sec (Wu and Lohman 2008) and the rate at which RecBC translocates along two non-complementary strands of ssDNA at 5 mM ATP is 671 ± 47 nt/sec (Chapter 3). Hence, $V_{un}/V_{trans} = 0.52$ which suggests that RecBC unwinds DNA using an active mechanism.

In a crystal structure of a RecBCD-DNA complex, the "arm" region of the RecB motor subunit is observed to interact with the duplex DNA ahead of the unwinding fork (Singleton, Dillingham et al. 2004; Saikrishnan, Griffiths et al. 2008). This arm domain could potentially be involved in destabilizing dsDNA during RecBC unwinding. Also, both RecBC and RecBCD can "melt-out" ~ 6 bp upon DNA binding in a Mg^{2+} dependent but ATP independent manner, further suggesting that RecBC is able to influence the stability of the duplex and can therefore unwind DNA using an active mechanism (Farah and Smith 1997; Wong, Lucius et al. 2005; Wong and Lohman 2008). For comparison, the *E. coli* RecQ protein has been shown to unwind DNA using an active mechanism and has a V_{un} (~80 bp/sec)/V_{trans} (~90 nt/sec) > 0.7 under a variety of experimental conditions (0-80% GC content and 3 to 11 pN external force), while the T4 gp41 helicase unwinds DNA using a passive mechanism and has a V_{un} (30-40 bp/sec)/V_{trans} (350-500 nt/sec) < 0.1 (Manosas, Xi et al. 2010).

Efficiency of ATP hydrolysis during RecBC catalyzed DNA unwinding and ssDNA translocation

Since we have been able to examine RecBC catalyzed DNA unwinding and translocation independently, we have determined the ATP coupling stoichiometry during these two processes in order to better understand the relationship between DNA unwinding and ssDNA translocation. The ATP coupling stoichiometry during RecBCD unwinding has been estimated to be ~ 2-3 ATP/bp unwound or 1-1.5 ATP/bp per motor, and for RecBC it has been estimated to be ~ 1.2-1.4 ATP/bp (Roman and Kowalczykowski 1989; Korangy and Julin 1994). Our result of 0.95 ± 0.08 ATP/bp unwound for RecBC is consistent with these observations. During ssDNA translocation, the RecBC primary translocase uses 0.81 ± 0.05 ATP/nt translocated while the secondary translocase consumes 1.12 ± 0.06 ATP/nt. These values suggest that the primary translocase activity uses ATP more efficiently than DNA unwinding while the secondary translocase activity uses ATP less efficiently than DNA unwinding; however, these differences likely result from the fact that the DNA substrates used to examine ATP hydrolysis during the RecBC primary and secondary translocase activities are different. When only the secondary translocase activity is monitored, RecBC remains bound to the ds/ss junction after DNA unwinding and uses its secondary translocase activity to reel in a 5' to 3' ssDNA extension whereas when only the primary translocase activity is monitored, RecBC can continue translocation along a 3' to 5' ssDNA extension uninterrupted (Chapter 3).

Interestingly, RecBC translocation along two non-complementary ssDNA extensions has an ATP coupling stoichiometry of 1.07 ± 0.09 ATP/nt. These substrates mimic those of DNA unwinding except the bases have been "pre-melted" and as a result, RecBC would not need to unwind the duplex. The fact that this value is the same within error as the value determined during DNA unwinding indicates that most of the energy, possibly all, obtained from ATP binding and hydrolysis is used to fuel RecBC translocation rather than to catalyze the strand separation reaction during DNA unwinding. This may be unique to the RecBC and perhaps RecBCD enzyme since either helicase can "melt-out" ~ 5-6 bp upon binding to DNA ends (Farah and Smith 1997; Wong, Lucius et al. 2005; Saikrishnan, Griffiths et al. 2008), and that the average kinetic step-size for RecBC and RecBCD unwinding is also ~ 4 bp (Lucius, Vindigni et al. 2002; Wu and Lohman 2008) with the potential caveat of static disorder.

We offer two potential unwinding models based on our observation that RecBC uses ~ 1 ATP/bp unwound and also ~ 1 ATP/nt translocated during DNA unwinding and ssDNA translocation. In one case, DNA unwinding is separate from ssDNA translocation (**Figure 8A**). If the hydrolysis state of the nucleotide is able to modulate RecBC between high and low affinity states for DNA binding, then RecBC can use its binding free energy to melt out 4-6 bp at once, and then translocation occurs subsequently using ~ 1 ATP/nt. An alternative model is that both DNA unwinding and ssDNA translocation occur simultaneously (**Figure 8B**) using 1 ATP/bp (or nt) and that the duplex is unwound as the DNA fork is translocated past the "separation pin" within the RecC subunit (Singleton, Dillingham et al. 2004; Rigden 2005). One way to discern between these two unwinding models is to examine RecBC unwinding in a single-molecule experiment using high resolution optical traps (Cheng, Dumont et al. 2007; Johnson, Bai et al. 2007). If DNA unwinding and translocation occur separately as depicted in **Figure 8A** and RecBC can melt out 4-6 bp at a time, then one would be able to observe bursts or steps of 4-6 bp during DNA unwinding. If however, DNA unwinding and translocation occur simultaneously using 1 ATP/bp as depicted in **Figure 8B**, then smaller bursts or steps of ~ 1 bp would be observed. These experiments will need to be conducted as a function of GC content, applied force, and ATP concentration in order to access whether the observed 4-6 bp steps are composed of smaller sub steps.

Comparison with other DNA helicases

The efficiency of ATP hydrolysis during ssDNA translocation of two other SF1 helicases, *E. coli* UvrD and *B. stereothermophilus* PcrA is estimated to be ~ 1 ATP/nt translocated using ensemble fluorescence approaches (Dillingham, Wigley et al. 2000; Tomko, Fischer et al. 2007). Based on structural studies of these two enzymes (Velankar, Soultanas et al. 1999; Lee and Yang 2006), the ATP coupling stoichiometry during DNA unwinding was inferred to be ~ 1 ATP/bp unwound although a direct comparison between the efficiency of ATP hydrolysis during DNA unwinding and ssDNA translocation has not been made for UvrD and PcrA. Such a comparison has been made for the ring-shaped hexameric bacteriophage T7 helicase (Kim, Narayan et al. 2002). During DNA unwinding, T7 unwinds 3-4 bp per molecule of dTTP hydrolyzed if the DNA substrate is rich in AT sequences (< 50% GC content) but only 1-2 bp are unwound per dTTP hydrolyzed if the DNA substrate is rich in GC sequences (Donmez and Patel 2008). During ssDNA translocation, T7 uses one dTTP to move along 2-3 bases of ssDNA (Kim, Narayan et al. 2002); hence the efficiency of dTTP hydrloysis during DNA unwinding and ssDNA translocation are comparable for the T7 helicase. Our measurement of ~ 1 ATP/bp unwound and also ~ 1 ATP/nt translocated for the RecBC enzyme indicates that T7 is uses dTTP more effciently for both DNA unwinding and ssDNA translocation. We have not at this time examined the influence of DNA base sequence composition on the efficiency of ATP hydrolysis during unwinding and translocation, and our unwinding experiments were performed using mixed sequence DNA substrates with ~40% GC content. It will be interesting to test whether RecBC would have the same ATP coupling stoichiometry when uniwnding DNA duplexes with higher or lower GC content. It has been shown that RecBCD can undergo forward and reverse motion during DNA unwinding (Perkins, Li et al. 2004). It is possible that RecBCD and perhaps RecBC may undergo futile ATP hydrolysis as a result of backwards motion and/or pausing and therefore does not utilize ATP as effciently as T7. The rates of T7-catalyzed DNA unwinding and of ssDNA translocation have also been compared directly. Although T7 translocates along ssDNA processively with a rate of 130-300 nt/sec, it unwinds dsDNA with a rate of only 15-30 bp/sec (Kim, Narayan et al. 2002; Jeong, Levin et al. 2004; Johnson, Bai et al. 2007). Hence, V_{un}/V_{trans} for T7 is ~ 0.1, which suggests that it uses a passive mechanism to unwind DNA. In fact, a strand exclusion model for DNA unwinding model has been proposed in which T7 translocates rapidly and processively along ssDNA with the ssDNA strand going through the center cavity of the hexameric ring (Ahnert and Patel 1997; Patel and Picha 2000). When T7 encounters a DNA duplex, it slows and must await for the bases to open transiently through thermal fluctuations before it can continue translocation, and the DNA strand along which T7 does not translocate is excluded from the center channel thereby preventing the two ssDNA strands from reannealing. Even though T7 uses dTTP effciently to unwind and to translocate along DNA, it unwinds DNA using a passive mechanism. It will be interesting to be similar comparisons between the rates of DNA unwinding and ssDNA translocation and also of the efficiency of ATP hydrolysis during these two processes for other ring-shaped hexameric helicases and non-hexameric SF1 enzymes.

Acknowledgements

This research was supported in part by the National Institute of Health through grant GM045948. We thank Thang Ho for synthesis and purification of all DNA substrates; Drs. Chris Fischer and Aaron Lucius for discussions of data analysis; Drs. Gerald Smith and Doug Julin for providing plasmids and cell lines.

Materials and Methods

Buffers and Reagents

All buffers were prepared with reagent grade chemicals and doubly-distilled water that was deionized further using a Milli-Q purification system (Millipore Corp., Bedford, MA). Solutions were filtered through 0.2 micron filters after preparation. Buffer M is 20 mM Mops-KOH (pH 7.0 at 25°C), 30 mM NaCl, 10 mM $MgCl_2$, 1 mM 2-ME, 5% (v/v) glycerol. Heparin stock solution was prepared by dissolving heparin sodium salt (Sigma, St. Louis, MO) in Buffer M and dialyzing the mixture extensively against Buffer M using 3500 molecular weight cut-off dialysis tubing. Heparin stock solution was stored at 4ºC until use and its concentration was determined by titration with Azure A as described (Tomko, Fischer et al. 2007). ATP stock solution was prepared as described previously and stored at -20ºC until use (Wu and Lohman 2008).

Proteins

E. coli RecB and RecC were purified separately and stored at -80°C as described (Lucius, Jason Wong et al. 2004). The RecBC heterodimer was reconstituted by mixing equal molar ratios of RecB and RecC on ice. RecBC was dialyzed against Buffer M at 4°C before use and its concentration was determined spectrophotometrically using an extinction coefficient of $\varepsilon_{280} = 3.9\times10^5$ $M^{-1}cm^{-1}$ (Wu and Lohman 2008). *E. coli* phosphate binding protein (PBP) was purified, labeled with coumarin (MDCC) (Invitrogen, Carlsbad, CA), and stored at -80ºC until use as described (Tomko, Fischer et al. 2007).

Oligodeoxynucleotides

DNA oligos, either unlabeled or labeled covalently with Cy3 or Cy5, were synthesized, purified, and their concentrations were determined as described (Wu and Lohman 2008). DNA stock solutions were stored at -20°C until use. The sequences of the DNA substrates are given in **Supplemental Table 1**.

Stopped-flow fluorescence experiments

All stopped-flow fluorescence measurements were collected using an SX.18MV stopped-flow apparatus (Applied Photophysics Ltd., Leatherhead, UK). All experiments were performed in Buffer M at 25°C.

DNA unwinding experiments were performed by incubating DNA substrate (40 nM) (L = 24, 29, 37, 40, 43, 48, 53, and 60 bp) with RecBC (200 nM) in one syringe of the apparatus and DNA unwinding was initiated by 1:1 mixing with ATP (20 μM, 75 μM, 150 μM, 240 μM, 832 μM, 2.8 mM, and 10 mM) and heparin (15 mg/mL) as described (Wu and Lohman 2008). Cy5 fluorescence was excited at 515 nm and its emission was collected at 570 nm using an interference filter (Oriel Corp., Stradford, CT) while Cy5 fluorescence was monitored simultaneously at all wavelengths > 665 nm using a cutoff filter (Oriel Corp., Stradford, CT).

Phosphate release experiments were performed by incubating DNA substrate (200 nM) with RecBC (20 nM) in one syringe of the instrument and the reaction was initiated by 1:1 mixing with ATP (150 μM), heparin (10 mg/mL), and PBP-MDCC (40 μM). Final conditions are therefore: 100 nM DNA, 10 nM RecBC, 75 μM ATP, 5 mg/mL heparin, and 20 μM PBP-MDCC in Buffer M. Identical experiments were performed without the DNA substrate to access the amount of phosphate contamination in buffers and reagents and also any background hydrolysis that may occur with RecBC. PBP-MDCC fluorescence was excited at 430 nm and its emission was collected at all wavelengths > 450 nm using a cutoff filter (Oriel Corp., Stradford, CT).

PBP-MDCC was calibrated by mixing the same ATP solution used in phosphate release experiments (150 μM ATP, 10 mg/mL heparin, and 40 μM PBP-MDCC) with various phosphate standards of 0, 0.5, 1.0, 1.5, 2.0, 2.5, 3.0, and 5 μM as described previously (Tomko, Fischer et al. 2007).

Analysis of DNA unwinding time courses

Global NLLS analysis of DNA unwinding time courses was performed using Conlin (kindly provided by Dr. Jeremy Williams and modified by Dr. Aaron Lucius) and IMSL C Numerical Libraries (Visual Numeric Incorporated, Houston, TX) as described previously (Wu and Lohman 2008). The uncertainties reported reflect 68% confidence interval limits determined from a 50 cycle Monte Carlo analysis as described (Lucius, Vindigni et al. 2002; Fischer and Lohman 2004; Fischer, Maluf et al. 2004; Lucius, Jason Wong et al. 2004)). Unwinding time courses were fit to **Equation 1** based on mechanism shown in **Scheme 1**, by obtaining the time-dependent formation of ssDNA, $f_{ss}(t)$, as the inverse Laplace transform of $F_{ss}(s)$ using numerical methods as described (Wu and Lohman 2008). For **Scheme 1**, $f_{ss}(t)$ is given by **Equation 1**:

$$\begin{aligned} f_{ss}(t) &= A_T \mathcal{L}^{-1} F_{ss}(s) \\ &= A_T \mathcal{L}^{-1}\left(\frac{k_{obs}^{n}(k_{NP}+sx)}{s(k_{NP}+s)(k_{obs}+s)^{n}}\right) \end{aligned} \qquad \text{(\textbf{Equation 1})}$$

where $F_{ss}(s)$ is the Laplace transform of $f_{ss}(t)$, $\mathcal{L}^{-1}$ is the inverse Laplace transform operator with s as the Laplace variable, A_T is the total amplitude for a given duplex length L, n is the number of unwinding steps with k_{obs} being the rate constant in between two successive unwinding steps, k_{NP} is the isomerization rate constant for the conversion of non-productive, $(RD)_{NP}$, to productive, $(RD)_L$, RecBC-DNA complexes, and x is the fraction of productively bound RecBC-DNA complexes. The average kinetic step-size, *m*, can be determined by NLLS analysis by replacing *n* in **Equation 1** with *L*/*m*. Alternatively, *m* can be determined from the slope of a plot of *n* vs *L*.

The plot of the macroscopic unwinding rate (mk_{obs}) versus [ATP] was fit to the Michaelis-Menton equation (**Equation 2)**

$$mk_{obs} = \frac{V_{\max}[ATP]}{K_M + ATP} \qquad \textbf{(Equation 2)}$$

Analysis of phosphate release kinetics

In order to determine the amount of phosphate released from the fluorescence signal obtained from phosphate release time courses, a calibration experiment was performed as described above by mixing the ATP, heparin, and PBP-MDCC solution with known concentrations of phosphate standard. These resulting traces were fit to a single exponential function ($Ae^{-kx} + C$) and the plateau value, C, was plotted versus phosphate standard concentration to obtain a calibration curve (**Supplemental Figure 1**). The fluorescence values from the phosphate release experiments fall within the linear region of the calibration curve and these time courses were analyzed using **Equation 3** which describes a burst of phosphate released followed by a steady-state phase of phosphate released.

$$Pi(t) = A_b(1 - e^{-k_b t}) + k_{ss}t \qquad \textbf{(Equation 3)}$$

Figure Legends

Figure 1. [ATP] dependence on RecBC catalyzed DNA unwinding. A-G). Unwinding time courses collected at 10 μM, 37.5 μM, 75 μM, 120 μM, 416 μM, 1.4 mM, and 5 mM ATP (*L* = 24, 29, 37, 40, 43, 48, 53, and 60 bp). Solid lines are simulations based on the

best fit parameters determined from NLLS analysis using **Equation** 1. The kinetic parameters are summarized in **Table 1**.

Figure 2. "*n* vs. *L*" plots. The number of unwinding steps "n" is plotted versus duplex length "L" at 10 μM, 37.5 μM, 75 μM, 120 μM, 416 μM, 1.4 mM, and 5 mM ATP. **A)**. 10 μM ATP: line of best fit is $n = 0.2433L + 0.0528$. **B**). 37.5 μM ATP: line of best fit is $n = 0.2311L - 0.0027$. **C)**. 75 μM ATP: line of best fit is $n = 0.2437L - 0.0023$. **D)**. 120 μM ATP: line of best fit is $n = 0.2483L + 0.0037$. **E)**. 416 μM ATP: line of best fit is $n = 0.2666L - 0.001$. **F)**. 1.4 mM ATP: line of best fit is $n = 0.2530L + 0.0008$. **G)**. 5 mM ATP: line of best fit is $n = 0.2514L + 0.1913$.

Figure 3. [ATP] dependence on RecBC unwinding summary. A). Average kinetic step-size, m, determined from NLLS analysis of the time courses in **Figure 1A-G** using **Equation 1** and also from the slope of the "n vs. L" plots shown in **Figure 2A-G**, is plotted versus [ATP]. The solid curve reflect an average of the values determined at each [ATP] ($m_{avg} = 4.0 \pm 0.3$ bp). **B).** Macroscopic unwinding rate, mk_{obs}, determined from NLLS analysis of the time courses in **Figure 1A-G** using **Equation 1** is plotted versus [ATP]. Solid curves are simulations based on the best fit parameters fitting the data to the Michaelis-Menton Equation (**Equation 2**) ($K_M = 131 \pm 23$ μM and $V_{max} = 317 \pm 14$ bp/s).

Figure 4. ATP coupling stoichiometry during RecBC unwinding. A). Phosphate release time courses collected from DNA substrates with duplex length $L = 24, 29, 37$,

40, 43, 48, 53, and 60 bp. Phosphate release kinetics is fit to **Equation 3** and smooth curves are simulations based on the best fit parameters given in **Table 2**. **B).** Plot of the burst amplitude as a function of duplex DNA length. Smooth line is a linear fit to the data (y = 0.9549x + 45.079).

Figure 5. ATP coupling stoichiometry of the RecBC primary translocase. A). Phosphate release time courses collected from DNA substrates with ssDNA extension length L = 15, 30, 45, 60, and 75 nt. Phosphate release kinetics is fit to **Equation 3** and smooth curves are simulations based on the best fit parameters given in **Table 2**. **B).** Plot of the burst amplitude as a function of ssDNA extension length. Smooth line is a linear fit to the data (y = 0.8132x + 32.16).

Figure 6. ATP coupling stoichiometry of the RecBC secondary translocase. A). Phosphate release time courses collected from DNA substrates with ssDNA extension length L = 15, 30, 45, 60, and 75 nt. Phosphate release kinetics is fit to **Equation 3** and smooth curves are simulations based on the best fit parameters given in **Table 2**. **B).** Plot of the burst amplitude as a function of ssDNA extension length. Smooth line is a linear fit to the data (y = 1.1233x + 43.14).

Figure 7. ATP coupling stoichiometry during RecBC translocation along twin ssDNA extensions. A). Phosphate release time courses collected from DNA substrates with twin ssDNA extensions of length L = 15, 30, 45, 60, and 75 nt. Phosphate release time courses collected from DNA substrates with ssDNA extension length L = 15, 30, 45,

60, and 75 nt. Phosphate release kinetics is fit to **Equation 3** and smooth curves are simulations based on the best fit parameters given in **Table 2**. **B).** Plot of the burst amplitude as a function of ssDNA extension length. Smooth line is a linear fit to the data (y = 1.0696x + 33.76).

Figure 8. Two potential models of RecBC catalyzed DNA unwinding. A). DNA unwinding occurs separately from ssDNA translocation. RecBC first binds and melts out 4-6 bp of a DNA end and translocation then follows using 1 ATP/nt. RecBC is able to use its binding free energy to melt out 4-6 bp to repeat the cycle. **B)**. DNA unwinding and translocation occur simultaneously. RecBC first binds and melts out 4-6 bp of a DNA end. DNA unwinding and translocation occur simultaneously using 1 ATP/bp unwound.

Supplemental Data

Supplemental Figure 1. PBP-MDCC calibration curve. A). PBP-MDCC calibration time courses obtained by mixing ATP, heparin, and PBP-MDCC solution with 0, 0.5, 1.0, 1.5, 2.0, 2.5, 3.0, and 5 μM phosphate standard. Time courses are fit to an exponential function and the plateau values are plotted in panel B. **B)**. Plateau values determined in panel A are plotted versus phosphate standard concentration in order to construct a calibration curve. The smooth line is a linear fit to the data (y = 0.6804x + 5.9469) and this curve is used to relate fluorescence intensities to the amount of phosphate released.

Supplemental Figure 2. Overlay of DNA unwinding and phosphate release kinetics. Phosphate release time course shown in **Figure 4A** (L = 40) is superimposed to the DNA unwinding time course shown in **Figure 1C** (L = 40)

Supplemental Figure 3. Overlay of translocation (primary) and phosphate release kinetics. Phosphate release time course shown in **Figure 5A** (L = 45) is superimposed to a translocation time course determined previously.

Supplemental Figure 4. Overlay of translocation (secondary) and phosphate release kinetics. Phosphate release time course shown in **Figure 6A** (L = 45) is superimposed to a translocation time course determined previously.

References

Ahnert, P. and S. S. Patel (1997). "Asymmetric interactions of hexameric bacteriophage T7 DNA helicase with the 5'- and 3'-tails of the forked DNA substrate." J Biol Chem **272**(51): 32267-32273.

Anderson, D. G. and S. C. Kowalczykowski (1997). "The Translocating RecBCD Enzyme Stimulates Recombination by Directing RecA Protein onto ssDNA in a χ-regulated Manner." Cell **90**: 77-86.

Arnold, D. A. and S. C. Kowalczykowski (2000). "Facilitated loading of RecA protein is essential to recombination by RecBCD enzyme." J Biol Chem **275**(16): 12261-12265.

Betterton, M. D. and F. Julicher (2005). "Opening of nucleic-acid double strands by helicases: active versus passive opening." Phys Rev E Stat Nonlin Soft Matter Phys **71**(1 Pt 1): 011904.

Bianco, P. R., L. R. Brewer, et al. (2001). "Processive translocation and DNA unwinding by individual RecBCD enzyme molecules." Nature **409**: 374-378.

Brune, M., J. L. Hunter, et al. (1998). "Mechanism of inorganic phosphate interaction with phosphate binding protein from Escherichia coli." Biochemistry **37**(29): 10370-10380.

Cheng, W., S. Dumont, et al. (2007). "NS3 helicase actively separates RNA strands and senses sequence barriers ahead of the opening fork." PNAS **104**(35): 13954-13959.

Delagoutte, E. and P. H. von Hippel (2002). "Helicase mechanisms and the coupling of helicases within macromolecular machines. Part I: Structures and properties of isolated helicases." Q Rev Biophys **35**(4): 431-478.

Dillingham, M. S., Spies, M., Kowalczykowski, S. C. (2003). "RecBCD enzyme is a bipolar helicase." Nature **423**: 893-897.

Dillingham, M. S., D. B. Wigley, et al. (2000). "Demonstration of unidirectional single-stranded DNA translocation by PcrA helicase: measurement of step size and translocation speed." Biochemistry **39**(1): 205-212.

Dillingham, M. S., D. B. Wigley, et al. (2002). "Direct measurement of single-stranded DNA translocation by PcrA helicase using the fluorescent base analogue 2-aminopurine." Biochemistry **41**(2): 643-651.

Donmez, I. and S. S. Patel (2008). "Coupling of DNA unwinding to nucleotide hydrolysis in a ring-shaped helicase." EMBO J **27**(12): 1718-1726.

Farah, J. A. and G. R. Smith (1997). "The RecBCD Enzyme Initiation Complex for DNA Unwinding: Enzyme Positioning and DNA Opening." J.Mol.Biol. **272**: 699-715.

Finch, P. W., A. Storey, et al. (1986). "Complete nucleotide sequence of the *Escherichia coli recB* gene." Nucleic Acids Research **14**: 8573-8582.

Finch, P. W., R. E. Wilson, et al. (1986). "Complete nucleotide sequence of the Escherichia coli recC gene and of the thyA-recC intergenic region." Nucleic Acids Res **14**(11): 4437-4451.

Fischer, C. J. and T. M. Lohman (2004). "ATP-dependent translocation of proteins along single-stranded DNA: models and methods of analysis of pre-steady state kinetics." J Mol Biol **344**(5): 1265-1286.

Fischer, C. J., N. K. Maluf, et al. (2004). "Mechanism of ATP-dependent translocation of E.coli UvrD monomers along single-stranded DNA." J Mol Biol **344**(5): 1287-1309.

Handa, N., P. R. Bianco, et al. (2005). "Direct visualization of RecBCD movement reveals cotranslocation of the RecD motor after chi recognition." Mol Cell **17**(5): 745-750.

Jeong, Y. J., M. K. Levin, et al. (2004). "The DNA-unwinding mechanism of the ring helicase of bacteriophage T7." Proc Natl Acad Sci U S A **101**(19): 7264-7269.

Johnson, D. S., L. Bai, et al. (2007). "Single-molecule studies reveal dynamics of DNA unwinding by the ring-shaped T7 helicase." Cell **129**(7): 1299-1309.

Kim, D. E., M. Narayan, et al. (2002). "T7 DNA helicase: a molecular motor that processively and unidirectionally translocates along single-stranded DNA." J Mol Biol **321**(5): 807-819.

Korangy, F. and D. A. Julin (1993). "Kinetics and processivity of ATP hydrolysis and DNA unwinding by the RecBC enzyme from Escherichia coli." Biochemistry **32**(18): 4873-4880.

Korangy, F. and D. A. Julin (1994). "Efficiency of ATP Hydrolysis and DNA Unwinding by the RecBC Enzyme from *Escherichia coli*." Biochemistry **33**: 9552-9560.

Kornberg, A., J. F. Scott, et al. (1978). "ATP utilization by rep protein in the catalytic separation of DNA strands at a replicating fork." J Biol Chem **253**(9): 3298-3304.

Kowalczykowski, S. C., D. A. Dixon, et al. (1994). "Biochemistry of homologous recombination in *Escherichia coli*." Microbiological Reviews **58**: 401-465.

Lee, J. Y. and W. Yang (2006). "UvrD Helicase Unwinds DNA One Base Pair at a Time by a Two-Part Power Stroke." Cell **127**(7): 1349-1360.
Lionnet, T., A. Dawid, et al. (2006). "DNA mechanics as a tool to probe helicase and translocase activity." Nucleic Acids Res **34**(15): 4232-4244.

Lohman, T. M. (1992). "*Escherichia coli* DNA helicases: mechanisms of DNA unwinding." Mol.Microbiol. **6**: 5-14.

Lohman, T. M., E. J. Tomko, et al. (2008). "Non-hexameric DNA helicases and translocases: mechanisms and regulation." Nat Rev Mol Cell Biol.

Lucius, A. L., C. Jason Wong, et al. (2004). "Fluorescence stopped-flow studies of single turnover kinetics of *E.coli* RecBCD helicase-catalyzed DNA unwinding." J. Mol. Biol. **339**(4): 731-750.

Lucius, A. L. and T. M. Lohman (2004). "Effects of temperature and ATP on the kinetic mechanism and kinetic step-size for *E.coli* RecBCD helicase-catalyzed DNA unwinding." J. Mol. Biol. **339**(4): 751-771.

Lucius, A. L., A. Vindigni, et al. (2002). "DNA unwinding step-size of E. coli RecBCD helicase determined from single turnover chemical quenched-flow kinetic studies." J Mol Biol **324**(3): 409-428.

Manosas, M., X. G. Xi, et al. (2010). "Active and passive mechanisms of helicases." Nucleic Acids Res.

Matson, S. W., D. W. Bean, et al. (1994). "DNA helicases: enzymes with essential roles in all aspects of DNA metabolism." Bioessays **16**(1): 13-22.

Patel, S. S. and K. M. Picha (2000). "Structure and function of hexameric helicases." Annu Rev Biochem **69**: 651-697.

Perkins, T. T., H. W. Li, et al. (2004). "Forward and reverse motion of single RecBCD molecules on DNA." Biophys J **86**(3): 1640-1648.

Rigden, D. J. (2005). "An inactivated nuclease-like domain in RecC with novel function: implications for evolution." BMC Struct Biol **5**: 9.

Roman, L. J. and S. C. Kowalczykowski (1989). "Characterization of the adenosinetriphosphatase activity of the Escherichia coli RecBCD enzyme: relationship of ATP hydrolysis to the unwinding of duplex DNA." Biochemistry **28**(7): 2873-2881.

Saikrishnan, K., S. P. Griffiths, et al. (2008). "DNA binding to RecD: role of the 1B domain in SF1B helicase activity." EMBO J **27**(16): 2222-2229.

Scott, J. F., S. Eisenberg, et al. (1977). "A mechanism of duplex DNA replication revealed by enzymatic studies of phage phi X174: catalytic strand separation in advance of replication." Proc Natl Acad Sci U S A **74**(1): 193-197.

Singleton, M. R., M. S. Dillingham, et al. (2004). "Crystal structure of RecBCD enzyme reveals a machine for processing DNA breaks." Nature **432**(7014): 187-193.

Smith, G. R. (1990). RecBCD Enzyme. Nucleic Acids and Molecular Biology. F. Eckstein and D. M. J. Lilley. Berlin, Springer Verlag**:** 78-98.

Spies, M., I. Amitani, et al. (2007). "RecBCD Enzyme Switches Lead Motor Subunits in Response to chi Recognition." Cell **131**(4): 694-705.

Spies, M., P. R. Bianco, et al. (2003). "A molecular throttle: the recombination hotspot chi controls DNA translocation by the RecBCD helicase." Cell **114**(5): 647-654.

Taylor, A. F. and G. R. Smith (2003). "RecBCD enzyme is a DNA helicase with fast and slow motors of opposite polarity." Nature **423**: 889-893.

Tomko, E. J., C. J. Fischer, et al. (2007). "A Nonuniform Stepping Mechanism for E. coli UvrD Monomer Translocation along Single-Stranded DNA." Molecular Cell **26**(3): 335-347.

Velankar, S. S., P. Soultanas, et al. (1999). "Crystal Structures of Complexes of PcrA DNA Helicase with a DNA Substrate Indicate an Inchworm Mechanism." Cell **97**: 75-84.

Wong, C. J. and T. M. Lohman (2008). "Kinetic control of Mg2+-dependent melting of duplex DNA ends by Escherichia coli RecBC." J Mol Biol **378**(4): 759-775.

Wong, C. J., A. L. Lucius, et al. (2005). "Energetics of DNA end binding by *E.coli* RecBC and RecBCD helicases indicate loop formation in the 3'-single-stranded DNA tail." J. Mol. Biol. **352**(4): 765-782.

Wong, C. J., R. L. Rice, et al. (2006). "Probing 3'-ssDNA Loop Formation in *E. coli* RecBCD/RecBC-DNA Complexes Using Non-natural DNA: A Model for "Chi" Recognition Complexes." J. Mol. Biol. **362**(1): 26-43.

Wu, C. G. and T. M. Lohman (2008). "Influence of DNA end structure on the mechanism of initiation of DNA unwinding by the Escherichia coli RecBCD and RecBC helicases." J Mol Biol **382**(2): 312-326.

Yarranton, G. T., R. H. Das, et al. (1979). "Enzyme-catalyzed DNA unwinding. A DNA-dependent ATPase from E. coli." J Biol Chem **254**(23): 11997-12001.

Yu, M., J. Souaya, et al. (1998). "The 30-kDa C-terminal domain of the RecB protein is critical for the nuclease activity, but not the helicase activity, of the RecBCD enzyme from *Escherichia coli*." Proc.Natl.Acad.Sci.,U.S.A. **95**: 981-986.

Yu, M., J. Souaya, et al. (1998). "Identification of the Nuclease Active Site in the Multifunctional RecBCD Enzyme by Creation of a Chimeric Enzyme." J.Mol.Biol. **283**: 797-808.

Table 1. RecBC unwinding kinetics summary

[ATP] (after 1:1 mixing)	mk_{obs} (bp/s)	k_{obs} (s^{-1})	m (bp)	k_{np} (s^{-1})	x
10 µM	19 ± 1	5 ± 2	4.1 ± 0.3	0.35 ± 0.13	0.85 ± 0.04
37.5 µM	61 ± 3	14 ± 4	4.3 ± 0.3	0.60 ± 0.10	0.84 ± 0.03
75 µM	114 ± 4	28 ± 5	4.1 ± 0.1	0.79 ± 0.21	0.84 ± 0.03
120 µM	162 ± 3	40 ± 7	4.0 ± 0.2	0.76 ± 0.17	0.82 ± 0.04
416 µM	239 ± 7	64 ± 11	3.8 ± 0.4	1.06 ± 0.25	0.81 ± 0.05
1.4 mM	295 ± 5	75 ± 8	4.0 ± 0.1	1.54 ± 0.14	0.83 ± 0.01
5 mM	305 ± 6	79 ± 10	4.0 ± 0.2	2.19 ± 0.28	0.82 ± 0.02
	V_{max} (bp/s)	**K_M (µM)**			
	317 ± 14	131 ± 23			

Table 2. Summary of phosphate release kinetics during RecBC unwinding and translocation

RecBC Unwinding	A_{burst} **(Pi/RecBC)**	k_{burst} **(s^{-1})**	k_{ss} **(s^{-1})**	**c = 0.95 ± 0.08 ATP/bp**
L = 24 bp	72 ± 2	1.99 ± 0.13	3.98 ± 0.14	
29 bp	78 ± 3	1.81 ± 0.06	4.27 ± 0.11	
37 bp	85 ± 1	1.53 ± 0.09	4.65 ± 0.08	
40 bp	87 ± 1	1.32 ± 0.05	5.56 ± 0.17	
43 bp	90 ± 2	1.14 ± 0.06	5.92 ± 0.14	
48 bp	95 ± 3	1.12 ± 0.04	6.29 ± 0.15	
53 bp	103 ± 4	0.90 ± 0.05	7.83 ± 0.08	
60 bp	113 ± 3	0.82 ± 0.03	7.96 ± 0.11	
Primary RecBC translocase	A_{burst} **(Pi/RecBC)**	k_{burst} **(s^{-1})**	k_{ss} **(s^{-1})**	**c = 0.81 ± 0.05 ATP/nt**
L = 15 nt	44 ± 1	2.41 ± 0.16	4.51 ± 0.17	
30 nt	55 ± 1	2.34 ± 0.09	4.98 ± 0.12	
45 nt	71 ± 2	2.21 ± 0.06	5.75 ± 0.06	
60 nt	81 ± 3	2.13 ± 0.05	6.28 ± 0.15	
75 nt	92 ± 2	2.07 ± 0.03	7.13 ± 0.08	
Secondary RecBC translocase	A_{burst} **(Pi/RecBC)**	k_{burst} **(s^{-1})**	k_{ss} **(s^{-1})**	**c = 1.12 ± 0.06 ATP/nt**
L = 15 nt	56 ± 1	2.51 ± 0.14	4.64 ± 0.09	
30 nt	81 ± 2	2.46 ± 0.07	5.02 ± 0.07	
45 nt	95 ± 1	2.31 ± 0.05	5.85 ± 0.16	
60 nt	108 ± 3	2.23 ± 0.03	6.57 ± 0.13	
75 nt	127 ± 3	2.10 ± 0.05	7.22 ± 0.15	
Translocation along twin ssDNA extensions	A_{burst} **(Pi/RecBC)**	k_{burst} **(s^{-1})**	k_{ss} **(s^{-1})**	**c = 1.07 ± 0.09 ATP/nt**
L = 15 nt	48 ± 1	2.48 ± 0.17	4.09 ± 0.14	
30 nt	69 ± 2	2.31 ± 0.06	4.57 ± 0.11	
45 nt	82 ± 2	2.28 ± 0.05	5.05 ± 0.07	
60 nt	95 ± 1	2.15 ± 0.06	5.54 ± 0.18	
75 nt	115 ± 7	2.08 ± 0.09	6.03 ± 0.13	

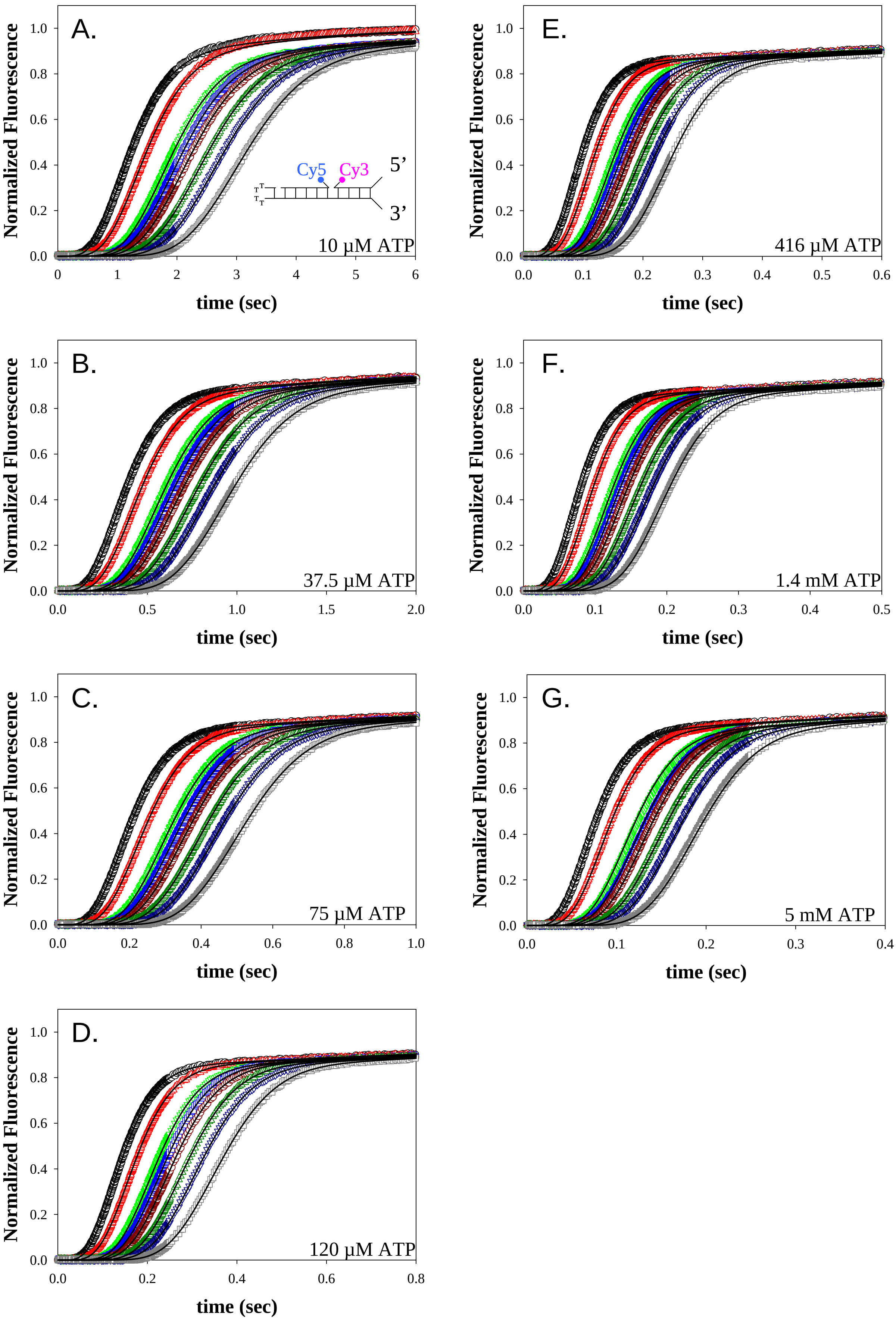
A.
Cy5
Cy3
5'
3'
10 μM ATP
B.
37.5 μM ATP
C.
75 μM ATP
D.
120 μM ATP
E.
416 μM ATP
F.
1.4 mM ATP
G.
5 mM ATP
Normalized Fluorescence
time (sec)

Figure 1

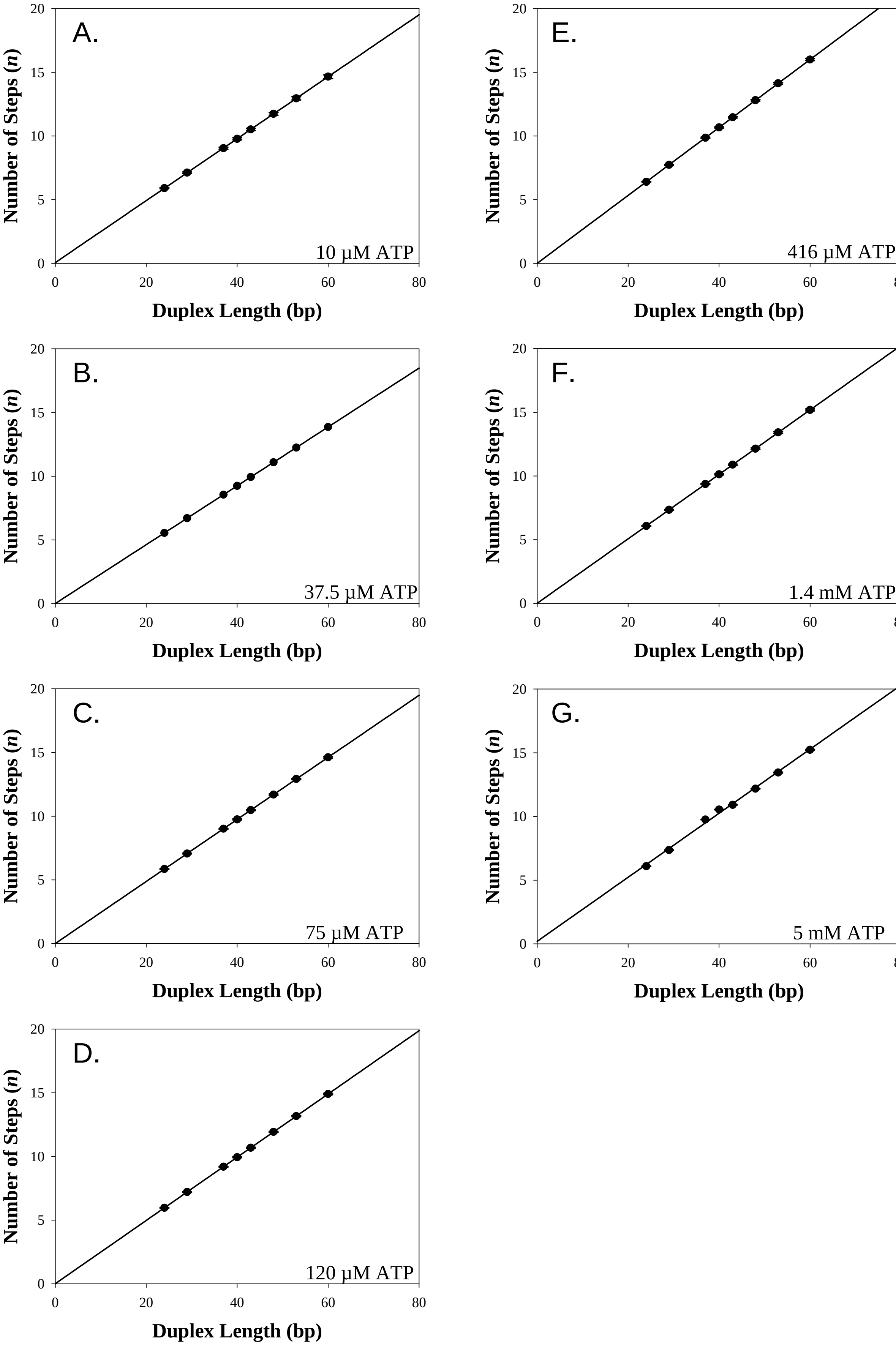
A.
10 µM ATP
B.
37.5 µM ATP
C.
75 µM ATP
D.
120 µM ATP
E.
416 µM ATP
F.
1.4 mM ATP
G.
5 mM ATP
Number of Steps (n)
Duplex Length (bp)
0
5
10
15
20
0
20
40
60
80

Figure 2

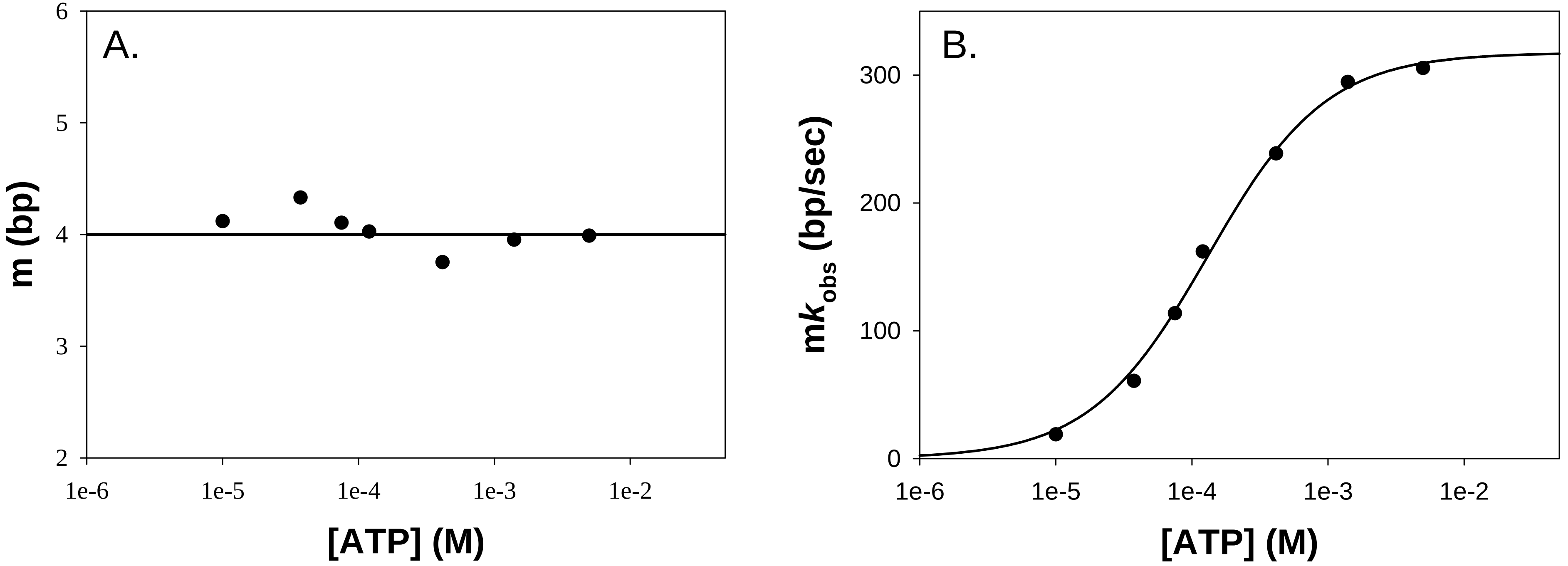
A.
m (bp)
6
5
4
3
2
1e-6
1e-5
1e-4
1e-3
1e-2
[ATP] (M)
B.
mk_{obs} (bp/sec)
300
200
100
0
1e-6
1e-5
1e-4
1e-3
1e-2
[ATP] (M)

Figure 3

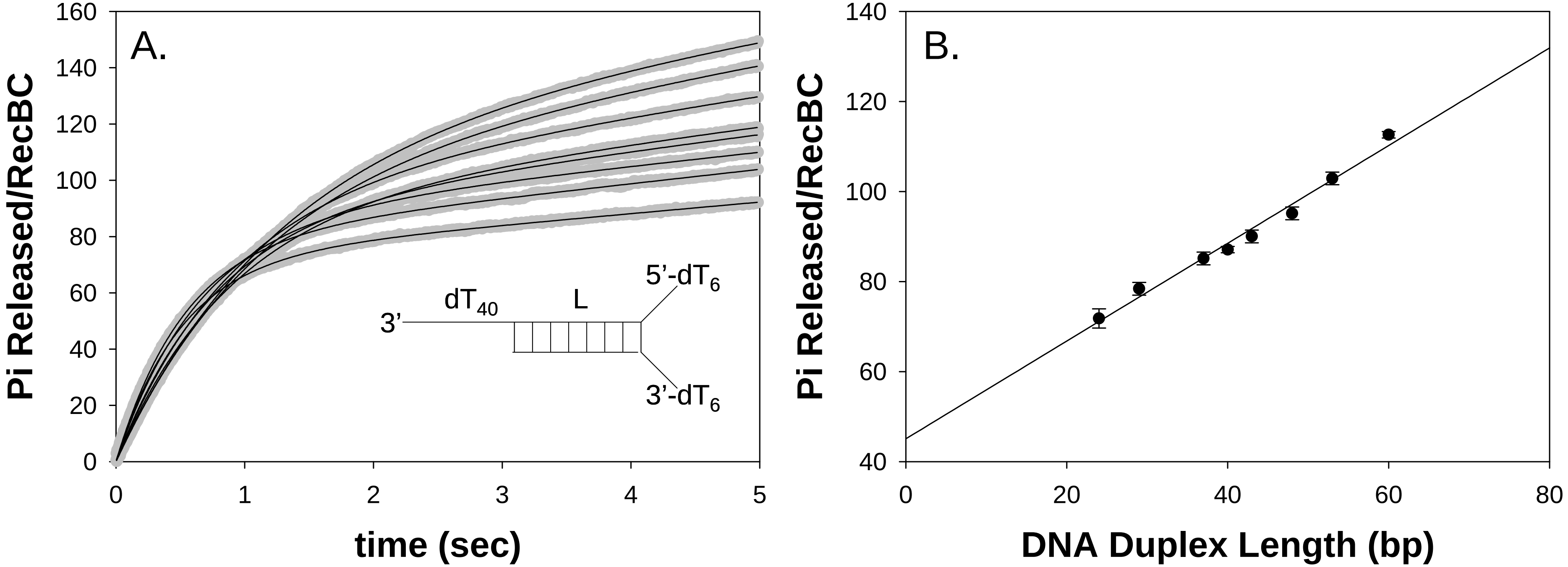
A.
B.
Pi Released/RecBC
time (sec)
DNA Duplex Length (bp)
3'
dT_{40}
L
5'-dT_6
3'-dT_6
0
20
40
60
80
100
120
140
160
0
1
2
3
4
5
0
20
40
60
80

Figure 4

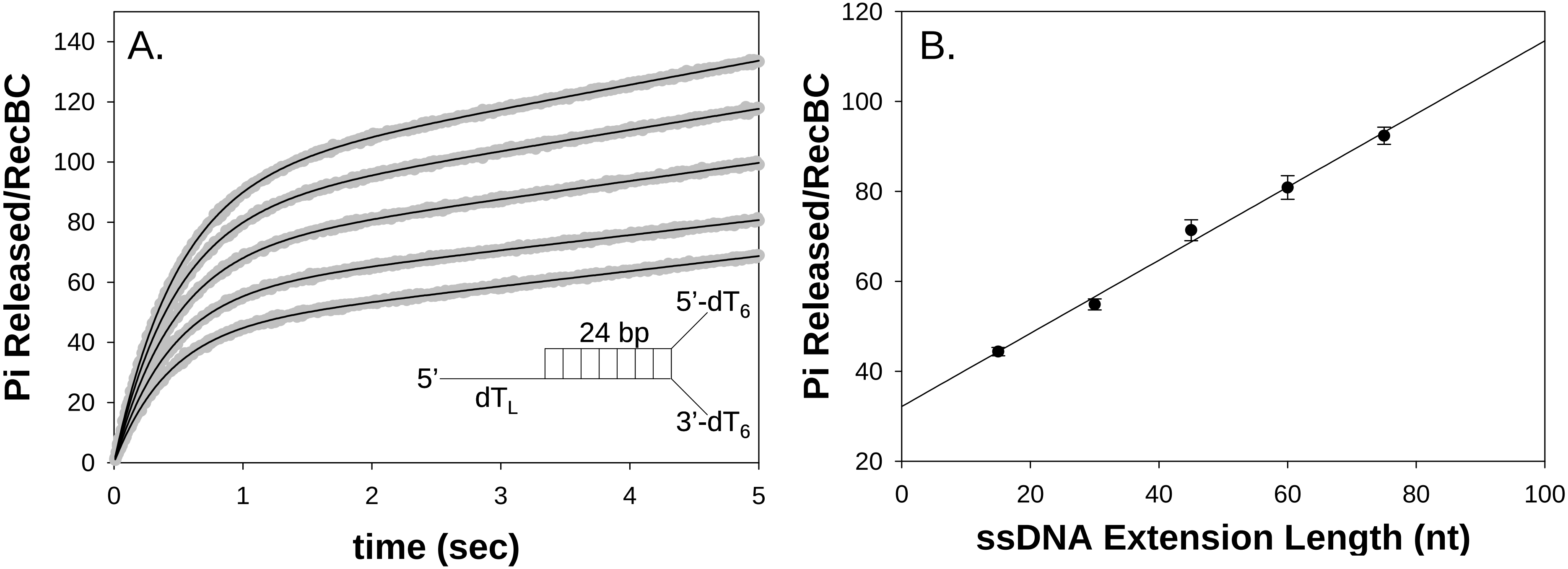
A.
B.
Pi Released/RecBC
time (sec)
ssDNA Extension Length (nt)
24 bp
5'
dT$_L$
5'-dT$_6$
3'-dT$_6$
0
20
40
60
80
100
120
140
1
2
3
4
5

Figure 5

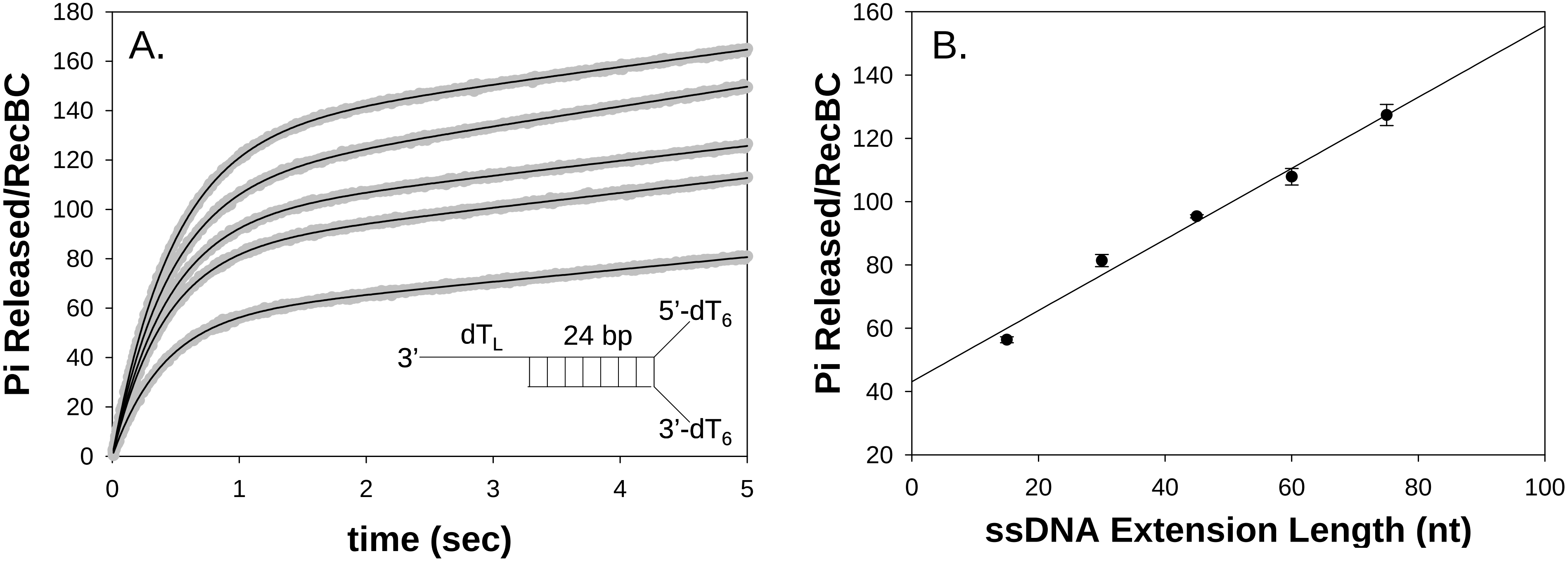
A.
Pi Released/RecBC
time (sec)
3'
dT$_L$
24 bp
5'-dT$_6$
3'-dT$_6$
B.
Pi Released/RecBC
ssDNA Extension Length (nt)

Figure 6

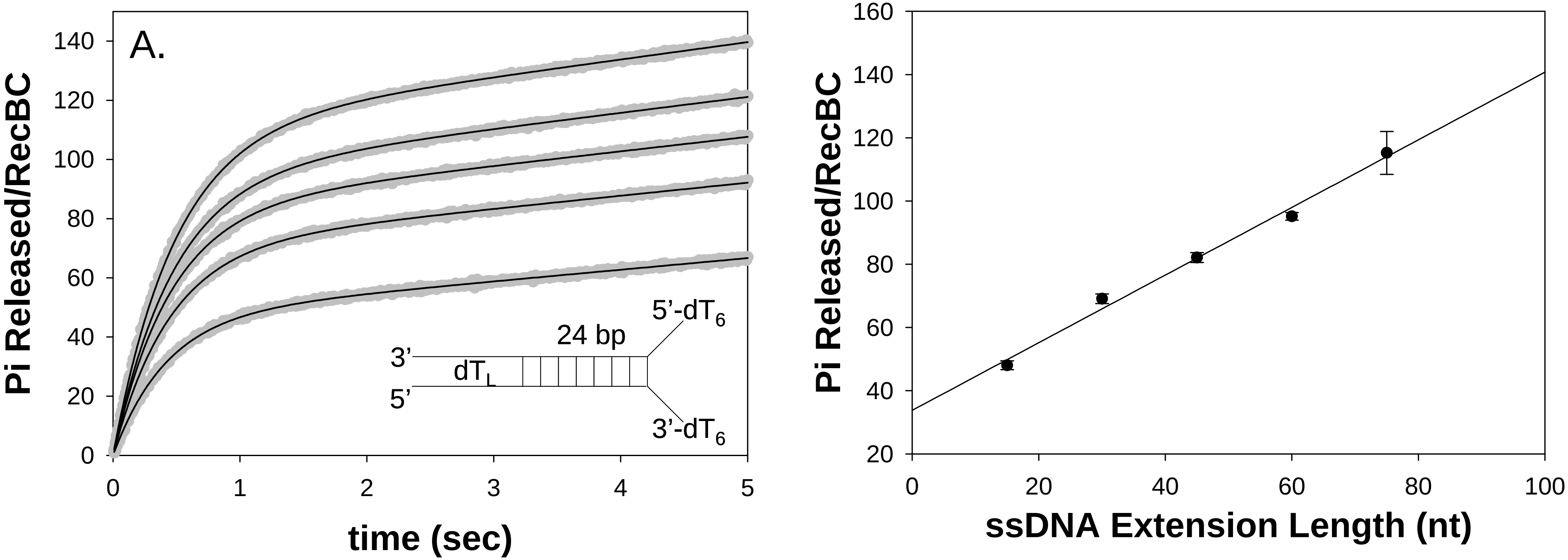
A.
Pi Released/RecBC
time (sec)
24 bp
3'
5'
dT$_L$
5'-dT$_6$
3'-dT$_6$
0
20
40
60
80
100
120
140
0
1
2
3
4
5
Pi Released/RecBC
ssDNA Extension Length (nt)
20
40
60
80
100
120
140
160
0
20
40
60
80
100

Figure 7

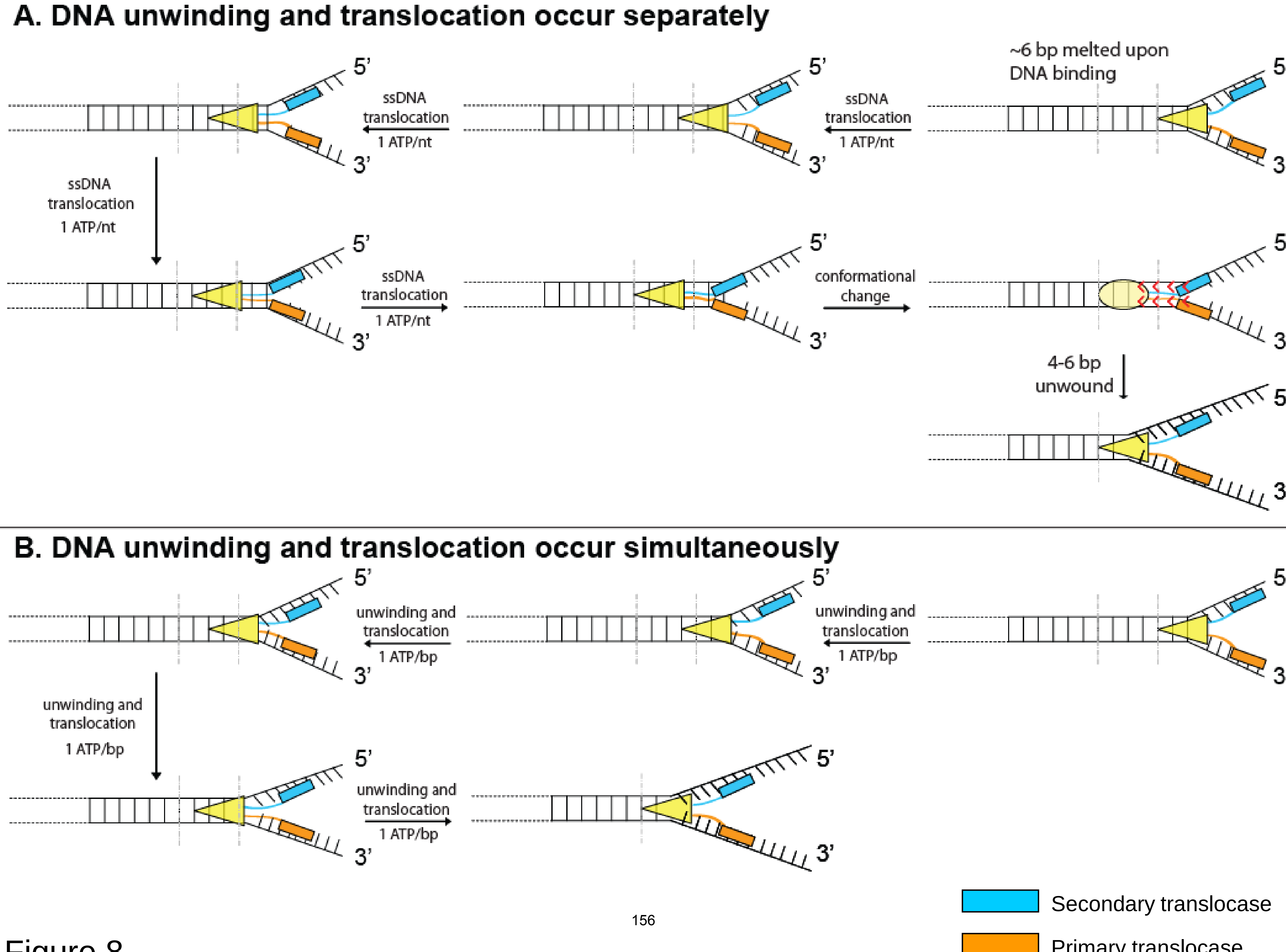
A. DNA unwinding and translocation occur separately
~6 bp melted upon DNA binding
ssDNA translocation
1 ATP/nt
conformational change
4-6 bp unwound
5'
3'
B. DNA unwinding and translocation occur simultaneously
unwinding and translocation
1 ATP/bp
Secondary translocase
Primary translocase

Figure 8

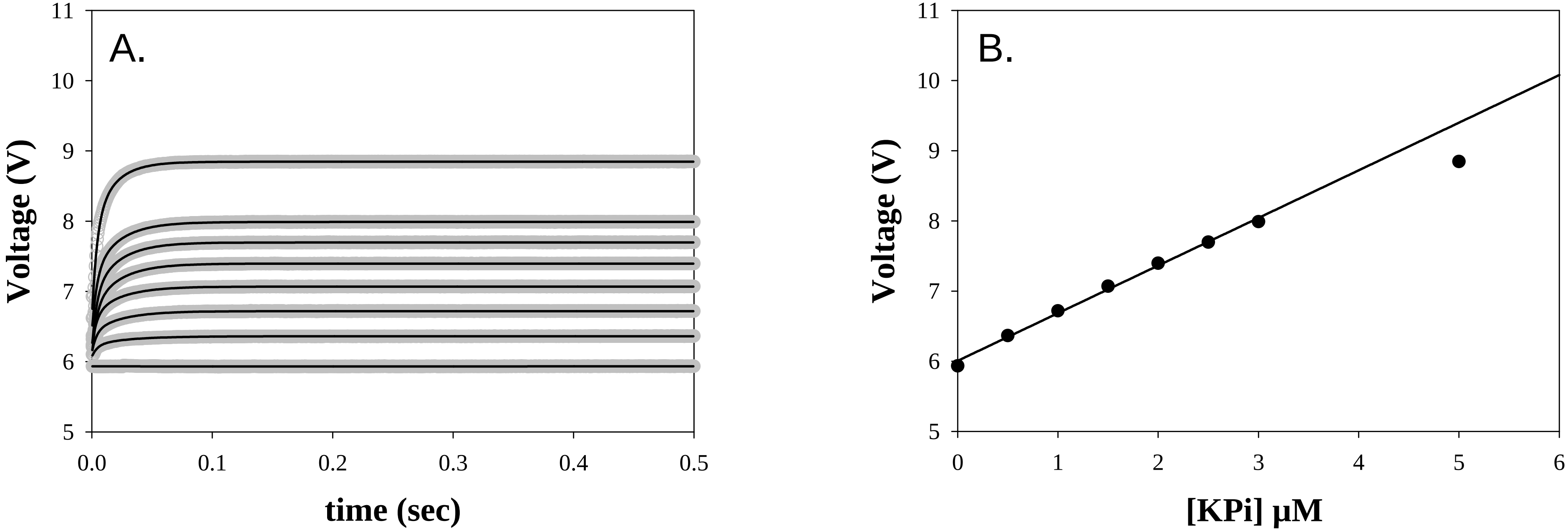

Supplementary Figure 1

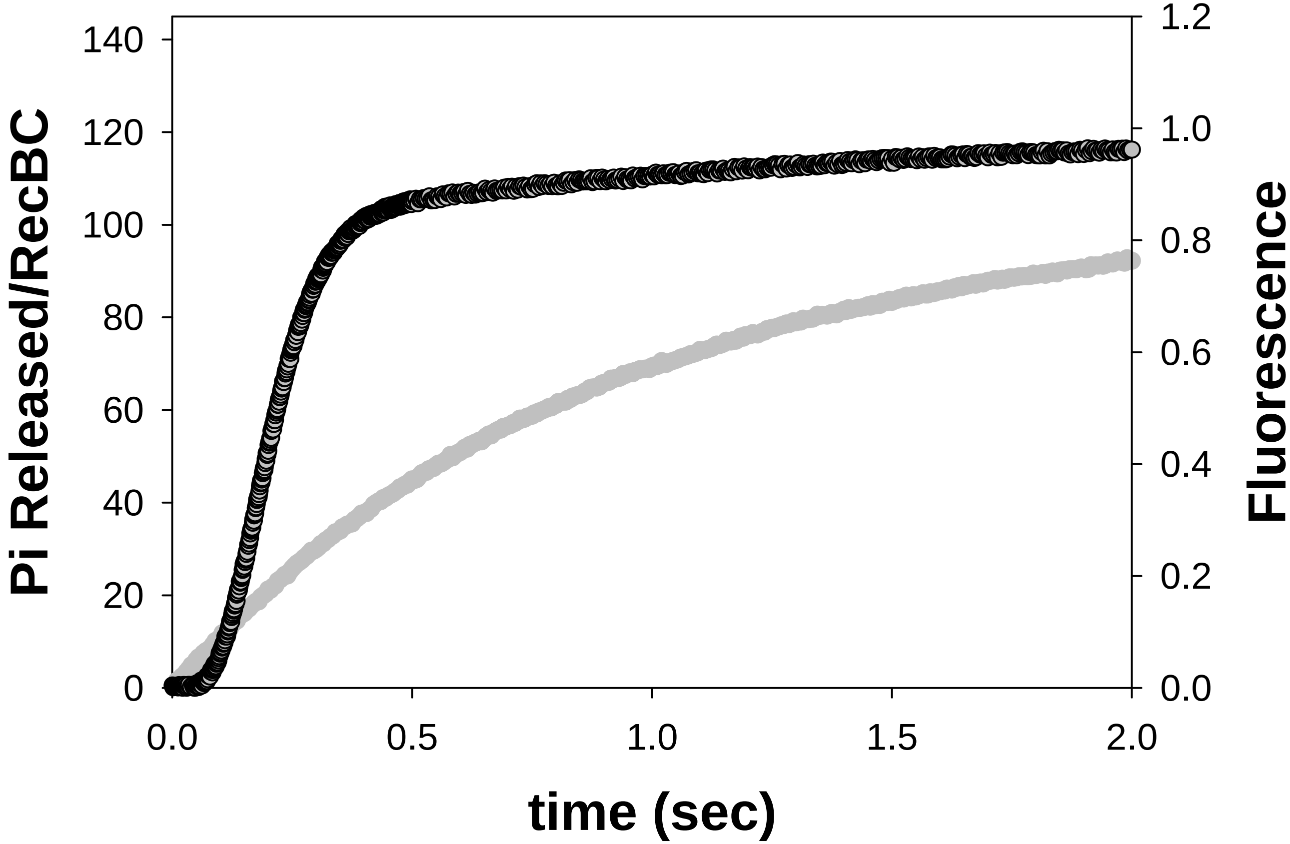

Supplementary Figure 2

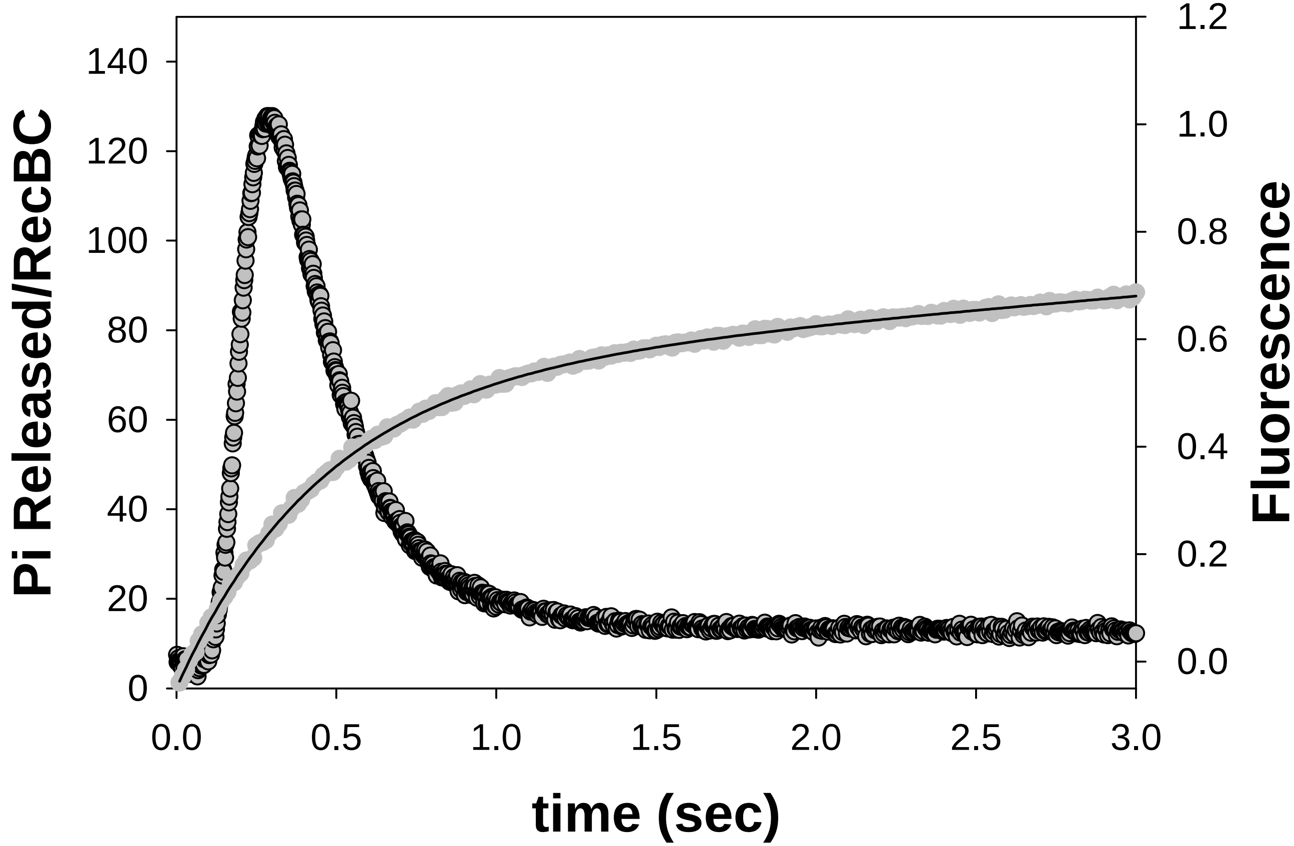

Supplementary Figure 3

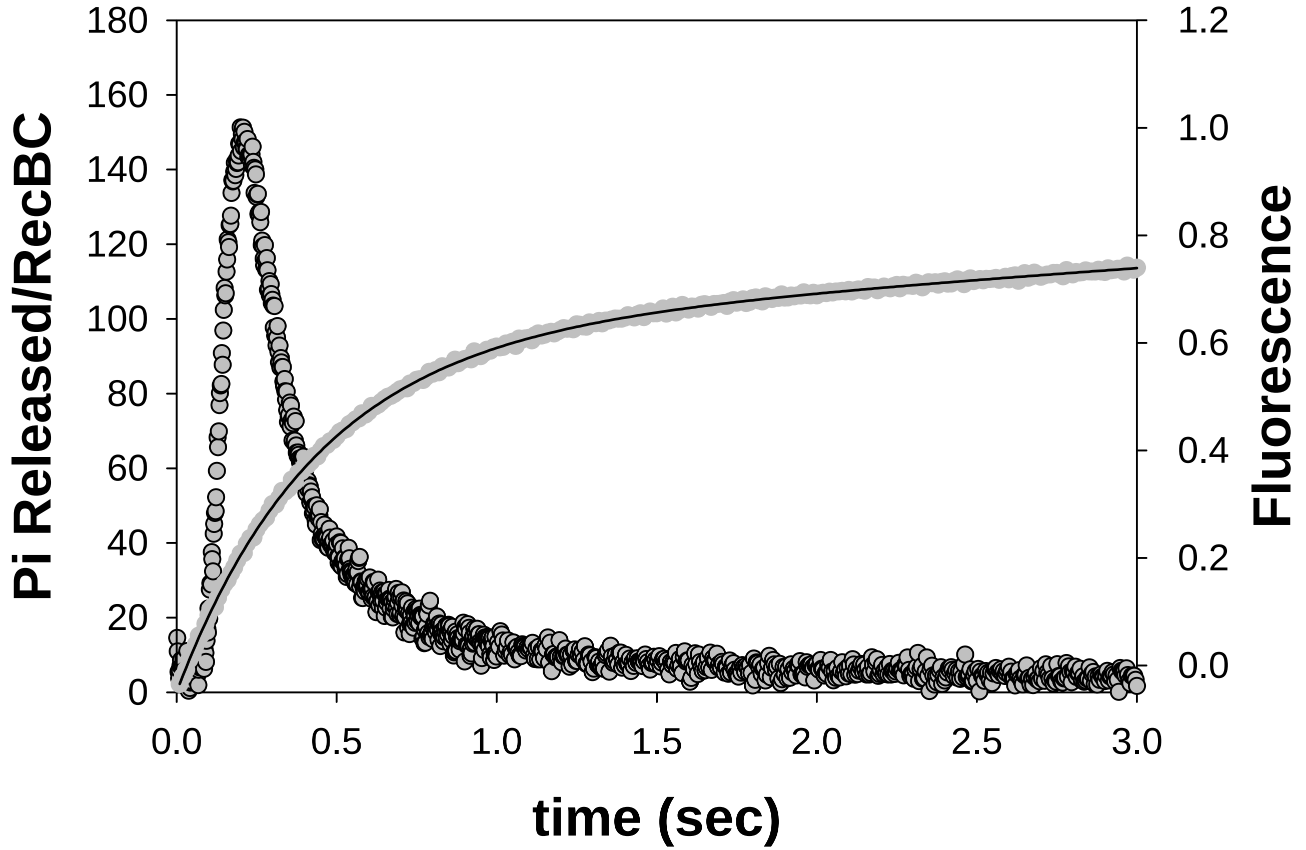

Supplementary Figure 4

Table S1. Sequences of DNA unwinding substrates

Substrate	Length (nt)*	DNA Sequence of Strand "A"
Ia	24	5'-$(dT)_6$ CCA TGG CTC CTG AGC TAG CTG CA(Cy3) G-3'
IIa	29	5'-$(dT)_6$ CCA TGG CTC CTG AGC TAG CTG CAG TAG C(Cy3)C-3'
IIIa	37	5'-$(dT)_6$ CCA TGG CTC CTG AGC TAG CTG CAG TAG CCT AAA GGA (Cy3)T-3'
IVa	40	5'-$(dT)_6$ CCA TGG CTC CTG AGC TAG CTG CAG TAG CCT AAA GGA TGA (Cy3)A-3'
Va	43	5'-$(dT)_6$ CCA TGG CTC CTG AGC TAG CTG CAG TAG CCT AAA GGA TGA AAC (Cy3)T-3'
Via	48	5'-$(dT)_6$ CCA TGG CTC CTG AGC TAG CTG CAG TAG CCT AAA GGA TGA AAC TAG GA(Cy3) T-3'
VIIa	53	5'-$(dT)_6$ CCA TGG CTC CTG AGC TAG CTG CAG TAG CCT AAA GGA TGA AAC TAG GAT CTT A(Cy3) T-3'
VIIIa	60	5'-$(dT)_6$ CCA TGG CTC CTG AGC TAG CTG CAG TAG CCT AAA GGA TGA AAC TAG GAT CTT ATG CTC CA(Cy3) T-3'
	Length (nt)	**DNA Sequence of Strand "B"**
Ib	56	5'-(Cy5) TAG CCT AAA GGA TGA AAC TAG GAT CTT ATG CTC CAT GGA TAC GTC GAG TCG CAT CC-3'
IIb	51	5'-(Cy5) TAA AGG ATG AAA CTA GGA TCT TAT GCT CCA TGG ATA CGT CGA GTC GCA TCC-3'
IIIb	43	5'-(Cy5) GAA ACT AGG ATC TTA TGC TCC ATG GAT ACG TCG AGT CGC ATC C-3'
IVb	40	5'-(Cy5) ACT AGG ATC TTA TGC TCC ATG GAT ACG TCG AGT CGC ATC C-3'
Vb	37	5'-(Cy5) AGG ATC TTA TGC TCC ATG GAT ACG TCG AGT CGC ATC C-3'
VIb	32	5'-(Cy5) CTT ATG CTC CAT GGA TAC GTC GAG TCG CAT CC-3'
VIIb	27	5'-(Cy5) GCT CCA TGG ATA CGT CGA GTC GCA TCC-3'
VIIIb	20	5'-(Cy5) GGA TAC GTC GAG TCG CAT CC-3'
	Length (nt)	**DNA Sequence of Strand "Hp"**
X	120	5'-AGA TCC TAG TGC AGG TTT TCC TGC ACT AGG ATC TGG ATG CGA CTC GAC GTA TCC ATG GAG CAT AAG ATC CTA GTT TCA TCC TTT AGG CTA CTG CAG CTA GCT CAG GAG CCA TGG TTT TTT-3'

DNA substrate I is formed by annealing DNA strands Ia, Ib, and X; DNA substrate II is formed by annealing DNA strands IIa, IIb, and X, etc.

Table S2. DNA substrate sequences used to determine the ATP coupling stoichiometry of RecBC catalyzed unwinding

Substrate	Annealed DNA Duplex Length (bp)	DNA Sequence
I	24	5'-$(dT)_6$ CCA TGG CTC CTG AGC TAG CTG CAG-3'-$(dT)_{40}$
II	29	5'-$(dT)_6$ CCA TGG CTC CTG AGC TAG CTG CAG TAG CC-3'-$(dT)_{40}$
III	37	5'-$(dT)_6$ CCA TGG CTC CTG AGC TAG CTG CAG TAG CCT AAA GGA T-3'-$(dT)_{40}$
IV	40	5'-$(dT)_6$ CCA TGG CTC CTG AGC TAG CTG CAG TAG CCT AAA GGA TGA A-3'-$(dT)_{40}$
V	43	5'-$(dT)_6$ CCA TGG CTC CTG AGC TAG CTG CAG TAG CCT AAA GGA TGA AAC T-3'-$(dT)_{40}$
VI	48	5'-$(dT)_6$ CCA TGG CTC CTG AGC TAG CTG CAG TAG CCT AAA GGA TGA AAC TAG GAT-3'-$(dT)_{40}$
VII	53	5'-$(dT)_6$ CCA TGG CTC CTG AGC TAG CTG CAG TAG CCT AAA GGA TGA AAC TAG GAT CTT AT-3'-$(dT)_{40}$
VIII	60	5'-$(dT)_6$ CCA TGG CTC CTG AGC TAG CTG CAG TAG CCT AAA GGA TGA AAC TAG GAT CTT ATG CTC CAT-3'-$(dT)_{40}$

DNA substrate I is formed by annealing strand I with a corresponding complementary DNA strand, which base pairs with only the mixed sequence in between the 5'-$(dT)_6$ and 3'-$(dT)_{40}$ ssDNA tails. DNA substrate II-VIII are formed in the same manner.

Table S3. DNA substrate sequences used to determine the ATP coupling stoichiometry of RecBC catalyzed ssDNA translocation

DNA	Length (nt)	DNA sequence
A	30	5'-$(dT)_6$ CCA TGG CTC CTG AGC TAG CTG CAG-3'
Ia	45	5'-$(dT)_{15}$ CTG CAG CTA GCT CAG GAG CCA TGG $(dT)_6$-3'
IIa	60	5'-$(dT)_{30}$ CTG CAG CTA GCT CAG GAG CCA TGG $(dT)_6$-3'
IIIa	75	5'-$(dT)_{45}$ CTG CAG CTA GCT CAG GAG CCA TGG $(dT)_6$-3'
IVa	90	5'-$(dT)_{60}$ CTG CAG CTA GCT CAG GAG CCA TGG $(dT)_6$-3'
Va	105	5'-$(dT)_{75}$ CTG CAG CTA GCT CAG GAG CCA TGG $(dT)_6$-3'
B	30	5'-CTG CAG CTA GCT CAG GAG CCA TGG $(dT)_6$-3'
Ib	45	5'-$(dT)_6$ CCA TGG CTC CTG AGC TAG CTG CAG $(dT)_{15}$-3'
IIb	60	5'-$(dT)_6$ CCA TGG CTC CTG AGC TAG CTG CAG $(dT)_{30}$-3'
IIIb	75	5'-$(dT)_6$ CCA TGG CTC CTG AGC TAG CTG CAG $(dT)_{45}$-3'
IVb	90	5'-$(dT)_6$ CCA TGG CTC CTG AGC TAG CTG CAG $(dT)_{60}$-3'
Vb	105	5'-$(dT)_6$ CCA TGG CTC CTG AGC TAG CTG CAG $(dT)_{75}$-3'

DNA substrates from **Figure 5A-5B** are formed by annealing DNA strand A with strands Ia-Va
DNA substrates from **Figure 6A-6B** are formed by annealing DNA strand B with strands Ib-Vb
DNA substrates from **Figure 7A-7B** are formed by annealing DNA strands Ia-Va with strands Ib-Vb

Appendix to Chapter IV

E. coli SSB binding to a ssDNA tail prevents RecBC loading

The hairpin containing DNA substrates used to examine DNA unwinding first presented in Chapter 2 are not suitable for examining phosphate release kinetics as discussed in Chapter 4. Therefore, I have used the DNA substrates shown in **Figure 4-S5A** and **S5B** and characterized RecBC's ability to initiate DNA unwinding from these DNA ends. I reasoned that a DNA substrate with a long 3' ssDNA tail (3'-dT_{40}), the end structure to which RecBC binds with weak affinity, and also having SSB binding to this tail will prevent RecBC from loading to the DNA end and therefore no DNA unwinding will be observed. As shown in **Figure 4-S5A**, when both DNA ends are blocked with SSB, RecBC cannot bind to the ds/ss junction and initiate DNA unwinding. If however, only one DNA end is occupied by SSB and the other end contains a high affinity RecBC loading site (**Figure 4-S5B**), RecBC is able to initiate DNA unwinding from the twin $(dT)_6$ junction. In fact, the time course of RecBC unwinding of a 24 bp DNA substrate shown in **Figure 4-S5B** is identical to the time course of RecBC unwinding of a 24 bp hairpin substrate presented in Chapter 2. I have used these DNA substrates and performed RecBC unwinding experiments as a function of DNA duplex length (time courses shown in **Figure 4-S6**) in order to determine the unwinding rate as well as the average kinetic step-size for DNA unwinding. Again, the best fit parameters shown in **Figure 4-S6** are in good agreement from those determined using the hairpin substrates. Alternatively, I have shown in Chapter 3 and Chapter 4 that RecBC will initiate unwinding from the unique loading site if DNA is present in excess of RecBC concentration.

A.

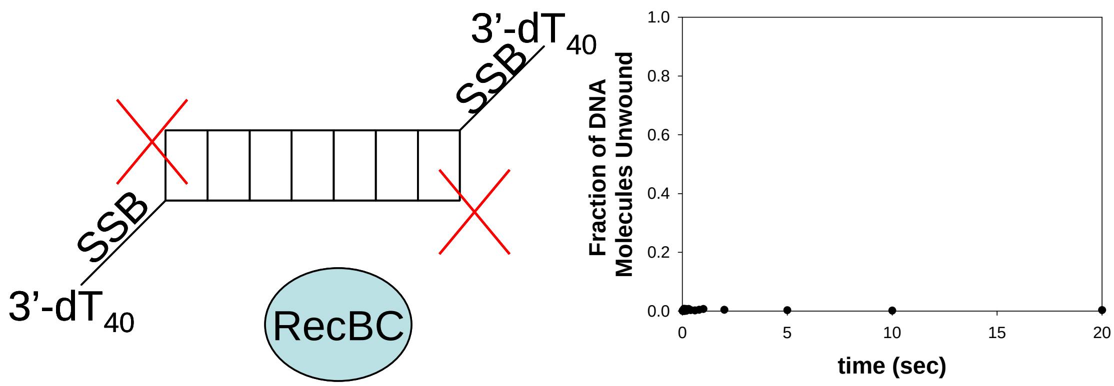

B.

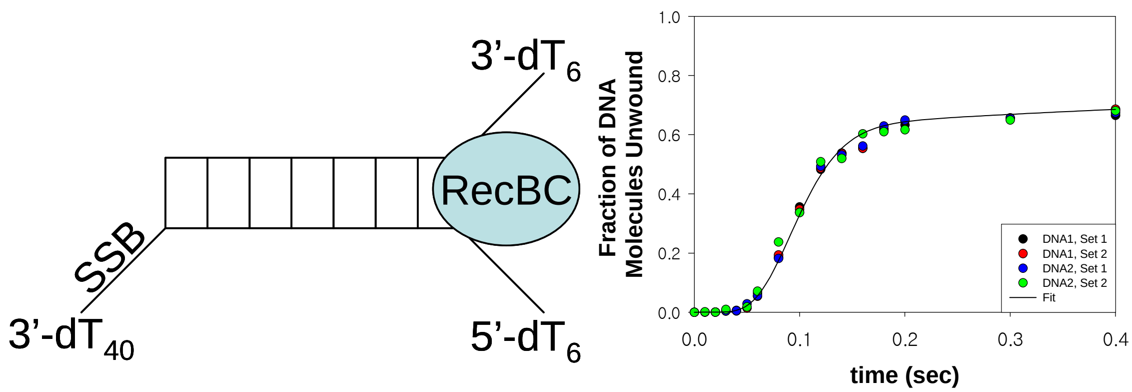

Figure 4-S5. *E. coli* SSB binding to the ssDNA tail prevents RecBC loading. A. a 24 bp substrate (2 nM) with a 3'-dT$_{40}$ ssDNA tail on either end of the duplex is pre-bound to SSB (20 nM tetramer). RecBC (20 nM) is then added to the mixture and DNA unwinding is initiated by mixing with ATP (150 µM) and heparin (10 mg/mL). No unwinding is observed. **B.** The same experiment was performed with a DNA substrate as depicted, which only has one 3'-dT$_{40}$ tail and a twin dT$_6$ RecBC loading site. Even in presence of SSB, RecBC is able to bind to the twin dT$_6$ junction and initiate DNA unwinding. The time course of DNA unwinding using this substrate (DNA 1) is identical to that obtained using a 24 bp hairpin substrate as shown in Chapter 2 (DNA 2).

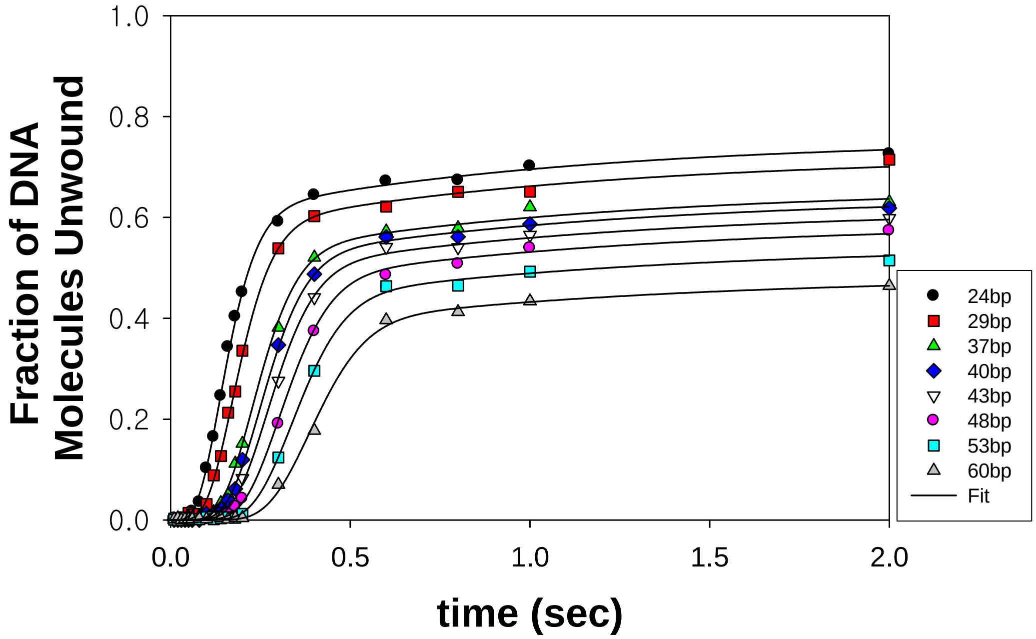

Figure 4-S6. RecBC unwinding at 150 μM ATP. 20 nM SSB is pre-bound to radiolabeled DNA substrate shown in **Figure 4-S5** (2 nM) to prevent RecBC loading onto the 3'-dT_{40} tail. 20 nM RecBC is then added to the mixture and DNA unwinding is initiated by mixing with 150 μM ATP and 10 mg/mL heparin. Unwinding time courses are analyzed using **Scheme 1**: $m = 4.2 \pm 0.3$ bp, $k_{obs} = 34 \pm 5$ sec^{-1}, $mk_{obs} = 145 \pm 3$ bp/sec, $k_{np} = 1.0 \pm 0.3$ sec^{-1}.

Chapter V

Summary

This thesis is part of a comprehensive study to dissect the mechanisms of DNA unwinding and translocation and also to understand the relationship between these two processes, using the *E. coli* RecBCD and RecBC helicases as model systems. Since RecBCD features two SF1 helicase motors (RecB and RecD) that function in unison in order to unwind DNA duplexes, mechanistic studies of this enzyme may provide information on any potential coupling or "cross talk" between the two motors. The individual subunits can be purified and characterized biochemically and either motor can be inactivated selectively in the holoenzyme by mutating a conserved lysine residue in the ATP binding site into a glutamine ($RecB^{K29Q}CD$ and $RecBCD^{K177Q}$) (Dillingham 2003; Taylor and Smith 2003; Dillingham, Webb et al. 2005). Furthermore, the RecBC heterodimer, which only possesses the RecB motor, still functions as a rapid and processive helicase (Korangy and Julin 1993); therefore, RecBCD and RecBC are good candidates with which to examine how ATP binding and hydrolysis is used to fuel DNA unwinding and translocation.

At the start of my thesis research, the minimal kinetic mechanism required to describe RecBCD catalyzed DNA unwinding had been determined (Lucius, Vindigni et al. 2002; Lucius, Jason Wong et al. 2004). In order for RecBCD to initiate DNA unwinding from a blunt end, it must first undergo two to three slow steps, and then unwinding occurs with a series of repeated limiting steps until the duplex is completely unwound. The functional significance of these additional initiation steps was not clear, and thus similar mechanistic studies have been performed with the RecBC enzyme to test whether it uses the same unwinding mechanism; however, unwinding experiments were difficult with RecBC due to low amplitude presumably because RecBC binds poorly to blunt ends. More recently, the energetics of RecBCD and RecBC binding to different DNA end structures were examined (Wong, Lucius et al. 2005). These studies indicate that RecBCD binds with optimal affinity to DNA ends possessing pre-existing 5'-$(dT)_{10}$ and 3'-$(dT)_6$ ssDNA tails while RecBC binds tightest to ends with pre-formed 5'-$(dT)_6$ and 3'-$(dT)_6$ ssDNA tails. Consistent with biochemical and structural studies, both RecBCD and RecBC can "melt out" ~ 6 bp upon binding to a DNA end in a Mg^{2+} dependent but ATP independent reaction (Farah and Smith 1997; Singleton, Dillingham et al. 2004; Saikrishnan, Griffiths et al. 2008; Wong and Lohman 2008).

In Chapter 2, I examined how various DNA end structures influence the mechanisms by which RecBCD and RecBC initiate DNA unwinding. First, I performed RecBC unwinding studies with its optimal binding substrate using techniques which were previously developed in the lab (Lucius, Maluf et al. 2003). When RecBC binds to DNA duplexes with pre-existing 5'-$(dT)_6$ and 3'-$(dT)_6$ tails, it can initiate DNA unwinding using a simple *n*-step sequential mechanism without the need for any additional initiation steps. NLLS analysis of these time courses indicate that RecBC unwinds DNA with an average kinetic step-size of 4.4 ± 0.1 bp and with an unwinding rate of 348 ± 5 bp/s (20 mM Mops-KOH, pH 7.0 at 25ºC, 10 mM NaCl, 10 mM $MgCl_2$, 5% (v/v) glycerol, 1 mM 2-mercaptoethanol). This is about two fold slower than the rate previously measured for RecBCD unwinding of blunt-ends (790 ± 23 bp/sec) (Lucius, Vindigni et al. 2002). Using the same methods, I also measured the rate of RecBCD unwinding from these twin $(dT)_6$ duplexes so the kinetic parameters could be compared directly with those of RecBC. These results are the same within error compared to those previously determined for blunt-end unwinding, which require two to three additional initiation steps (Wu and

Lohman 2008). Interestingly, when the 5' ssDNA tail length at the loading site is extended to ten nucleotides, RecBCD unwinding can be described by a simple *n*-step model without the need for any additional initiation steps. RecBC unwinding of these 5'-$(dT)_{10}$, 3'-$(dT)_6$ substrates with the same unwinding rate and also step-size when compared to RecBC unwinding of the twin $(dT)_6$ duplexes. Taken together, these data indicate the additional steps needed to describe RecBCD unwinding of blunt-ends and twin $(dT)_6$ duplexes involve the loading of the 5' DNA end onto the RecD subunit. If the 5' ssDNA end is pre-loaded into RecD using a longer 5' tail or if RecD is not present (RecBC unwinding), then these initiation steps are not observed (Wu and Lohman 2008).

Additional experiments, however, will be necessary to dissect these minimal DNA unwinding mechanisms further. For example, the RecBCD and RecBC unwinding kinetics are biphasic (Lucius, Vindigni et al. 2002; Wu and Lohman 2008). The simplest explanation for this observation is that RecBC(D)-DNA complexes exist in both productive and non-productive forms and that the non-productive complexes must first isomerize into the productive form before unwinding can occur (Ali and Lohman 1997; Lucius, Maluf et al. 2003). Although we can detect this isomerization step kinetically, the functional and structural basis of this isomerization remains unclear. Preliminary studies of the length of the 3' ssDNA tail on RecBC unwinding indicate that the unwinding contribution from productive RecBC-DNA complexes decreases when the 3' ssDNA tail is extended beyond six nucleotides. These data correlate well with equilibrium experiments which showed that when RecBC binds to a DNA end with a 3' tail length greater than six nucleotides, a ssDNA loop is formed (Wong, Rice et al. 2006). This looped structure may be associated with a non-productive complex and inhibit DNA unwinding by RecBC. Also, the mechanism by which RecBC and RecBCD "melt-out" DNA ends upon DNA binding has not been examined. It is possible that some fraction of RecBC(D)-DNA complexes are not melted (or only partially melted) and are giving rise to these non-productive complexes. To test this hypothesis, the DNA melting mechanism can be investigated by pre-forming RecBC(D)-DNA complexes in the absence of Mg^{2+} and initiating melting by rapid mixing with a buffer containing Mg^{2+} ions. The conformation of the DNA end can be monitored by either labeling the DNA end fluorescently or by incorporating nucleotide analogs such as 2-aminopurine or 6-methyl-isoxanthopterin into the last 4-6 nucleotides, which have different spectroscopic signatures when in ssDNA or dsDNA (Bjornson, Wong et al. 1996; Singleton, Roca et al. 2007). DNA unwinding experiments can also be performed as a function of $MgCl_2$ concentration or alternatively, DNA unwinding can be initiated by addition of Mg^{2+} in order to probe the influence of Mg^{2+} and DNA melting on this isomerization step.

In Chapter 3, I examined the translocation mechanisms of the RecB monomer and the RecBC heterodimer to better understand the relationship between DNA unwinding and translocation. RecB initiates translocation from random sites within ssDNA and moves with a rate of 803 ± 13 nt/sec in the 3' to 5' direction, as expected for a 3' to 5' helicase. This is about two times faster than the RecBC unwinding rate (348 ± 5 bp/sec) determined under the same solution conditions. After RecBC unwinds a 24 bp initiation duplex, it can continue to move along the ssDNA extension in the 3' to 5' direction with a rate of 909 ± 51 nt/sec (Cy3) or 1030 ± 53 nt/sec (Fluorescein), which is slightly faster than RecB monomer translocation. Interestingly, in performing these experiments, I have discovered that RecBC also possesses a secondary translocase activity which enables it translocate along the opposite DNA strand (i.e.: along a 5’ to 3’ ssDNA extension) with a similar rate (990 ± 49 nt/sec (Cy3), 1187 ± 61 (Fluorescein)). In fact, RecBC can utilize these two translocase activities to move along two non-complementary ssDNA extensions simultaneously albeit with a slower rate (671 ± 47 nt/sec).

The structural basis for the secondary translocase is still unclear. However, based on a RecBCD-DNA crystal structure, there are two regions within RecBC which comes in contact of the 5’ terminating DNA strand: the “arm” domain of RecB and the “dead” nuclease domain of RecC (Singleton, Dillingham et al. 2004; Rigden 2005). The RecB arm is observed to come in contact of the DNA ahead of the unwinding fork while the RecC dead nuclease is observed to interact with the unwound 5’-terminating ssDNA strand, the strand opposite of which RecB operates. Therefore, RecB ATPase activity can potentially control either of these regions allosterically in order to drive the secondary translocase. Future mutation and deletion studies can be employed to test this hypothesis and to examine the structural basis for this secondary translocase activity. This novel discovery and the use of these partial duplex substrates will facilitate subsequent translocation studies of the RecBCD enzyme and its single motor mutants ($RecB^{K29Q}CD$ and $RecBCD^{K177Q}$). These experiments will enable us to examine ssDNA translocation of the RecB and RecD motors independently so that we can compare these results with those of DNA unwinding in order to better understand the relationship between these two processes.

Since RecBC and RecBCD can be synchronized to initiate translocation from a unique site, we can examine whether these proteins can displace protein blocks on the DNA during translocation. For example, I have performed preliminary studies to test whether either the primary or secondary RecBC translocase activities can displace *E. coli* SSB bound to a ssDNA extension. However, additional work will be necessary since the results are inconclusive. This is because the translocation kinetics are difficult to interpret due to the fact that both SSB and RecBC can influence Cy3 fluorescence intensity as described in Chapter 3. Alternatively, instead of labeling the ssDNA end fluorescently with Cy3, it can be labeled with biotin and the DNA substrate can be radiolabeled with ^{32}P and bound to streptavidin, and similar translocation and protein displacement experiments can be performed (Morris and Raney 1999). The relative mobility shift of the DNA substrate with streptavidin bound versus those with streptavidin displaced by RecBC on a native polyacrylamimde gel could potentially be used to observe translocation by the RecBC primary and secondary translocases. Using this type of assay could overcome the complicated fluorescence signal changes observed with RecBC, SSB, and Cy3.

We do not know at this time whether the secondary translocase within RecBC is functional when RecD is present (ie: in the RecBCD enzyme). Because RecD unwinds DNA with 5' to 3' translocation directionality, this motor subunit translocates along the ssDNA strand along which the RecBC secondary translocase operates. This can be addressed by examining the ssDNA translocation kinetics of RecBCD and RecBCD^{K177Q} (and also RecB^{K29Q}CD) using the approaches presented in Chapter 3. In this way, RecBC will be in complex with RecD but this subunit will be catalytically dead. These translocation experiments will also allow us to determine whether the RecB and RecD motor subunits function as independent motors or whether there is some sort of coupling or communication between these two SF helicases mediated through RecC.

In Chapter 4, I examined the efficiency of ATP hydrolysis during DNA unwinding and translocation by RecBC using a phosphate release assay (Brune, Hunter et al. 1998; Dillingham, Wigley et al. 2000; Dillingham, Wigley et al. 2002; Tomko, Fischer et al. 2007). The ATP coupling stoichiometry for both DNA unwinding and ssDNA translocation can be compared independently, which will help us better understand the relationship between these two processes. Thus far, an ATP coupling stoichiometry of ~ 1 ATP/nt translocated has been estimated for the UvrD and PcrA helicases (Dillingham, Wigley et al. 2000; Tomko, Fischer et al. 2007). Based on structural studies, the efficiency of ATP hydrolysis during DNA unwinding by these helicases has been inferred to be 1 ATP/bp unwound (Velankar, Soultanas et al. 1999; Lee and Yang 2006), although this has yet to be shown biochemically. An estimate of ~ 2-3 ATP/bp unwound was estimated for RecBCD unwinding by taking the ratio of the steady-state unwinding rate and the steady-state rate of ATP hydrolysis (Korangy and Julin 1993; Korangy and Julin 1994). The efficiency of ATP hydrolysis during RecBC unwinding is estimated to be 1.2-1.4 ATP/bp with a similar approach (Korangy and Julin 1993; Korangy and Julin 1994). Using a phosphate release assay, I was able to monitor the pre-steady state rate of ATP hydrolysis under single turnover conditions. During DNA unwinding, RecBC consumes on average 0.95 ± 0.08 ATP/bp unwound, which is similar to the ~ 1 ATP/bp unwound proposed for other SF1 enzymes. RecBC translocation along ssDNA in the 3' to 5' direction using its primary translocase activity utilizes on average 0.81 ± 0.05 ATP/nt translocated while its secondary translocase requires on average 1.12 ± 0.06 ATP/nt. Simultaneous translocation along two non-complementary strands has a ATP coupling stoichiometry of 1.07 ± 0.09 ATP/nt, which is the same within error as the value determined for RecBC unwinding. These results indicate that the large majority of ATP hydrolyzed, possibly all, is used to fuel RecBC translocation rather than the strand separation reaction during DNA unwinding. This may be unique to the RecBC and RecBCD enzymes since either protein can “melt-out” 5-6 bp upon DNA binding (Farah and Smith 1997; Singleton, Dillingham et al. 2004; Wong, Lucius et al. 2005; Wong and Lohman 2008). Therefore, if the nucleotide state can modulate the relative affinity of RecBC(D) for DNA, then the melting of 5-6 bp can occur when RecBC(D) switches between tight and loose DNA binding states while ATPase activity is used to drive unidirectional translocation. This model suggests then that RecBC(D) would melt out 5-6 base pairs at once, and then translocation follows using 1 ATP/nt. We cannot at this point rule out an alternative model in which DNA unwinding and translocation occur concurrently, and that translocation occurs using 1 ATP/nt but unwinding occurs simultaneously as the two DNA strands are pulled into the “separation-pin” on the RecC subunit (Singleton, Dillingham et al. 2004). In order to discern between these two unwinding models, single molecule unwinding experiments using high resolution optical traps can determine whether DNA unwinding (consequently base pair melting) occurs in 4-6 bp steps. Similar to the future directions outlined in Chapter 2, studies of the mechanism of DNA melting in addition to mutation studies of the separation pin on the unwinding properties of RecBC and also RecBCD will also help us access the validity of these two DNA unwinding models.

In summary, the thesis outlines mechanistic unwinding and translocation studies of the *E. coli* RecBC and RecBCD helicases. Hopefully, this research will facilitate subsequent studies of the RecBC and RecBCD enzymes or other motor proteins which will help us better understand how these molecular motors can convert the chemical energy from NTP binding and hydrolysis to mechanical energy and drive nucleic acid unwinding and translocation.

References

Abdel-Monem, M., H. Durwald, et al. (1976). "Enzymic unwinding of DNA. 2. Chain separation by an ATP-dependent DNA unwinding enzyme." Eur J Biochem **65**(2): 441-449.

Abdel-Monem, M., H. Durwald, et al. (1977). "DNA unwinding enzyme II of Escherichia coli. 2. Characterization of the DNA unwinding activity." Eur J Biochem **79**(1): 39-45.

Abdel-Monem, M. and H. Hoffmann-Berling (1976). "Enzymatic unwinding of DNA. 1. Purification and characterization of a DNA-dependent ATPase from Escherichia coli." Eur J Biochem **65**(2): 431-440.

Ali, J. A. and T. M. Lohman (1997). "Kinetic measurement of the step size of DNA unwinding by Escherichia coli UvrD helicase." Science **275**(5298): 377-380.

Anderson, D. G. and S. C. Kowalczykowski (1997). "The Translocating RecBCD Enzyme Stimulates Recombination by Directing RecA Protein onto ssDNA in a χ-regulated Manner." Cell **90**: 77-86.

Arnold, D. A. and S. C. Kowalczykowski (2000). "Facilitated loading of RecA protein is essential to recombination by RecBCD enzyme." J Biol Chem **275**(16): 12261-12265.

Betterton, M. D. and F. Julicher (2005). "Opening of nucleic-acid double strands by helicases: active versus passive opening." Phys Rev E Stat Nonlin Soft Matter Phys 71(1 Pt 1): 011904.

Bianco, P. R., L. R. Brewer, et al. (2001). "Processive translocation and DNA unwinding by individual RecBCD enzyme molecules." Nature **409**: 374-378.

Bianco, P. R. and S. C. Kowalczykowski (2000). "Translocation step size and mechanism of the RecBC DNA helicase." Nature **405**: 368-372.

Bjornson, K. P., I. Wong, et al. (1996). "ATP hydrolysis stimulates binding and release of single stranded DNA from alternating subunits of the dimeric E. coli Rep helicase: implications for ATP-driven helicase translocation." J Mol Biol **263**(3): 411-422.

Brune, M., J. L. Hunter, et al. (1998). "Mechanism of inorganic phosphate interaction with phosphate binding protein from Escherichia coli." Biochemistry **37**(29): 10370-10380.

Brendza, K. M., W. Cheng, et al. (2005). "Autoinhibition of *Escherichia coli* Rep monomer helicase activity by its 2B subdomain." Proc Natl Acad Sci U S A **102**(29): 10076-10081.

Delagoutte, E. and P. H. von Hippel (2002). "Helicase mechanisms and the coupling of helicases within macromolecular machines. Part I: Structures and properties of isolated helicases." Q Rev Biophys **35**(4): 431-478.

Dillingham, M. S., M. R. Webb, et al. (2005). "Bipolar DNA translocation contributes to highly processive DNA unwinding by RecBCD enzyme." J Biol Chem **280**(44): 37069-37077.

Dillingham, M. S., Spies, M., Kowalczykowski, S. C. (2003). "RecBCD enzyme is a bipolar helicase." Nature **423**: 893-897.

Dillingham, M. S., D. B. Wigley, et al. (2002). "Direct measurement of single-stranded DNA translocation by PcrA helicase using the fluorescent base analogue 2-aminopurine." Biochemistry **41**(2): 643-651.

Dillingham, M. S., D. B. Wigley, et al. (2000). "Demonstration of unidirectional single-stranded DNA translocation by PcrA helicase: measurement of step size and translocation speed." Biochemistry **39**(1): 205-212.

Eisenberg, S., J. D. Griffith, et al. (1977). "ϕX174 *cistron A* protein is a multifunctional enzyme in DNA replication." Proc.Natl.Acad.Sci.USA **74**: 3198-3202.

Ellis, N. A., J. Groden, et al. (1995). "The Bloom's syndrome gene product is homologous to RecQ helicases." Cell **83**: 655-666.

Farah, J. A. and G. R. Smith (1997). "The RecBCD Enzyme Initiation Complex for DNA Unwinding: Enzyme Positioning and DNA Opening." J.Mol.Biol. **272**: 699-715.

Finch, P. W., A. Storey, et al. (1986). "Complete nucleotide sequence of *recD*, the structural gene for the α subunit of Exonuclease V of *Escherichia coli*." Nucleic Acids Research **14**: 8583-8594.

Finch, P. W., A. Storey, et al. (1986). "Complete nucleotide sequence of the *Escherichia coli recB* gene." Nucleic Acids Research **14**: 8573-8582.

Finch, P. W., R. E. Wilson, et al. (1986). "Complete nucleotide sequence of the Escherichia coli recC gene and of the thyA-recC intergenic region." Nucleic Acids Res **14**(11): 4437-4451.

Fischer, C. J. and T. M. Lohman (2004). "ATP-dependent translocation of proteins along single-stranded DNA: models and methods of analysis of pre-steady state kinetics." J Mol Biol **344**(5): 1265-1286.

Fischer, C. J., N. K. Maluf, et al. (2004). "Mechanism of ATP-dependent translocation of E.coli UvrD monomers along single-stranded DNA." J Mol Biol **344**(5): 1287-1309.

German, J., M. M. Sanz, et al. (2007). "Syndrome-causing mutations of the BLM gene in persons in the Bloom's Syndrome Registry." Hum Mutat **28**(8): 743-753.

Gorbalenya, A. E. and E. V. Koonin (1993). "Helicases: amino acid sequence comparisons and structure-function relationships." Curr.Op.Struct.Biol. **3**: 419-429.

Hall, M. C. and S. W. Matson (1999). "Helicase motifs: the engine that powers DNA unwinding." Mol Microbiol **34**(5): 867-877.

Handa, N., P. R. Bianco, et al. (2005). "Direct visualization of RecBCD movement reveals cotranslocation of the RecD motor after chi recognition." Mol Cell **17**(5): 745-750.

Hickson, I. D. (2003). "RecQ helicases: caretakers of the genome." Nat Rev Cancer **3**(3): 169-178.

Hickson, I. D., S. L. Davies, et al. (2001). "Role of the Bloom's syndrome helicase in maintenance of genome stability." Biochem Soc Trans **29**(Pt 2): 201-204.

Korangy, F. and D. A. Julin (1994). "Efficiency of ATP Hydrolysis and DNA Unwinding by the RecBC Enzyme from *Escherichia coli*." Biochemistry **33**: 9552-9560.

Korangy, F. and D. A. Julin (1993). "Kinetics and processivity of ATP hydrolysis and DNA unwinding by the RecBC enzyme from Escherichia coli." Biochemistry **32**(18): 4873-4880.

Kowalczykowski, S. C., D. A. Dixon, et al. (1994). "Biochemistry of homologous recombination in *Escherichia coli*." Microbiological Reviews **58**: 401-465.
Lohman, T. M. and K. P. Bjornson (1996). "Mechanisms of helicase-catalyzed DNA unwinding." Annu Rev Biochem **65**: 169-214.

Lee, J. Y. and W. Yang (2006). "UvrD Helicase Unwinds DNA One Base Pair at a Time by a Two-Part Power Stroke." Cell **127**(7): 1349-1360.

Lohman, T. M., E. J. Tomko, et al. (2008). "Non-hexameric DNA helicases and translocases: mechanisms and regulation." Nat Rev Mol Cell Biol.

Lohman, T. M., J. Hsieh, et al. (2003). DNA Helicases, Motors that Move Along Nucleic Acids: Lessons from the SF1 Helicase Superfamily. NY, Academic Press.

Lohman, T. M. (1992). "*Escherichia coli* DNA helicases: mechanisms of DNA unwinding." Mol.Microbiol. 6: 5-14.

Lucius, A. L., C. Jason Wong, et al. (2004). "Fluorescence stopped-flow studies of single turnover kinetics of *E.coli* RecBCD helicase-catalyzed DNA unwinding." J. Mol. Biol. **339**(4): 731-750.

Lucius, A. L. and T. M. Lohman (2004). "Effects of temperature and ATP on the kinetic mechanism and kinetic step-size for *E.coli* RecBCD helicase-catalyzed DNA unwinding." J. Mol. Biol. **339**(4): 751-771.

Lucius, A. L., N. K. Maluf, et al. (2003). "General methods for analysis of sequential "n-step" kinetic mechanisms: application to single turnover kinetics of helicase-catalyzed DNA unwinding." Biophys J **85**(4): 2224-2239.

Lucius, A. L., A. Vindigni, et al. (2002). "DNA unwinding step-size of E. coli RecBCD helicase determined from single turnover chemical quenched-flow kinetic studies." J Mol Biol **324**(3): 409-428.

Maluf, N. K., C. J. Fischer, et al. (2003). "A Dimer of *Escherichia coli* UvrD is the active form of the helicase in vitro." J. Mol. Biol. **325**(5): 913-935.

Manosas, M., X. G. Xi, et al. (2010). "Active and passive mechanisms of helicases." Nucleic Acids Res.

Matson, S. W., D. W. Bean, et al. (1994). "DNA helicases: enzymes with essential roles in all aspects of DNA metabolism." Bioessays **16**(1): 13-22.

Matson, S. W. and A. B. Robertson (2006). "The UvrD helicase and its modulation by the mismatch repair protein MutL." Nucl. Acids Res **34**(15): 4089-4097.

Morris, P. D. and K. D. Raney (1999). "DNA Helicases Displace Streptavidin from Biotin-Labeled Oligonucleotides." Biochemistry **38**: 5164-5171.

Niedziela-Majka, A., M. A. Chesnik, et al. (2007). "Bacillus stearothermophilus PcrA Monomer Is a Single-stranded DNA Translocase but Not a Processive Helicase in Vitro." J. Biol. Chem. **282**(37): 27076-27085.

Patel, S. S. and I. Donmez (2006). "Mechanisms of Helicases." J. Biol. Chem. **281**(27): 18265-18268.

Patel, S. S. and K. M. Picha (2000). "Structure and function of hexameric helicases." Annu Rev Biochem **69**: 651-697.

Perkins, T. T., H. W. Li, et al. (2004). "Forward and reverse motion of single RecBCD molecules on DNA." Biophys J **86**(3): 1640-1648.
Rigden, D. J. (2005). "An inactivated nuclease-like domain in RecC with novel function: implications for evolution." BMC Struct Biol **5**: 9.

Rigden, D. J. (2005). "An inactivated nuclease-like domain in RecC with novel function: implications for evolution." BMC Struct Biol **5**: 9.

Roman, L. J., A. K. Eggleston, et al. (1992). "Processivity of the DNA helicase activity of Escherichia coli recBCD enzyme." J Biol Chem **267**(6): 4207-4214.

Roman, L. J. and S. C. Kowalczykowski (1989). "Characterization of the adenosinetriphosphatase activity of the Escherichia coli RecBCD enzyme: relationship of ATP hydrolysis to the unwinding of duplex DNA." Biochemistry **28**(7): 2873-2881.

Roman, L. J. and S. C. Kowalczykowski (1989). "Characterization of the helicase activity of the Escherichia coli RecBCD enzyme using a novel helicase assay." Biochemistry **28**(7): 2863-2873.

Saikrishnan, K., S. P. Griffiths, et al. (2008). "DNA binding to RecD: role of the 1B domain in SF1B helicase activity." EMBO J **27**(16): 2222-2229.

Serebrov, V. and A. M. Pyle (2004). "Periodic cycles of RNA unwinding and pausing by hepatitis C virus NS3 helicase." Nature **430**(6998): 476-480.

Singleton, M. R., M. S. Dillingham, et al. (2007). "Structure and Mechanism of Helicases and Nucleic Acid Translocases." Annu Rev Biochem **76**: 23-50.

Singleton, S. F., A. I. Roca, et al. (2007). "Probing the structure of RecA-DNA filaments. Advantages of a fluorescent guanine analog." Tetrahedron **63**(17): 3553-3566.

Singleton, M. R., M. S. Dillingham, et al. (2004). "Crystal structure of RecBCD enzyme reveals a machine for processing DNA breaks." Nature **432**(7014): 187-193.

Smith, G. R. (1990). RecBCD Enzyme. Nucleic Acids and Molecular Biology. F. Eckstein and D. M. J. Lilley. Berlin, Springer Verlag**:** 78-98.

Spies, M., I. Amitani, et al. (2007). "RecBCD Enzyme Switches Lead Motor Subunits in Response to chi Recognition." Cell **131**(4): 694-705.

Spies, M., P. R. Bianco, et al. (2003). "A molecular throttle: the recombination hotspot chi controls DNA translocation by the RecBCD helicase." Cell **114**(5): 647-654.

Spies, M., M. S. Dillingham, et al. (2005). "Translocation by the RecB motor is an absolute requirement for {chi}-recognition and RecA protein loading by RecBCD enzyme." J. Biol. Chem. **280**(44): 37078-37087.

Taylor, A. F. and G. R. Smith (2003). "RecBCD enzyme is a DNA helicase with fast and slow motors of opposite polarity." Nature **423**: 889-893.

Tomko, E. J. (2010). Transient-State Kinetic Studies of the *E. coli* UvrD Monomer Translocation Along Single-Stranded DNA. Biochemistry and Molecular Biophysics. St. Louis, Washington University School of Medicine. **Ph.D:** 380.

Tomko, E. J., C. J. Fischer, et al. (2007). "A Nonuniform Stepping Mechanism for E. coli UvrD Monomer Translocation along Single-Stranded DNA." Molecular Cell **26**(3): 335-347.

Velankar, S. S., P. Soultanas, et al. (1999). "Crystal Structures of Complexes of PcrA DNA Helicase with a DNA Substrate Indicate an Inchworm Mechanism." Cell **97**: 75-84.

Webb, M. R. (2010). "Fluorescent biosensors to investigate helicase activity." Methods Mol Biol **587**: 13-27.

Wong, C. J. and T. M. Lohman (2008). "Kinetic control of Mg2+-dependent melting of duplex DNA ends by Escherichia coli RecBC." J Mol Biol **378**(4): 759-775.

Wong, C. J., R. L. Rice, et al. (2006). "Probing 3'-ssDNA Loop Formation in *E. coli* RecBCD/RecBC-DNA Complexes Using Non-natural DNA: A Model for "Chi" Recognition Complexes." J. Mol. Biol. **362**(1): 26-43.

Wong, C. J., A. L. Lucius, et al. (2005). "Energetics of DNA end binding by *E.coli* RecBC and RecBCD helicases indicate loop formation in the 3'-single-stranded DNA tail." J. Mol. Biol. **352**(4): 765-782.

Wu, C. G. and T. M. Lohman (2008). "Influence of DNA end structure on the mechanism of initiation of DNA unwinding by the Escherichia coli RecBCD and RecBC helicases." J Mol Biol **382**(2): 312-326.

Yarranton, G. T., R. H. Das, et al. (1979). "Enzyme-catalyzed DNA unwinding. A DNA-dependent ATPase from E. coli." J Biol Chem **254**(23): 11997-12001.

Yu, M., J. Souaya, et al. (1998). "The 30-kDa C-terminal domain of the RecB protein is critical for the nuclease activity, but not the helicase activity, of the RecBCD enzyme from *Escherichia coli*." Proc.Natl.Acad.Sci.,U.S.A. **95**: 981-986.

Yu, M., J. Souaya, et al. (1998). "Identification of the Nuclease Active Site in the Multifunctional RecBCD Enzyme by Creation of a Chimeric Enzyme." J.Mol.Biol. **283**: 797-808.